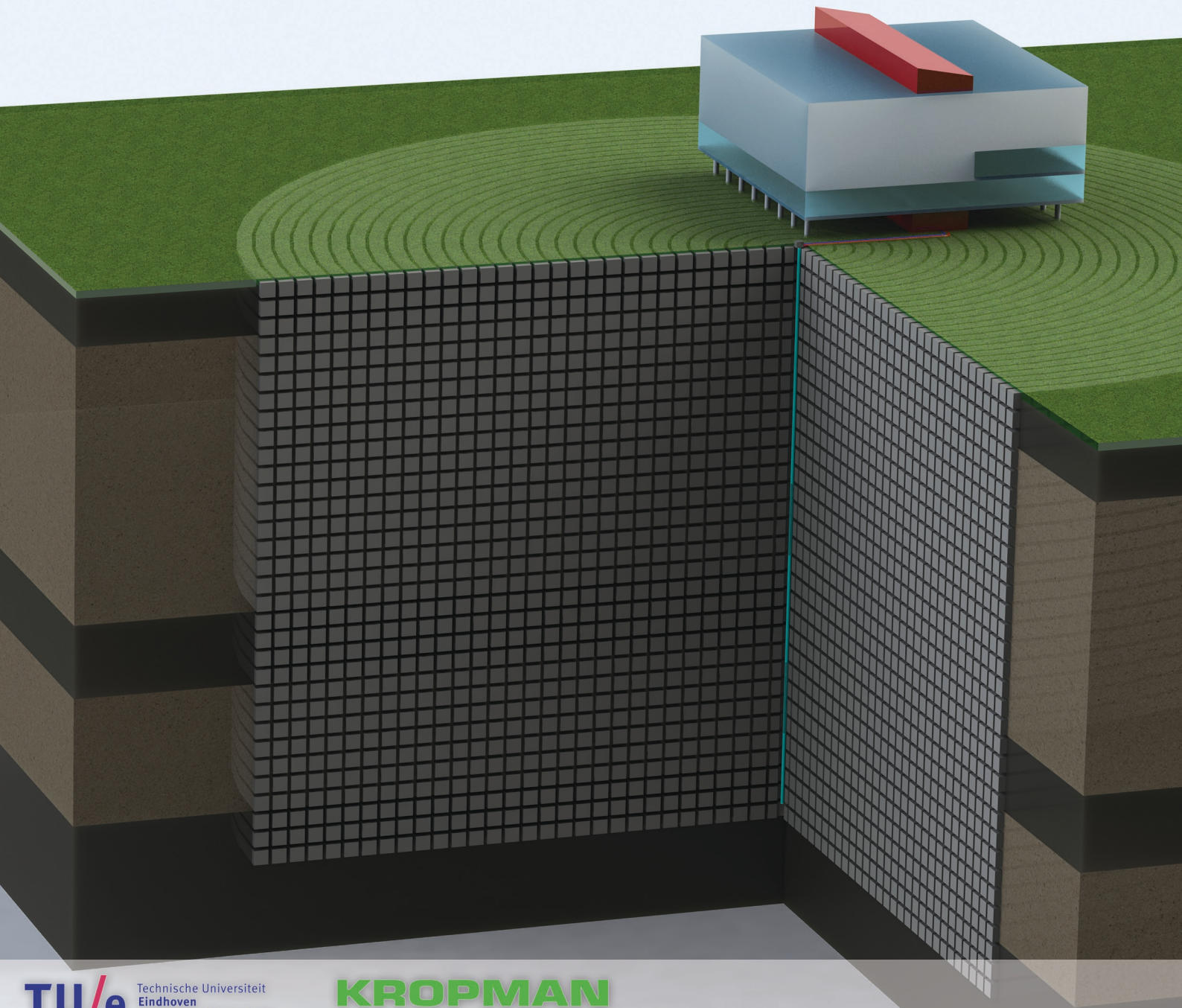


# MAINTAINING ATEs BALANCE USING CONTINUOUS COMMISSIONING AND MODEL PREDICTIVE CONTROL

*Development of a reference model and analysis of method potential  
based on a case study at the Kropman Utrecht office*

*Master thesis*

*J.H.K. Hoving  
January 2015*



# ***MAINTAINING ATES BALANCE USING CONTINUOUS COMMISSIONING AND MODEL PREDICTIVE CONTROL***

*Development of a reference model and analysis of method potential  
based on a case study at the Kropman Utrecht office*

*Master thesis*

*January 2015*

## ***Author:***

J.H.K. Hoving  
Master Sustainable Energy Technology  
Eindhoven University (s124057)  
University of Twente (s0125016)

## ***Department:***

Building Services  
Unit Building Physics and Services  
Department of the Built Environment  
Eindhoven University of Technology (NL)

## ***Graduation committee:***

Prof. ir. W. Zeiler  
Prof. dr. ir. T.H. van der Meer  
Ir. J.F.B.C. Haan  
Dr. R. Li  
Ir. G. Boxem

*Chair of committee*  
*Program director*  
*Company supervisor*  
*Internal member*  
*Internal member*

*Eindhoven University*  
*University of Twente*  
*Kropman Installatietechniek*  
*Eindhoven University*  
*Eindhoven University*

# ABSTRACT

---

A rapidly growing amount of office buildings in the Netherlands is using an Aquifer Thermal Energy Storage (ATES) system. An ATES system uses a well pump to extract cold groundwater for cooling. The returned warm water is injected and stored in a second well. During winter this warm water is used for heating and the returned cold water is injected again in the first well. An optimal functioning ATES system can significantly reduce energy use and CO<sub>2</sub> emissions of an office building.

An essential condition for optimal ATES operation is the thermal balance of the system. Office buildings typically store much more heat than cold, causing the entire underground slowly to heat up and causing cooling capacity problems on the long term. This is compensated by using cold outdoor air to store additional cold during the winter, called regeneration. In this research two methods are evaluated to keep the thermal storage in balance. Continuous Commissioning (CC) is used to check if the expected amount of energy is actually stored in the ATES system. Model Predictive Control (MPC) is used to control the amount of regenerated cold to maintain the ATES balance. The key element in both methods is the reference model to calculate the expected stored amount (CC) and use as model for MPC.

A reference model is constructed based on the Kropman Utrecht case study building and contains three main blocks: The ATES, Heating/Ventilation/Air-conditioning (HVAC) and load simulation. For the ATES system a lightweight finite element simulation method is developed, based on an axisymmetric grid. An additional method is developed to reconstruct the injected water temperatures and volumes, because these are not measured in the case study installation. The HVAC and load simulation models are based on logged building management system (BMS) data. The use of BMS data has the large advantage that models are easily configured and can automatically adjust to changes in the building.

The analysis of CC revealed a combination of hardware and software problems. Around 30% of the generated cold is not stored in the ATES system and around 10% of the heat did not need to be stored in the ATES. The use of district heat can be reduced by 60%. Using the current regeneration strategy, the building should generate a significant surplus of cold instead of heat. Using MPC it was possible to keep the ATES in balance over a simulated 20 years period. By using a slight cold surplus as target, the effect of exceptionally warm winters is minimal and extraction temperatures are very constant.

For the case study building it can be concluded that the combination of CC and MPC, using the developed reference model, is capable of automatically maintaining the ATES balance. Because the case study building type and size is comparable to the majority of the new Dutch office buildings, it is expected that large parts of the method are universally applicable.

# PREFACE

---

This thesis is the result of my graduation research for the master Sustainable Energy Technology at the University of Twente. I choose the master SET because I believe the transition from fossil fuels to sustainable energy is one of the largest and most interesting technological challenges the world faces in the coming decades. During the various courses of the master, the sheer size of the sustainable challenge became clear. Sustainable energy is partly about developing and optimizing new technologies, but an even larger challenge is found in integrating all technologies into concepts that provides the same reliability as fossil fuel. A research field that is on the forefront of integrating multiple sustainable technologies into actual systems is building services for the built environment.

Starting this research I had no experience at all in building services. I did a bachelor Applied Physics, so I understood the processes but never saw an actual heat pump or air handling unit. This fresh approach proved to be a bit of a handicap sometimes, but also provided several new insights and proved to be an advantage in 'out-of-the-box' thinking. While performing this research one of the main challenges of this field became apparent. Energy is not saved by designing buildings with a reduced energy use, but by making buildings actually save energy. The yearly energy bills represent the buildings energy use and not the framed energy certificate on the wall.

In this research an attempt is done to develop a bridge between the energy bill and the energy certificate. I believe that using methods like continuous commissioning the gap between research, design and reality can be closed and truly sustainable buildings can be constructed. On the other hand I learned to put the challenge for sustainability in perspective. Goals like comfort and reliability are at least equally important and can outweigh the energy efficiency.

Because the University of Twente does not have a building services department, this research is performed under supervision of the Eindhoven University. I would like to thank prof. Wim Zeiler for offering me the opportunity to graduate at this field and supervising the research. I really appreciated the given freedom in performing the research and the provided feedback. The interesting conversations about the construction sector helped me to put the research in perspective.

I also would like to thank my supervisor at Kropman, Jan-Fokko Haan, and all direct colleagues in the O&T team. Every time I had some novice questions you all took the time to give me a crash course on various topics. During the research I was trusted with full access to the BMS and Priva software, the master key of the building and all measurement equipment. This really helped in getting familiar with the building and acquiring the required data. Overall I had a great time at the office in Utrecht.

During the writing of the report I had several interesting meetings at the Eindhoven University. In special I would like to thank Gert Boxem, Rongling Li, Basar Bozkaya and Christian Finck for the discussions and provided help on getting an understandable structure in the thesis.

Finally I would like to thank my parents for supporting me during my time as student. This thesis concludes an exciting and inspiring period at (and around) the University. I'm really grateful for making this possible.

Jasper Hoving

*Utrecht, January 2015*



# INDEX

---

|   |            |
|---|------------|
| <b>ABSTRACT .....</b>                               | <b>I</b>   |
| <b>PREFACE .....</b>                                | <b>II</b>  |
| <b>INDEX .....</b>                                  | <b>III</b> |
| <b>1. INTRODUCTION.....</b>                         | <b>1</b>   |
| 1.1 Background .....                                | 1          |
| 1.2 Problem analysis .....                          | 2          |
| 1.3 Research introduction .....                     | 4          |
| 1.4 Research structure .....                        | 7          |
| 1.5 Case study introduction .....                   | 9          |
| <b>2. ATES SYSTEM MODEL.....</b>                    | <b>10</b>  |
| 2.1 Introduction.....                               | 10         |
| 2.2 Aquifer simulation method .....                 | 13         |
| 2.3 Aquifer side data reconstruction method .....   | 22         |
| 2.4 Implementation of control software method ..... | 32         |
| 2.5 Discussion .....                                | 37         |
| <b>3. HVAC SYSTEM MODEL .....</b>                   | <b>39</b>  |
| 3.1 Introduction.....                               | 39         |
| 3.2 Air handling unit simulation method .....       | 46         |
| 3.3 Local cooling simulation method .....           | 55         |
| 3.4 Heat pump simulation method.....                | 59         |
| 3.5 Discussion .....                                | 63         |
| <b>4. LOAD SIMULATION MODEL .....</b>               | <b>64</b>  |
| 4.1 Introduction.....                               | 64         |
| 4.2 Load curves reconstruction method .....         | 64         |
| 4.3 State selection method .....                    | 71         |
| 4.4 Discussion .....                                | 74         |
| <b>5. MODEL APPLICATION.....</b>                    | <b>75</b>  |
| 5.1 Continuous commissioning analysis .....         | 75         |
| 5.2 Model predictive control analysis.....          | 80         |
| 5.3 Discussion .....                                | 83         |
| <b>6. CONCLUSIONS AND RECOMMENDATIONS .....</b>     | <b>84</b>  |
| 6.1 Conclusions .....                               | 84         |
| 6.2 Recommendations .....                           | 86         |
| <b>REFERENCES .....</b>                             | <b>87</b>  |

# 1. INTRODUCTION

## 1.1 BACKGROUND

The worldwide depletion of fossil fuels, increasing energy prices and climate change have led to sharpened building regulations and the need to design more energy efficient buildings. Buildings constructed during the last decade have high standards of air-tightness and insulation. For all buildings these measures achieve a significant improvement in heating demand and comfort. For office (and comparable) buildings however there is an additional advantage.

Because office buildings typically have a high internal heat load (heat generated by people, lighting and equipment), the required amount of external heat is relatively low compared to residential or utility buildings. As result, the required amount of cooling is significantly higher than the average building. Nowadays modern office buildings have reached the insulation quality at which the amount of cooling required during the summer roughly equals the amount of heating needed during the winter. Hypothetically this means that if all heat could be stored within the building, no external heat source would be needed throughout the year.

The storage of such large amounts of (low quality / temperature) heat within the building would require vast amounts of high heat capacity materials like thick stone walls (as in churches, castles) or phase change materials (PCMs). A more feasible option is to store the energy outside the building. An increasingly popular solution is energy storage in the groundwater below the building. This groundwater is stored in porous sand layers, called *aquifers*. Therefore, this method is called Aquifer Thermal Energy Storage (ATES). Using this method the seasonal storage effect of an expensive high thermal mass building can be achieved with a cheaper lightweight building construction and an external ATES system.

The principle of an ATES system is based on transferring groundwater between two separated storage wells. During summertime water is extracted from the coldest well and used to cool the building. During cooling, the water temperature increases from approximately 8°C to 16°C. The heated water is injected in the warmer well and stored until winter season. During winter the extraction/injection flow is reversed and the heated water (which still has a temperature of approx. 14 °C) is pumped back to the building. Using a heat pump the heat is extracted and converted to higher temperatures to heat the building. The water is cooled to approx. 6°C and is injected in the cold well. A heat exchanger between the groundwater and the building system water is used to avoid contamination of the water.

The storage wells can be located horizontally or vertically spaced to each other (Figure 1-1). A horizontally spaced system is called a doublet and has the highest thermal capacity because the total length of the well can be used to inject or extract water. A vertically spaced system is called a mono-well. A mono-well has less capacity, but is significantly cheaper because only one borehole is needed. This research will focus on a mono-well system, as this system is used at the Kropman Utrecht office (the used case study for this research).

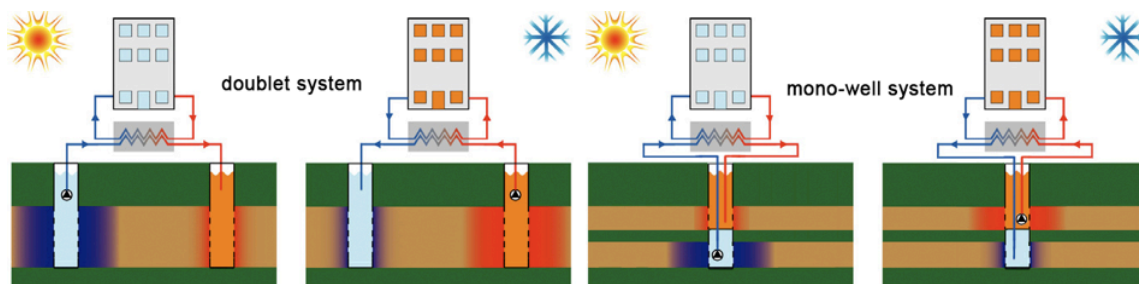


Figure 1-1 – Doublet and mono-well ATES systems (modified from [1])

For efficient and profitable application of a mono-well ATES system there are a few boundary conditions, which make the Dutch soil structure particularly suitable.

- The groundwater level should be relatively close to the ground level, to avoid expensive deep drilling. In the Netherlands the groundwater level is usually within 20 meters below the ground level.
- The natural flow in the groundwater should be low to avoid the stored heat/cold flowing away. Due to the flat Dutch landscape, the annual groundwater flow is only a few meters per year.
- To use two vertically spaced wells (a mono-well), there should be an impermeable layer of clay to avoid a short-cut water flow between the storage wells. A large part of the Dutch soil consists of alternating layers of sand and clay, making it likely that a suitable separation layer can be found.

An optimal performing ATES system can deliver very efficient cooling. The case-study system for example uses a 2 kW well pump that delivers 20 m<sup>3</sup>/h of cooling water with a  $\Delta T$  of 8K between extraction and injection. This equals roughly 200 kW of cooling power, a *Coefficient of Performance* (COP) of 100. For comparison, a regular (compression based) cooling system reaches a COP between 4 and 6 [2]. The energy gains (compared to a conventional system) for heating are not that significant, because the stored low temperature heat is not directly applicable in the building. The heating performance of the ATES system depends mainly on the coupled heat pump, which has a COP of around 4 [2]. However, assuming an average Dutch electricity generation efficiency of 42% [3], this is still a 60% higher efficiency than natural gas boilers and is required to provide the cold water storage supply.

Because of these favorable conditions, the use of ATES systems in the Netherlands has become increasingly popular since the first installations in 1990. In 2013 there were over 2000 installations in use and this number is expected to grow to 10.000 (worst-case) or 20.000 (best-case) in the year 2020 [4].

## 1.2 PROBLEM ANALYSIS

Although the theoretical performance of ATES systems looks promising, the soil conditions are optimal and the heating and cooling loads of an office building in the Dutch climate are ideal; in reality the performance of the installed systems is not fulfilling expectations. As frequently reported in Dutch newspapers and professional journals [5], [6], [7], the performance of 70% of the ATES systems in the Netherlands is not as successful as designed. Almost 30% of these systems is performing even worse than when conventional heating / cooling methods would be applied [7].

A wide diversity of causes is responsible for these underperforming systems. Based on a selection of case studies [8], [9], [10], articles, experiences of engineers at Kropman and personal experience during the research, an analysis of the main problems is made. These problems can be categorized in four groups (Figure 1-2), depending on the moment in time.

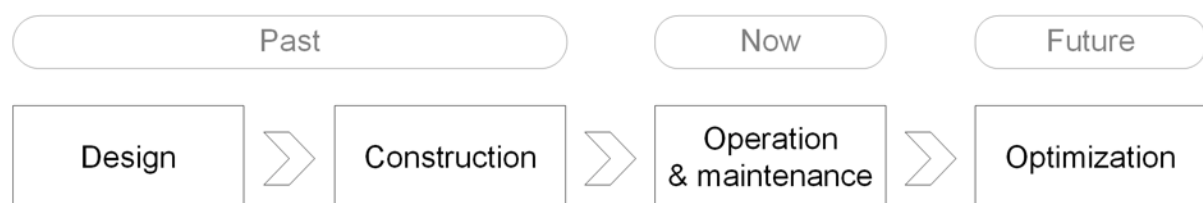


Figure 1-2 - Categorization of main ATES-related problems

### DESIGN CHALLENGES

The design of an ATES coupled *Heating, Ventilation and Air Conditioning* (HVAC) system is significantly more complex than a conventional system for a number of reasons:

- The extraction temperature of the wells is variable throughout the year
- The typically applied high temperature cooling systems are very sensible to variations in the supply water temperature, because of a small  $\Delta T$  to the indoor air temperature
- During extraction of warm water simultaneously the cold well must be injected with a suitable chilled water temperature (and vice versa)
- The ATES-system cannot deliver heating and cooling at the same moment, while buildings do need simultaneously heating and cooling during spring and autumn. Systems must be designed to optimally buffer and redistribute thermal energy in order to supply a net heating or cooling load to the ATES
- Partial loads (which are already notoriously complex in conventional systems) are even more complex if also the storage side  $\Delta T$  must be taken into account

Although engineers are well aware of these complexities, the majority of the systems are designed using a conventional method: Design the installation for full capacity operation during a predefined minimum (for heating) and maximum (for cooling) ambient temperature and assume the system to work between these temperatures (which are by far the most hours per year).

### CONSTRUCTION DEVIATIONS

The more complex an HVAC system is, the higher the risk of deviations between the original plan and what is actually built. Although a system seems to be quite straightforward on a principle diagram, the actual piping labyrinth of cramped utility rooms can be very confusing. It is not uncommon that systems are not functioning because:

- Advisors, mechanical engineers, software engineers and contractors all use different version of systems drawings.
- Construction mistakes, incorrect connected piping and faulty placed, configured or even missing sensors and valves.
- Last minute (undocumented) changes in the construction due to problems discovered at the building site.

Using new techniques like Building Information Modeling (BIM) this should be reduced, but actual construction of the systems shall always be vulnerable to human errors.

### OPERATION AND MAINTENANCE DIFFICULTIES

Because the original performance calculations are made for full capacity operation (for a few hours per year), it is difficult to evaluate how the system is operating during partial load. The dynamic nature of storage based systems causes maintenance difficulties; for example:

- Unlike conventional systems, heating and cooling are always coupled (by both the heat pump as the storage wells). A problem at the cold-water side of the system can cause heating problems and vice versa.
- A similar difficulty is found in the coupled distribution and storage. A setpoint change of the distribution (loads) side can significantly influence the stored energy.
- A high number of system states are needed for buffering and redistribution. It can be difficult to discover which state causes problems under which circumstances.
- Only the problems at the distribution side are noticed directly by a lack of heating or cooling capacity in the building. Problems on the storage side of the system have no direct effect, but are revealed in the next season by performance problems of the ATES.

The fundamental difference between conventional systems and ATES based systems is the 'charging' of the storage. This aspect complicates maintenance because of the long-term effects. Imagine for example a technician standing in the utility room of a building during summer season with the assignment to 'fix the decreased cooling capacity of the ATES'. Obviously this is not possible, because the problems are caused by the lack of stored cold in the winter.

### *OPTIMIZATION OF PERFORMANCE*

The named difficulties in designing, constructing, operating and maintaining an ATES coupled system can be directly connected to problems in optimization of performance. In a system that does not perform as 'expected', it won't be a surprise that optimizations are also not performing as expected. For this reason optimization is often done by trial and error. The system is operated for a few years and after that period the settings are tuned to compensate heat or cold shortage. This requires frequent (and expensive) human intervention in the settings. A few common optimization difficulties are:

- The performance of an ATES system is coupled to the cumulative yearly loads, which makes it hard to evaluate the optimization results after one rainy summer or a very cold winter. A change in the storage strategy should be evaluated over several seasons to evaluate its results. This makes the trial-and-error method not suitable on short-term.
- If a conventional system has performance problems, a mechanic can solve these problems within a day of cleaning, repairing, replacing and fine-tuning of the equipment and directly measure the results. Due to the storage aspect, performance optimization can only be measured after several years and the result is highly dependent on climate and building use variations.

In short, it is very complicated (or even impossible) to optimize something when the process that must be optimized is not sufficiently understood and the effects are not directly measurable or predictable.

## **1.3 RESEARCH INTRODUCTION**

As can be concluded from the problem analysis, the performance problems of ATES systems are not so much found in the initial hardware design of the ATES and HVAC system (although there is room for improvement). The main problem is found in the *understanding, monitoring and prediction* of the systems behavior and thermal charging and discharging behavior of the aquifer. To guarantee reliable and robust ATES operation, the storage process must be monitored on short-term events (monitor the past hours/days) and the long-term operation (predict the future months/year). The two analyzed methods to do this are respectively continuous commissioning (short-term) and model predictive control (long-term).

### **1.3.1 CONTINUOUS COMMISSIONING**

Because the long-term performance of the ATES system is the cumulative result of all hour-to-hour events, the key of gaining control over the total stored energy is to monitor each individual event. This can be done by applying a continuous commissioning (CC) system in the building. Continuous commissioning is based on the principle commissioning. This is done when a building is finished and handed over to the owner. All equipment is tested and measured to check if it operates according to the design specifications. CC is an automated real-time version of commissioning to secure that all systems keep operating according to their specifications.

An example of the usability of CC can be given using a heat pump that does not perform as intended during winter. In the building nothing will be noticed, because the remainder of the heat load is supplied by the back-up heating systems. The stored cold however will be significantly less than accounted for, creating cooling problems in the following summer. Using continuous



commissioning this can be noticed immediately, while using conventional methods this will be noticed indirectly (and much later) via a cooling capacity shortage, expensive back-up heating energy bills and a thermal ATES imbalance.

It is important to realize continuous commissioning is a *concept*, not an actual *method*. Methods for CC are currently under development by several research institutes and for various case-study buildings [11]. However, a uniform method is not yet developed and it still is a kind of ‘umbrella term’ for a large variety of possible implementation methods. One of those methods could be model-based fault detection. As shown in Figure 1-3 this method can compare measured sensor values with a model that simulates ‘correct system behavior’.

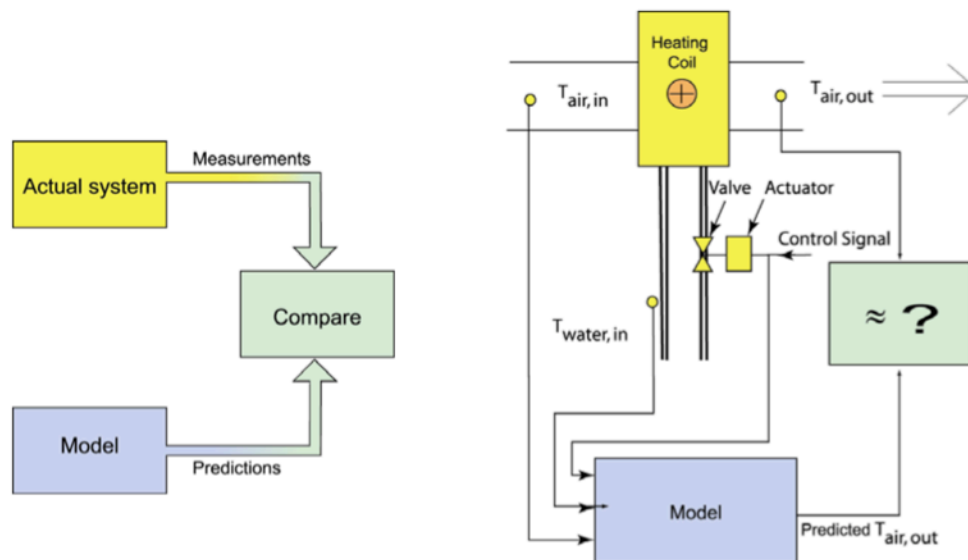


Figure 1-3 - The concept of model-based fault detection and its application to a heating coil (from [11])

If a value deviates significantly for a longer time, a warning is generated in the buildings management system (BMS). The main challenge in this method is the development of this ‘correct behavior’ or reference model.

The goal of this research is *explicitly not* to provide an implementation for the fault detection method. An analysis of the comparison between a reference model and the actual (measured) performance is given. If deviations are caused by actual problems in the system, the fault detection method might be capable of detecting these. The goal of the analysis is to determine if model-based fault detection is a suitable tool to detect ATES-affecting building problems.

### 1.3.2 MODEL PREDICTIVE CONTROL

Even if (as result of implementing continuous commissioning) the building operates exactly as intended, this does not imply that the ATES will achieve a thermal balance. The stored amounts of energy are influenced by climate variations (i.e. warmer winters) or variations in building use (i.e. internal heat load, building occupancy); these are *uncontrollable* input variables. For this reason ATES-coupled systems are usually combined with possibilities for regeneration capacity, which supplies additional *controllable* amounts of energy to the storage to restore balance. The main challenge is to define how much regeneration is required (because of the uncontrollable part) and how to realize it.

The analyzed method for this goal is model predictive control (MPC) [12]. MPC is not a specific control strategy, but a broad range of methods that all use a (simplified) model of the system for behavior prediction and as input for the control strategy. MPC is a more intuitive (human) way of controlling a system. It is for example easily compared with the decision if we need to bring an

umbrella (by using the weather forecast) or the needed force on the brake pedal while driving a car in traffic (by making a prediction of the surrounding cars' behavior and risks) [13]. Conventional controllers only take the past and current situation in account (find an umbrella when it starts to rain and hit the brake when hitting something).

In Figure 1-4 the basic principle of MPC is shown. An essential component of MPC is the *Prediction Horizon*. The prediction horizon states within how much time from point 'k' the reference trajectory (target state) should be reached. The sample time is the interval between recalculation of the new control inputs.

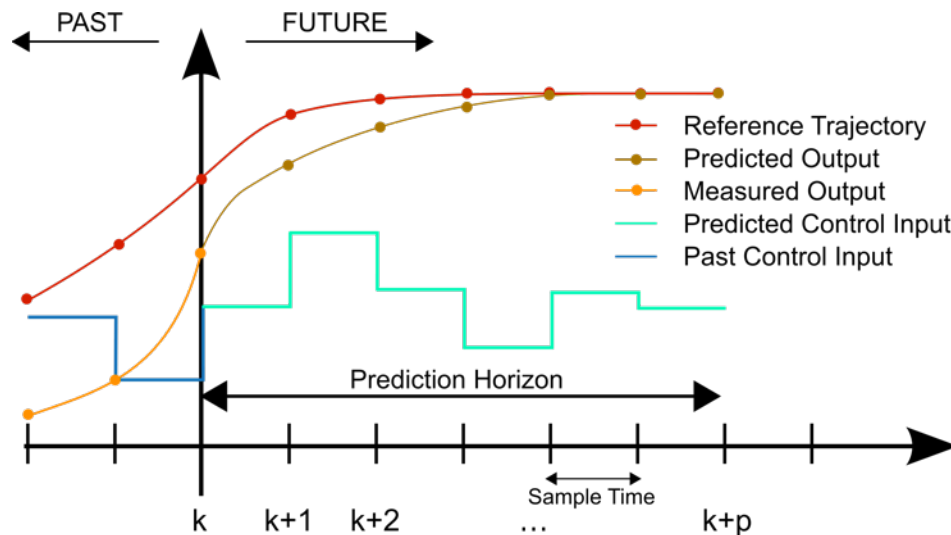


Figure 1-4 - MPC basic principle [14]

In this research an analysis is made if MPC is capable of maintaining the thermal ATES balance. A reference trajectory is set on the required amount of stored cold during the winter and MPC is used to control the amount of regenerated energy. If the stored amount of cold deviates from the reference trajectory, the control input or regeneration is adapted to reach the reference trajectory within the prediction horizon. A simulated analysis is performed (not an actual implementation) to check if the suggested MPC method is capable of maintaining the thermal balance.

The combination between CC and MPC is essential, because the MPC values are only applicable if the actual system does behave as the reference model suggests. The latter is ensured by implementing model-based CC.

### 1.3.3 RESEARCH QUESTIONS

As can be derived from the previous two sections, the key element in both continuous commissioning and model predictive control is the development of an accurate reference simulation model. The more accurate this model, the higher the potential of both methods. The model should be an integral solution for the ATES behavior (the storage), HVAC system performance and heating / cooling loads, because only by analyzing the whole combination a predictive model can be constructed. The model must be capable of adapting to changes in building use or equipment performance. This implies the model should be merely based on data extracted from the building management system (BMS). A model based on this method uses data generated by the building and is not based on static assumptions or calculations. The general modeling concept is: 'Learning from the past how the building will behave in the future'.

This research is based on a case-study building, the Kropman office in Utrecht (NL), of which the ATES system has a structural yearly surplus of stored heat. This results in cooling problems during summer and high-energy use for regeneration. In the original designs a surplus of cold was expected [9], which makes the case-study interesting for both CC as MPC.

The research has two main parts:

## 1) Model development

*How to develop a reference model for the Kropman Utrecht case-study building?*

Sub questions:

- How to model the ATES system using BMS data?
- How to model the HVAC components using BMS data?
- How to model the heating and cooling load using BMS data?

## 2) Model application

*Are continuous commissioning and model predictive control suitable tools to maintain the ATES balance of the Kropman building?*

Sub questions:

- Which problems could be found by implementing continuous commissioning?
- Can model predictive control maintain the ATES balance?

The focus of this research is the development of the reference model, which is the most essential and challenging part.

## 1.4 RESEARCH STRUCTURE

As introduced, this thesis contains two main parts: model development and model application. The main structure is shown in Figure 1-5.

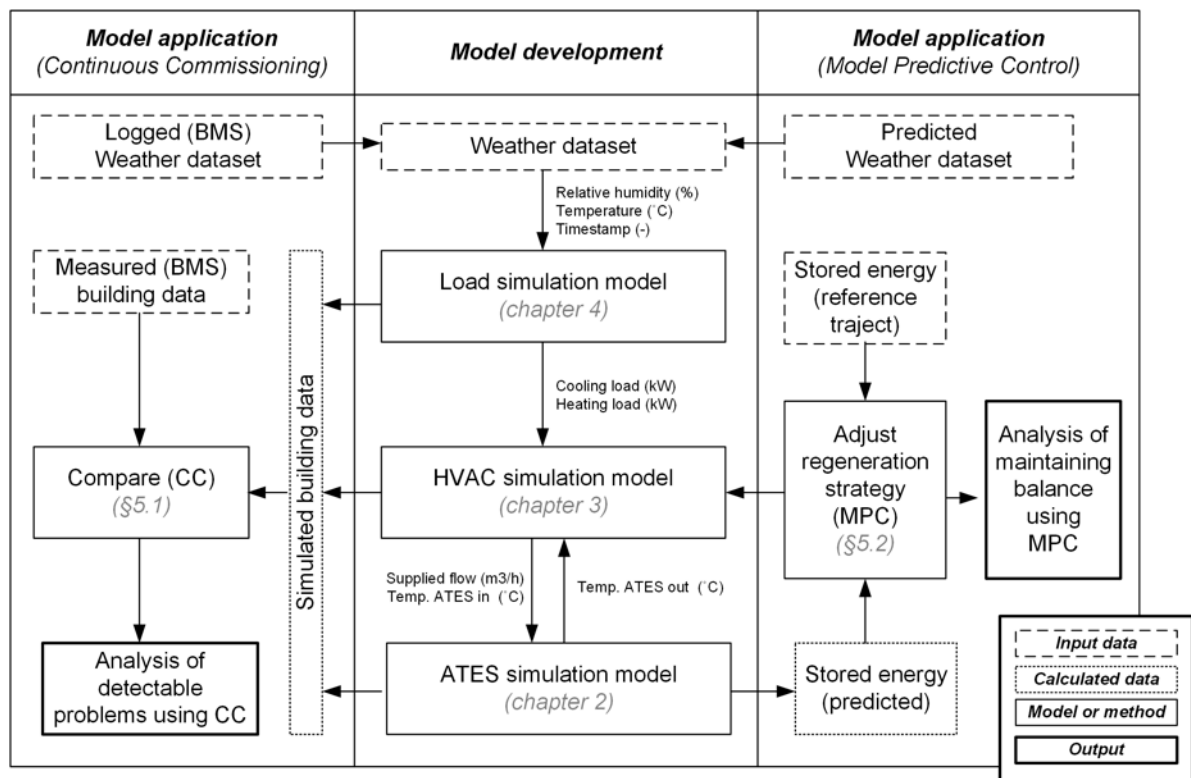


Figure 1-5 - Main thesis structure

### 1.4.1 MODEL DEVELOPMENT

To introduce the structure of the developed reference model, only the center column of Figure 1-5 is relevant. The complete reference model is based on three separate models:

1. The **load simulation model** calculates the heating and cooling loads using the weather data as input.
2. The **HVAC simulation model** calculates which flows and temperatures are supplied to the ATES as function of the calculated loads and weather conditions.
3. The **ATES simulation model** calculates the temperature that is supplied back to the building and how the thermal energy is stored in aquifer.

The models are introduced in the reverse order, because this makes it easier to understand how the parts are connected and why certain methods are used.

#### ATES SIMULATION MODEL

In chapter 2 the used ATES model is introduced. A method is presented to simulate the aquifer temperature distribution. Using this method the model can calculate how much energy is stored in the ATES wells and what the expected extraction temperature is. Additional methods are presented to analyze the performance of the well pumps and the heat exchanger. Using a final method that simulates the control software, the entire combination of storage wells, pumps and heat exchanger is simulated. The total model can calculate the outgoing temperature as function of the ingoing temperatures and flows and simultaneously model the effect on the temperature distribution in the storage wells.

#### HVAC SYSTEM SIMULATION MODEL

Chapter 3 introduces the configuration of the buildings HVAC system, how it is operated (the states) and the main components. The system is analyzed from the ATES point of view. All components that do not directly influence the ATES system are left out or simplified using assumptions. The chapter contains three methods to simulate the air-handling unit, the local cooling systems and the heat pump. The focus of these methods is to predict the component behavior mainly based on BMS data, instead of the manufacturers specifications. Using this method, the model can be implemented very easily and eventually monitor or adjust to changing performance over the years.

#### LOAD SIMULATION MODEL

Chapter 4 introduces the developed method to predict how cooling and heating loads are distributed over the buildings HVAC components. Again the modeling methods are based on BMS data to make the model as realistic as possible. It also provides the opportunity to easily readjust the model if parts of the building are not in use. The chapter ends with how the combination of heating curves and load curves influences the selection of system states.

### 1.4.2 MODEL APPLICATION

Chapter 5 analyses the two applications of the reference model, as showed in the left and right column of Figure 1-5. First continuous commissioning is analyzed by comparing the simulated data with the actual building data. Deviating results are analyzed and the hardware or software related causes are named.

The second part of chapter 5 presents the used MPC method for adjusting the regeneration strategy. The method simulates how a predefined storage target can be reached during the reference winter dataset and adapts to the energy stored during the actual winter. A 20-year simulation is performed to analyze if the system is capable of maintaining the energy balance in the ATES.

## 1.5 CASE STUDY INTRODUCTION

The developed model is based on a case study on the office of Kropman in Utrecht. Kropman is a large HVAC installation company ( $\pm 800$  employees) in the Netherlands with a broad experience on installation, manufacturing, design and ICT solutions. The office in Utrecht houses approx. 150 employees. The building is constructed in 2004 and has a GFA (gross floor area) of roughly 5500 m<sup>2</sup>, which is a typical size of a Dutch office building [15]. The GFA is divided in 3300 m<sup>2</sup> office space and 2200 m<sup>2</sup> for storage, restaurant, entree hall and other general spaces. The building has two wings, both holding 4 floors, which are separated by a large atrium. The atrium is closed in by the wings and two towers containing staircases, elevators, toilets and the majority of the technical installations. The wings contain large open offices with small (meeting) rooms and offices at both ends. Figure 1-6 shows a photo impression of the building.

The building is constructed using the industrial, flexible & demountable (IFD) building method. Buildings constructed with the IFD method are constructed with straightforward industrial methods as a bolted steel frame and prefab concrete floors. The design is based on large open floors without any internal walls. This makes the buildings highly flexible in their use and easy to readjust to future needs.

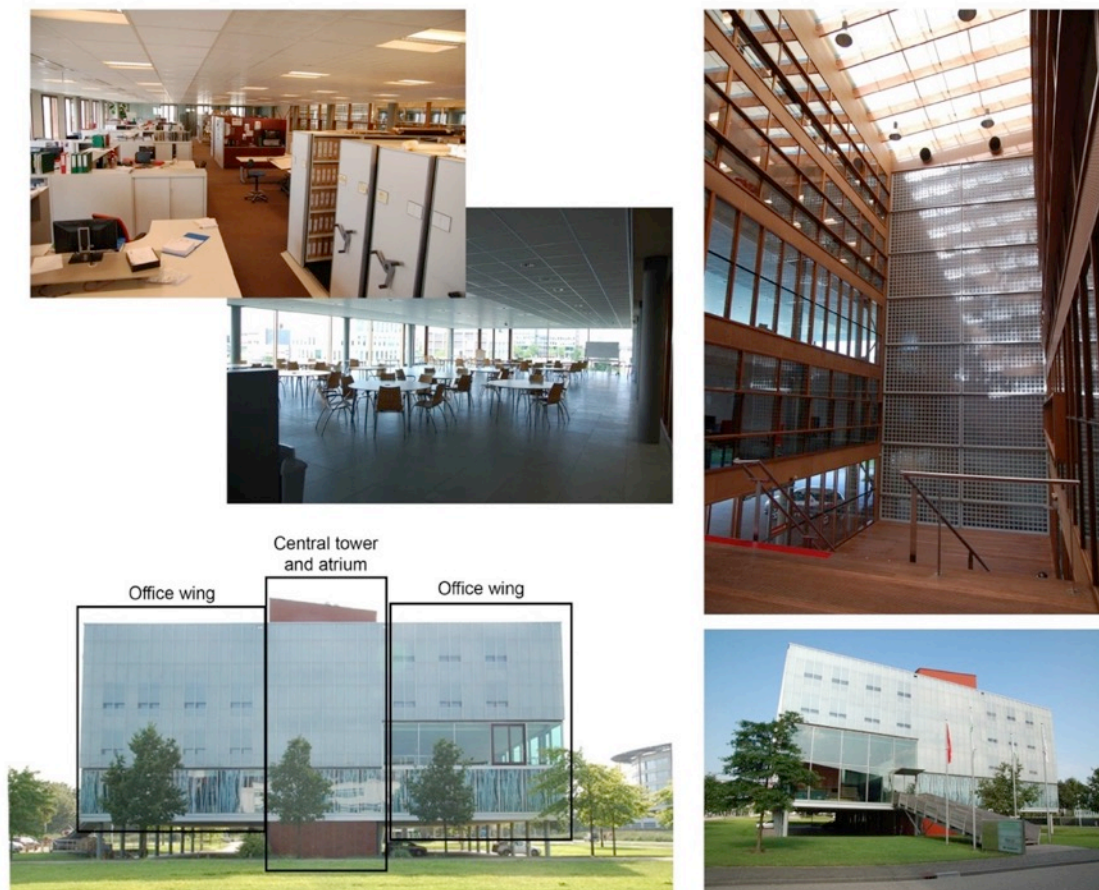


Figure 1-6 - Impression of the Kropman Utrecht office (offices, restaurant, atrium and outside view)

The building is equipped with a building management software (BMS) system, InsiteView, which logged most flows, temperatures, pressures, valve settings, setpoints and energy uses of the systems since its commissioning in 2004. Around 500 values have been logged every 8 minutes since then. In total the BMS has a dataset of about 250 million data points. Because the building systems are managed by the company itself, there are possibilities to adjust settings and perform tests and manual measurements.



## 2. ATES SYSTEM MODEL

---

This chapter describes the modeling of the ATES system and includes all components that are inseparably connected to the energy storage process. The chapter starts with an introduction of the system, the problem description and an overview of the used methods. Next the three required methods are introduced to simulate the complete ATES system.

### 2.1 INTRODUCTION

The used mono-well system is the GT-15, which is developed and installed by GeoComfort, a specialized company in ATES systems. The GT-15 is a so-called 'Turn-key' ATES system. It is installed as complete integrated solution containing the well, groundwater pumps, heat exchanger, valves, electric hardware and a software system to control the components. First the hardware is introduced followed by the modeling methods of this chapter.

#### 2.1.1 MONO-WELL HARDWARE

The mono-well is constructed using two connected pipes, which form the outer structure of the well. The upper part has a diameter of 0.8 meters and houses the heat exchanger and the valves. The lower part has a diameter of 0.5 meters and houses the two well pumps (schematic overview in Figure 2-1). This pipe contains two filters at the depth of the storage aquifers to prevent sand entering the pumps and water circuit. The entire construction of heat exchanger, valves, pipes and pumps is suspended in the well. Figure 2-2 shows a photo of the actual equipment lifted by a crane during maintenance at the lower well pump (not visible).

The main distinctive feature of a mono-well is the complete system of pumps, valves and heat exchanger operates below natural water level. This way of constructing an ATES system has two advantages. Technically the groundwater is never 'pumped up', because the entire process is operated below groundwater level. This simplifies a lot of permit application procedures and also avoids problems with groundwater protection regulations. Secondly, it does have the advantage that the groundwater system is kept under pressure. Because the water pumped from a depth of 50 meters is stored under high pressure, it will release gas when it is depressurized. Below groundwater level the surrounding water pressure prevents this depressurization.

During well drilling the extracted material is analyzed and recorded in the drilling report [16]. The revealed ground structure is shown in Figure 2-1. The yellow layers are sand layers containing the aquifers and the brown layers are the impermeable clay layers that separate the aquifers. The warm and cold storage aquifers are separated by two thin (one meter) clay layers. It could be possible the layers disappear a few meters further away from the well, which causes water flows between the warm and cold well (so-called interference). The drilling report does not provide information about a possible clay layer below the well to seal the lower end of the aquifer. Using a database of ground profiles provided by the Dutch government [17], all surrounding (<1000 meter distance) measurements show a clay layer at 60 meters depth. It is assumed that this layer is also present below the case study well.

The mono-well system has two operation modes; heating and cooling. The water supplied by the building can vary roughly between 5°C and 25°C. The systems software is designed to return this water with a (setpoint) temperature of 12°C, flowing in the same (clockwise) direction. Therefore, the supplied heating or cooling capacity depends on the supplied  $\Delta T$  (deviation from 12°C) and flow rate. The systems software adjusts the extracted warm or cold water flow to reach 12°C.

The valves between the well pumps and heat exchanger ensure the water is always flowing in the same direction through the heat exchanger. Using this method the heat exchanger is used in

counter-flow configuration, which is the most effective way for heat exchange. Table 2-1 introduces the variables of this simulation part. The flow and temperature variables are coded from the heat exchanger point of view; using subscript 'a' for aquifer side, 'b' for building side, 'in' for the incoming stream and 'out' for the outgoing stream.

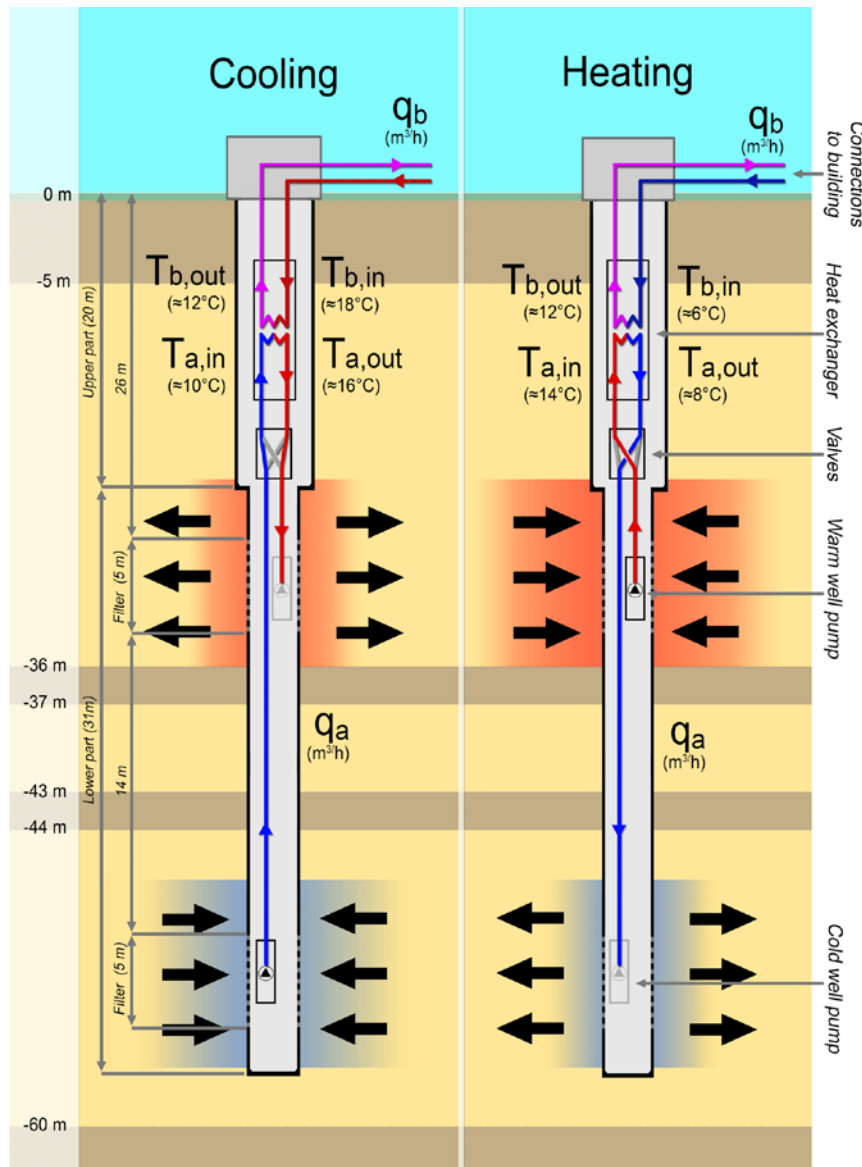


Figure 2-1 – Schematic overview mono-well in heating and cooling mode

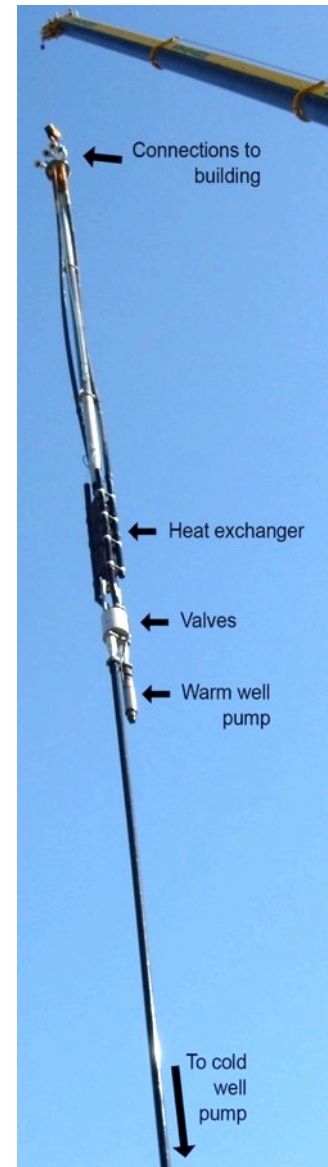


Figure 2-2 - Picture of ATES installation lifted by a crane

| Variable    | Unit   | Measured? | Description   |
|-------------|--------|-----------|---|
| $T_{a,in}$  | [°C]   | No        | Water temperature, aquifer side in (extracted groundwater)          |
| $T_{a,out}$ | [°C]   | No        | Water temperature, aquifer side out (injected groundwater)          |
| $q_a$       | [m³/h] | No        | Water flow, aquifer side (controlled by well pump)                  |
| $T_{b,in}$  | [°C]   | Yes       | Water temperature, building side in (supplied from building system) |
| $T_{b,out}$ | [°C]   | Yes       | Water temperature, building side out (returned to building system)  |
| $q_b$       | [m³/h] | Yes       | Water flow, building side (controlled by building systems)          |

Table 2-1 – Variables in ATES system

### 2.1.2 GENERAL SIMULATION METHOD

The main challenge of this simulation part is created by absence of sensors to measure or log data in the groundwater part of the system. The only data known is the percentage of power on which the well pumps are operating ( $\eta_{\text{pump}}$ ), but this value does not provide any direct information without knowing the corresponding flow curve. In essence the goal of this chapter is to model the behavior of the ATEs system, without having any measurements of the groundwater system at all.

To create a simulation model of the complete ATEs system three methods are developed as shown in Figure 2-3.

**Method 1** is the method for the ATEs simulation (so only the aquifer storage part) based on data of extracted and injected water data. This data is not available but will be calculated in method 2. This method is explained in section 2.2.

**Method 2** is the method to calculate the heat exchanger and well pump characteristics. Using this method the injected and extracted water temperature data for the ATEs model (method 1) can be calculated. The method uses all available data logged in the building management system. This method is explained in section 2.3.

**Method 3** is the method in which the logged well pump data is replaced by the simulation of the control software. Using this method the return temperature to the building ( $T_{b,\text{out}}$ ) can be predicted. In the final model the HVAC part (chapter 3) calculates the supplied flow ( $Q_b$ ) and temperature ( $T_{b,\text{in}}$ ) and this method calculates the return temperature. The method is explained in section 2.4

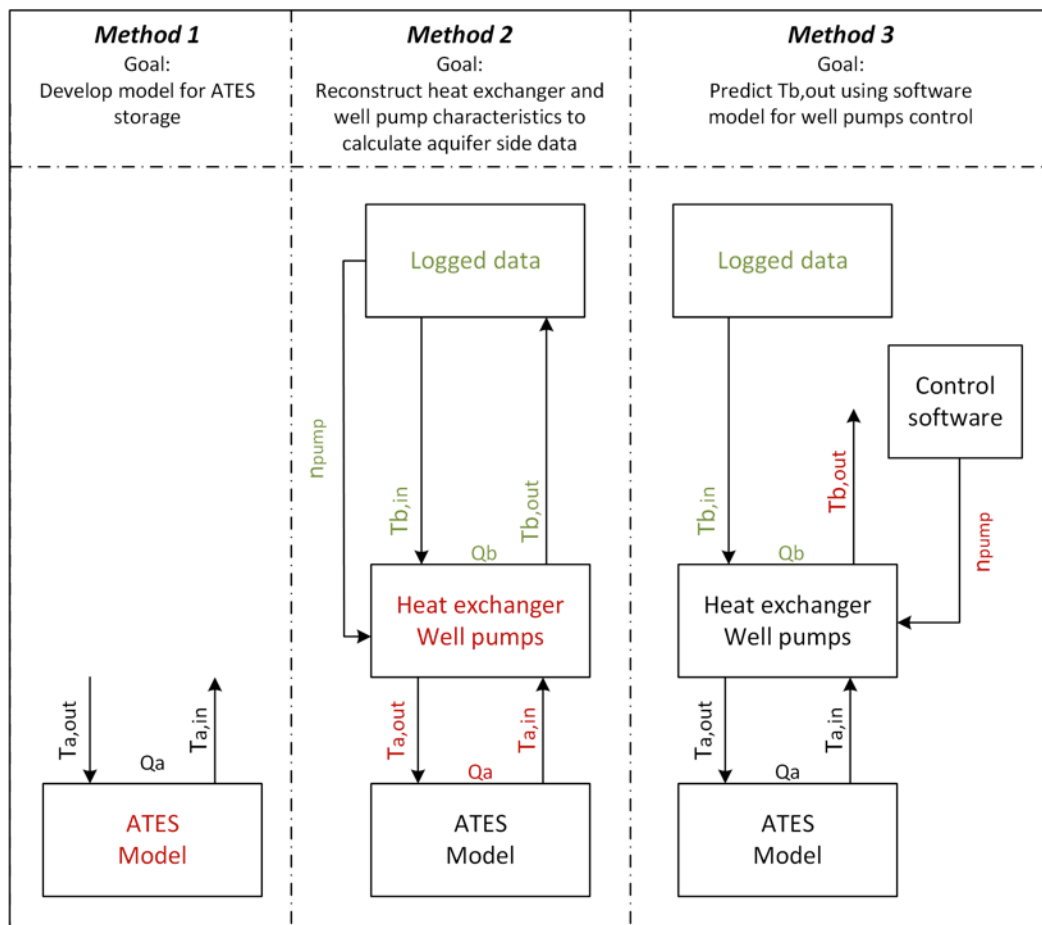


Figure 2-3 - ATEs modeling methods (goal = red, used data = green)

## **2.2 *AQUIFER SIMULATION METHOD***

This section introduces the aquifer simulation method. The goal of this method is to simulate the temperature distribution in the aquifers (and thereby the expected extraction temperatures), as function of the injected water temperatures. This is essential for both the 'bookkeeping' of the stored energy as well the behavior of the coupled components. It first explains why a new simulation method is chosen on top of all existing methods, next the calculation method is explained and finally the model is validated.

### **2.2.1 *INTRODUCTION***

For the simulation of ATEs systems a large variety of methods and software tools is available. To explain why a new method is developed for this research first an analysis of requirements and existing methods is made. The main requirements for the method are:

- A final (long term) goal is to implement the model in the building management software for the automated monitoring. For this reason specialized commercial (/closed source) simulation software is far from ideal to be used.
- The methods 2 and 3 need the output from the aquifer simulation and vice versa. For this reason it is highly preferred that both models are simulated in the same simulation software. For the research process preferably MATLAB is used and for future implementation the methods must be translatable to a generic software language.
- Because all logged data points since commissioning (650.000 measurements) should be included in the simulation to derive the correct aquifer temperature distribution profile, the method must be quite fast.
- For the iterative solving of the problem, the complete 650.000-point dataset must be evaluated numerous times. This requires an even faster simulation tool to create a practical method.

These requirements do narrow the possibilities for an appropriate tool significantly. Roughly, there are three methods to simulate the ATEs:

1. Use of open source simulation software with a 'bridge' to MATLAB. An example can be the combination of MODFLOW [18] and MFLab [19]
2. Use of a model that is developed natively in MATLAB, like MaxSym [20]
3. Development of a new lightweight simulation model designed specifically for mono-well ATEs systems.

Option 1 is not a realistic method, because there should be a continuous data exchange between both programs by exporting and importing data via data files. Even if this only takes a tenth of a second, the processing of the complete dataset will add over a 1000 minutes to the total calculation time. Option 2 is a safe choice, but uses a variety of MATLAB specific functions that would be difficult to transfer to another software language. Based on this analysis, it was worth a try to develop a new method using only the bare essentials needed to simulate the ATEs. The next section analyzes which aspects should be simulated for this model.

### **2.2.2 *AQUIFER SIMULATION ASPECTS***

A study on aquifer simulation methods reveals a large variety of research fields that are studying groundwater behavior. It is not only studied to evaluate ATEs systems, but also for example pumping of drinking water [21], [22], contamination spreading [23], seawater intrusion [24] and high temperature heat storage [25]. Although they are studying the same area, the different goals justify different simplifications. Furthermore, the geological structure can make a huge difference. Simulation of groundwater behavior in anisotropic mountainous terrain is more complicated than the isotropic flat structure of the Dutch aquifers. To establish which aspects are essential for the

simulation, an analysis of the case study mono-well is done, followed by an analysis of the best simulation grid.

### *SELECTION OF ESSENTIAL SIMULATION ASPECTS*

To make a profound assessment on which simplifications are allowed for the simulation of the aquifer used by the Kropman mono-well, an analysis of the main aspects in groundwater simulation is done.

#### **1) Natural groundwater flow**

Natural groundwater flow is caused by a difference in the natural groundwater level, called the hydraulic head. As always in nature, a fluid flows from the highest hydraulic head to the lowest causing natural flow. The differences in hydraulic head can be caused by varying rainwater infiltration or by height differences (mountains). At the Kropman mono-well location the slope in hydraulic head is 13.3 cm/km [26]. Using the hydraulic conductivity of 27 m/day derived in [27], the average natural flow can be calculated at 1.3 meter/year. The storage well area is spread out over an area with a much larger diameter, therefore the effect of groundwater flow is negligible.

#### **2) Hydraulic head variation due to well pumping**

When a considerable amount of water is extracted from the aquifer, the hydraulic head will decrease significantly because of a 'water shortage' in the pumping zone. For (drinking) water extraction this subsoil water level can drop several meters, making the pump work harder to extract the same amount of water and influencing the flow direction. In the GeoComfort mono-well the flows are relatively small (<20 m<sup>3</sup>/h) [28] and not continuous. This causes only a drawdown of less than a meter [29] and does not have a significant influence.

#### **3) Flow induced water mixing**

During injection and extraction of groundwater, different chemical compositions of groundwater are mixed. For example in mono-well ATEs systems, water from a deep aquifer (containing higher amounts of salt) is mixed with water from a less deep aquifer [27]. Although this is an interesting effect, it is highly unlikely to influence the performance of the ATEs and thus is not much of interest for this application.

#### **4) Flow induced temperature mixing**

When warm water is injected in a colder aquifer, the thermal energy in the water mixes with the existing water and the aquifer sand to reach a new equilibrium temperature. The mixing of different temperature water flows is obviously one of the main processes that determine the temperature profile of the aquifer.

#### **5) Buoyancy effects**

Warm water has a lower density than cold water and has the tendency to flow upwards. As investigated in [30] this has a quite significant effect when injecting water of 50 to 90°C. Using water of 30°C the effect is hardly visible. The injected water temperature of the mono-well is around 18°C so the effect is assumed to be negligible.

#### **6) Conduction**

Thermal energy storage in an aquifer will require temperature differences between the stored water and the surroundings, which will inevitably lead to conduction losses. Although the temperature differences are relatively small, water and clay are also not very good insulators. This makes conduction also an important factor in ATEs simulation.

### **Overview**

One can conclude that the main aspects to simulate ATEs behavior of the case study are temperature mixing and conduction. The model developed in this research is only applicable to similar cases justifying equal assumptions. It is not applicable, for instance when higher temperature differences are used or when there is a significant natural flow.



## SELECTION OF SIMULATION GRID

The most common method to simulate the thermal distribution in an aquifer system is to use a finite element simulation. Crucial in the efficiency of design of such a simulation model is the selection of an appropriate grid capable of simulation the essential phenomena. The lowest number of elements will give the fastest model, but can also reduce accuracy. The use of symmetry or reducing dimensions can make the model made faster while sustaining the same accuracy. A selection of commonly used grids is evaluated on their ability to model:

- Radial flows (due to injection or extraction)
- Vertical flows (due to injection in partially penetrated aquifers or buoyancy)
- Horizontal flows (natural groundwater flow)
- Interference between axial aligned wells (mono-well configuration)
- Difficulty of implementation in building management software

To give an indication of the grid calculation speed, an element number will be given based on a 2 meter grid spacing, 50 meters horizontal range (from well) and 40 meters aquifer thickness. Table 2-2 shows the various possible simulation grids that are commonly used for ATEs simulation.



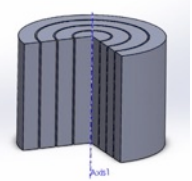
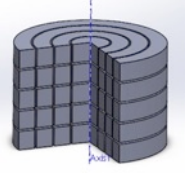
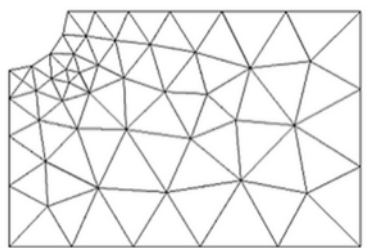
| <b>2-D Cartesian (top-down)</b>   |   | <b>3-D Cartesian</b>  |   |
|---|---|---|---|
| <p>This grid maps the temperature distribution in a square grid from a top-down view. This is an ideal grid to model interference between multiple horizontal distributed wells and to simulate the effect of natural groundwater flows. Simulation of vertical flows or vertical interference is not possible.</p> <p>[Element indication: 2.500]</p>  |   | <p>This grid adds the vertical dimension to the 2-D Cartesian grid using cubic elements. All effects can be simulated (although radial flows are a more difficult). The downside is the number of elements, which makes the model very slow and harder to implement.</p> <p>[Element indication 50.000]</p> |   |
| <b>1-D Axisymmetric</b>   |   | <b>2-D Axisymmetric</b>   |   |
| <p>This grid simulates a series of hollow cylindrical volumes around the injection well. It can only model radial flows. This model is very easy to implement.</p> <p>[Element indication: 25]</p>  |  | <p>This grid adds a vertical dimension to the 1-D axisymmetric grid. This enables the grid to model vertical flows and interference. Groundwater flow cannot be modeled because this is not a vertical or axisymmetric flow. This model is easy to implement.</p> <p>[Element indication: 500]</p>          |  |
| <b>Polygon mesh grid</b>  |   |    |   |
| <p>A polygon mesh grid is used in specialized software (like Comsol) and uses elements of different sizes and shapes. The smallest elements will be used at the area close to the well and they will become gradually larger at distance. This grid allows all effects to be modeled, but is almost impossible to implement in building management software without specific knowledge.</p> <p>[Element guess &lt;50.000]</p> |   |   |   |

Table 2-2 - Various grids for finite element simulation

### Schematic overview

In Table 2-3 an overview is given of the grids. It is clear that axisymmetric models have the advantage of low element numbers by reducing one dimension using symmetry. The axisymmetric models can simulate radial flow and interference quite simple. The downside is the lacking possibility to simulate the natural flow. The alternatives (the Cartesian grids) perform better at this field, but are performing worse at element numbers (speed). Because natural flow is negligible, the 2-D axisymmetric grid seems to be the best choice.

|                | Cart. (2D) | Cart (3D) | Axisym. 1D | Axisym. 2D | Polymesh |
|----------------|------------|-----------|------------|------------|----------|
| Radial flow    | +/-        | +/-       | ++         | ++         | +        |
| Vertical flow  | --         | ++        | --         | ++         | +        |
| Natural flow   | ++         | ++        | --         | --         | +        |
| Interference   | --         | ++        | --         | ++         | +        |
| Elements       | 2.500      | 50.000    | 25         | 500        | <50.000  |
| Implementation | +/-        | -         | ++         | +          | --       |

Table 2-3 - Assessment of simulation grids

### 2.2.3 AQUIFER SIMULATION METHOD THEORY

There are three sub-methods needed to make this method work. First a method is needed to calculate the flow patterns in a 2D-axisymmetric grid. Next a method is needed to calculate the effect of water mixing with the sand and finally a method to calculate the conduction between the elements. These methods are introduced in this section.

#### CALCULATION OF FLOW PATTERN

A large advantage in the use of an axisymmetric grid (and the neglecting of the horizontal groundwater flow) is found in the fact that the flow pattern can be simplified to a 2D model. A 2-dimensional water flow problem can be solved by calculating the streamlines. Although the water is not flowing freely (in for example a shallow water tank) but through a porous sand structure, the method is still applicable. The sand increases the pressure drop uniformly in all directions, so it does not affect the flow direction.

The streamline method is based on the intuitive fact that water will always try to evenly spread out its flow velocity pattern. When this pattern is not averaged out, the velocity differences will create pressure differences. Because water flows always from a higher pressure to a lower pressure, these differences are again directly averaged out. The method is illustrated by Figure 2-4 from (and further explained in) *Fluid Mechanics* [31]. In the left figure the boundary values are set. Streamline 0 and 5 follow the impermeable lower and upper boundary, the others are evenly spread between the other grid points on the open left and right end. By iteratively calculating the average of the four neighbors for the other (non boundary) grid points, the streamline distribution can be derived (the right figure).

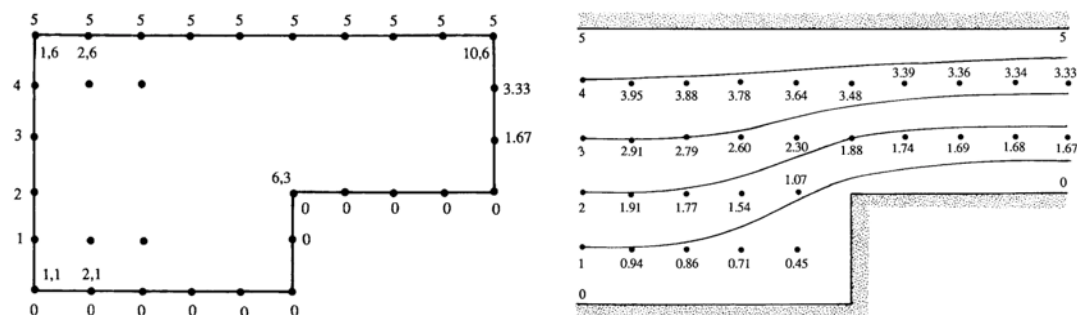


Figure 2-4 - Streamline calculation method (from [31])

$$U_r = -\frac{\partial \psi}{\partial z} \quad \text{and} \quad U_z = \frac{\partial \psi}{\partial r} \quad (2.1-2.2)$$

$$U_r = -\frac{\partial \psi}{\partial z} \quad \text{and} \quad U_z = \frac{\partial \psi}{\partial r} \quad (2.1-2.2)$$

**Figure 2-6 - Streamline method - Averaging method**

Figure 2-8 - Streamline method – Calculated flows

Page | 17

### AQUIFER WATER MIXING

When water flows between grid elements, the amount of energy transported depends on the transported amount of water and temperature difference between these elements. For each element the ingoing and outgoing energy is calculated using the flow patterns and the element temperatures calculated in the previous iteration (Figure 2-9).

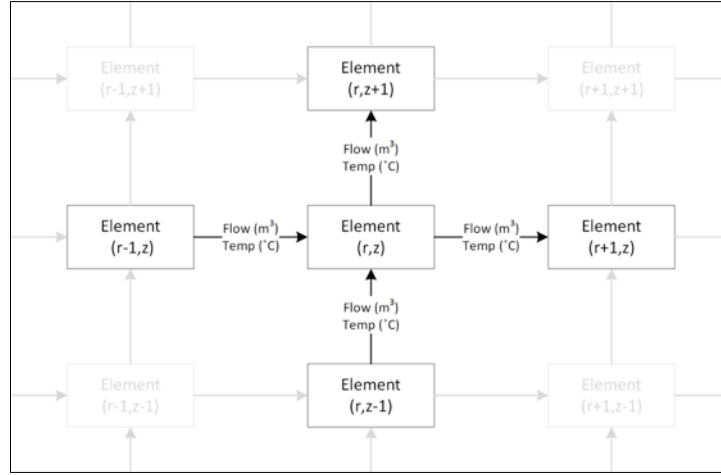


Figure 2-9 - Energy flow between grid elements

The new temperature can be calculated using an energy balance (equation 2.3). The equation calculates the original energy content of the element, sums the energy content of all ingoing flows, distracts the outgoing flows and calculates the new temperature based on the new element energy content. The energy content of the flow is calculated by multiplying the flow ( $Q_{in}$ ), temperature ( $T$ ), timestep ( $t$ ) and volumetric heat capacity of water ( $C_{water}$ ). The variables used in this equation are shown in table 2.3.

$$T_{new} = \frac{T_{old} * V * C_{aqui} + \sum Q_{in,i} * t * T_i * C_{water} - \sum Q_{out,i} * t * T_i * C_{water}}{V * C_{aqui}} \quad (2.3)$$

| Variable       | Unit     | Description                                     |
|----------------|----------|---|
| $T_{old/new}$  | [°C]     | The old and new element temperature             |
| $V$            | [m³]     | Element volume                                  |
| $C_{aqui}$     | [MJ/m³K] | Specific heat capacity aquifer (sand and water) |
| $C_{water}$    | [MJ/m³K] | Specific heat capacity water                    |
| $Q_{out/in,i}$ | [kg/h]   | Water flow in/out element 'i'                   |
| $t$            | [h]      | Timestep of simulation                          |
| $T_i$          | [°C]     | Temperature of element 'i'                      |

Table 2-4 - Variables of equation 2.3

### AQUIFER HEAT CONDUCTION

For the heat conduction between the elements, a similar method can be applied. The transferred energy depends on the temperature difference, heat conduction and contact area between the elements. The contact area is calculated using equations 2.4 and 2.5 for radial ( $r$ ) and axial ( $z$ ) direction.

$$A_r = 2\pi n_r l^2 \quad (2.4)$$

$$A_z = \pi * (n_r l)^2 - \pi * ((n_r - 1)l)^2 \quad (2.5)$$

Using equation 2.6 the thermal resistance between two elements can be calculated. By summing the energy flowing in and out the element, the new temperature can be calculated (equation 2.7). The used variables are introduced in Table 2-1, except the ones that are already used in equation 2.3.

$$R_i = \frac{\lambda_i}{l} * A_i \quad (2.6)$$

$$T_{new} = \frac{T_{old} * V * C_{aqui} + \sum \frac{T_{old} - T_i}{R_i}}{V * C_{aqui}} \quad (2.7)$$

| Variable    | Unit              | Description                           |
|-------------|-------------------|---------------------------------------|
| $n_r$       | [-]               | Element number in radial direction    |
| $\lambda_i$ | [W/mK]            | Thermal conductivity between elements |
| $l$         | [m]               | Grid size (distance between elements) |
| $A_i$       | [m <sup>2</sup> ] | Contact area between elements         |
| $R_i$       | [W/K]             | Thermal resistance between elements   |

Table 2-5 - Variables of equation 2-4 to 2-7

## 2.2.4 ATES MODEL CONFIGURATION

In section 2.2.3 the general theory is introduced to model an ATES system using the streamline method. This section introduces the configuration to adjust this model to the mono-well system used at Kropman.

First the dimensions of the simulation grid are defined. The soil layers are based on the drilling profile used during construction of the well [16]. The grid is based on a grid size of 2 meters, which is empirically chosen. A smaller grid (1 meter) increases the calculation time with a factor 4 without improving accuracy. A larger grid size (5 meter) smoothens the short-term storage effects (during spring and autumn) too much because of the large volume of the first elements. Table 2-6 shows the used dimensions. The cold aquifer bottom and simulation depth are an estimate based on other (deeper) drillings in the close proximity, because they are not defined in the drilling profile. The simulation length is defined by analyzing at which radial distance there the thermal influence of the ATES is negligible according to the simulation.

| Variable                | Value [m] | Grid point |
|-------------------------|-----------|------------|
| Top warm aquifer        | 7         | 4          |
| Top filter warm well    | 25        | 13         |
| Bottom filter warm well | 31        | 16         |
| Bottom warm aquifer     | 35        | 18         |
| Top cold aquifer        | 45        | 23         |
| Top filter cold well    | 45        | 23         |
| Bottom filter cold well | 51        | 26         |
| Bottom cold aquifer     | 57        | 29         |
| Simulation depth        | 64        | 32         |
| Simulation length       | 60        | 30         |

Table 2-6 - Grid dimensions



Using the defined grid dimensions, the ideal flow pattern can be calculated (Figure 2-10). The constructed m-file is also capable of simulating interference flows (Figure 2-11). In order to realize this the boundary streamline values (as introduced in 2.2.3) are changed to allow an adjustable fraction of the streamlines going through the clay layer and the remainder via the aquifers. Because the pressure difference between both aquifers decreases with  $1/r$ , the streamlines are distributed with this ratio.

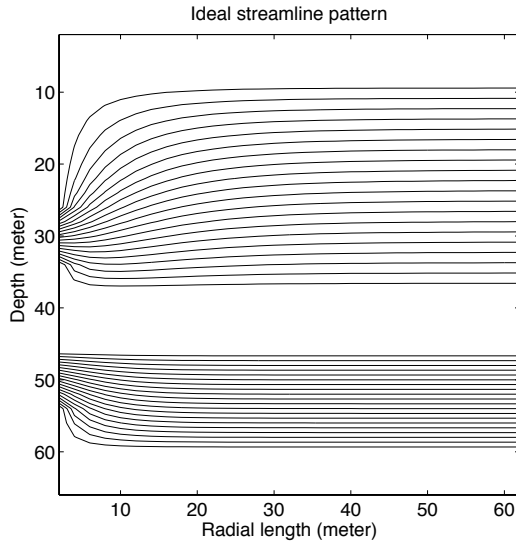


Figure 2-10 - Streamlines of ideal ATES

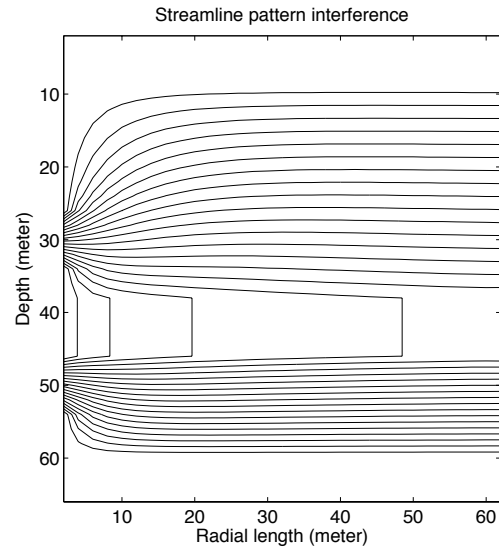


Figure 2-11 - Streamline pattern with interference

The calculation method introduced in section 2.2.3 needs three soil specific properties: the heat capacity of the various layers, the conduction between these layers and the natural temperature distribution. The used heat capacities and conductivities are based on a similar Dutch ATES system used for a research project [32] (Table 2-7).

| Description                    | Variable         | Value | Unit                  |
|--------------------------------|------------------|-------|-----------------------|
| Volumetric heat capacity water | $C_{H_2O}$       | 4.2   | [MJ/m <sup>3</sup> K] |
| Volumetric heat capacity sand  | $C_{sand}$       | 1.5   | [MJ/m <sup>3</sup> K] |
| Volumetric heat capacity clay  | $C_{clay}$       | 2.5   | [MJ/m <sup>3</sup> K] |
| Porosity aquifer               | $n$              | 0.35  | [-]                   |
| Conductivity aquifer           | $\lambda_{aqui}$ | 2.5   | [W/mK]                |
| Conductivity clay              | $\lambda_{clay}$ | 1.7   | [W/mK]                |

Table 2-7 - Heat capacity and conduction values [32]

The volumetric heat capacity of the aquifer layer can be calculated by using the ratio between water and sand (equation 2.8). For the conductivity between a layer of sand and a layer of clay the average conductivity is used.

$$C_{aqui} = n * C_{H_2O} + (1 - n) * C_{sand} \quad (2.8)$$

For the start of the simulation the natural temperature distribution is needed. This is the original distribution of temperatures over the grid elements before the ATES was used. The top layer of soil has on average the same temperature as the average yearly outdoor temperature, which is 10.4 °C [33]. For every 100 meter depth, the soil temperature increases with 2°C [32] as result of heat flowing from the core of the earth. The natural temperature as function of the depth ( $z$ ) is calculated using equation 2.9.

$$T_{nat} = T_{mean} + 0.02z \quad (2.9)$$

The last step is the definition of the boundary values of the temperature distribution as shown Figure 2-12. The conduction between the upper layer and the outdoor temperature is used to define the temperature of the first elements. For the lower layer a constant temperature based on equation 2.9 is assumed. The last vertical row of elements is defined by only calculating the effects in z-direction and is not influenced by radial (storage) effects. This row simulates the natural surrounding water temperature of the ATES.

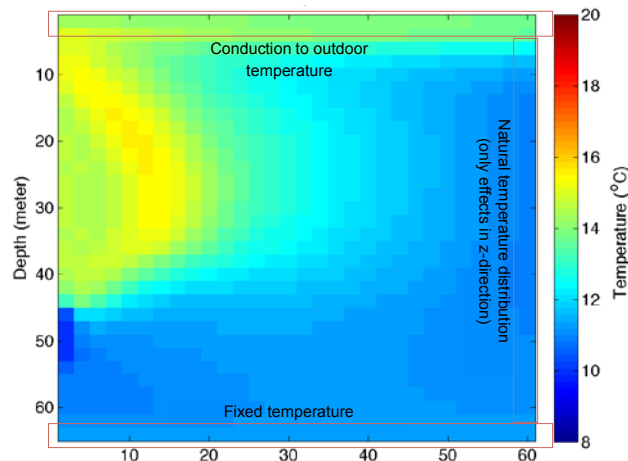


Figure 2-12 - Boundary values ATES temperature distribution

## 2.2.5 METHOD RESULTS

The best way to evaluate and validate the results of this method is to use a dataset of injection and extraction temperatures and compare them to the extraction temperatures predicted by the method. Because there are no aquifer side temperatures and flow data available, this is not possible for the case-study system. A dataset of another building (the ING-House in Amsterdam) is used to check the accuracy of the method. Although this is a doublet system (two separate wells) the calculation method is similar. To avoid confusion by introducing a different ATES configuration the simulation is presented in Appendix A. As shown in Figure 2-13 the results are in general accurate within  $\pm 0.2$  °C, except for a few deviations caused by start/stop cycles and low flow. If the ground water is not extracted continuously and at high flow, it exchanges heat to the surrounding soil and causes deviations in the measurements. The average accuracy is sufficient for this research. Simulation of these 5 years of data (300.000 values) takes roughly 30 seconds, which is suitable for the intended purpose.

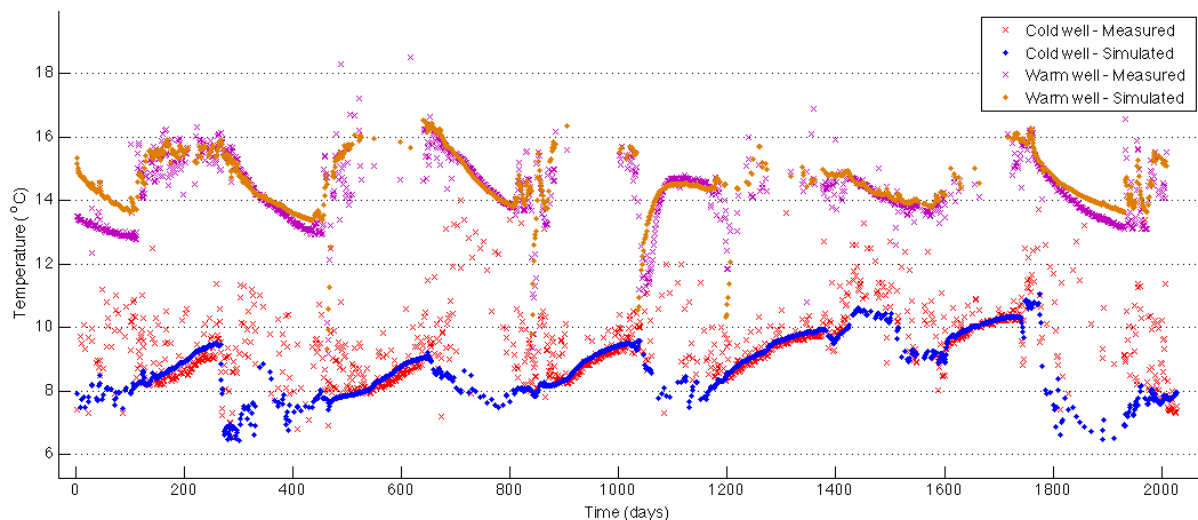


Figure 2-13 - ATES simulation results ING-House

## 2.3 AQUIFER SIDE DATA RECONSTRUCTION METHOD

The developed ATES model is only of use when the injection and extraction temperatures and flows are known. This section introduces the method how this data can be reconstructed. First the available dataset and the interpretation method is introduced. Next the reconstruction method and the corresponding calculation methods are presented. As result the reconstructed characteristics are presented and the accuracy is evaluated.

### 2.3.1 DATASET HANDLING

The building management software InsiteView has recorded the sensors monitoring the ATES system every 8 minutes since 2004. A short example of the dataset is shown in Table 2-8. Only the measured value at the sampling moment is stored, so no averaging or filtering is applied. An iteration of storing all values of the BMS takes around 5 minutes, so the values stored for the specific 'timestamp' are not recorded at the same moment. The storage order or time offset is not known. There are a few additional remarks on the dataset:

- The values 'Tb\_in', 'Tb\_out' and 'Qb' are directly logged by InsiteView and should be seen as reference. Although this is the most complete dataset, it has also unexpected values. As marked in **green**, 'Tb\_out' is higher than 'Tb\_in' while the other data suggests the system is continuously in cooling mode.
- The bits 'Heating' and 'Cooling' are also directly logged, but there is a delay between sending the bit and starting or stopping the well pump (as marked in **blue**).
- The pump percentage and current are logged by the GeoComfort controller and are extracted by InsiteView. Also those values do not always match each other, have a timestamp mismatch or are missing data due to data extraction errors). It is also unknown which pump (warm/cold well) is active (marked in **red**).
- The well pumps always start at 100% and slowly lower the flow to the required value. Those startup values are not representative of the effective groundwater flow (marked in **red**).

In short, there is data available about the well pumps operation, but this data should be used with great care and must be filtered for steady states based on the temperature and flow data. However, this data sample is an example of start/stop behavior. During continuously cooling (summer) or heating (winter) the data is more consistent.

| Timestamp      | Sensors     |            |           | Priva software    |                   | Geocomfort controller |            |
|----------------|-------------|------------|-----------|-------------------|-------------------|-----------------------|------------|
|                | Tb_out (°C) | Tb_in (°C) | Qb (m3/h) | Cooling state (-) | Heating state (-) | n_pump (%)            | I_pump (A) |
| 16-05-11 07:35 | 10.6        | 15.5       | 6.2       | 0                 | 0                 | 0                     | 0          |
| 16-05-11 07:43 | 10.8        | 15.4       | 6.3       | 0                 | 0                 | 0                     | 0          |
| 16-05-11 07:51 | 11.7        | 13.5       | 6.6       | 1                 | 0                 | 76                    | 3.23       |
| 16-05-11 07:59 | 12.8        | 13.0       | 6.6       | 1                 | 0                 | 30                    | 2.44       |
| 16-05-11 08:07 | 10.1        | 16.2       | 6.3       | 1                 | 0                 | 30                    | 2.44       |
| 16-05-11 08:15 | 10.7        | 15.2       | 6.3       | 0                 | 0                 | 30                    | 2.46       |
| 16-05-11 08:23 | 10.8        | 14.7       | 6.9       | 0                 | 0                 | 0                     | 0          |
| 16-05-11 08:31 | 12.0        | 13.3       | 7.3       | 1                 | 0                 | 90                    | 3.58       |
| 16-05-11 08:39 | 12.9        | 13.8       | 6.7       | 1                 | 0                 | 30                    | 2.46       |
| 16-05-11 08:47 | 9.9         | 15.7       | 6.8       | 1                 | 0                 | 30                    | 2.44       |
| 16-05-11 08:55 | 10.8        | 14.6       | 7.0       | 1                 | 0                 | 0                     | 0          |
| 16-05-11 09:03 | 11.1        | 14.6       | 7.8       | 0                 | 0                 | 30                    | 0          |
| 16-05-11 09:11 | 11.2        | 14.8       | 8.0       | 1                 | 0                 | 31                    | 2.46       |
| 16-05-11 09:19 | 11.3        | 14.6       | 7.9       | 1                 | 0                 | 30                    | 2.42       |
| 16-05-11 09:27 | 11.4        | 13.9       | 7.5       | 1                 | 0                 | 30                    | 2.44       |
| 16-05-11 09:35 | 13.3        | 12.9       | 6.9       | 1                 | 0                 | 30                    | 2.44       |
| 16-05-11 09:43 | 11.6        | 14.8       | 6.8       | 1                 | 0                 | 30                    | 2.46       |
| 16-05-11 09:51 | 10.2        | 14.4       | 7.4       | 0                 | 0                 | 30                    | 2.42       |
| 16-05-11 09:59 | 11.0        | 14.5       | 7.9       | 0                 | 0                 | 0                     | 0          |
| 16-05-11 10:07 | 11.3        | 14.7       | 8.1       | 1                 | 0                 | 100                   | 0          |
| 16-05-11 10:15 | 11.3        | 14.7       | 8.0       | 1                 | 0                 | 33                    | 2.48       |
| 16-05-11 10:23 | 11.2        | 14.7       | 8.0       | 1                 | 0                 | 30                    | 2.46       |
| 16-05-11 10:31 | 12.0        | 14.0       | 8.0       | 1                 | 0                 | 30                    | 2.42       |

Table 2-8 - Example of ATES dataset

To find out in which state the mono-well is operating, the building side flow data is filtered using these conditions:

- Cooling state is active if:
  - The building-side flow ( $q_b$ ) is  $> 2 \text{ [m}^3/\text{h]}$
  - The supplied temperature ( $T_{b,in}$ ) is  $> 12 \text{ }^\circ\text{C}$
  - The temperature difference over the ATES ( $T_{b,in} - T_{b,out}$ ) is at least  $1 \text{ }^\circ\text{C}$
- Heating state is active if:
  - The building-side flow ( $q_b$ ) is  $> 2 \text{ [m}^3/\text{h]}$
  - The supplied temperature ( $T_{b,in}$ ) is  $< 10 \text{ }^\circ\text{C}$
  - The temperature difference over the ATES ( $T_{b,out} - T_{b,in}$ ) is at least  $1 \text{ }^\circ\text{C}$
- Otherwise the system is in rest state and the data is ignored

For every time a heating or cooling state is started (after rest),  $0.8 \text{ m}^3$  is transferred between the wells to compensate for the full capacity well pump startup flows (as explained in Appendix B).

### 2.3.2 RECONSTRUCTION METHOD

For the modeling of the integrated mono-well system, three sub-models are needed:

1. A curve to relate the pump flow ( $q_a$ ) to the capacity percentage ( $n_{\text{pump}}$ ).
2. A curve to relate the building flow ( $q_b$ ) to the heat transfer function of the heat exchanger
3. The model of method 1 that models extraction temperatures ( $T_{a,in}$ ) of the ATES.

These three sub-models all have the problem they can only be calculated (1 & 2) or evaluated (3) when the other two are known. The method used in this part is based on iteratively comparing assumed characteristics with calculated characteristics. When the assumptions for all sub-models correspond with the calculated values (so an iteration of the three steps) without the need to adjust any assumption) the combination is assumed to be correct. There is no hard evidence that these are the actual characteristics, only that the combination of assumptions forms a solution to the problem. Because there are three 'unknowns', three calculation steps are needed to evaluate the assumed values. This section introduces the calculation structure. The required background and equations are introduced in the next section (2.3.3).

#### Step 1. Calculate well pump flow as function of the well pump percentage

The diagram in Figure 2-14 shows the structure of this first step. Using assumptions for the ATES groundwater model, the extracted water temperature ( $T_{a,in}$ ) is given. Using assumptions for the heat transfer coefficient and the logged building side water flow data,  $T_{a,out}$  and  $q_a$  is calculated. By plotting this groundwater flow ( $q_a$ ) as function of the well pump frequency ( $n_{\text{pump}}$ ), the flow function is derived. Also  $T_{a,out}$  and  $q_a$  are used as input for the ATES model, to calculate the new groundwater temperature distribution.

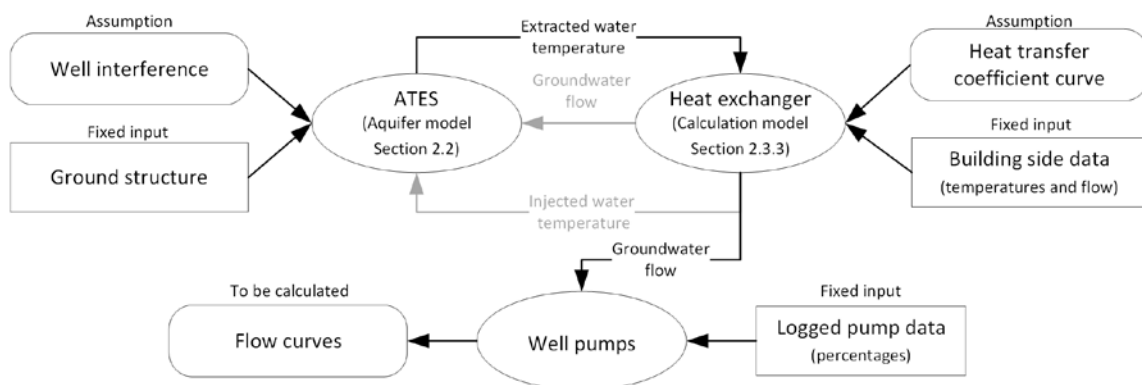


Figure 2-14 - Method to calculate groundwater flow

## Step 2. Calculate heat transfer coefficient

Figure 2-15 shows the structure used for step 2. Using the previously derived pump flow curve and the pump data (percentages) the heat transfer coefficient curve of the heat exchanger can be calculated. In first sight it may look like this method reconstructs the heat exchanger assumption (circular reasoning), because it uses the same groundwater flows. In reality however the groundwater flows calculated in the first step are very scattered. The well pump linearization produces much more realistic and accurate flow data. The goal of this step is to (iteratively) find the best match between flow characteristics and heat transfer coefficient. Every time the heat transfer coefficient is adjusted, the whole ATEs model must also be recalculated because it also influences the injection temperature.

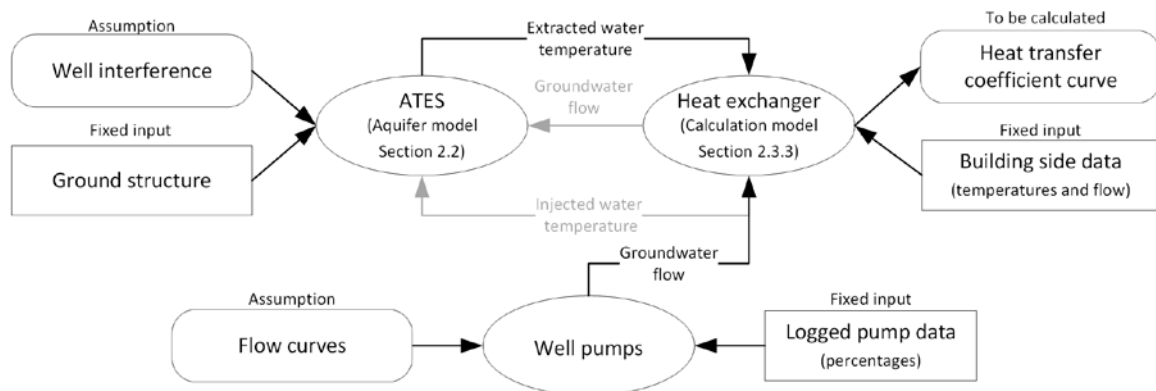


Figure 2-15 - Method to calculate the heat transfer coefficient

## Step 3. Evaluate ATEs groundwater model input

The third step is to use both the results of step 1 and 2 to reconstruct the extracted water temperature and compare it to the predicted extraction temperatures. Deviation at the start of the heating or cooling season can indicate a wrong calculated injection temperature (defined by the heat exchanger). Deviations at the end of the season (when storage is empty) can indicate the need to adjust the interference.

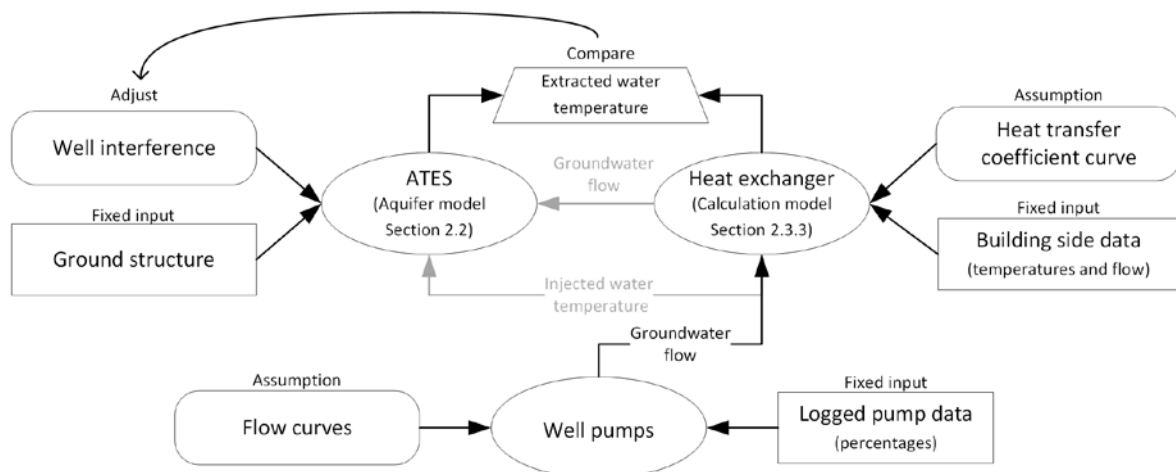


Figure 2-16 - Method to reconstruct extracted water temperatures

When in all three steps the calculated and assumed values match, a solution is found for the needed sub-models. Again, this is no guarantee to be the only possible and correct solution. However, if the method matches several years of historical data, it is likely that it will also match the future behavior.

### 2.3.3 CALCULATION METHODS

The reconstruction method is based on calculations on the heat exchanger. The heat exchanger used in the mono-well is a plate heat exchanger and is used in counter-flow configuration. This section introduces the fundamental physics of a heat exchanger and three calculation models for the steps used in the method.

#### HEAT EXCHANGER PHYSICS

The transferred heat in a heat exchanger can be described by two aspects: the temperature difference between both sides and the thermal conductivity or heat transfer function. The temperature difference is defined using the *logarithmic mean temperature difference* method (LMTD). The LMTD is calculated using equation 2.10, using the temperature difference at the warm side ( $\Delta T_w$ ) and the cold side ( $\Delta T_c$ ) (as in Figure 2-17).

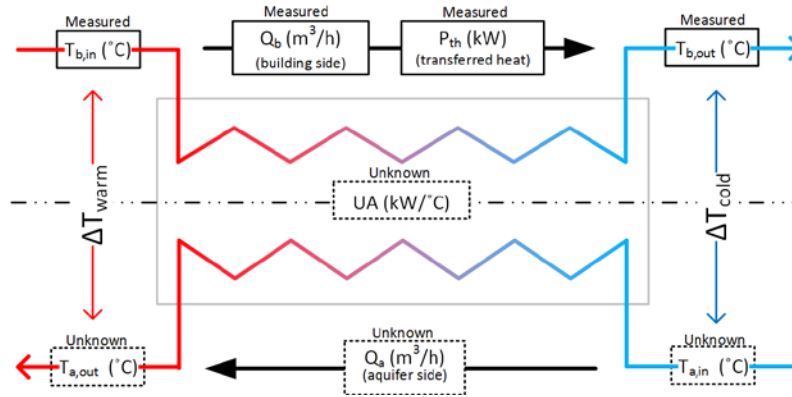


Figure 2-17 - Heat exchanger diagram

$$LMTD = \frac{\Delta T_{warm} - \Delta T_{cold}}{\ln\left(\frac{\Delta T_{warm}}{\Delta T_{cold}}\right)} \quad (2.10)$$

Using the LMTD, the transferred heat (kW) is calculated using equation 2.11. The unknown variables in this calculation are the thermal transfer coefficient (U) times the heat exchanger internal conduction area (A). The area (A) is a constant value and the transfer coefficient (U) is defined by equation 2.12 from [34].

$$P_{th} = LMTD * U * A \quad (2.11)$$

$$\frac{1}{U} = \frac{1}{h_{t,building}} + \frac{1}{h_{hex}} + \frac{1}{h_{t,aquifer}} \quad (2.12)$$

This equation shows the overall heat transfer coefficient is based on three components:

- $h_{t,building}$  Conductivity between building side water and heat exchanger material
- $h_{hex}$  Conductivity through the heat exchanger material
- $h_{t,aquifer}$  Conductivity between heat exchanger material and aquifer side water

The  $h_{hex}$  factor is a constant, depending on the material and thickness of the heat exchanger. The other two are depended on the *Reynolds* number. During turbulent flow (typical for plate heat exchangers) the Reynolds number is proportional to the fluid velocity [34]. So, the overall heat transfer function ( $U \cdot A$ ) is a function of the fluid velocity at both sides of the heat exchanger. Because the aquifer side flow is calculated using the UA-function, it would further complicate the method to include this flow in the calculation of the UA value. For that reason it is assumed that the aquifer flow is proportional to the building flow within a certain range (depending on software limitations introduced in section 2.4.1). This implies that the UA-function can be expressed as function of the building side flow.

## HEAT EXCHANGER SOLVING METHODS

As introduced in section 2.3.2, there are three methods needed to calculate or reconstruct the missing values for the ATEs model.

### Step 1. Calculation of injection temperature and flow

The first method is the method to calculate the aquifer side flow ( $Q_a$ ) and aquifer injection temperature ( $T_{a,in}$ ) as shown in Figure 2-18. All building side values are measured and assumptions are used for the UA value and the extraction temperature.

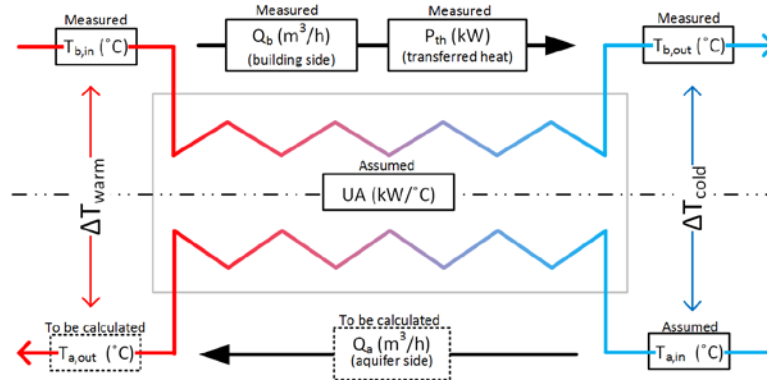


Figure 2-18 - Heat exchanger calculation - Method 1

Using equation 2.13 the LMTD is calculated and because the  $T_{a,out}$  is the only unknown in equation 2.10, this can be solved by rewriting equation 2.10 to equation 2.14. The resulting aquifer side flow is calculated using  $\Delta T_a$  and  $P_{th}$ .

$$LMTD = \frac{P_{th}}{UA} \quad (2.13)$$

$$T_{a,out} = T_{b,in} + LMTD * W \left( -e^{-\frac{\Delta T_{cold}}{LMTD}} * \frac{\Delta T_{cold}}{LMTD} \right) \quad (2.14)$$

In equation 2.14 the *Lambert W* function  $W(x)$  is used (  $Y = X * \exp(X)$  solves to  $X = W(Y)$  ) and is needed to solve the natural logarithm in equation 2.10. The Lambert W function has several branches of solutions, of which -1 and 0 are the primary solutions. As visible in Figure 2-19 the function is only continuous if switched between branches at  $x = (-1) * \exp(-1)$ . For equation 2.14, the following 'if-statement' is used:

- If  $\Delta T_{cold} > LMTD$  → Use the 0<sup>th</sup> branch
- If  $\Delta T_{cold} = LMTD$  → The solution if  $W(x) = -1$
- If  $\Delta T_{cold} < LMTD$  → Use the -1<sup>th</sup> branch

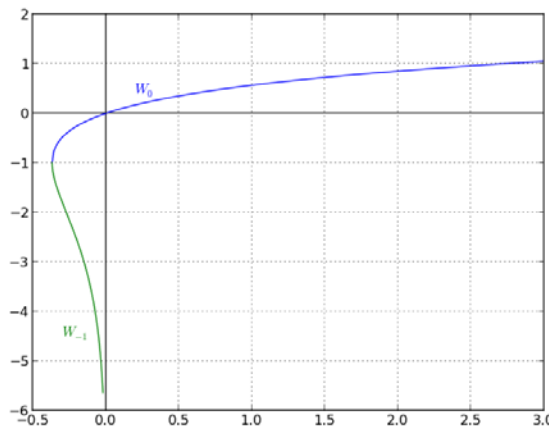


Figure 2-19 - Branches of the Lambert W function [35]



### Step 2. Calculation of UA factor

The calculation of the UA factor is done using the aquifer flow ( $Q_a$ ) calculated using the well pump percentages (Figure 2-20). Via the energy balance the temperature of the injected water ( $T_{a,out}$ ) can be calculated. Because now all temperatures are known, the LMTD can be calculated using equation 2.10 and the UA-value via equation 2.13.

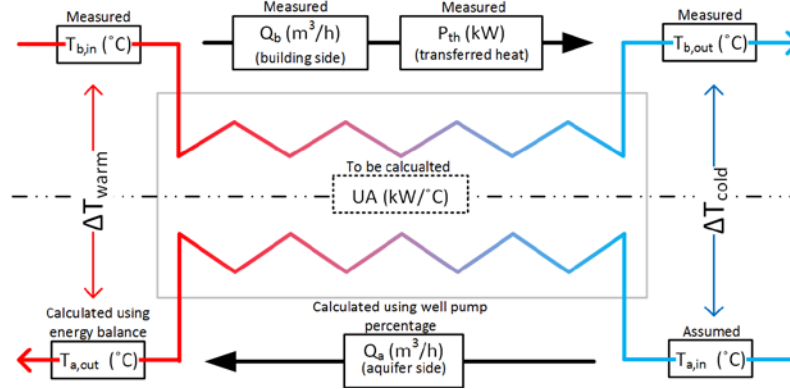


Figure 2-20 - Heat exchanger calculation - Method 2

### Step 3. Reconstruction of extracted water temperature

For reconstruction of the temperature of extracted water ( $T_{a,in}$ ) the flow is calculated using the well pump percentage (Figure 2-21). Because the flow and transferred heat are known, the temperature difference over the aquifer side ( $\Delta T_a$ ) can be calculated.

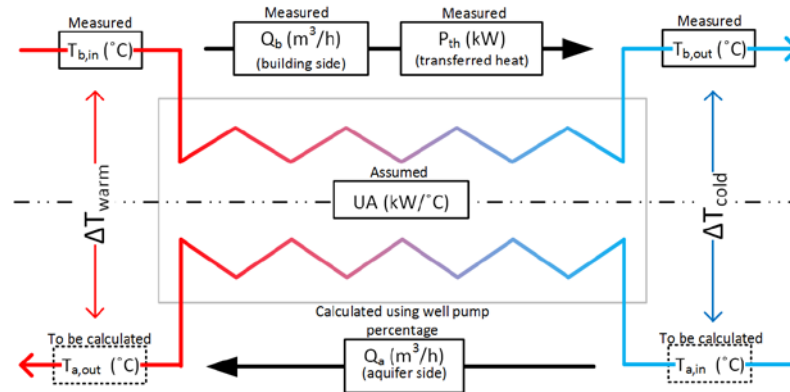


Figure 2-21 - Heat exchanger calculation - Method 3

Equation 2.15 and 2.16 prove that the difference between the warm/cold side  $\Delta T$  values equals the aquifer/building side  $\Delta T$  values. This difference is named  $\Delta T_{rel}$ , the relative temperature difference, and can be substituted in the LMTD equation (2.17) and solved to equation 2.18. Once  $\Delta T_{cold}$  is known, the other temperatures can be solved using energy balances.

$$\Delta T_b + \Delta T_{cold} = \Delta T_a + \Delta T_{warm} \quad (2.15)$$

$$\Delta T_b - \Delta T_a = \Delta T_{warm} - \Delta T_{cold} = \Delta T_{rel} \quad (2.16)$$

$$LMTD = \frac{\Delta T_{warm} - \Delta T_{cold}}{\ln\left(\frac{\Delta T_{warm}}{\Delta T_{cold}}\right)} = \frac{\Delta T_{rel}}{\ln\left(\frac{\Delta T_{cold} + \Delta T_{rel}}{\Delta T_{cold}}\right)} \quad (2.17)$$

$$\Delta T_{cold} = \frac{\Delta T_{rel}}{e^{LMTD} - 1} \quad (2.18)$$

### 2.3.4 DATA RECONSTRUCTION RESULTS

The results of this method are separated in five different parts. First the dataset interpretation is evaluated and a check on conservation of energy of the ATES model is done. Using these two steps it is possible to check if all measured stored energy is actually stored in the model. Next the results of the three steps of the explained iterative method are presented. A graphical overview of the calculated temperature ATES distributions is shown in appendix C.

#### DATASET INTERPRETATION

The GeoComfort control system continuously (approx. 10 seconds) reads the temperature and flow sensor values and calculates the stored energy. In Table 2-9 these yearly values from InsiteView (imported from the GeoComfort system) are compared to the stored energy amount reconstructed using the conditions stated in section 2.3.1. Clearly, the data cannot be reconstructed as accurate as the direct measurements. In the first two years there is data missing because of startup software problems, making 2004 and 2005 data not representative for actual behavior. In 2010 there were problems with the power supply to the cold well pump, which explains part of the cooling mismatch. Other deviations are probably caused by the start/stop cycles of heat pump, which cannot be accurately reconstructed using the 8-minute data.

| Year   | Cooling             |                     |                  | Heating             |                     |                  | Imbalance           |                     |                  |
|--------|---------------------|---------------------|------------------|---------------------|---------------------|------------------|---------------------|---------------------|------------------|
|        | InsiteView<br>[MWh] | Simulation<br>[MWh] | Deviation<br>[%] | InsiteView<br>[MWh] | Simulation<br>[MWh] | Deviation<br>[%] | InsiteView<br>[MWh] | Simulation<br>[MWh] | Deviation<br>[%] |
| 2004   | 105.0               | 179.4               | 41.5%            | 32.2                | 6.5                 | -395.4%          | 72.8                | 172.9               | 57.9%            |
| 2005   | 143.6               | 122.1               | -17.6%           | 86.4                | 108.4               | 20.3%            | 57.2                | 13.8                | -315.2%          |
| 2006   | 195.1               | 184.2               | -5.9%            | 72.8                | 78.8                | 7.6%             | 122.3               | 105.4               | -16.1%           |
| 2007   | 146.7               | 147.3               | 0.4%             | 82.6                | 80.5                | -2.6%            | 64.1                | 66.8                | 4.0%             |
| 2008   | 122.2               | 103.6               | -17.9%           | 77.1                | 58.5                | -31.8%           | 45.1                | 45.1                | 0.0%             |
| 2009   | 123.7               | 130.7               | 5.3%             | 89.1                | 76.1                | -17.0%           | 34.6                | 54.5                | 36.6%            |
| 2010   | 102.9               | 83.1                | -23.8%           | 146.4               | 141.7               | -3.3%            | -43.5               | -58.6               | 25.8%            |
| 2011   | 106.4               | 103.9               | -2.4%            | 81.4                | 77.6                | -4.9%            | 25.0                | 26.3                | 5.0%             |
| 2012   | 109.5               | 105.6               | -3.7%            | 83.9                | 76.6                | -9.5%            | 25.6                | 29.0                | 11.6%            |
| 2013   | 140.0               | 137.8               | -1.6%            | 102.7               | 95.8                | -7.2%            | 37.3                | 42.0                | 11.3%            |
| Summed | 1295.1              | 1297.8              | 0.2%             | 854.5               | 800.7               | -6.3%            | 440.6               | 497.1               | 12.8%            |

Table 2-9 - Comparison of simulated and monitored energy storage

#### CONSERVATION OF ENERGY IN THE METHOD

The second test is to compare the thermal energy transferred from the building to the heat exchanger with the energy stored in the ATES. A check on conservation of energy is applied to the total calculation method (from building side, via the heat exchanger to the storage system). To do this test, the conduction is assumed to be zero to ensure no energy is conducted to surrounding layers. The stored energy is analyzed by calculating the temperature difference between the natural temperature and the simulated temperature per element multiplied by the volumetric capacity. Table 2-10 shows the imbalances between injected and stored energy are almost the same, which is prove for the conservation of energy within the model.

| Year | Injected energy |               |                    | Stored energy |               |                    |
|------|-----------------|---------------|--------------------|---------------|---------------|--------------------|
|      | Heat<br>[MWh]   | Cold<br>[MWh] | Imbalance<br>[MWh] | Heat<br>[MWh] | Cold<br>[MWh] | Imbalance<br>[MWh] |
| 2004 | 179.4           | 6.5           | 172.8              | 172.6         | -0.1          | 172.7              |
| 2005 | 301.5           | 114.9         | 186.6              | 189.5         | 3.0           | 186.5              |
| 2006 | 485.7           | 193.7         | 292.0              | 294.1         | 1.5           | 292.6              |
| 2007 | 632.9           | 274.2         | 358.7              | 367.7         | 8.2           | 359.5              |
| 2008 | 736.6           | 332.7         | 403.9              | 408.8         | 4.1           | 404.7              |
| 2009 | 867.3           | 408.9         | 458.4              | 467.2         | 8.0           | 459.2              |
| 2010 | 950.4           | 550.6         | 399.8              | 429.9         | 29.2          | 400.6              |
| 2011 | 1054.3          | 628.2         | 426.1              | 448.5         | 21.6          | 427.0              |
| 2012 | 1159.9          | 704.9         | 455.1              | 476.7         | 20.8          | 455.9              |
| 2013 | 1297.8          | 800.7         | 497.1              | 514.3         | 16.3          | 497.9              |

Table 2-10 - Validation of ATES model energy conservation

## RECONSTRUCTION OF WELL PUMP CURVES

Using step 1 of this method the curves of the well pumps and heat exchanger are reconstructed. Figure 2-22 shows the curve of the cold (lower) well pump and Figure 2-23 shows the curve of the warm (upper) well pump.

The curves can be fitted using equation 2.19 and 2.20. All fits in this research are evaluated by the *coefficient of determination*, also known as  $R^2$ . The closer this value is to 1, the better the fit. Both curves start at 30% because this is the minimum pump capacity. Values below 30% are excluded from fitting, even as the 100% values they are clearly startup effects.

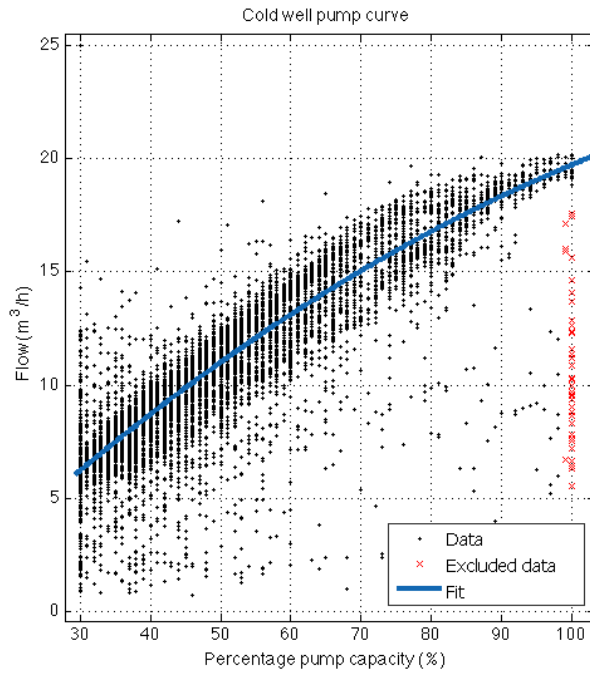


Figure 2-22 - Cold well pump

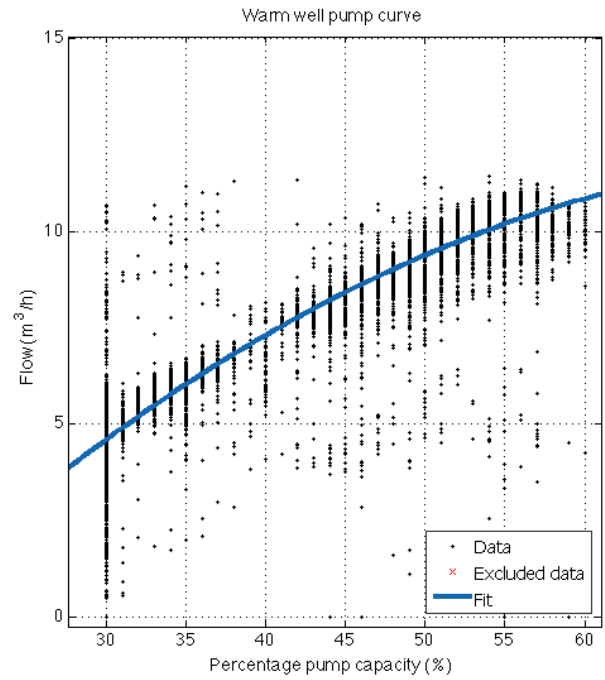


Figure 2-23 - Warm well pump

$$Q_{cold} = -9.2 \cdot 10^{-4} * x^2 + 0.312x - 2.33 \quad (R^2: 0.957) \quad (2.19)$$

$$Q_{warm} = -3.1 \cdot 10^{-3} * x^2 + 0.490x - 7.28 \quad (R^2: 0.973) \quad (2.20)$$

The cold well pump flow shows a neat fit over the whole range. The warm well has no data above 60%, because the maximal percentage is proportionally limited (in the control software) to the building side. The maximum flow is around 14 (m<sup>3</sup>/h) (which roughly 60% of the proportional limit, as introduced in section 2.4.1).

## RECONSTRUCTION OF HEAT TRANSFER COEFFICIENT CURVES

Using step 2 of the method the plots of the heat transfer coefficient (the AU-function) of the heat exchanger are reconstructed. The fits are split in two parts: on the red line the well pump is operating at the minimum capacity of 30% (so only building flow is variable) and on the green line the well pump flow increases proportional with the building flow (both flows are variable).

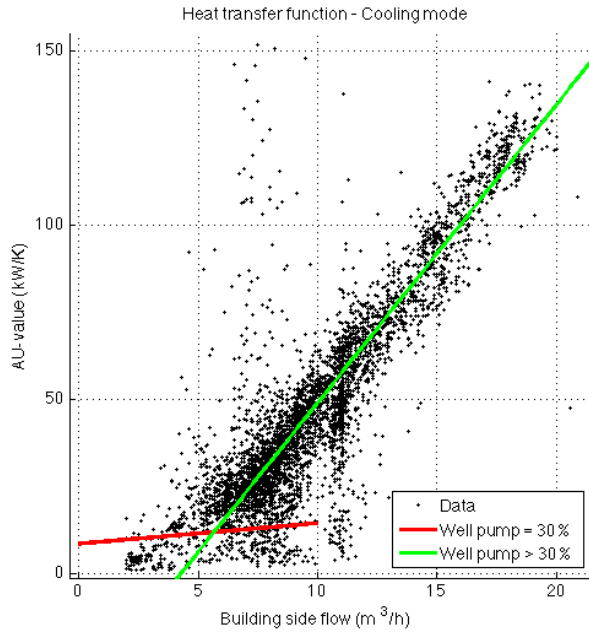


Figure 2-24 - Heat exchanger transfer function cooling

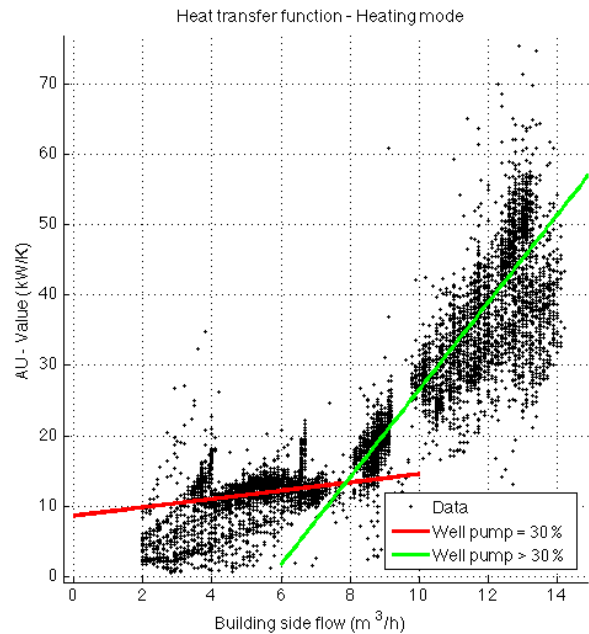


Figure 2-25 - Heat exchanger transfer function heating

Theoretical a third fit should be used for the case that well pump operates constantly at 100% (higher than 18 m<sup>3</sup>/h for cooling and 24.5 m<sup>3</sup>/h for heating as explained in section 2.4.1). For heating this never occurs and for cooling it occurs only a few hours per year, which provide not enough data for this fit.

These curves are fitted using equations 2.21-2.23. Equation 2.21 is fitted on the data of the heating state, but is also used as 30% curve for the cooling state. Because the cooling state is hardly used at minimal capacity, there are not enough data points for an accurate fit. On the other hand, because it is rarely operating at minimal capacity the effect of this assumption will also be not very significant.

$$AU_{30\%} = 0.590 * Q + 8.65 \quad (R^2: 0.96) \quad (2.21)$$

$$AU_{cool} = 8.54 * Q - 36.97 \quad (R^2: 0.956) \quad (2.22)$$

$$AU_{heat} = 6.21 * Q - 35.54 \quad (R^2: 0.839) \quad (2.23)$$

The two curves should intersect at the same points as the proportional limit (section 2.4.1) and the 30%-limit. For the cooling state this should be 7.35 (m<sup>3</sup>/h) and is fitted at 7.86 (m<sup>3</sup>/h). For the heating state this should be 5.40 (m<sup>3</sup>/h) and is fitted at 5.73 (m<sup>3</sup>/h).

### EXTRACTION TEMPERATURE COMPARISATION

In the third and last step the ATES model simulation method is compared with the reconstructed ATES extraction temperatures (Figure 2-26). As explained, the **reconstructed value** is a **direct** calculation based only on the assumed heat exchanger and well pumps characteristics. The **ATES model value** is the **cumulative** result of all injected water volumes and the mixing and conduction calculations in the ATES model. If these two match, the combination of assumptions is a solution. The cold well simulation seems to be accurate except for the summer of 2010 and some deviations at the start of each cooling season. The warm well shows larger deviations, probably caused by the large numbers of start-stops. The extracted temperature decreases quickly for the fact that there is a huge surplus of heat. This suggests a significant interference between the wells. For the ATES model an interference flow of 20% is assumed. A higher interference gives a better fit for the warm well (steeper temperature descent), but also increases the cold well temperatures too much for the model to be solvable.

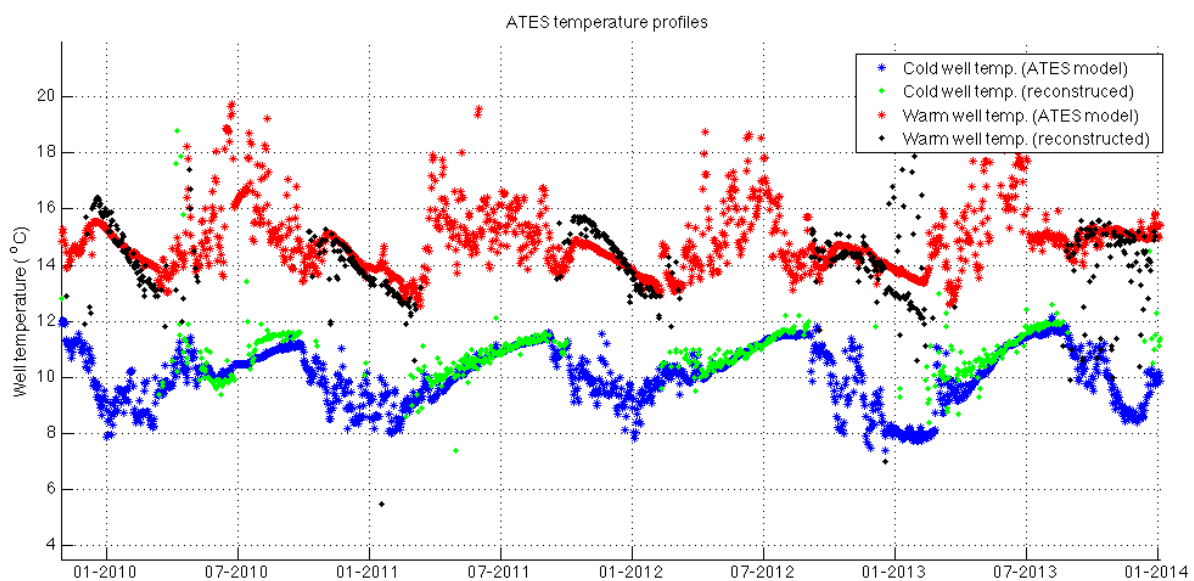


Figure 2-26 - Simulated and reconstructed ATES temperature

## 2.4 IMPLEMENTATION OF CONTROL SOFTWARE METHOD

The research methods upon now are used to reconstruct the behavior based on historical data. To predict the future behavior, the control strategy of the well pumps must be included in the model. This section introduces the control software, the required calculation method and evaluates the simulation results.

### 2.4.1 CONTROL SOFTWARE INTRODUCTION

The 'turn-key' solution developed by GeoComfort, includes a stand-alone software system to control the well pumps. This software is linked to the buildings software system that gives a signal when cooling or heating should be enabled. If one of those modes is enabled, the GeoComfort software is responsible for the operation of the pumps. The software uses measurements of three sensors in the pipes connecting the building with the mono-well: ( $T_{b,in}$ ), ( $T_{b,out}$ ) and ( $q_b$ ).

The software uses some internal rules to ensure the stored (aquifer side) water has a suitable temperature. If for instance the natural water temperature is 12 °C, the same amount of energy can be stored in 2 m<sup>3</sup> water of 10 °C as in 1 m<sup>3</sup> water of 8 °C. The latter is preferred however, because the colder water can provide a higher peak cooling capacity and less water displacement is needed. To achieve this, the maximum groundwater flow must be restricted, with as possible side effect that the supplied water temperature will deviate from the 12 °C setpoint.

The cooling state of the mono-well is controlled using three rules:

1. The cold well pump only operates if  $q_b$  is higher than 1.5 m<sup>3</sup>/h
2. The cold well pump maximum flow is proportionally limited to  $q_b$  using 18 m<sup>3</sup>/h = 100% and 0 m<sup>3</sup>/h is 0%, with a minimum of 30% (Figure 2-27)
3. The cold well pump maximum flow is proportionally limited to  $T_{b,in}$  using 15°C = 100% and 11°C = 0%, with a minimum of 30% (Figure 2-28)

In all cases the minimum value has priority over the maximum value, because the pumps need a minimum flow to operate and provide cooling to the pump motor. Also the lowest maximum value prioritized over the highest. The grey shaded areas show the range the system can vary its well pump flow. The value is increased or decreased using a PID (*Proportional-Integral-Derivative*) controller until the setpoint temperature (for  $T_{b,out}$ ) of 12°C is reached.

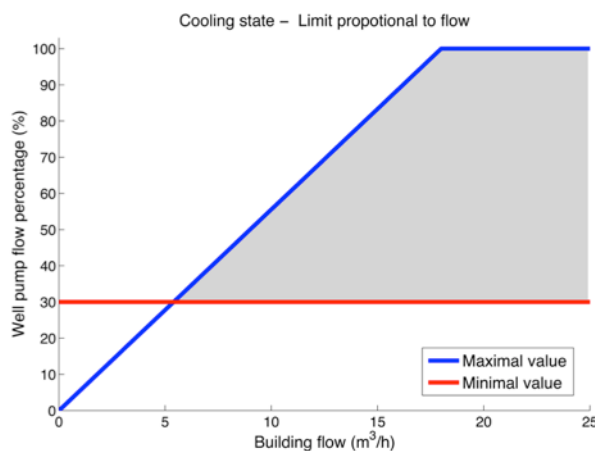


Figure 2-27 - Cooling state pump flow limit 2

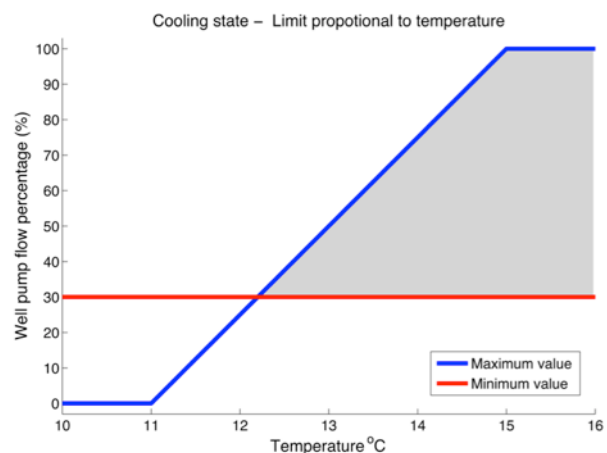


Figure 2-28 - Cooling state pump flow limit 3

For the heating state a comparable set of four rules is defined:

1. The warm well pump only operates if  $q_b$  is higher than 1.5 m<sup>3</sup>/h
2. The warm well pump maximum flow is proportionally limited to  $q_b$  using 24.5 m<sup>3</sup>/h = 100% and 0 m<sup>3</sup>/h = 0%, with a minimum of 30% (Figure 2-29)
3. The warm well pump **maximum** flow is proportionally limited to  $T_{b,in}$  using 8°C = 100% and 10°C = 0%, with a minimum of 30% (Figure 2-30)
4. The warm well pump **minimum** flow is proportionally limited to  $T_{b,in}$  using 2°C = 100% and 6°C = 0% (to prevent freezing) (Figure 2-30)

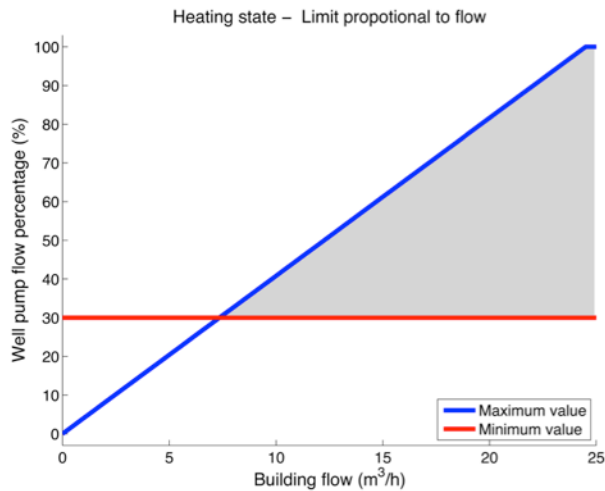


Figure 2-29 - Heating state pump flow limit 2

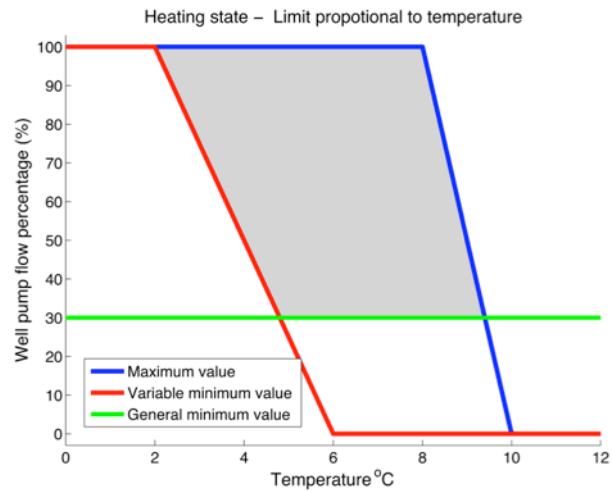


Figure 2-30 - Heating state pump flow limit 3 and 4

Again, in all cases the minimum value has priority over the maximum value, the lowest maximum value is prioritized of the higher and the grey shaded areas show the range the system can vary its well pump flow.

## 2.4.2 CALCULATION METHOD

Using the 'solved' ATES model, heat exchanger and well pump characteristics, a similar heat exchanger model can be used to predict the supplied water temperature to the building system. The problem to be solved is shown in Figure 2-31.

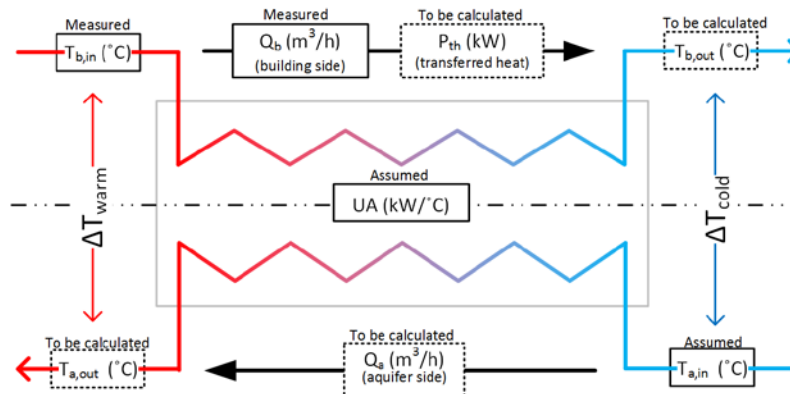


Figure 2-31 - Heat exchanger calculation – Prediction method



The way to solve this problem is a little more complicated than the other three, because the control software is included in this solving method. First step 1 of section 2.3 is used to calculate the needed aquifer flow to reach the setpoint temperature of  $T_{b,out} = 12^{\circ}\text{C}$ . Next the relations defined in 2.4.1 are used to define the maximum and the minimum pump frequency and flow. There are three possibilities:

- The calculated flow is lower than the minimum flow: the minimum flow is used
- The calculated flow is between minimum and maximum flow: solution is correct
- The calculated flow is higher than the maximum flow: the maximum flow is used

For the first and third option the problem is changed to Figure 2-32. On both sides the flows and ingoing temperatures are known, but the transferred heat is unknown (and so both outgoing temperatures). This can be solved using the 'Effectiveness - Number of Transfer Units' ( $\epsilon$ -NTU) method [36].

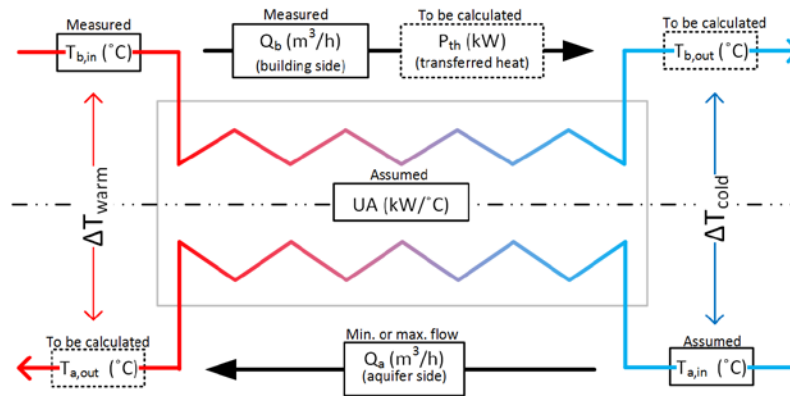


Figure 2-32 - Heat exchanger calculation

The  $\epsilon$ -NTU method uses a number of calculation steps. First the minimal and maximal heat capacity rate is calculated (equation 2.24)

$$C_{min} \left[ \frac{kW}{^{\circ}\text{C}} \right] = \min(Q_a, Q_b) * 4.2 \quad \text{and} \quad C_{max} \left[ \frac{kW}{^{\circ}\text{C}} \right] = \max(Q_a, Q_b) * 4.2 \quad (2.24)$$

Using these values, three variables are calculated; the heat capacity ratio  $C_r$ , the NTU and the effectiveness  $E$  (equation 2.25).

$$C_r = \frac{C_{min}}{C_{max}}, \quad NTU = \frac{UA}{C_{min}} \quad \text{and} \quad E = \frac{1 - \exp[-NTU(1 - C_r)]}{1 - C_r \exp[-NTU(1 - C_r)]} \quad (2.25)$$

Finally the transferred heat is calculated using equation (2.26). When the transferred heat is known, the outgoing temperatures can be calculated.

$$P_{th} [kW] = E * C_{min} (T_{a,in} - T_{b,in}) \quad (2.26)$$

### 2.4.3 SIMULATION RESULTS

Figure 2-33 shows the result of the control software simulation. The showed dataset is the winter of 2011-2012, because in 2012-2013 a lot of well pump data is missing and 2013-2014 was an unusual warm winter, which generated only a small amounts of data. The green and the yellow line are equal to the plot of Figure 2-26. Again, at the start of the winter the ATES model temperature is a bit lower and at the end slightly higher.

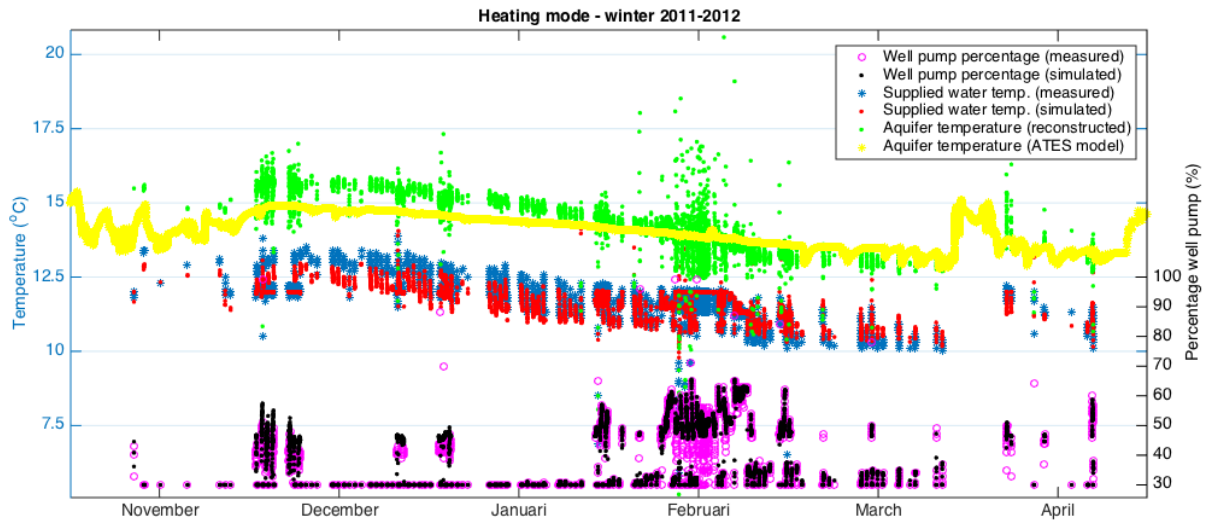


Figure 2-33 - Simulation results heating state

Figure 2-34 shows a more close up version of the plot above. The most important conclusion of these results is to notice that if the result of method 2 is accurate (so the yellow and green line match), the prediction of the supplied water temperature to the building ( $T_{b,out}$ ) and the well pump percentage are also accurate. The other way around, if method 2 was not successful the result of method 3 also deviates. This makes sense, because simulating software logic using software logic can hardly go wrong. The weakest link is the prediction of the extraction temperature.

Closer analysis of graph shows several groups in the data. These are nights or weekends, where the heat pump is continuously active. On the left half the results are quite accurate, but in the right half the behavior is very unstable. This variation is caused by the slow response of the ATES-system to changes in temperature or flow.

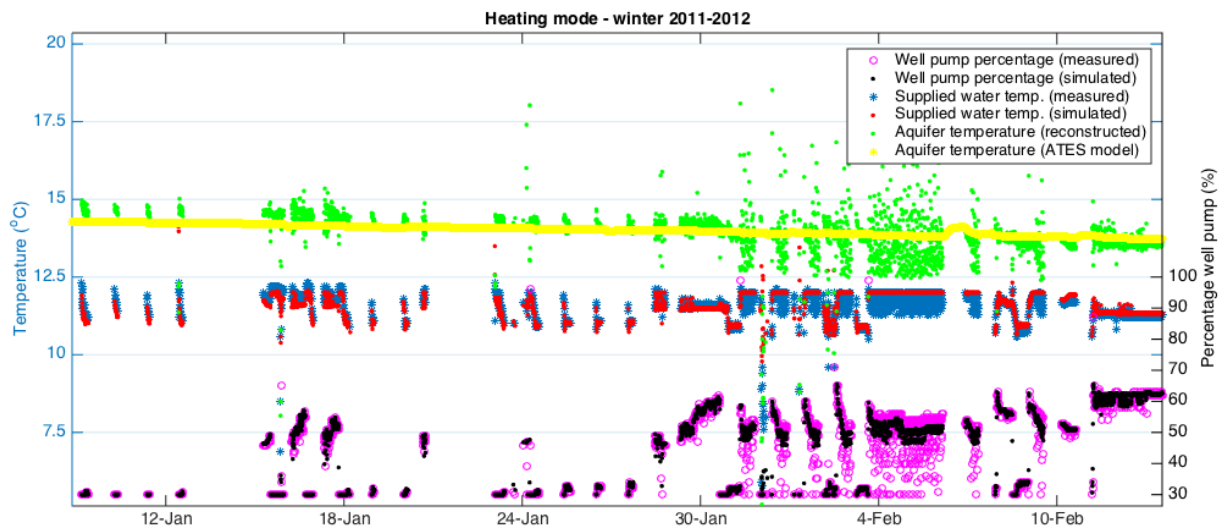


Figure 2-34 - Simulation results heating state (detail)

The same two plots are created for the cooling mode. Figure 2-35 shows the simulation results of the summer of 2013. Again the main analysis here is not if all measured and simulated values over the entire year do match (because they do not). The main analysis is that *if* the results of method 2 (green and yellow) do match, the temperatures and well pump percentages do also match.

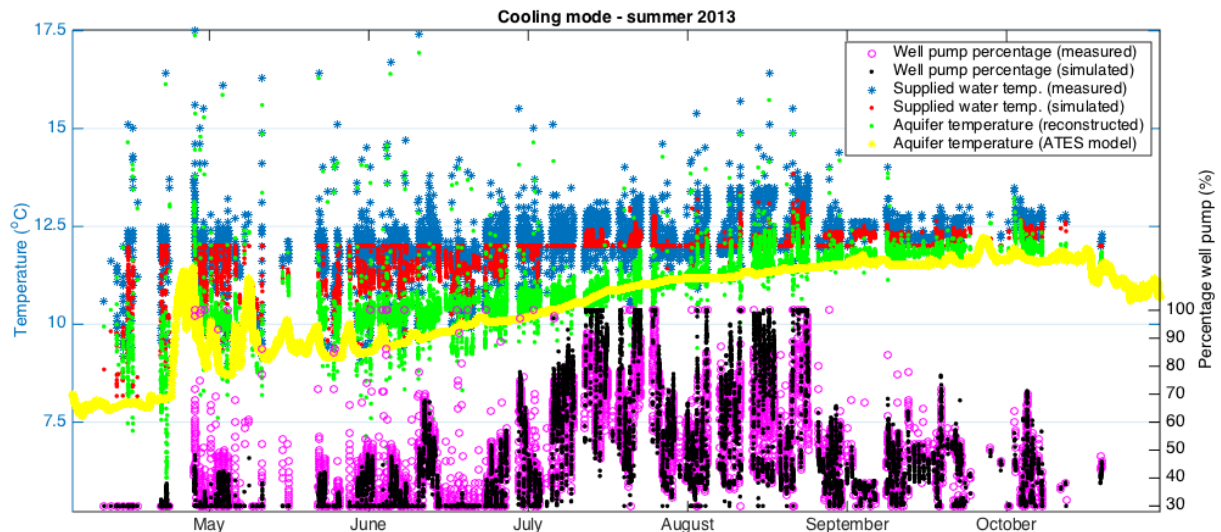


Figure 2-35 - Simulation results cooling state

Figure 2-36 shows the close-up containing four weeks of data, recognizable on the groups of five weekdays. Equal to the heating state the results match well when the ATES temperature is correctly predicted. Remarkable is that in the week of 31th of August the model structurally suggests a higher well pump percentage and (as result) a lower supplied water temperature. Analysis of this deviation during last summer revealed a very long integration time of the maximum limit (it takes over an hour to reach 100%) and very short (<30 sec) periodical decreases of the building side flow as cause. The well pump slowly increases capacity to 100%, but is set back to 80% by the flow limit every ~10 minutes.

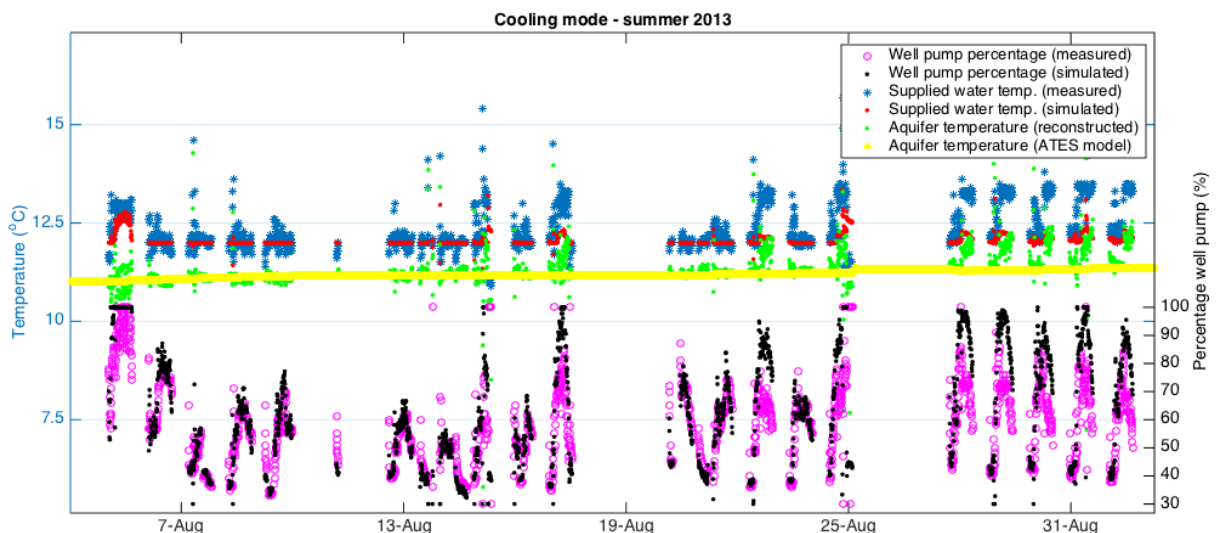


Figure 2-36 - Simulation results cooling state (detail)

## 2.5 DISCUSSION

In this chapter an attempt was done to simulate the case-study ATEs system while literally no data at all was available on the groundwater part of the system. The developed methods proved to be capable of solving a significant part of the puzzle. First a recap of the used method is given followed by a discussion of the results.

### 2.5.1 RECAP

In this chapter three main methods are introduced:

- 1) A method for simulation of the energy storage in the aquifer (the aquifer model)
- 2) A method for characteristics of well pumps and the heat exchanger (the component model)
- 3) A method for the used control software (the software model)

This combination of *aquifer*, *component* and *software* simulation can be seen as universal way to simulate the interaction between the complete ATEs-system and the building. For each specific case-study object, each of these modeling parts must be fulfilled with a suitable method.

The main goal of the **aquifer** model is to predict the temperature of the extracted water, based on the logged injection temperatures. For the case-study building a specialized (light-weight) aquifer model is developed. This model is universally applicable, as long as the system allows equal simplifications. If not, for example systems with a high natural flow or significant non-axial interference (doublets/clusters), another aquifer model should be used.

The main goal of the **component** model is to find characteristics of well pumps and the heat exchanger. If the aquifer flow and temperatures are measured, this model is very simple and concerns only the fitting of logged data. For the case-study a more complex method is used to reconstruct the missing aquifer data and to calculate the required fits.

The main goal of the **software** model is to simulate how the well pumps are controlled. This part probably is unique for the configuration of each control software system. The method to calculate the resulting water flows is universally applicable, because it only uses general heat transport laws.

The combination of these methods has as main goal to calculate the return temperature ( $T_{b,out}$ ) to the building, for the combination of supplied flow ( $q_b$ ) and temperature ( $T_{b,in}$ ) by the HVAC system introduced in chapter 3. The stored amount of energy is used for the 'bookkeeping' of MPC.

### 2.5.2 DISCUSSION

The aquifer model proved to be capable of providing a very quick simulation method, with an accuracy that is sufficient for predicting the effect of the storage temperatures on the building systems (accuracy within  $<1K$ ). On the other hand, for the isotropic and flat Dutch aquifers very significant deviations were not expected (based on the analysis of allowed simplifications).

The component model using the data reconstruction method was the most difficult part of this chapter. The main problems where:

- It proved to be difficult to reconstruct the stored amounts of energy from the dataset. An inaccurate dataset is a debatable starting point for a reconstruction simulation.
- For the heat exchanger the assumption was made of the aquifer side flow being proportional to building side flow. This assumption was necessary, because otherwise the problem became too complicated to solve. In reality these flows are not strictly proportional, causing deviations in the fits.

- The analysis of results is complicated, because by comparing the predicted and reconstructed extraction temperatures (as only possible check), it is not possible to conclude which part is deviating.

The results of the reconstruction method can be discussed from two points of views. From a *scientific angle*, the method is not very solid and it is hard to make an estimation of the accuracy of the results. The method could only be evaluated if aquifer measurements were available. From a *practical angle*, the method reveals usable data from a chaotic plain-text dataset. Even taking the uncertainties into account, this is already significantly more useful than the currently available logging methods. For the complete model, the reconstructed data is accurate enough to construct a realistic model of the ATEs-system performance.

The software model only showed accurate results when the predicted ATEs temperature matched the reconstructed temperature. This makes sense, because deviations of the aquifer and component methods influence the result of the software method. The simulation of the software itself was accurate, but it is not surprising that software simulation using software gives accurate results.

Although the total method presented in this chapter has its weak points, the results are still a huge improvement on conventional monitoring methods. The limited possibilities and uncertainties in the data reconstruction method, emphasizes the need to measure aquifer side temperatures and flows. Implementation of the developed aquifer method in the BMS will make already a huge difference in monitoring and understanding the ATEs system, which was one of the main issues introduced in chapter 1.

## 3. HVAC SYSTEM MODEL

This chapter introduces the methods to simulate the HVAC system (Heating, Ventilation, Air Conditioning). It focuses only on the aspects that influence the water flows to the ATES system and is explicitly not intended as complete building simulation method. Accordingly, the main goal is to simulate which temperature and flow is supplied to the ATES system introduced in chapter 2. First an introduction of the system is given and next the modeling methods for the main components are introduced.

### 3.1 INTRODUCTION

Like a typical ATES coupled system, the HVAC system is designed for low-exergy [37] operation (using low temperature ( $<50\text{ }^{\circ}\text{C}$ ) heating water and high temperature ( $>10\text{ }^{\circ}\text{C}$ ) cooling water). The low temperature heating is needed to reach a high efficiency on the heat pump and the high temperature cooling is needed to directly utilize the cold water supplied by the ATES system. The system is mainly based on heating and cooling via the ventilation air. First air distribution system is introduced, next the hydronic (water-based) distribution network and finally the various operation states.

#### 3.1.1 AIR DISTRIBUTION

Figure 3-1 shows the main structure of the air distribution system. The system uses a constant airflow and is only active during office hours (6 am till 9 pm). A more detailed version of the diagram can be found in appendix D.

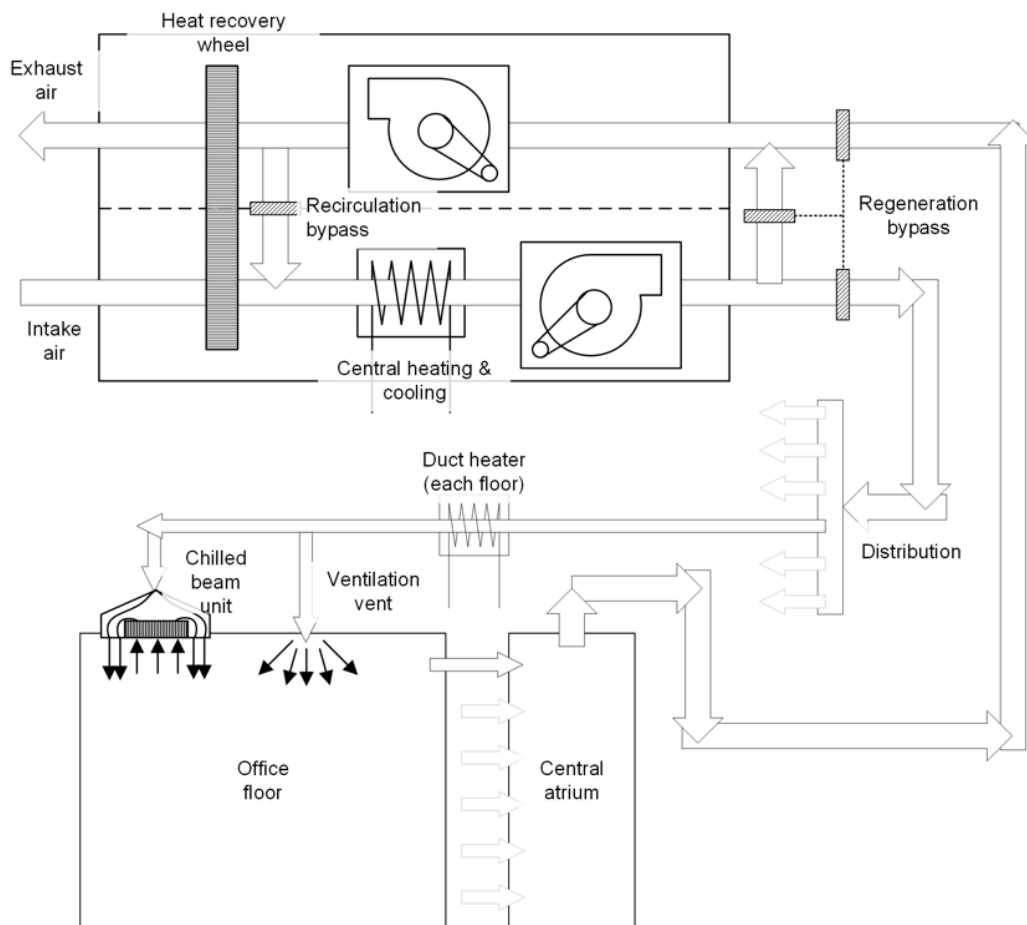


Figure 3-1 - Air distribution diagram

The intake air is preheated or cooled by the *heat recovery wheel* or the central (change-over) *cooling/heating coil*. The air is distributed through the building and passes a *duct heater* on every office floor to provide heating per floor. The air is supplied to the office spaces using *chilled beam units* (at the small offices and close to the windows) and using *ventilation vents* (throughout the open-plan offices). The surplus of air transferred to the *central atrium*, where the air of all offices is collected. At the top of the atrium the air is extracted by the AHU and transferred via the *heat recovery wheel* to the air exhaust.

The system has two bypass options: *recirculation* and *regeneration*. The recirculation option can be used to recirculate air within the building (and though minimize ventilation losses). This is useful to increase reheating speed of the building, because in the early hours the need for fresh air is minimal. However, in reality this feature is never used because the heat recovery wheel has sufficient heat recover capacity. The regeneration bypass is used to provide additional cooled water to the ATES system during the winter, to restore the balance of stored energy. The intake air is directly transferred to the return duct and the exhaust fan, enabling a kind of 'dry cooler' function in the AHU.

### 3.1.2 WATER DISTRIBUTION AND COMPONENTS

The water distribution system transfers the heat and cold from the 'generating components' to the 'distributing components'. Other than conventional building systems, the system in the Kropman office is quite sophisticated and offers a lot of possibilities to (re)distribute the heating and cooling loads. The main generating components are:

**The ATES system:** As already introduced in chapter 2, the ATES system always tries to supply water of 12 °C to the building. The maximum heating or cooling capacity of the system depends on the extraction temperatures and the temperature difference over the heat exchanger. During standard operating conditions the ATES system can deliver a rated capacity of roughly 150 kW ([28]) of heating or cooling power for a  $\Delta T$  of 8K.

**The heat pump:** The 12°C water supplied by the ATES system can be directly used for cooling, but for heating a heat pump (type: Thermia Robust 45-U/M [38]) is used. The capacity of the heat pump is  $\pm 50$  kW, which should be enough to provide >90% of the yearly heating energy. The heat pump is a single-stage (on/off) type. Two buffer vessels of 800 liters are coupled to the warm and cold side to provide the heating or cooling when the heat pump is off.

**The district heating:** The district heating is used to provide peak heating when total heating load is higher than the maximum capacity of the heat pump. It can also be used as backup heating or alternative heating in the (unlikely) case of a cold surplus in the ATES system. The system is connected via a heat exchanger to the district heating pipes which provide water of 90°C. The rated capacity of the system is 120 kW.

The distribution components are separated in *central* and *local* distribution. Central distribution is provided via the air handling unit and depends only on the outdoor temperature and the heating curve. Local distribution is provided on office level and depends on the local heating or cooling load per office. The main distribution components are:

**AHU heating/cooling coil:** The coil in the air handling unit can be used for both heating and cooling (+ dehumidification) using a change-over principle. For cooling mode the coil is directly coupled to the ATES system. In heating mode the coil is coupled via a heat exchanger to the warm water distribution system.

**Local heating group:** The local heating group is the combination of all chilled beam units, duct heaters and floor heating(/cooling) systems. The chilled beam unit (approx. 100 units) and duct heaters (8 units) are already introduced in the air distribution section. The floor heating is used on



the first floor (above the car parking) and in the restaurant. Only combined supply and return temperatures are measured in this system, so the system is analyzed as one complete group.

**Local cooling group:** The local cooling group is the combination of all chilled beam units (approx. 100 pieces) and floor cooling systems (only first floor and restaurant). Based on design flows, the chilled beam units account for 80% of the capacity of this group. Because only the combined supply and return temperatures of this system are measured, the system is analyzed as one complete group.

All components are linked by the water distribution system, which uses various valves and pumps to distribute the water through the building. The general principle diagram of the water distribution system is shown in Figure 3-2 (larger version in appendix E). This diagram is quite difficult to understand, so the separate system states are introduced in the next section.

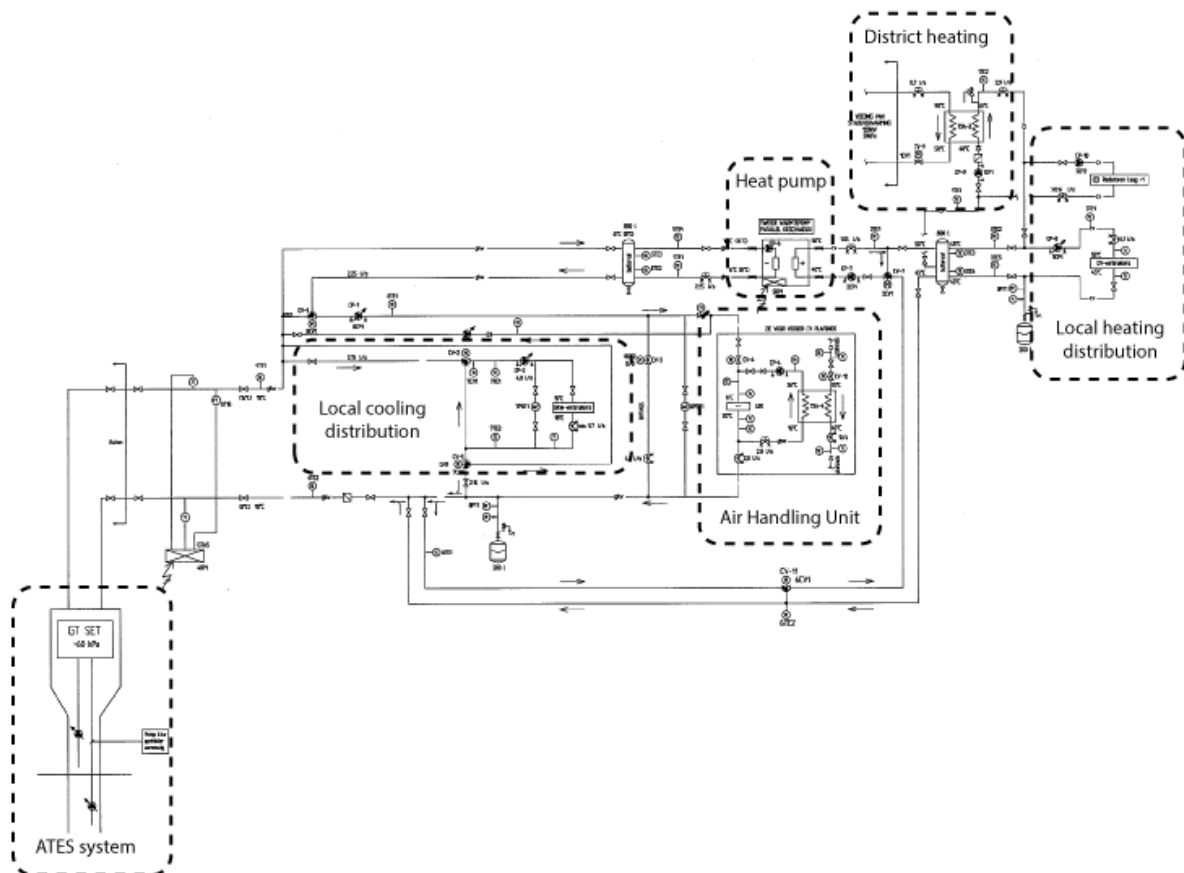


Figure 3-2 - Principle diagram water distribution

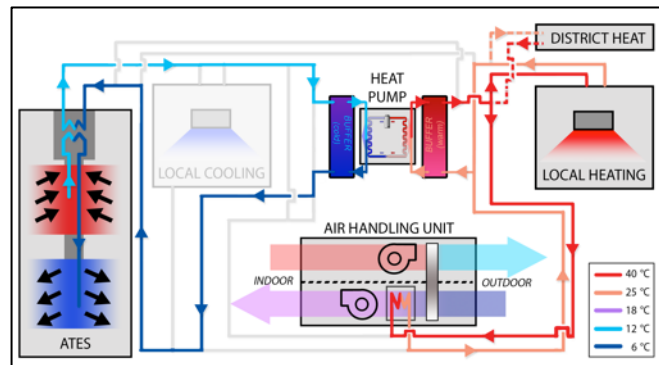
### 3.1.3 SYSTEM STATES

The states of the distribution network are defined by the buildings control software. This software is based on a technical description that describes how the system should operate. The model is constructed according to the states described in this original document [39]. In reality there are some deviations between the original description and the actual software. These deviations are caused by bugs, manual overridden settings or faults in the implementation. This section introduces the states as they were intended in the original design. Table 3-1 and Table 3-2 show the states during office hours. Table 3-3 and Table 3-4 show the states outside office hours.

### Building states during office hours (weekdays 6.00-21.00 hour)

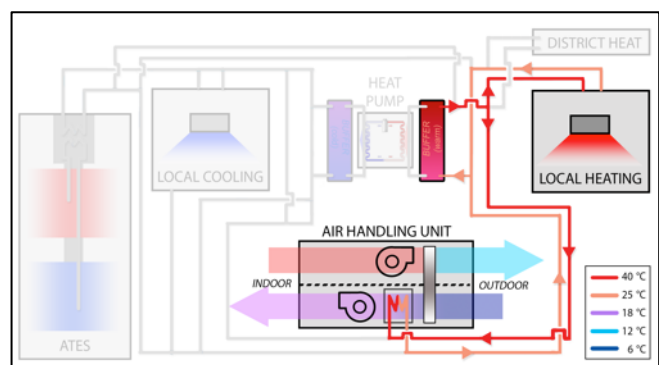
#### State 1a. Only heating (estimated < 5 °C) - Heat pump active

If the air temperature after the heat recovery wheel is lower than the required temperature according to the heating curve, additional central heating in the AHU is supplied. Chilled water produced by the heat pump is stored in the ATES system. When the heat pump cannot deliver enough heating capacity, the district heating supplies the needed additional heating power.



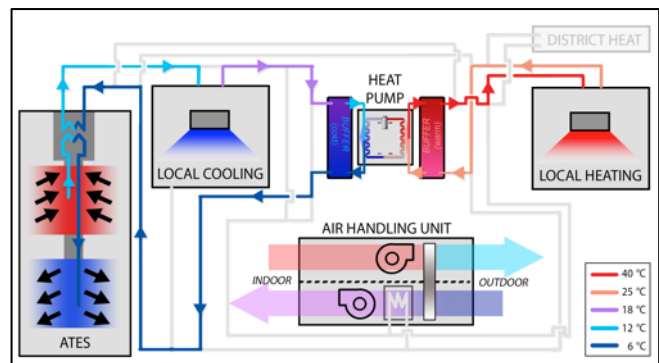
#### State 1b. Only heating (estimated < 5 °C) - Heat pump inactive

If the total heat load is lower than the heating capacity of the heat pump, the surplus of produced heat is stored in the buffer vessel. When the buffer vessel has reached the setpoint temperature, the heat pump and ATES are shut down. The heating load is supplied from the buffer vessel.



#### State 2a. Redistribution of heat (estimated 5-13 °C) – Heat pump active

If no central heating is required, the supply water pump of the local cooling group is started. The water supplied to the heat pump is preheated by the local cooling. If in this state the local cooling demand is lower than the chilled water production by the heat pump, the surplus of cold is stored in the ATES.



#### State 2b. Redistribution of heat (estimated 5-13 °C) – Heat pump inactive

If the heated water buffer is filled, the heat pump is switched off and the local heating load is supplied by the buffer vessel. The return water from the local cooling system is transported to the AHU coil and used to preheat the air. The more heat supplied by the local cooling, less heat needs to be recovered by the heat recovery wheel.

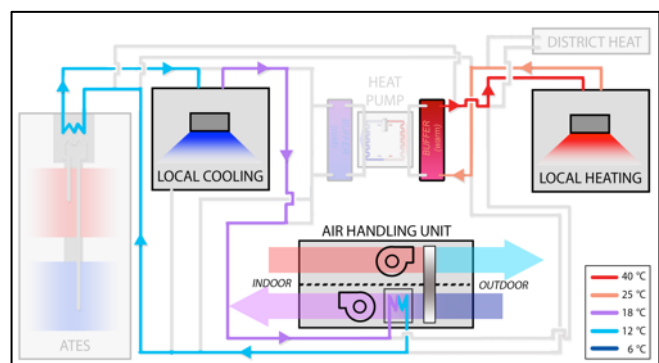


Table 3-1 - System states during office hours (part 1)

State 3a. Redistribution and ATES cooling (*estimated 13-17 °C*) - Heat pump active

The diagram illustrates a district heating and cooling system. It features a central 'DISTRICT HEAT' source connected to a 'HEAT PUMP' and a 'LOCAL HEATING' unit. A 'LOCAL COOLING' unit is also connected to the 'HEAT PUMP'. The 'HEAT PUMP' is connected to an 'AIR HANDLING UNIT' which has 'INDOOR' and 'OUTDOOR' air flows. A legend indicates temperatures: 40 °C (red), 25 °C (orange), 18 °C (purple), 12 °C (blue), and 6 °C (dark blue). The 'ATES' (Adsorption Thermal Energy Storage) unit is shown on the left, connected to the 'LOCAL COOLING' unit.

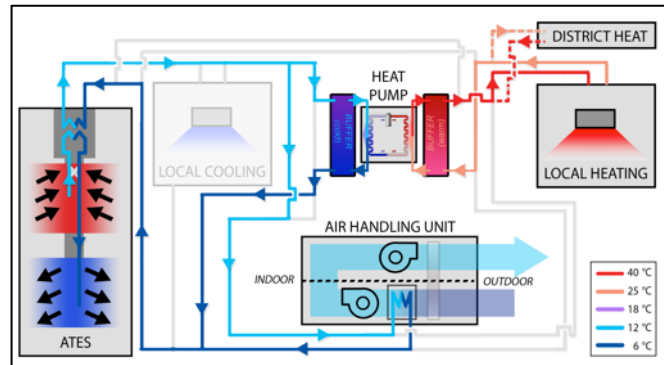
The diagram illustrates a district heating and cooling system. It features a central 'DISTRICT HEAT' source connected to 'LOCAL COOLING' and 'LOCAL HEATING' units. A 'HEAT PUMP' is shown between the local units and the district heat source. An 'AIR HANDLING UNIT' is shown with 'INDOOR' and 'OUTDOOR' air flows. A legend indicates temperatures: 40 °C (red), 25 °C (orange), 18 °C (purple), 12 °C (blue), and 6 °C (dark blue).

The diagram illustrates a district heating and cooling system. It features a central 'DISTRICT HEAT' source connected to 'LOCAL COOLING' and 'LOCAL HEATING' units. A 'HEAT PUMP' is shown between them. An 'AIR HANDLING UNIT' is connected to the local cooling and heating units, with arrows indicating 'INDOOR' and 'OUTDOOR' air flow. A legend on the right shows temperature ranges for different flow types: 40 °C (red), 25 °C (orange), 18 °C (purple), 12 °C (blue), and 6 °C (dark blue).

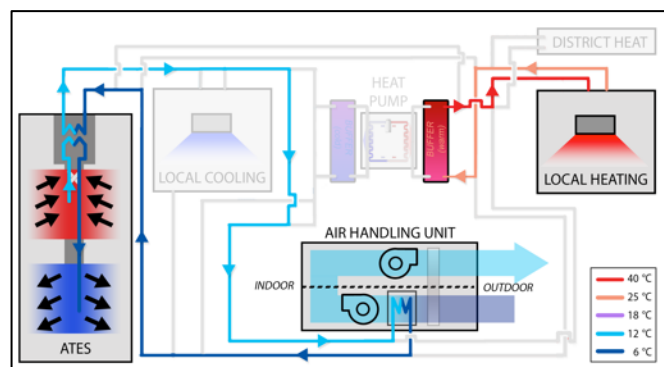
Page | 43

**Building states outside office hours (21.00-6.00 hours & weekends)****State 1a. Regeneration of the ATES system (below 4°C) – Heat pump active**

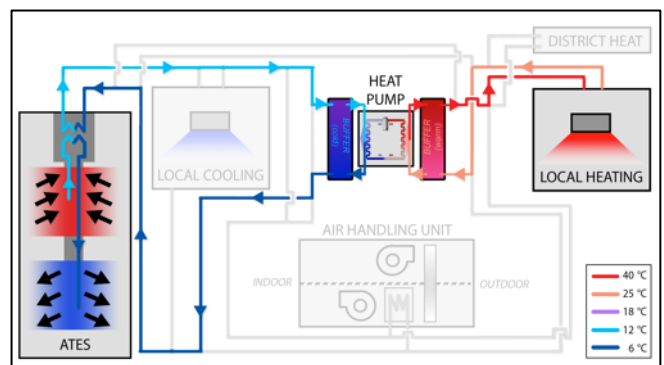
Depending on the setpoint to start regeneration (4°C) the bypass in the AHU is opened and the cold airflow is used to supply cold water to the ATES. Parallel to this flow the heat pump is used to supply heat to the building. The district heating is used if the heating load is higher than the maximal heat pump capacity.

**State 1b. Regeneration of the ATES system (below 4°C) – Heat pump inactive**

Same as above, but with heat pump inactive.

**State 2a. Only heating (4-15 °C) - Heat pump active**

Only local heating is active using the heat pump. Cold is stored in the ATES system. The rest of the system is inactive.

**State 2b. Only heating (4-15 °C) - Heat pump inactive**

Same as above, but with heat pump inactive. The heat is supplied from the buffer vessel and the rest of the system is inactive.

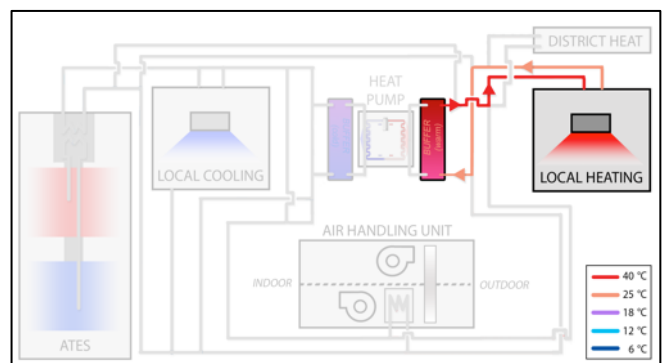


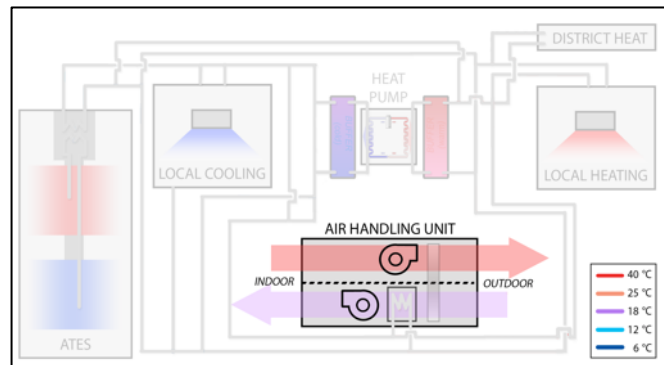
Table 3-3 - System states outside office hours (part 1)

---

**Building states outside office hours (21.00-6.00 hours & weekends)****State 3. Night ventilation (15-23 °C)**

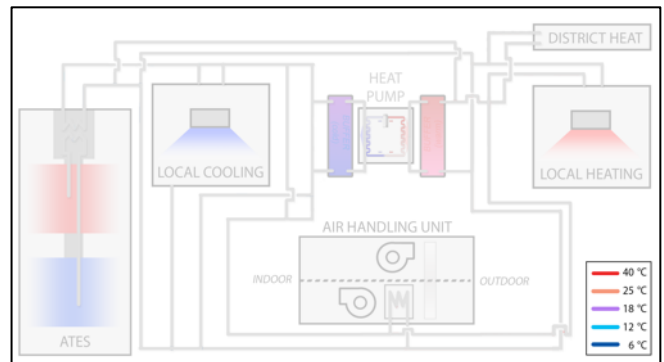
---

The colder outdoor air is used to cool down the building upon the average room temperature gets below a predefined temperature setpoint. When this setpoint is reached the AHU is turned off and the building is in rest (state 4). The behavior during this state is not important for ATES simulation, because both states do not directly influence the ATES system.

**State 4. Rest (>23 °C or when night ventilation has cooled the building sufficiently)**

---

All systems inactive.



---

Table 3-4 - System states outside office hours (part 2)

---

As can be concluded from the various system states, the simulation of the influence of the HVAC system on the ATES system can be simulated using methods for three main components: the air handling unit, the local cooling group and the heat pump. All heating components do only influence the ATES via heat pump. The summed load of all heating components is sufficient for simulations (without analyzing the separate parts).

### 3.2 AIR HANDLING UNIT SIMULATION METHOD

The air handling unit is a combination of components with as main goal to supply cleaned and conditioned air to the offices, under almost all outdoor conditions. Figure 3-3 shows the main components and the important sensors (temperature (T), moisture (M) and pressure difference (dP)). The main focus of this section is to analyze the behavior of the central coil. This section introduces the needed theoretic background, analyzes the data, explains the calculation method and evaluates method results. Before using any of the data an extensive check was performed on all sensors and airflows. These are presented in appendices D and E.

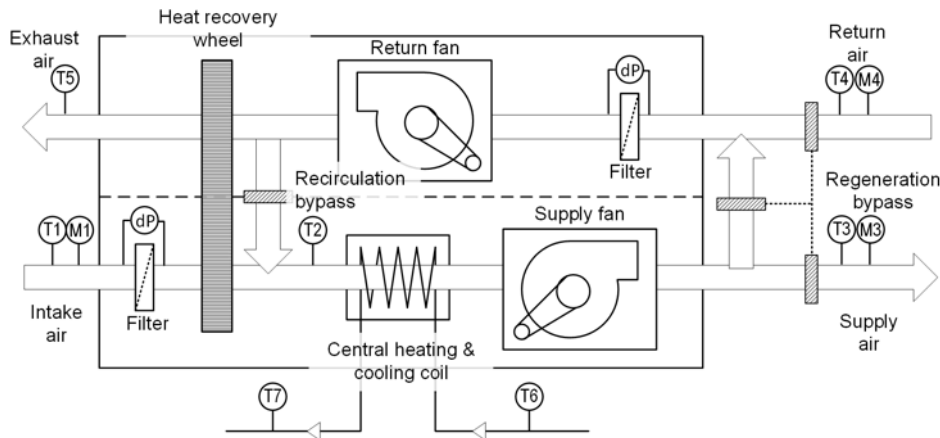


Figure 3-3 - Schematic AHU overview

#### 3.2.1 THEORETICAL BACKGROUND

The central heating and cooling coil is from a thermodynamic point of view equal to the heat exchanger introduced for the ATES system, but heat is transferred between water and air instead of water and water. Other differences are that moisture in air condensates while cooled down and that the calculation of the heat transfer factor is somewhat more complex when both air as water flow are variable.

##### CONDENSATION

When air is cooled down, the relative humidity (RH) increases. This is caused by the fact that warmer air can contain more moisture compared to cold air. The temperature at which 100% relative humidity is reached is called the dew-point temperature. When the air is cooled even further, the moisture starts to condensate and the air is dehumidified.

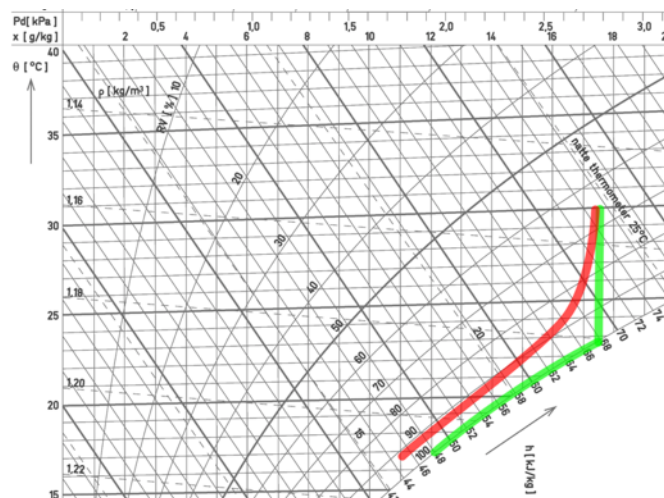


Figure 3-4 - Dehumidifying air in the Mollier diagram

The process can be visualized using a Mollier-diagram (Figure 3-4). When air is cooled from 30 °C and 65% RH to 17 °C, the **green** line shows the theoretical path. First the humidity increases to 100% at 22.5 °C and next condensation starts while cooling further down to 100% RH at 17 °C. This process removes 5.5 grams of water per kg air. The energy needed to cool down one kg of air (sensible heat) is 12 KJ and the energy needed to condensate the water (latent heat) is 14 KJ. This sensible/latent energy ratio indicates the importance of accurate condensation modeling.

In reality the **red** line is followed and 100% RH will never be reached. To cool down the air to 17 degrees, the coil surface temperature must be significant lower in order to extract enough heat. This causes locally more condensation than theoretically required. This phenomenon combined with very turbulent airflows, re-evaporation of condensate, local pressure differences and leaking air makes the prediction of this process very complex. The cooling coil in the case study AHU dehumidifies the air to a RH between 91% and 98%.

There are several methods to simulate this behavior. According to [40] there are two categories; the theoretical and empirical methods. Theoretical methods (which is the majority of the methods) simulate the dehumidifying behavior using the exact physical parameters, which make implementation for buildings quite difficult and specialized work. Also it is debatable how accurate these model results are for older (>10 year) cooling coils, due to fouling on the coil surface [41]. The found empirical models are not capable of modeling the complete behavior of a cooling coil using the building data, but only using experimental setups.

For this research a very simplified method is used to predict the condensation. Using data analysis the amount of condensing moisture is plotted as function of the number of degrees below the dew temperature. Depending on the operating settings of the system, the coil will develop a specific 'condensation-pattern' which can be used to simulate air dehumidification.

## HEAT TRANSFER

The main difference between the ATES heat exchanger and the AHU cooling coil is the fact that both flows (air/water) are variable and not proportional to each other. Both the airflow and water flow are independent variables and have different boundary layer characteristics for variable flow.

The method used to calculate the heat transfer function is to reconstruct the three different heat resistance parts (equation 3.1). First the minimal 'fixed' heat resistance is calculated using the value during maximal water flow and maximal airflow. Next the effects of decreasing the water flow and airflow are analyzed separately to find a fit-equation. The resulting (combined) equation is only valid within the fitted flow range.

$$\frac{1}{AU} = R_{th,bound-air} + R_{th,bound-water} + R_{fixed} \quad (3.1)$$

It is assumed that the wet surface of the coil does not significantly influences the heat transfer characteristics according to the modeling method used in [42].

### 3.2.2 COOLING STATE SIMULATION METHOD

A common challenge in solving a heat exchanger problem with unknown flows is that the solution can only be found by iterative calculation. Both the heat transfer factor (AU) as the LMTD are depending on the water flow, which makes formulation of a direct (analytical) solution impossible.

All calculations on absolute/relative humidity and dew-points are done using the MATLAB scripts from the HAM-Lab site of the TU/e [43]. The goal of this method is to find the water flow through the cooling coil and the temperature of the return water. During cooling mode the airflow is assumed to be constant. The method uses four steps to find the correct solution.



### STEP 1 – PREPARATION

The first step is to calculate the cooling load that should be supplied by the cooling coil. The ingoing air temperature ( $T_{afterHRW}$ ) (eq. 3.2) is calculated using the outdoor temperature ( $T_{outdoor}$ ), the HRW efficiency ( $\eta_{hrw}$ ) (appendix F) and assumed average return air temperature of 28°C (Figure 4-5). Using the heating curve ( $T_{supply}$ ), fan dissipation ( $dT_{dis, fan}$ ) and the specific heat capacity of the air flow ( $\dot{m}_{air} * C_{air}$ ) the sensible cooling load can be calculated (equation 3.3). The latent cooling load is calculated using the condensation curve and the latent heat of condensing water ( $L_{water}$ ) (equation 3.4). The total cooling load is the sum of both (equation 3.5).

$$T_{afterHRW} = \min(T_{outdoor}, T_{outdoor} - \eta_{hrw}(T_{outdoor} - 28)) \quad (3.2)$$

$$P_{sens} = (T_{afterHRW} - T_{supply} - dT_{dis, fan}) * \dot{m}_{air} * C_{air} \quad (3.3)$$

$$P_{lat} = X_{cond} * \dot{m}_{air} * L_{water} \quad (3.4)$$

$$P_{coil} = P_{sens} + P_{lat} \quad (3.5)$$

### STEP 2 – DIRECT ATES COOLING

In this step a solution is searched using the water supplied by the ATES system (approx. 12°C). Using the LMTD method introduced in equation 2.10 & 2.11 the transferred heat is calculated for an assumed flow. Starting at the minimum flow (0.1 l/s) a solution is searched to find the flow at which the same amount of heat is transferred as needed according to equation 3.3. If the flow needs to be larger than the maximum flow (2.8 l/s) the solution is found using step 3 (Figure 3-5).

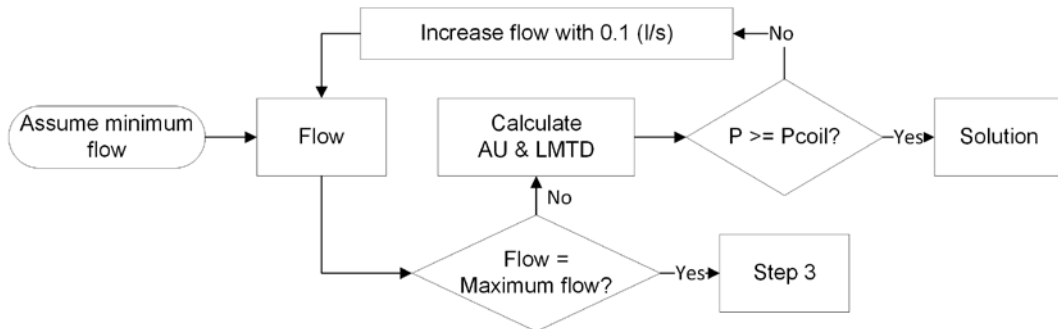


Figure 3-5 - AHU cooling calculation method - Step 2

### STEP 3 – ADDITIONAL HEAT PUMP COOLING

When the heat pump is used to precool the water (according to state 4b in section 3.1.3), the supply temperature is calculated using equation 3.6. The solving method is now slightly changed to Figure 3-6.

$$T_{water, sup} = T_{b, out} - \frac{P_{hp, cool}}{\dot{m}_{water} * C_{water}} \quad (3.6)$$

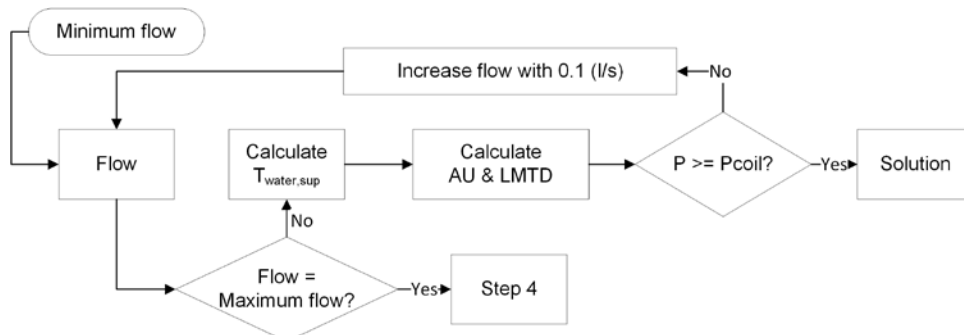


Figure 3-6 - AHU cooling calculation method - Step 3

#### STEP 4 – INCREASE SUPPLY AIR TEMPERATURE

If no solution can be found using maximum flow and maximum heat pump capacity, the setpoint of the supply air (as set in the AHU heating curve) cannot be reached. As shown in Figure 3-7 the supply temperature  $T_{\text{supply}}$  is increased step by step to find a temperature where the transferred cooling load ( $P$ ) matches the needed cooling load ( $P_{\text{coil}}$ ).

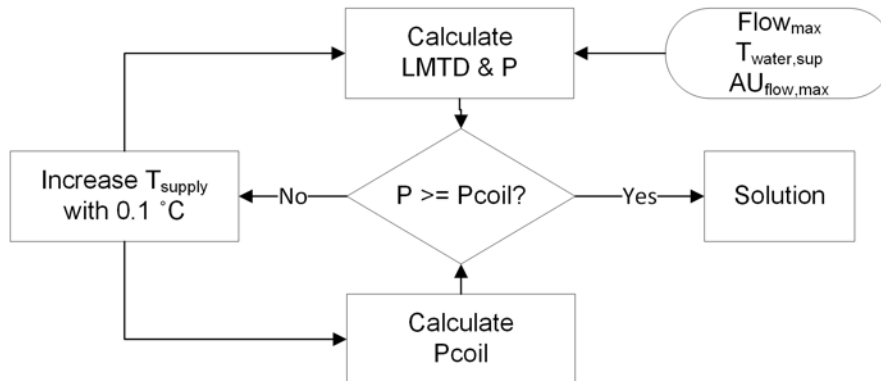


Figure 3-7 - AHU cooling calculation method - Step 4

When the matching water flow is found, the return temperature is easily calculated using the transferred heat and the supply temperature.

#### 3.2.3 REGENERATION CALCULATION METHOD

The regeneration state uses a similar series of sub-states and steps to supply chilled water to the ATES system. The software is designed with as main goal to cool down the water flow to a temperature between 6.5 and 6.2 °C. There are three steps used to achieve this:

##### STEP 1 – MAXIMUM AIRFLOW, MINIMUM WATER FLOW

Because maximum regeneration airflow (25700 m<sup>3</sup>/h) and minimum water flow (2.0 l/s) are constant and the supplied temperatures are known, the NTU method (as introduced in 2.4.2) can be used to calculate the chilled water temperature. There are two options:

- The temperature is 6.5°C or higher, than the solution is correct
- The temperature is below 6.5 °C, than step 2 is used

##### STEP 2 – INCREASE WATER FLOW

Equal to step 2 of the cooling method, the flow is iteratively increased by 0.1 (l/s) until the setpoint of 6.5°C is reached again. If the maximum flow (3.0 l/s) is reached and the return temperature gets below 6.2 °C step 3 is used.

##### STEP 3 – DECREASE AIRFLOW

This step uses the same method as used for step 2, but than by decreasing the airflow until the setpoint of 6.2 °C is reached.

In the actual installation there is an additional protection thermostat that switches off the AHU when the coil gets below zero degrees to prevent freezing damage. Historical data shows this thermostat has never been triggered (upon temperatures of -10°C), so there is no need to take this effect into account.

### 3.2.4 DATA ANALYSIS

This section introduces the method to use data analysis to reconstruct the heat transfer function of the AHU coil and the condensation profile.

#### CONDENSATION PROFILE

The condensation profile is calculated by filtering the dataset on all events where the AHU coil is in cooling mode (valve opened). The dew point and absolute humidity are calculated using the RH (sensors M1 & M3), temperature (sensors T1 & T3) and the scripts from [43]. Figure 3-8 shows little or no condensation when cooled to 5 °C before the dew temperature. Below the dew temperature the condensation steeply increases. Between those points a transition zone is visible. The profile is fitted with the exponential function in equation 3.7.

$$\Delta X = 0.88 * e^{0.40 * \Delta T} \quad (R^2: 0.947) \quad (3.7)$$

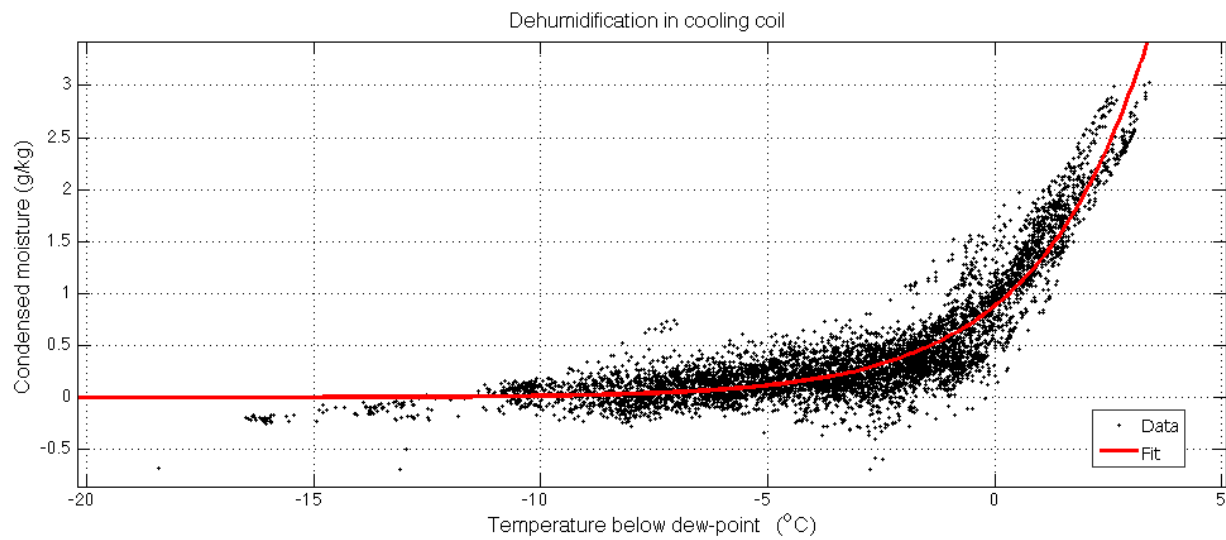


Figure 3-8 - Dehumidification profile

#### HEAT TRANSFER FUNCTION

As introduced, the method to determine the three thermal resistance factors uses the case with maximum flow at both sides as 'fixed' reference resistance. The maximum flow at both sides (air & water) is achieved during regeneration state. The water flow can be measured using the flow sensor over the ATES system, when only flow over the AHU coil is active. Otherwise the water flow is measured using the  $\Delta T$  over the coil ( $T_6/T_7$ ) and the transferred heat ( $P_{coil}$ ).

The airflow is **constant** during office hours (23.000 m<sup>3</sup>/h) and maximum regeneration flow (25.700 m<sup>3</sup>/h). The airflow is **variable** during regeneration, when the water flow is constant and maximal (3.0 l/s). The variable airflow is calculated using equation (3.8) based on conservation of energy. The heat supplied by the water flow through the coil and the fan dissipation (appendix F) has to equal the amount of heat added to the airflow. Figure 3-9 shows the calculated profile, which can be fitted with equation 3.9.

$$\varphi_{air} = \frac{P_{fan,dis} + (T_7 - T_6) * 3.0 * 4.2}{(T_5 - T_2) * 1.2 \text{ (kJ/m}^3\text{)}} \quad (3.8)$$

$$\varphi_{air} = 1069 * P_{fan} + 3886 \quad (R^2: 0.998) \quad (3.9)$$

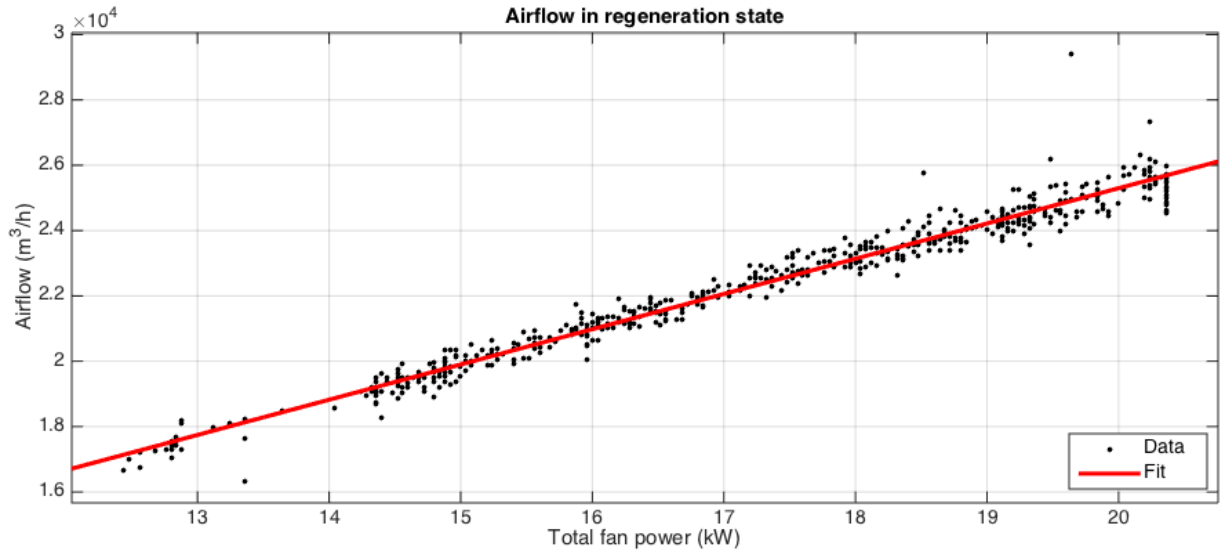


Figure 3-9 - Variable airflow fit

Using equation 3.9 the heat transfer function of Figure 3-10 (variable air flow) is plotted (and fitted with equation 3.10). The transferred heat is calculated using the same method as equation 3.8. The LMTD is calculated using the water temperature difference over the coil (T6/T7) and the air temperature sensor T2 and T5 (corrected for the dissipation of both fans).

$$AU_{airflow} = 4.793 \times 10^{-4} * \varphi_{air} + 4.223 \quad (R^2: 0.998) \quad (3.10)$$

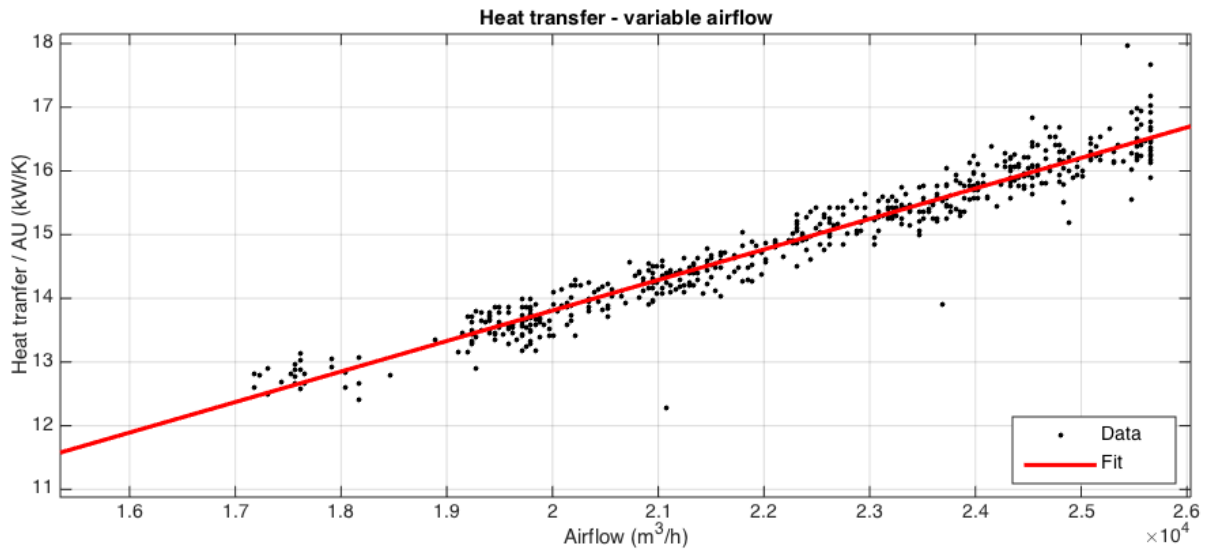


Figure 3-10 - Heat transfer during variable airflow (regeneration state)

The heat transfer at the maximum airflow is 16.5 (kW/K), so minimal thermal resistance is the inverse value, 0.0606 (K/kW). The additional thermal resistance when the airflow is lower than the reference case (25700 m³/h) is calculated using equation 3.11.

$$R_{airflow} = \frac{1}{4.793 \times 10^{-4} * \varphi_{air} + 4.22} - 0.0606 \quad (3.11)$$

After distracting the additional resistance caused by the lower airflow during office hours (23000 versus 25700 m<sup>3</sup>/h), the effect of the variable water flow is plotted (Figure 3-11) and fitted with equation 3.12. The assumption that the heat transfer coefficient does not change significantly when condensing seems justified by the relative straight scatterplot.

$$AU_{waterflow} = \frac{0.42 * \varphi_{water}^2 + 15.49 * \varphi_{water} - 2.446}{\varphi_{water} + 1.93} \quad (R^2: 0.994) \quad (3.12)$$

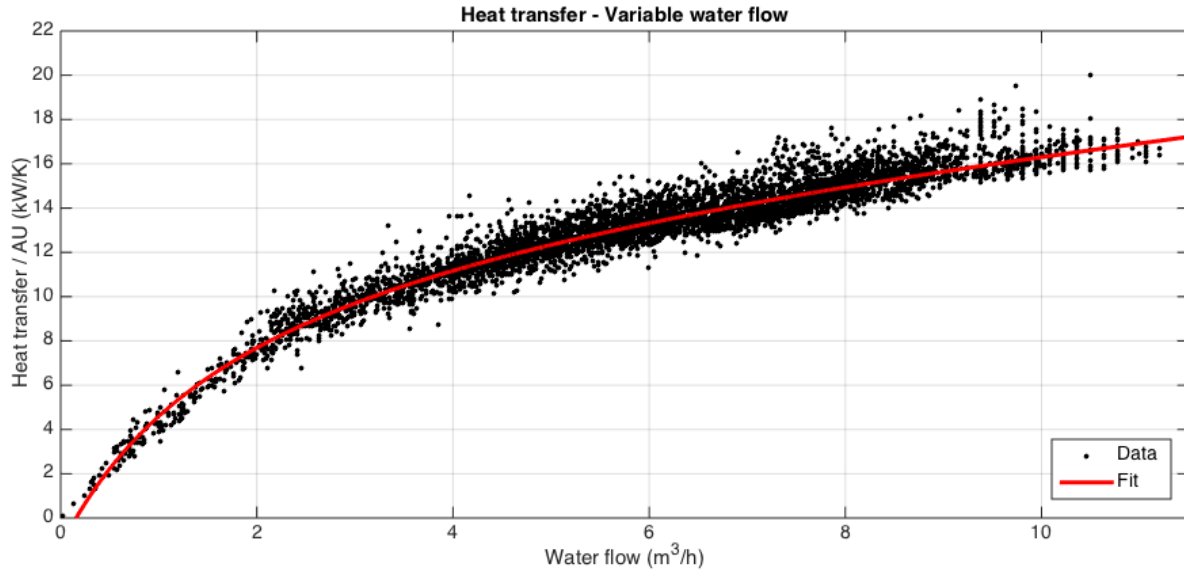


Figure 3-11 - Heat transfer during variable water flow

Equation 3.13 gives the thermal resistance of water flows. The inversed sum of the three resistances (fixed, water and air) can be simplified to equation 3.14, which is the main heat resistance equation for the AHU coil. This equation is only valid for airflows between 17.000 and 25700 m<sup>3</sup>/h and water flows between 0 and 11 m<sup>3</sup>/h, because the equation is based on data within this range (Figure 3-10 & Figure 3-11).

$$R_{waterflow} = \frac{\varphi_{water} + 1.93}{0.42 * \varphi_{water}^2 + 15.49 * \varphi_{water} - 2.446} - 0.0606 \quad (3.13)$$

$$AU_{coil} = \left( \frac{\varphi_{water} + 1.93}{0.42 * \varphi_{water}^2 + 15.49 * \varphi_{water} - 2.446} + \frac{1}{4.793 * 10^{-4} * \varphi_{air} + 4.22} - 0.0606 \right)^{-1} \quad (3.14)$$

### 3.2.5 RESULTS

As introduced, the AHU coil is evaluated in cooling and regeneration state. Both use the same heat transfer equation (3.14), but they differ in goal and control strategy method (introduced in sections 3.2.2 and 3.2.3).

#### AHU COIL - COOLING STATE

To evaluate the accuracy of the cooling state model, three aspects are evaluated: the absolute humidity of the supply air, the water flow and the return temperature. The input data (T2, T3 & T6) for this graph is a filtered dataset for all events where the cooling valve is open. The result is a simulation of 'continuous' cooling operation during summer days. Figure 3-12 shows a fragment of these simulation results. In general, the flows and temperatures are accurate if the absolute humidity is simulated accurate. A deviation of the temperature is compensated by an opposing deviation of the flow to ensure the same amount of heat is transferred.

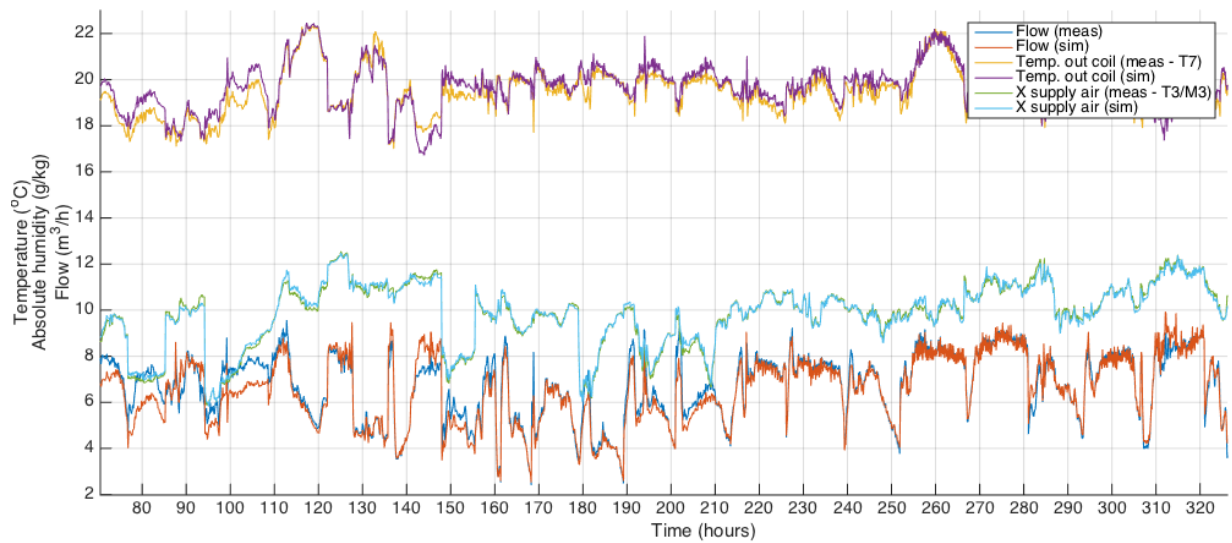


Figure 3-12 - Simulation AHU cooling state

#### AHU COIL - REGENERATION STATE

Simulation results of the regeneration state (Figure 3-13) show a comparable accuracy. The same method of dataset filtering (but now for each event where the regeneration valve is opened) is used to create a test dataset of continuous winter days in regeneration mode.

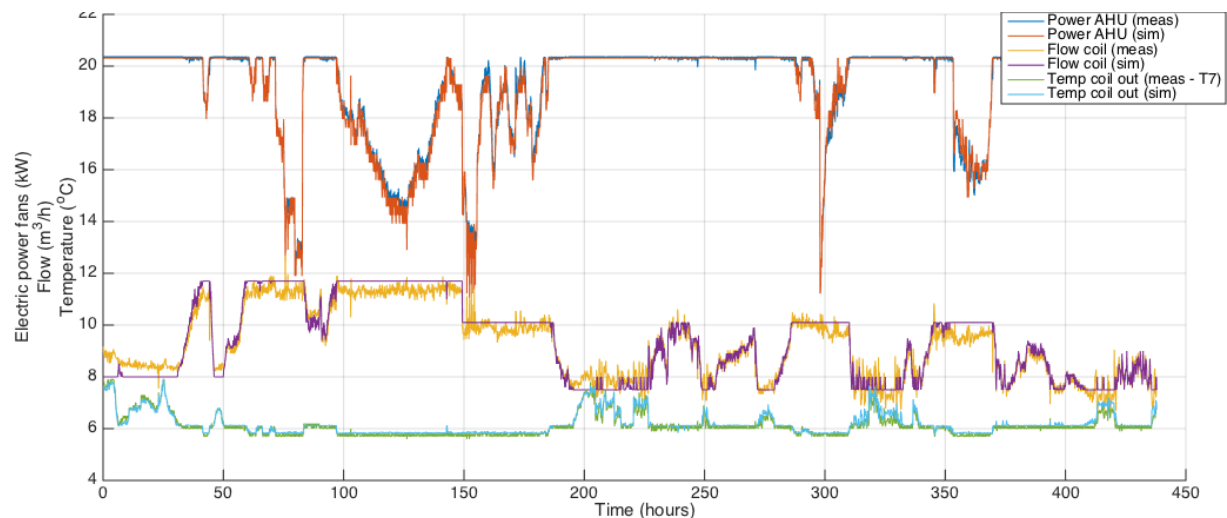


Figure 3-13 - Simulation AHU regeneration state

As visible in the plot, the minimal and maximal water flows are differing before and after hour 150. This is caused by a design simplification of the system. Instead of using a pressure controlled pump and (balancing) valves for a constant minimal and maximal flow, the pump is operated at 50% for minimum flow and at 80% for maximum flow. After hour 150 the pump of the heat pump circuit is simultaneously active, causing a larger summed flow and pressure drop over the ATES heat exchanger, which causes a decrease of the flow over the AHU coil. A pressure controlled pump would compensate this by increasing its capacity to (for example) 90% and maintain the same maximum flow of 3.0 (l/s). To compensate this, the minimum and maximum flows are adjusted for the part where the heat pump circuit is active.

### 3.2.6 DISCUSSION

In this section two main aspects of the AHU were analyzed: the physical characteristics (heat transfer and air flows) and the simulation of the control strategy.

The physical characteristics were reconstructed using data analysis. This method was chosen explicitly to simulate the behavior as simple but still realistic as possible. The resulting plots showed quite good results compared to the simplicity of the method. However, there are two significant downsides on this method:

First, the method heavily relies on sensor accuracy (which is  $\pm 0.8^{\circ}\text{C}$  and  $\pm 3\%\text{RH}$  in commonly used air sensors [44]). Before manual determination of the offsets of all sensors (using a calibrated measurement tool – Appendices E&F), the results were significantly worse. Because the sensors are originally intended only for monitoring and controlling the system, not a very large accuracy was needed. However, if in the future methods like these are implemented, it is essential to use more accurate sensors and plan a periodical recalibration routine.

Secondly, the method used the assumption of a constant flow (water or air) to calculate the variation in the other flow (based on conservation of energy). This was necessary because there was no separate flow meter installed in series with the coil. For this case it was possible to solve using this trick and manual measurements of the constant flows, but new systems are often using variable airflow systems. This means both sides become variable and a separate measurement of the water flow becomes essential. For the case study system it would increase the robustness of the method, by eliminating the need for a constant flow assumption.

The control strategy was simulated using the method described in the actual software (similar to the ATES software simulation). In cooling mode it was not useful to simulate the supply water temperature and supply air temperature because of the following reasons:

- A software bug prevents the transition between state 4b (precooling with heat pump) and state 4a (ATES cooling), so the heat pump keeps running until the HVAC is shut down.
- A part of the (warm) local cooling return water is leaked into the supply water of the AHU cooling coil, making the actual supply temperature unpredictable.
- Kropman employees change the central heating curve quite often (>10 times per year), while the method assumes fixed heating curve setpoints.

In regeneration mode there were two deviations from the explained software simulation method:

- The maximum water flow was not constant, because it is not pressure controlled.
- Instead of the outdoor temperature ( $T_1$ ) the coil intake temperature ( $T_2$ ) was used, because air leaks through the recirculation valve and the HRW.

In the application of the method for CC the complete control strategy is used, so the impact of these deviations can be analyzed. For now, the model was adjusted to match reality, but the final goal of CC is to 'adjust reality' (detect and fix problems) to match the model.



### 3.3 LOCAL COOLING SIMULATION METHOD

The 'local cooling group' is the combined system of over a hundred chilled beam units and three floor cooling systems. The behavior of this system is mainly influenced by the indoor temperature, the cooling load and the supplied water temperature. This section explains the method to predict the water flow and temperature generated by this combined group.

#### 3.3.1 THEORETICAL BACKGROUND

As introduced, the system consists of chilled beam units (80% of the capacity) and floor cooling systems (20%). The software strategy that controls the supplied water temperature is the main input variable for both systems. The background of those three systems is introduced in this part.

##### CHILLED BEAM UNITS

The principle of a chilled beam unit is demonstrated in Figure 3-14. Fresh (centrally heated or cooled) air is supplied from above and accelerated via the small cavities (nozzles) at the left and right side. The high velocity air creates a lower pressure inside the unit (like airplane wings), drawing warmer office air through the heat exchanger in the chamber above. By circulating warm or cold water through the heat exchanger, the air can be heated or cooled. The air is mixed with the fresh supply air and recirculates into the office space. The unit automatically controls the heating or cooling water supply, to reach the demanded room temperature setpoint.

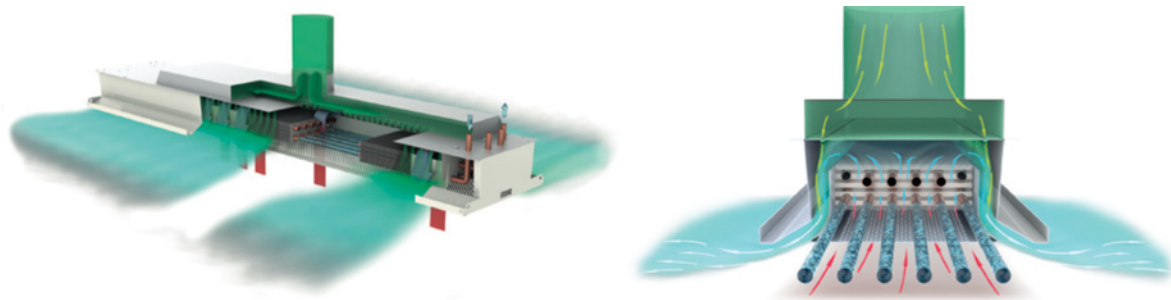


Figure 3-14 - Air flow principle of a chilled beam unit [45]

According to the datasheet [45] (OKNI 300-1800 / 90m<sup>3</sup>/h) the cooling capacity of a single unit is roughly 300 Watt, using supply water of 15 °C and an indoor temperature of 22 °C. A higher cooling capacity can be achieved by increasing the temperature difference. If the indoor temperature is 25 °C, the unit can deliver 450 Watts of cooling using the same supply water temperature and flow. The same 450 Watts can also be achieved using 12°C supply water and a 22°C room temperature. The temperature increase of the return water is respectively 1.5°C and 2.2°C, using a maximal water flow of 2.8 liter per minute. This already indicates that the effect of varying room temperatures within the building is not expected to be very large.

##### FLOOR COOLING

On the first floor level and the restaurant floor cooling is applied. For the restaurant it is the main cooling source and for the first floor it is used as additional cooling. The concept of floor cooling is simply circulating chilled water through the floor heating system. Because cold air floats down, the cooling effect of floor cooling is not very large.

Like the chilled beam units, the return temperature will be influenced by the average indoor temperature. The floor cooling systems are coupled to the cooling group via a heat exchanger, which significantly reduces influence on the temperature. Because floor cooling (at maximal/design capacity) only uses 20% of the local cooling water flow, the effect on the return water temperatures is expected to be small.

## SUPPLY WATER TEMPERATURE

The main control strategy of the local cooling group is the supplied water temperature. Other than the cooling coil in the AHU, condensation of air on floor cooling or chilled beam units should be avoided at all times. To ensure this the supply water temperature is always kept above the dew-point temperature of the AHU's return air (measured with T4/M4). This is done by mixing supply water with the warmer return water using a three-way valve. The temperature is kept at minimal 15 degrees (to ensure the return temperature is high enough for storage in the ATES) and is increased when the dew temperature is higher.

In the AHU section already a method is introduced to simulate the dehumidification of the supply air. To predict the humidity of the return air, the amount of added moisture during ventilation through the building must be taken into account. Because the building does not have a lot of plants, has no (operational) kitchen and is not very crowded, the moisture increase is expected to be not very significant. By calculating the dew temperature (using the methods from [43]) the offset on the default supply temperature of 15 °C is calculated.

### 3.3.2 DATA ANALYSIS

As introduced, the local cooling group behavior is related to the average indoor temperature. The average indoor temperature is calculated by averaging the temperatures of the five large open offices. The cooling load is reconstructed by distracting the AHU cooling load from the total load on the ATES system. Figure 3-15 shows the relation between both, which can be fitted by equation 3.15. The large deviations in the plot are caused (for example) by local setpoint variations (controlled by presence detection), errors in the AHU load calculation and local internal heat load variations. As visible in the graph, the average indoor temperature is indeed related to the total local cooling load. The variations in average indoor temperatures are relative small.

$$T_{indoor} = 3.15e-4 * P_{cool,loc}^2 - 5.31e-4 * P_{cool,loc} + 22.2 \quad (R^2: 0.915) \quad (3.15)$$

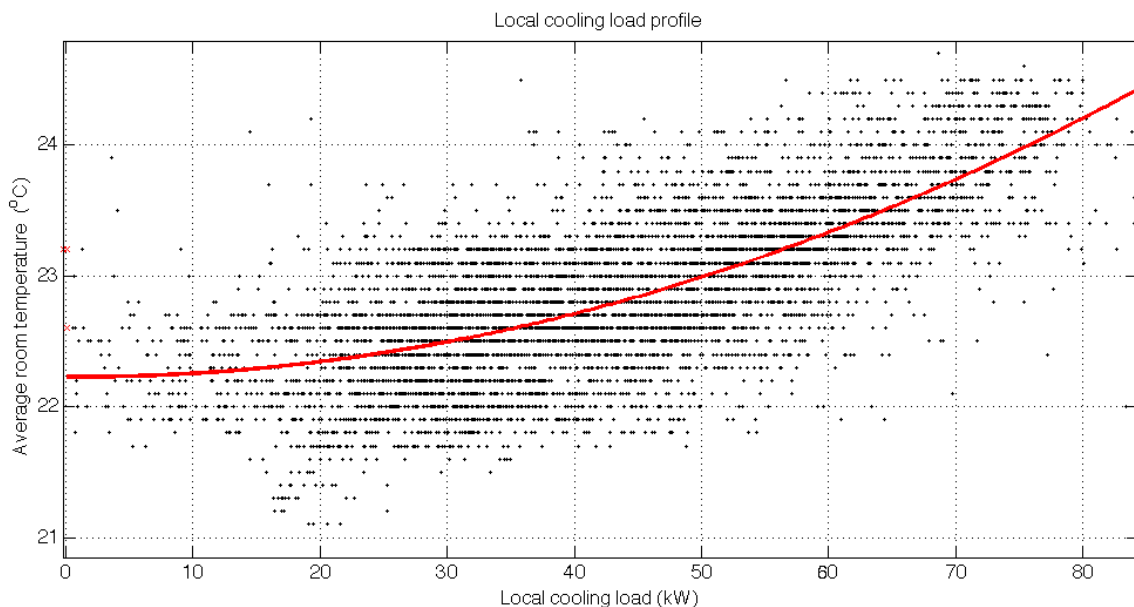


Figure 3-15 - Local cooling load versus average room temperature

Figure 3-16 shows the return temperature as function of the average room temperature. The graph shows a clear relation between those values. From the graph can be concluded that the variation in return temperature is low and in majority of the events between 16.5°C and 17.5°C. This implies that the varying total load mainly influences the flow and not the temperature. The graph can be fitted using equation 3.16.

$$T_{return} = 0.367 * T_{indoor} + 8.76 \quad (R^2: 0.981) \quad (3.16)$$

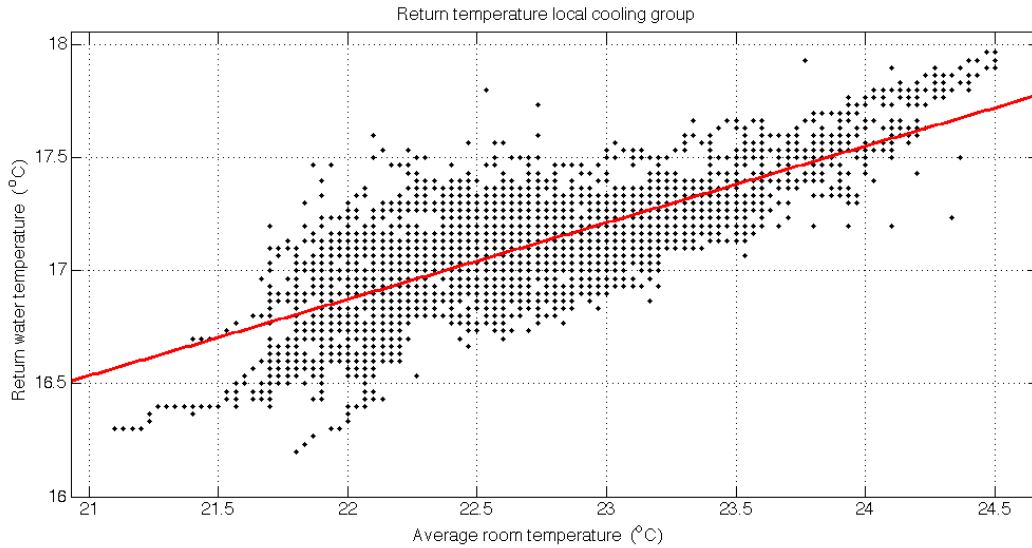


Figure 3-16 - Return temperature versus room temperature

The supply water temperature of the local cooling group is controlled using the humidity of the return air. The humidity of the supply air is simulated using the AHU model. To predict the return air humidity, the average amount of added moisture is analyzed. Figure 3-17 shows the moisture increase between supply and return air varies over the day and is on average 0.3 (g/kg). Per hour this equals 8.3 kg of moisture production in the building. An average human produces 30-60 grams of moisture per hour during light activity [46]. During office hours there are roughly 100-150 people in the building, which explains the majority of the moisture production. The average amount of 0.3 g/kg has no significant influence on the return air humidity.

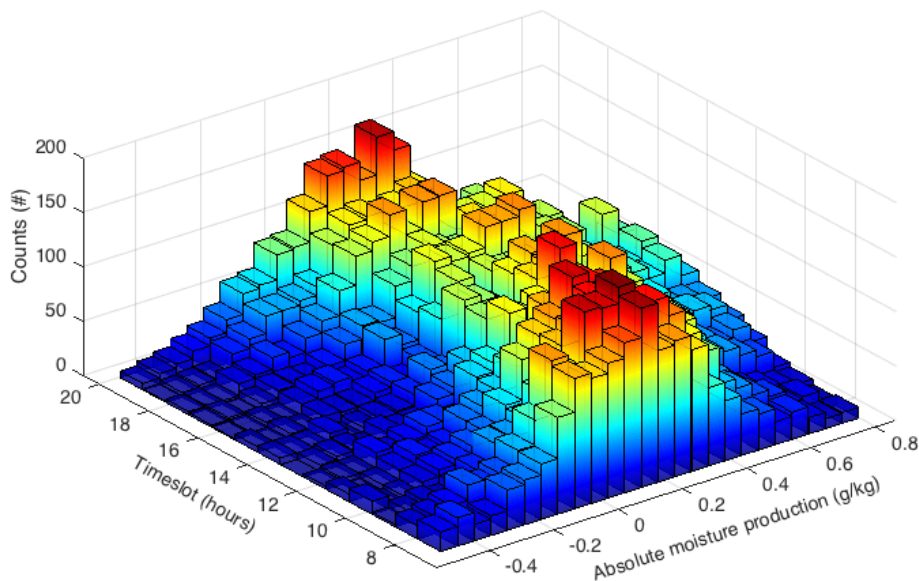


Figure 3-17 - Moisture production

### 3.3.3 RESULTS

For evaluation of local cooling group simulation method, the same dataset as for the AHU section is used. Three aspects are simulated:

- The supply water temperature is calculated based on the dew-point temperature of the return air (calculated from simulated supply air + 0.3 g/kg).
- The return water temperature is calculated as function of the cooling load plus the dew-point temperature offset.
- The flow is calculated using the cooling load and the  $\Delta T$  between supply and return.

Figure 3-18 shows simulation results of a part of the dataset. The supply and return temperatures are predicted within 0.5°C accuracy for the majority of time. If the simulated  $\Delta T$  deviates (caused by supply or return deviation), flow is obviously also deviating.

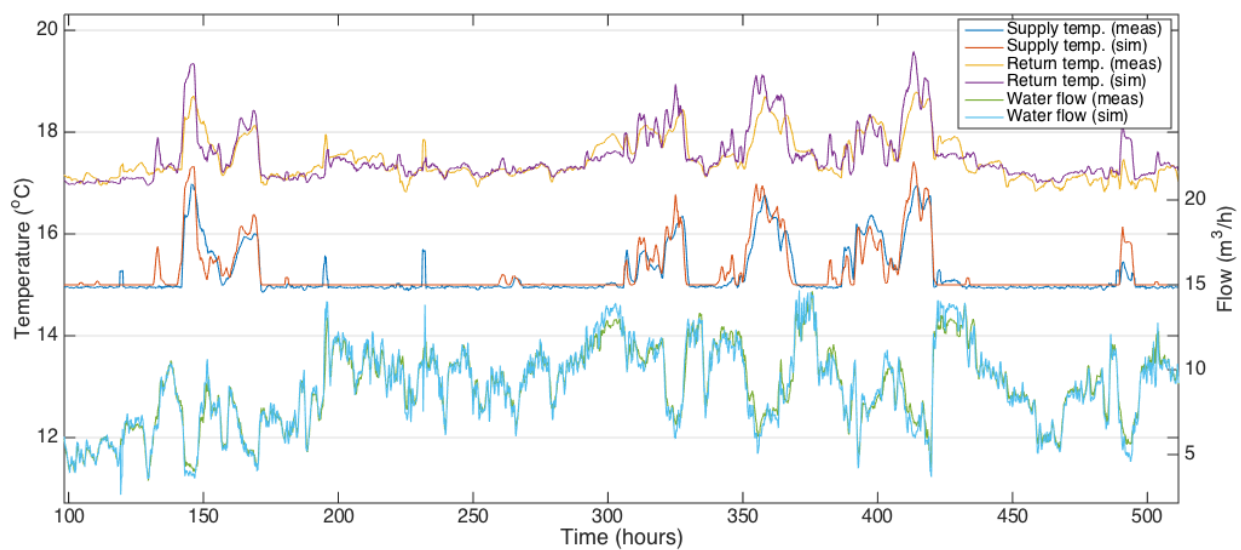


Figure 3-18 - Local cooling group simulation

### 3.3.4 DISCUSSION

Analysis of the local cooling group proved that this group behaves quite predictable, although it consists of over a hundred individual units and floor cooling systems. An explanation can be found in the fact that both water and indoor air temperatures hardly fluctuate over the year. The supplied air (room temperature) is constantly between 22°C and 25°C and the water temperature between 15°C and 17°C. In buildings with larger temperature variations (older buildings or rooms with very large occupancy variations) this method probably is not applicable.

### 3.4 HEAT PUMP SIMULATION METHOD

The remaining method for the HVAC part is the simulation of the heat pump behavior. The main goal of this section is simulation of the supplied water temperature and flow to the ATES system, as function of the warm water temperature. This section introduces the background, method, data analysis and an evaluation of results.

#### 3.4.1 THEORETICAL BACKGROUND

The heat pump extracts heat from the cold-water circuit and transports it to the warm-water circuit using an electrical compressor and an evaporating and condensing gas cycle (comparable to a refrigerator). The installed heat pump has a very straightforward on/off design, which makes its behavior easily predictable. The simulation method is based on two components: efficiency and compressor electricity use.

The thermal efficiency of a heat pump is called the COP (Coefficient of Performance), which is the ratio between produced heat and the added electric energy. The COP depends on the temperature difference between the cold side (evaporator) and the warm side (condenser). The theoretical efficiency is determined using the Carnot efficiency (eq. 3.17). The actual achieved COP is a factor of the Carnot COP. This factor is called the irreversibility factor ( $k$ ) (eq. 3.18).

$$\text{COP}_{\text{carnot}} = \frac{\bar{T}_{\text{warm}}}{\bar{T}_{\text{warm}} - \bar{T}_{\text{cold}}} \quad (3.17)$$

$$k = \frac{\text{COP}_{\text{actual}}}{\text{COP}_{\text{carnot}}} \quad (3.18)$$

The temperatures are in degrees Kelvin and the mean values are calculated using the LMTD method. The  $k$ -factor varies as function of both COP's, depending on the heat pump design. Every heat pump is designed for an optimal temperature range, where it achieves the highest  $k$ -factor.

The electricity use of a heat pump depends on the amount of work the compressor performs (as with any engine). When the  $\Delta T$  between condenser and evaporator increases, the required pressure for the gas to condensate increases [47]. This increases compressor load and so electricity use. It has the counter intuitive effect that a higher COP can result in less heating capacity, because the compressor uses less electricity.

#### 3.4.2 HEAT PUMP SIMULATION METHOD

Because of the simple design, the mean temperatures over the condenser and evaporator side are the only two variables that influence the performance of the heat pump. Figure 3-19 shows the schematic overview of the heat pump and buffer vessels.

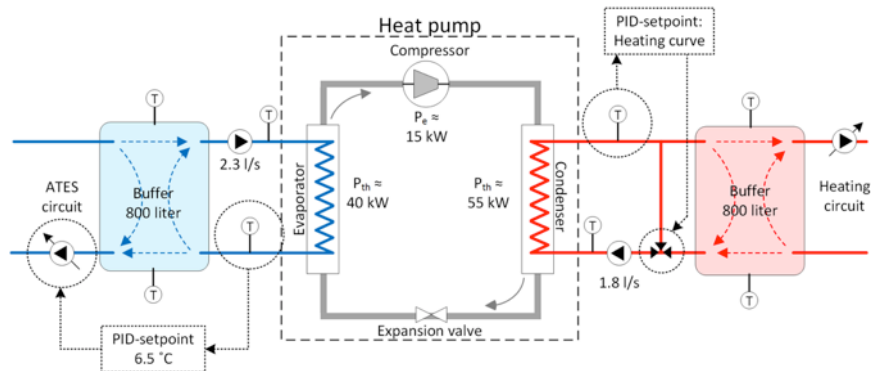


Figure 3-19 - Heat pump system diagram

The cold (ATES circuit) water flow through the cold buffer vessel is PID-controlled to keep the return temperature on the evaporator side at 6.5 °C. The  $\Delta T$  over the evaporator is roughly 4 °C, so the mean evaporator side temperature is 8.5 °C. The flow over the ATES circuit is slightly lower than over the heat pump circuit, because of the larger temperature difference (12°C / 6.5°C for the ATES circuit versus 10.5°C / 6.5°C for the heat pump circuit). Because the flow over the heat pump is higher, the supplied temperature to the ATES circuit can be safely assumed to be also 6.5 °C. Using this assumption the ATES circuit flow can be calculated using equation 3.19.

$$q_{heatpump}[l/s] = \frac{P_{hp, evap}}{(T_{ATES} - 6.5) * 4.2} \quad (3.19)$$

Because the evaporator side temperature is assumed to be constant (at 8.5 °C), the condenser side temperature is the only variable of the heat pump behavior. The condenser side temperature is controlled by a heating curve and a PID-controller. The PID controls the 3-way valve in the supply water, which recirculates a part of the heated water to reach higher supply temperatures. The  $\Delta T$  over the condenser is roughly 7°C. The heat pump is started when the upper buffer temperature sensor drops below the heating curve temperature and stops when the bottom buffer sensor gets above the heating curve temperature. This causes a variable condenser side temperature during this start/stop cycle. In the beginning the supply temperature is approx. 7 °C below the heating curve and the return temperature is equal to the heating curve. At the end of the cycle the supply temperature is nearly equal to the heating curve and the return temperature is 7 °C above the heating curve. It is assumed that the average condenser temperature over a cycle is equal to the heating curve.

### 3.4.3 DATA ANALYSIS

In this section the data extracted from the BMS is analyzed to find the needed data fits. The used dataset contains the data of 2013 and values are filtered on steady state operation (>2 time samples) without the first value (to exclude startup effects). Figure 3-20 shows the k-factor is decreasing at higher Carnot COP's. This (correctly) indicates the heat pump is optimized for (high  $\Delta T$ ) heating use instead of being a cooling machine. The k-factor is fitted using equation 3.20.

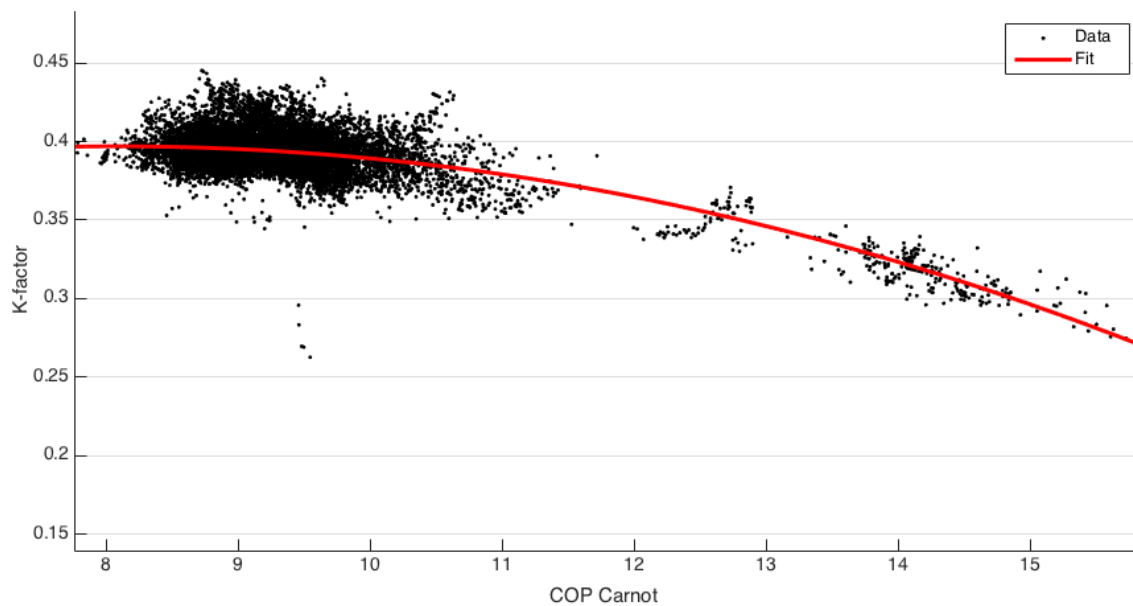


Figure 3-20 - Heat pump K-factor / irreversibility factor

$$k = -0.0021 * COP_{carnot}^2 + 0.034 * COP_{carnot} + 0.259 \quad (R^2: 0.949) \quad (3.20)$$



Figure 3-21 shows the heat pump electricity use. The electricity use is reconstructed from the difference between heating and cooling capacity. The actual electricity use can be higher, because of energy losses and auxiliary energy use (pumps, electronics). As predicted, the electricity use (proportional to the compressor load) increases at lower COP's. The graph is fitted using equation 3-21.

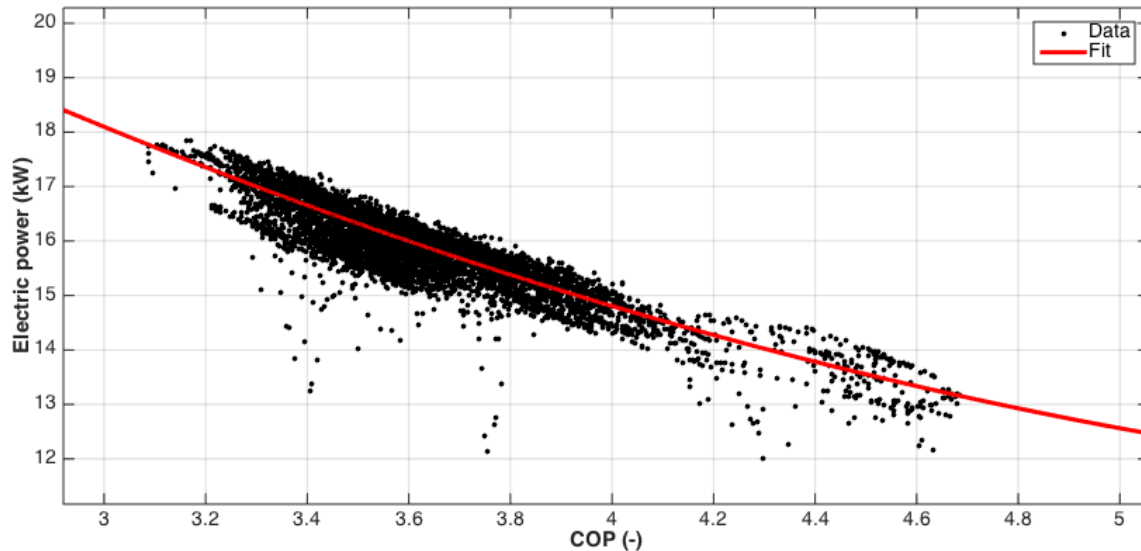


Figure 3-21 - Electricity use heat pump

$$P_{el} = 0.523 * COP^2 - 6.95 * COP + 34.3 \quad (R^2: 0.81) \quad (3.21)$$

Figure 3-22 shows the measured mean condenser temperature and the heating curve. In the heating mode (-5°C to 15°C) the temperature varies  $\pm 5^\circ\text{C}$ . In cooling mode the temperature is 5°C higher than expected. The deviations are mainly caused by leaking of the 3-way mixing valve in the condenser circuit (Figure 3-19), which is further described in appendix J.

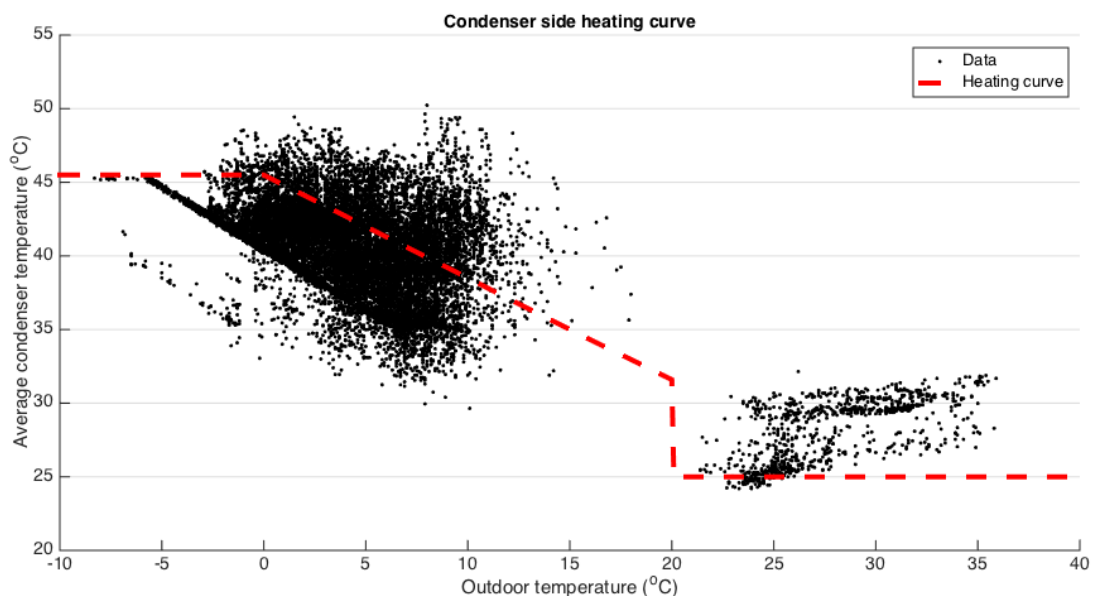


Figure 3-22 - Heat pump heating curve analysis

### 3.4.4 RESULTS

Using the derived equations in this chapter, the behavior of the heat pump is calculated in five steps:

- 1) The condenser temperature is derived from the heating curve and outdoor temperature
- 2) The Carnot COP is calculated from the mean condenser temperature and the assumed evaporator temperature of 8.5 °C
- 3) The actual COP is calculated using the k-factor equation
- 4) The electricity use is calculated based on the actual COP
- 5) Using the electricity use and actual COP the heating and cooling capacity is calculated

As shown in Figure 3-22 the main inaccuracy of this calculation is caused by the mismatch between condenser temperature and heating curve. For that reason only step 2 to 5 are evaluated. Figure 3-23 shows the results of the simulation versus the actual measurements. The measured values are filtered on steady state operation (>2 time samples) and a mean evaporator temperature within 1 °C of the assumed 8.5 °C. The simulated curves on average match the measurements, but with a scattered distribution.

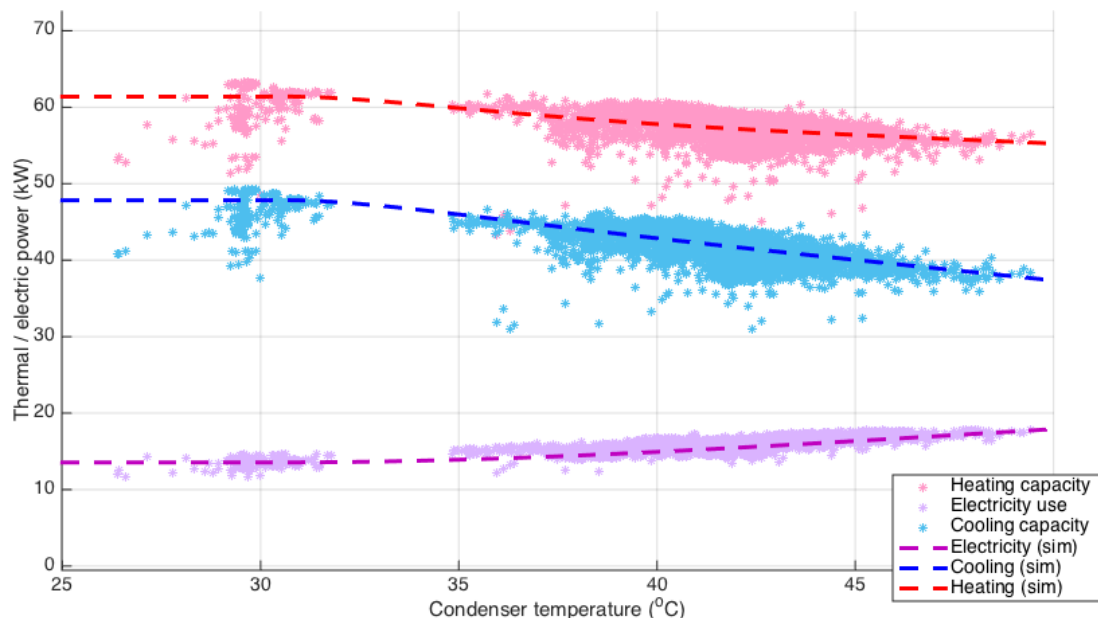


Figure 3-23 - Heat pump performance at variable condenser temperature

### 3.4.5 DISCUSSION

The analysis of the heat pump data and development of this simulation method reveals a key challenge for this way of modeling. *To predict the behavior of a component, the component itself has to behave predictable.* The cyclic on/off behavior of the heat pump can be simulated using a much shorter time interval (for example 10 seconds), but with the logged 8-minute data it is difficult to analyze the short-term fluctuations. Nevertheless, the general behavior of the heat pump showed to be predictable as function of the condenser temperature. The actual effect of the large condenser temperature variations showed to be minimal, because the capacities do vary only a few percent within a 5°C range of condenser temperatures (Figure 3-23).

From an (software) engineer's point of view, it makes sense to use the large (cyclic) temperature swings for filling the buffer vessel. It utilizes the maximal buffer capacity and reduces the number of starts and stops. From an energetic point of view however, the condenser temperature is too high for efficient operation. This could be solved by increasing the condenser side flow and hence reducing the condenser  $\Delta T$ . In the current situation however, the implementation of a heating curve makes hardly any sense.



### 3.5 DISCUSSION

In this chapter the configuration of the HVAC system is explained and the methods are introduced to simulate the water flow and temperature supplied to the ATES simulation method of chapter 2. This section gives a short recap of the used method and a general discussion.

#### 3.5.1 RECAP

In chapter 2 the method is explained how the ATES heats or cools the water from the buildings HVAC system. The main goal of this chapter is to simulate the water temperatures and flows as input for the simulation model of chapter 2. First the systems components and states are analyzed and next a simulation method for each main component is presented. This chapter is very case study specific, but parts could be possibly applied to other buildings.

The **AHU simulation method** is constructed around the heat transfer function of the central cooling coil. This coil is used in both the cooling and regeneration state of the AHU. For both states a method is explained and evaluated to simulate the water temperature and flow supplied back to the ATES. The method of reconstructing the heat transfer function from historical data is probably universally applicable to other AHU systems.

The **local cooling simulation method** is not based on a physical phenomena or process (like heat transfer for instance), but on the return water temperatures filtered from historical data. The method is more like finding a 'fingerprint' of the combined behavior of all chilled beam units. The method needs the local cooling load as input, for which a method is defined in section 4.2.

The **heat pump simulation method** is based on reconstructing the elementary characteristics of the heat pump (k-factor and electricity use). This method is applicable to all single stage (on/off type) heat pumps. Although this method simulates how the heat pump behaves when active, it does not define for what period the heat pump is active. This is defined in section 4.3.

Although this chapter introduced all possible states and needed component methods, it is not a complete simulation model. The influence of the actual building (the heating and cooling loads) is missing. These are introduced in chapter 4.

#### 3.5.2 DISCUSSION

Because the modeling results are already discussed per method, only a general discussion of the methods is given in this section. All methods have in common that they are based on historical data instead of manufacturer specifications. The methods proved that data analysis is a powerful tool for reconstructing relations of underlying physical phenomena and the construction of simulation models. To successfully apply these methods, three conditions must be met:

- **Sensor accuracy.** The actual accuracy of used temperature sensors is currently  $\pm 1K$ , which is not accurate enough for these methods. Installation of more accurate sensors ( $\pm 0.1K$ ) and periodically calibration is required.
- **Minimize assumptions.** Because the HVAC parts do not have separate flow sensors, assumptions for constant (water / air) flows were needed. This decreases accuracy and increases the need for human intervention in the model. Placement of more flow sensors in the system increases simplifies modeling and increases model robustness.
- **Dataset coherence.** As introduced in chapter 2, the logging of all sensors in the building takes around 5 minutes. So, as statistical average, the supply and return temperature of a HVAC part are measured 2.5 minutes apart. For an accurate dataset, logging should be done within a few seconds.

If methods like these are implemented in future buildings, these conditions should be taken into account during the design process of the buildings HVAC system.

## 4. LOAD SIMULATION MODEL

---

This chapter completes the reference model, by explaining the loads and states simulation model. A method for analysis of historical data is introduced and the way this data is interpreted and implemented in the reference model.

### 4.1 INTRODUCTION

As explained in section 3.5, the goal of this chapter is to simulate the local cooling load, the heating load and the buildings HVAC system states (as introduced in section 3.1). As introduced in the research structure (Figure 1-5) these loads are simulated as function of weather data (containing a timestamp, outdoor temperature and humidity).

For simulation of the loads for the reference model there are two possible methods: theoretical modeling of the building or reconstructing from historical data.

- Theoretical modeling would imply the use of calculation models based on insulation values, internal heat loads, etc. to simulate the theoretical heating and cooling loads. The results differ (almost per definition) from the actual loads.
- Reconstruction from historical data uses the logged loads in the past, to predict the future loads. These results are more accurate, but non-optimal behavior in the past is also included in the reference model and though in the prediction model.

For continuous commissioning (CC), the theoretic modeling would be the most suitable method. Using this method an indication can be given how much the actual behavior deviates from the theoretical behavior. If reconstruction from historical data is used, only deviations from the historical performance can be detected. For model predictive control (MPC), the historical data method is preferred. Sub-optimal behavior in the past is probably also present in the future, and should be included in the prediction model.

Because the focus of this research is 'maintaining the ATES balance', the accuracy of the reference model for MPC is the most important aspect. Also, with keeping the future goal of automated implementation (CC and MPC) in mind, learning from historical data is more useful than manual theoretic simulation. Every change in building use (empty floors, changing internal heat loads) requires a new (manually performed) theoretical simulation. For further research however, theoretical modeling is an interesting addition.

This chapter introduces two methods. Section 4.2 introduces the method to reconstruct the load profiles. Section 4.3 introduces the method to use these load profiles to define in which state the building is operating.

### 4.2 LOAD CURVES RECONSTRUCTION METHOD

For the load curves reconstruction method the total heating and cooling load of the building is analyzed. This is needed, because the AHU heating curve is changed quite often by Kropman employees with access to the BMS. A change in heating curve temperatures causes:

- For heating: a change in the recovered heat (by the HRW) versus the actively generated heat (by the heat pump / district heating)
- For cooling: a change in cooling load of the AHU versus the local cooling systems

With the total loads as starting point, the component specific loads are calculated as function of the heating curve. This section introduces the theoretic background, method, data analysis and results.

#### 4.2.1 THEORETICAL BACKGROUND

The goal of this method is to analyze the heating and cooling load, as function of the outdoor temperature, using historical load data. To achieve this, a black box approach of the building is used. All summed ingoing and outgoing energy flows are plotted as function of the outdoor temperature. A separation between datasets ‘during office hours’ and ‘outside office hours’ is made, because the use and operation of the building differs significantly. This method is only valid when two constrains are applicable:

First, the average indoor temperature has to be relatively constant throughout time. For instance, if a building cools down significantly during nighttime ( $> 5 \text{ }^{\circ}\text{K}$ ), the thermal mass of the building is influencing the heating loads. While cooling down, heating loads are lower than expected and during reheating they are much higher. As visible in Figure 4-1, the average room temperature throughout the year is quite constant around the statistic mean of  $22.5 \text{ }^{\circ}\text{C}$  ( $\sigma = 0.83 \text{ K}$ ).

Secondly, the internal heat load should have little fluctuations throughout the day or fluctuations must be related to the outdoor temperature. The Kropman Utrecht office has the advantage to have a very constant use. The occupancy of employees is spread out between 6 am to 8 pm. During these times the office lights are always on, because of the large open offices. Due to outside blinds on all sun facing facades, the influence of sunlight is minimal and assumed to be related to the outdoor temperature. A more extensive analysis is given in appendix H.

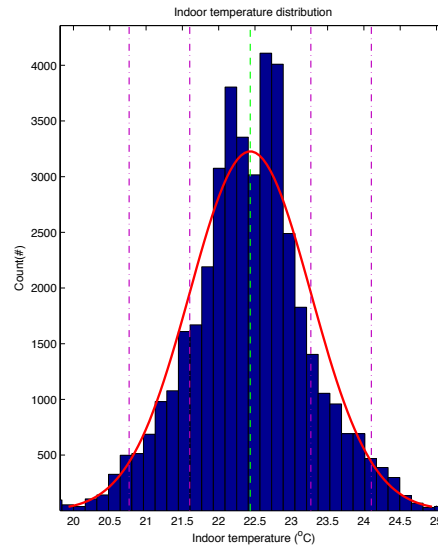


Figure 4-1 – Average indoor temperature histogram (Dataset 2013)

The total heating and cooling loads are calculated using equation 4-1 to 4-4. The heating load is the sum of the supplied heat by the heat pump in heating mode ( $P_{hpheat,con}$ ), district heating ( $P_{distheat}$ ) and heat recovery wheel in heating mode ( $P_{hrw,heat}$ ). Outside office hours the heat recovery wheel is not active. The cooling load is calculated using the cooling energy supplied by the ATES ( $P_{ATES,cool}$ ) and the heat recovery wheel in cooling mode ( $P_{hrw,cool}$ ). The difference between the generated cold (by heat pump ( $P_{hpheat,evap}$ ) or during regeneration ( $P_{AHU,reg}$ )) and the stored cold ( $P_{ATES,heat}$ ) is the redistributed cold within the building and is a cooling load. During day time the cooling load is corrected for the latent cooling load ( $P_{AHU,lat}$ ) and the electricity use of the heat pump in cooling mode ( $P_{hpcool,el}$ ).

$$P_{heat,day}[kW] = P_{hpheat,con} + P_{distheat} + P_{hrw,heat} \quad (4.1)$$

$$P_{heat,night}[kW] = P_{hpheat,con} + P_{distheat} \quad (4.2)$$

$$P_{cool,day}[kW] = P_{ATES,cool} + P_{hrw,cool} + (P_{hpheat,evap} - P_{ATES,heat}) - P_{AHU,lat} - P_{hpcool,el} \quad (4.3)$$

$$P_{cool,night}[kW] = P_{ATES,cool} + (P_{hpheat,evap} + P_{AHU,reg} - P_{ATES,heat}) \quad (4.4)$$

#### 4.2.2 METHOD

By analyzing the load curves of the building the total heating and cooling load is calculated independently of heating curves or other setpoints. The goal of this section is to introduce the methods to predict heat pump and local cooling loads from these curves. The used heating curve for this research is defined as in Figure 4-2.

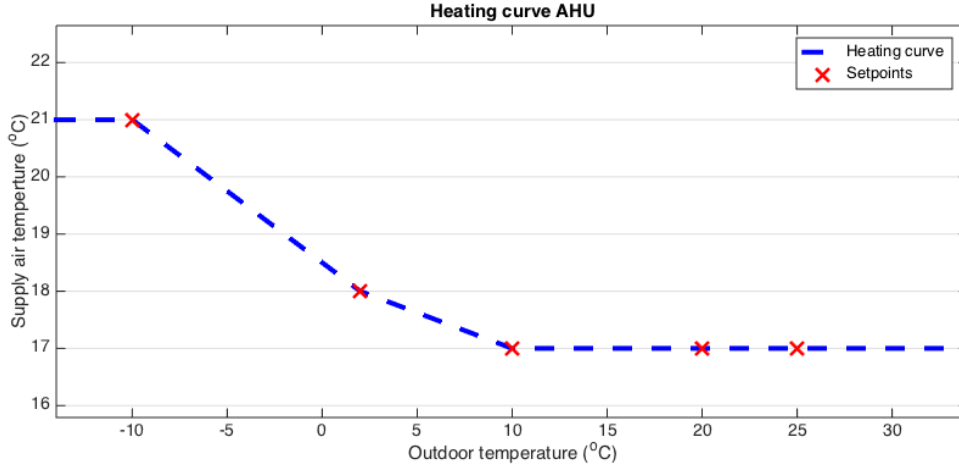


Figure 4-2 - Heating curve for supplied ventilation air

#### HEAT PUMP LOAD

The heat pump load is simulated by solving equations 4.1 and 4.2. If the heating load delivered by the heat recovery wheel is known, the remaining amount must be delivered by the heat pump and district heating. The HRW heating load is calculated using equation 4.5, 4.6 and 4.7. First the minimum outdoor temperature is calculated at which the HRW could reach the needed supply temperature (equation 4.5). Above this temperature the angular velocity is lowered and the supplied heat is calculated using the difference between the outdoor temperature ( $T_{outdoor}$ ) and the heating curve supply temperature ( $T_{sup} - \Delta T_{fan}$ ) (equation 4.6). Below the minimum temperature, the HRW is at full angular velocity and heating load is calculated using the efficiency and temperature difference (equation 4.7).

$$T_{hrw,min} = \frac{\eta_{hrw} * T_{return} - (T_{supply} - \Delta T_{fan})}{(\eta_{hrw} - 1)} \quad (4.5)$$

$$if (T_{outdoor} \geq T_{hrw,min}) \quad P_{hrw,heat} = (T_{sup} - \Delta T_{fan} - T_{outdoor}) * 1.2 * \varphi_{supply} \quad (4.6)$$

$$if (T_{outdoor} < T_{hrw,min}) \quad P_{hrw,heat} = \eta_{hrw} * (T_{return} - T_{outdoor}) * 1.2 * \varphi_{supply} \quad (4.7)$$

Using equation 4.8 and 4.9 the distribution is calculated. The heat pump load is the minimum of the remaining heating load and the maximum heating capacity. The remainder is supplied by the district heating (eq. 4.9).

$$P_{hp} = \min(P_{heat} - P_{hrw,heat}, P_{hp,max}) \quad (4.8)$$

$$P_{dist,heat} = P_{heat} - P_{hrw,heat} - P_{hp} \quad (4.9)$$

### LOCAL COOLING LOAD

For local cooling a similar method is applied. The total sensible cooling load is reduced by the heat recovery wheel (in cooling mode) and the sensible cooling load delivered by the AHU cooling coil (equation 4.11). The heat recovery wheel capacity is calculated using equation 4.10. The AHU cooling load is calculated using the supply air temperature calculated in section 3.2.

$$P_{hrw,cool} = \eta_{hrw} * (T_{outdoor} - (T_{return} + \Delta T_{fan})) * 1.2 * \phi_{supply} \quad (4.10)$$

$$P_{local,cool} = P_{cool} - P_{hrw,cool} - P_{ahu,sens} \quad (4.11)$$

The heat recovery wheel efficiency and fan dissipation temperatures are calculated in appendix F. The return air temperatures are analyzed in the next section, as function of the outdoor temperature.

### 4.2.3 DATA ANALYSIS

For this analysis a dataset of one year (2013) is used, based on hourly intervals. An interval of an hour is long enough to smooth out the start/stop behavior of the heat pump and district heating, but short enough to account for outdoor temperature variations during the day. The 'during office hours' data for is filtered on all events between 6 and 21 hours during weekdays. All events where the AHU is not active are filtered out to account for holidays.

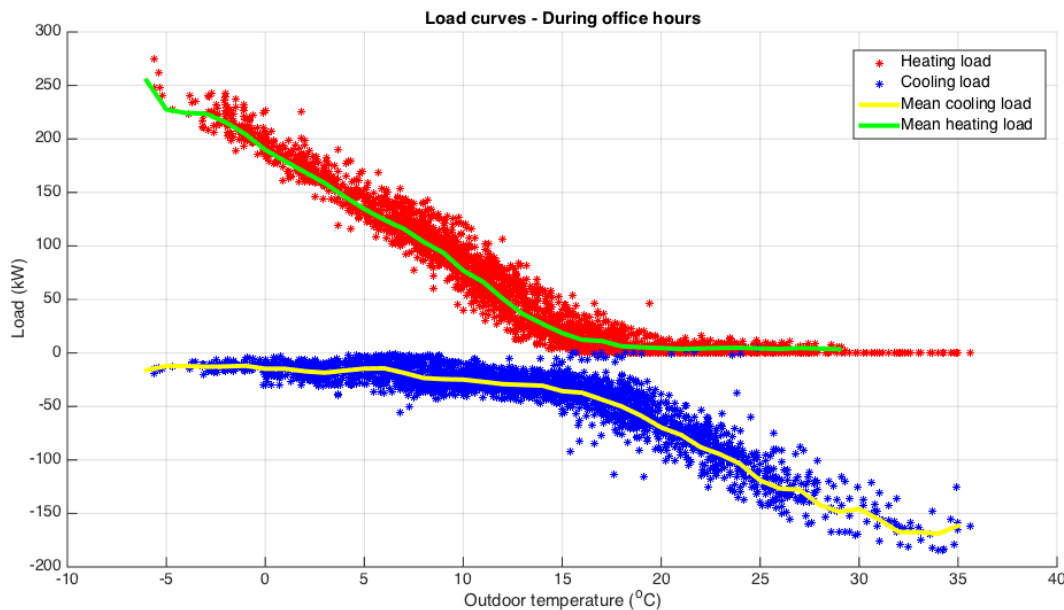


Figure 4-3 - Load curves (office hours)

Figure 4-3 shows the load profiles with the fitted mean curves during office hours. The heating load shows a nice straight curve below 15°C, but does not decrease completely to zero on warmer days. This is caused by the air leaks between the exhaust and intake air (via the HRW and startup valve (Appendix F)) causing unwanted heat recovery. The cooling load is not decreasing to zero, because there is a structural mismatch between the generated cold at the heat pump evaporator and the stored cold in the ATES. The difference between those is defined as cooling load (eq. 4.3), but is caused by leaks between the heating and cooling system (Appendix J). During higher outdoor temperatures (>20°C) the cooling load roughly follows a straight line, until the maximum cooling capacity is reached (>30°C).

Figure 4-4 shows the load profiles outside office hours. This graph shows several deviations from the expected behavior described by the system states. The first mayor deviation is that outside office hours, there should be no cooling load at all. Below 10°C the same problem is found as during office hours, as the difference between generated and stored cold is interpreted as cooling load. Below 4°C this gets even worse, because then also regeneration is active which increases the leaking effect. Between 10°C and 15°C the cooling load is created a software bug. Between these temperatures, night ventilation, ATES cooling and district heating are started simultaneously causing large waste of energy.

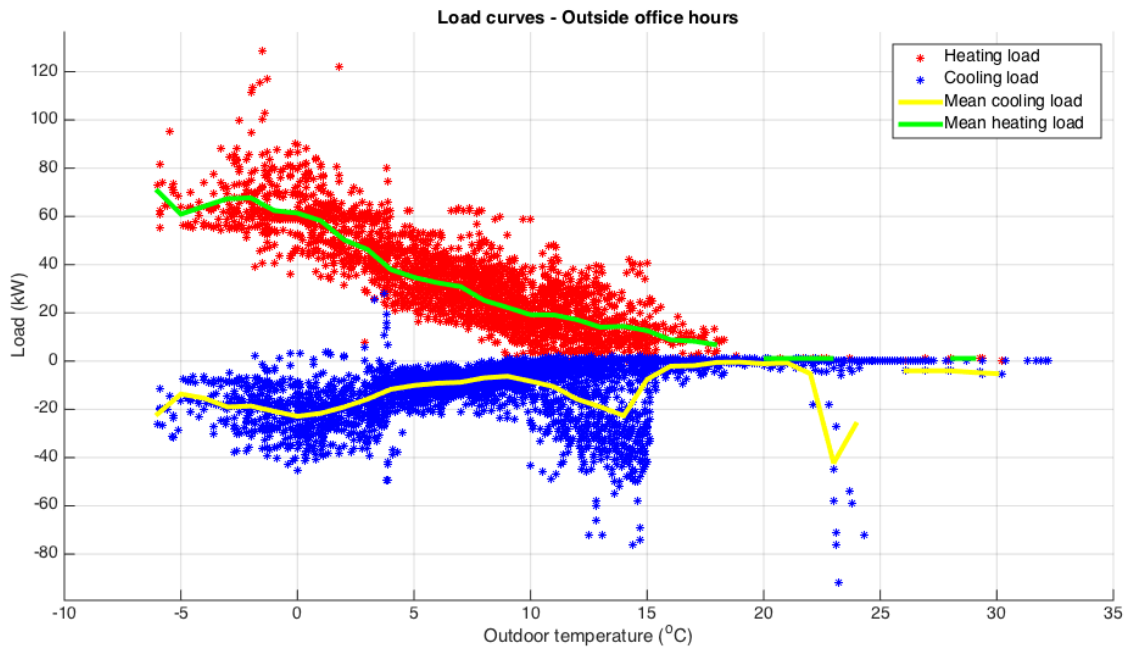


Figure 4-4 - Load curves (outside office hours)

Figure 4-5 shows the data analysis for the return air temperatures, as input for the HRW. The lower value is assumed to be 21°C (for maximal heat recovery) and the upper value is assumed at 28 °C (for cooling mode). The high return temperatures are caused by the central atrium, that creates a chimney effect. The warm air floats to the top of the atrium, where the AHU exhaust fan intake is (Figure 3-1).

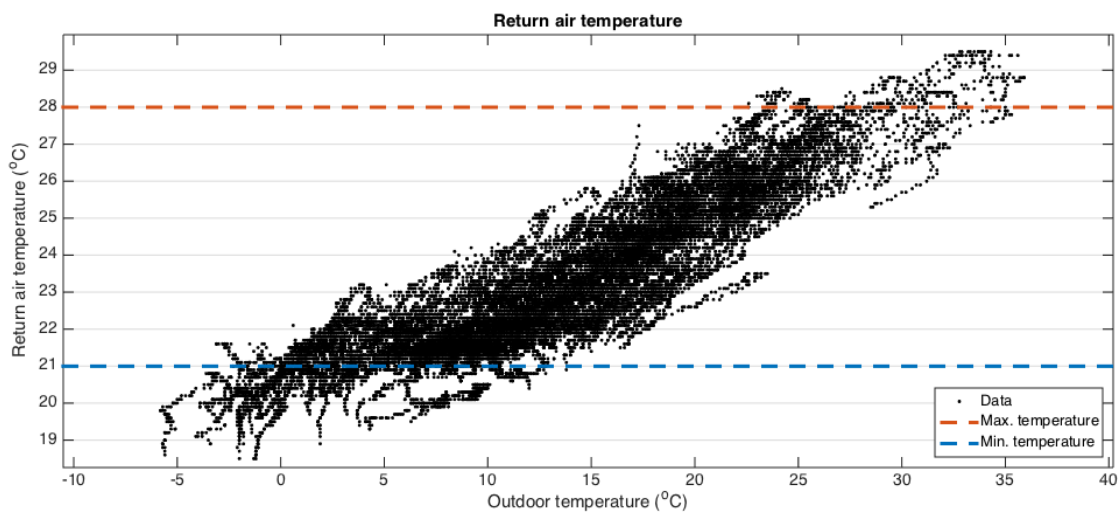


Figure 4-5 - Return air temperature for heat recovery wheel calculations

#### 4.2.4 RESULTS

The goal of this method is to calculate the local cooling (during office hours) and heat pump load (during and outside office hours). The analysis of load data showed the building has a significant amount of cooling load during conditions (outside office hours and during winter days) where no cooling load should be present. These cooling loads proved to be (Appendix J) leaks to the heating system and are cancelled out versus the heating load. Extrapolation using linear curve fitting is used to predict loads below  $-4^{\circ}\text{C}$  and above  $25^{\circ}\text{C}$ .

Figure 4-6 shows the reconstructed heating load curves. Below  $4^{\circ}\text{C}$  the heat pump is continuously operating and district heating is needed to provide the additional (peak) heating. Above  $17^{\circ}\text{C}$  there is no heating load, because heat pump operation is blocked.

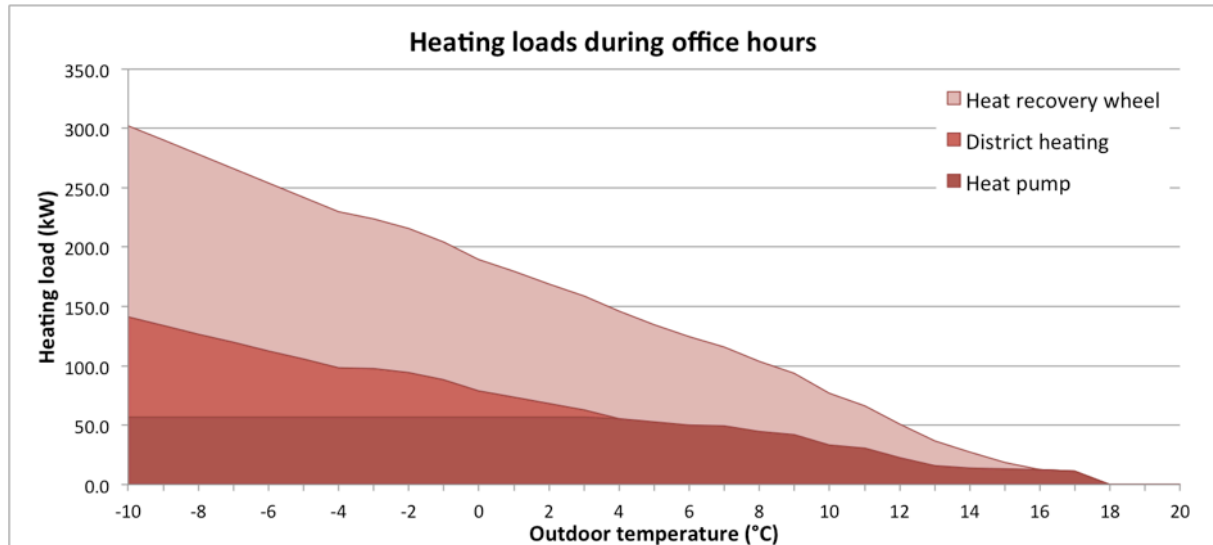


Figure 4-6 - Heating loads (office hours)

Figure 4-7 shows the reconstructed cooling loads. Local cooling starts at  $4^{\circ}\text{C}$  (lower values are ignored) and around  $16^{\circ}\text{C}$  the central cooling is started. Above  $29^{\circ}\text{C}$  the heat recovery wheel can extract cooling from the colder return air.

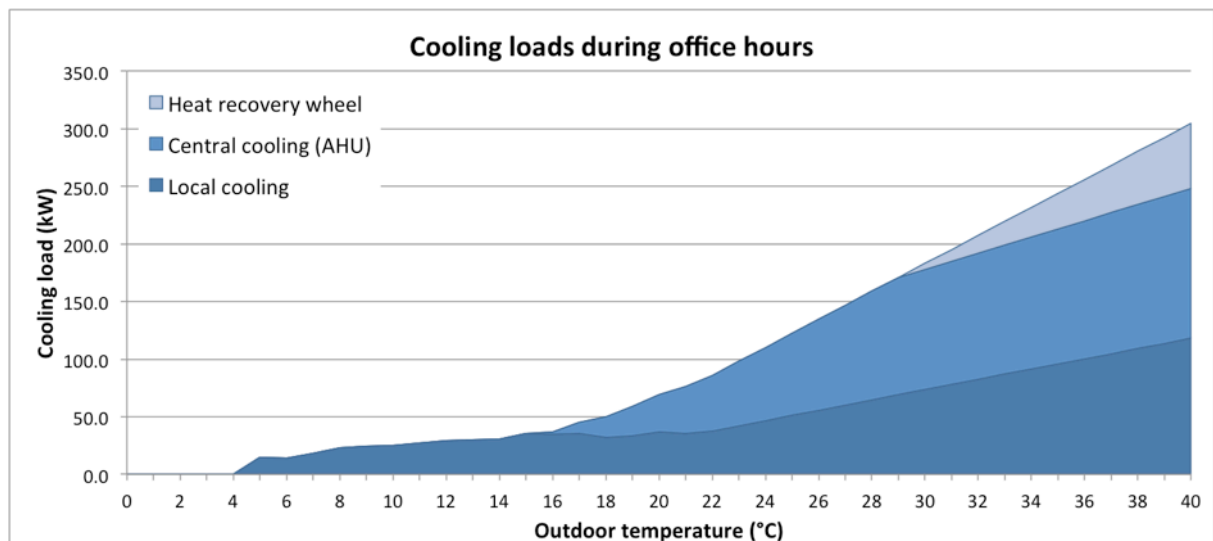


Figure 4-7 - Cooling loads (office hours)

Outside office hours only the heating load curves are needed (cooling is not active). The cooling load found in the data analysis (Figure 4-4) is cancelled out versus the heating load, because it is caused by leaks between both circuits. As example, around 0°C there is +60 kW heating load and -20 kW cooling load. The effective heating load (so without leaking) is 40 kW and is used in the heating curve (Figure 4-8). A linear extrapolation is applied of the data below 0 °C.

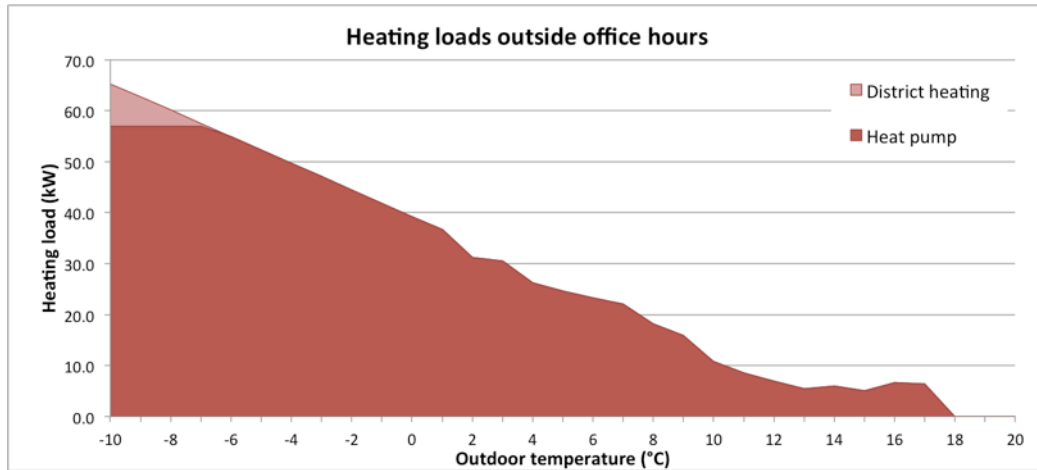


Figure 4-8 - Heating loads (outside office hours)

#### 4.2.5 DISCUSSION

The analysis of the buildings load curves already proved to be an interesting method to find deviations in the buildings behavior. Even without specific knowledge on the building, the data analysis graphs provide a quick insight in the 'health' of the buildings curves. Heating loads during summer, cooling loads during winter or unexpected 'bumps' in the curves indicate something is wrong.

The method is based on the assumption that local (individual office level) heating and cooling systems are capable of maintaining a constant indoor temperature (22.5 °C) independently of the supplied air temperature (within reasonable ranges). In reality there are two deviations that complicate this assumption.

First, the setpoints of the individual rooms in the building are controlled by presence detection sensors. If someone is present the setpoint is 22.5 °C and if the room is empty the setpoint is 10 °C. As result, when the employee leaves for a meeting the chilled beam unit starts cooling at full capacity and when he is back it start heating again at full capacity. This causes a lot of scattering in the load profile.

Secondly, the floor heating/cooling systems are not configured to reach a room temperature setpoint, but to maintain a constant (heating curve controlled) supply water temperature. As result, the actual heating or cooling loads have no relation at all to the theoretic loads and room temperatures vary randomly between 18°C and 25 °C.

Again an earlier mentioned rule applies: *To predict the buildings behavior, the building has to behave predictable*. The application of more sophisticated load prediction models (like [48], including variable internal heat loads, solar intensities, wind speeds, etc.) can produce far more accurate results, but only if the majority of problems in the building is fixed.

In the scope of this research (maintaining the ATES balance), the presented long-term mean values are sufficient to detect structural deviations (for continuous commissioning) and predict building long-term building behavior (for model predictive control).



### 4.3 STATE SELECTION METHOD

The method to complete the reference model is the selection of the systems state, of all possible states introduced in section 3.1. This section introduces the state selection method and the equations to calculate the flow and temperature supplied to the ATES simulation method of chapter 2.

#### 4.3.1 STATE SELECTION METHOD

The states introduced in section 3.1.3 are separated in main states (1, 2, 3, 4) and heat pump activity dependent sub-states (a, b). The switch-points between the main states *outside* office hours are operated based on the fixed temperature settings already introduced. The switch-points *during* office hours are selected by the following equations.

##### State 1<->2

The switch-point temperature between these states is defined by the temperature at which the AHU needs no additional heating via in the coil (equation 4.12 / equal to equation 4.5). As long as the coil is used for heating (state 1) the coil cannot be used to supply cooling water for local cooling (state 2).

$$T_{sw,1-2} = \frac{\eta_{hrw} * T_{return} - (T_{supply} - \Delta T_{fan})}{(\eta_{hrw} - 1)} \quad (4.12)$$

##### State 2<->3

The switch-point between the supply of cooling water via the AHU (state 2) and via the ATES (state 3) is defined by the point where the heating load supplied by the heat recovery wheel equals the needed cooling load for the local cooling group (equation 4.13).

$$T_{sw,2-3} = find(T_{outdoor}) \text{ where } [P_{hrw,heat} = P_{cool,local}] \quad (4.13)$$

##### State 3<->4

The switch-point between simultaneously heating and cooling (state 3) and only cooling (state 4) is defined by the temperature where central cooling is needed (equation 4.14).

$$T_{sw,3-4} = find(T_{outdoor}) \text{ where } [T_{heatingcurve} - \Delta T_{fan} = T_{outdoor}] \quad (4.14)$$

##### Substates a (heat pump on) & b (heat pump off)

The heat pump activity is defined in operating minutes per hour. These are calculated using the ratio between heat pump heating capacity (as function of the condenser temperature of Figure 3-22) and the predicted heating load (equation 4.15).

$$t_{hp}[min] = \frac{P_{hp,load}}{P_{hp,max}} * 60 \quad (4.15)$$

### 4.3.2 STATE SELECTION DURING OFFICE HOURS

Figure 4-9 shows the calculated switch points and the minutes of heat pump activity based on the reconstructed load curves. As visible, only state 2 and 3 supply simultaneously heating and cooling. In state 4 the heat pump is also active for additional cooling, but this is already calculated in the method of section 3.2.2.

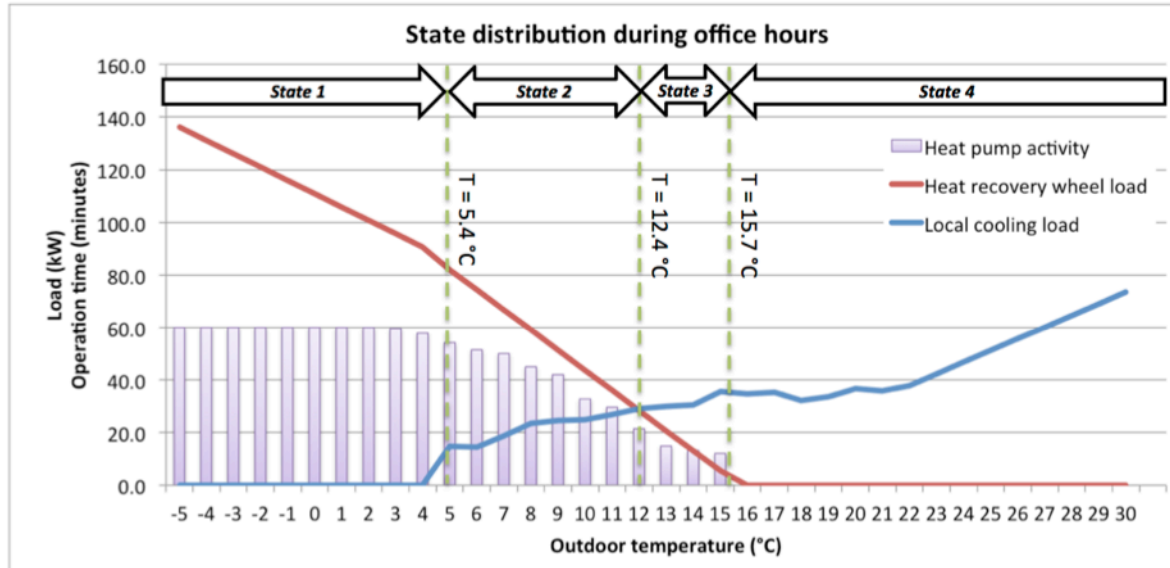


Figure 4-9 - States during office hours

Table 4-1 shows the equations for calculating the flows ( $Q_b$ ) and temperatures ( $T_{b,in}$ ) supplied to the building side of the ATES system heat exchanger (Figure 2-17). The variables ( $T_{loc}$ ,  $q_{loc}$ ) and ( $T_{ahu}$ ,  $q_{ahu}$ ) are the results of the methods for the local cooling group and the air handling unit.  $Avg_w()$  is the flow-weighted average of both temperatures within the brackets.

| State | HP  | Flow over ATES HEX (l/s)   | Temperature to ATES HEX (°C)  |
|-------|-----|--|---|
| 1     | On  | $Q_b = \frac{P_{hp,evap}}{4.2 * (T_{b,out} - 6.5)}$                  | $T_{b,in} = 6.5$  |
|       | Off | (-)  | (-)   |
| 2     | On  | $Q_b = \frac{P_{hp,evap} - P_{cool,local}}{4.2 * (T_{b,out} - 6.5)}$ | $T_{b,in} = 6.5$  |
|       | Off | (-)  | (-)   |
| 3     | On  | $Q_b = \frac{P_{hp,evap}}{4.2 * (T_{b,out} - 6.5)} + q_{loc}$        | $T_{b,in} = avg_w(6.5, T_{loc})$  |
|       | Off | $Q_b = q_{loc}$  | $T_{b,in} = T_{coolloc,out}$  |
| 4     | Off | $Q_b = q_{loc} + q_{ahu}$  | $T_{b,in} = avg_w(T_{loc}, T_{ahu})$                                      |
|       | On  | $Q_b = q_{loc} + q_{ahu}$  | $T_{b,in} = avg_w(T_{loc}, T_{ahu}) + \frac{P_{hp,cond}}{4.2 * q_{ates}}$ |

Table 4-1 - ATES flow and temperature equations during office hours

### 4.3.3 STATE SELECTION OUTSIDE OFFICE HOURS

A similar analysis is made for the states outside office hours (Figure 4-10). Here the switch-points are fixed setpoints based on the outdoor temperature. During these states the load is only used to predict the minutes of heat pump activity.

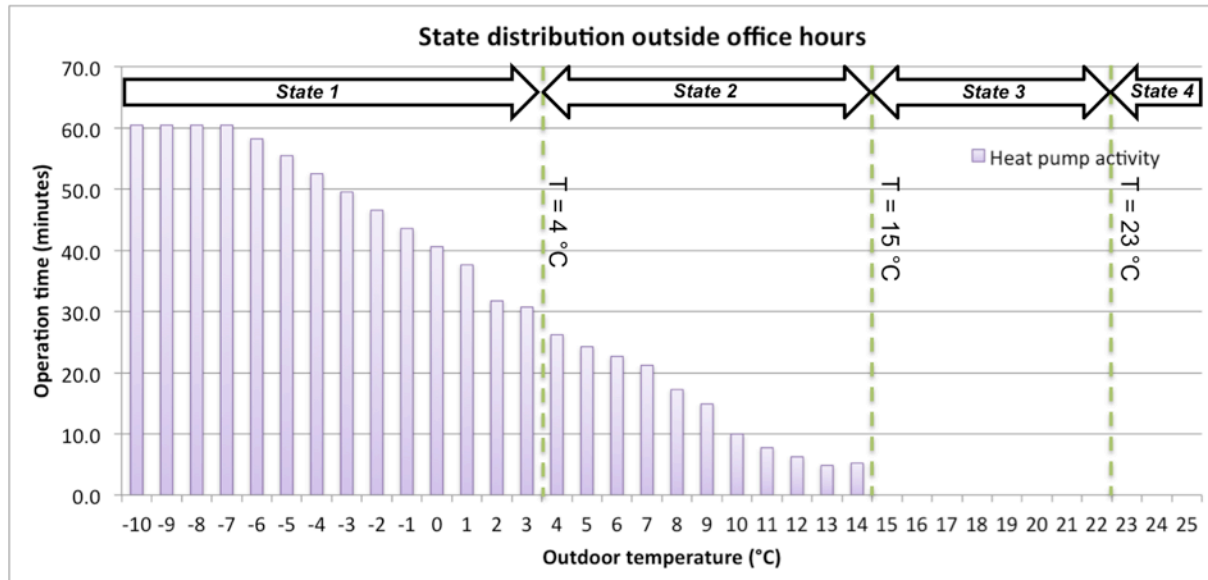


Figure 4-10 – States outside office hours

Table 4-2 shows the corresponding equations needed to calculate the flows and temperatures outside office hours. In state 1 the regeneration method results ( $T_{reg}$ ,  $q_{reg}$ ) are used to simulate the regeneration.

| State | HP  | Flow over ATES HEX (l/s)  | Temperature to ATES HEX (°C)      |
|-------|-----|---|-----------------------------------|
| 1     | On  | $Q_b = \frac{P_{hp, evap}}{4.2 * (T_{b, out} - 6.5)} + q_{reg}$ | $T_{b, in} = avg_w(6.5, T_{reg})$ |
|       | Off | $Q_b = q_{reg}$   | $T_{b, in} = T_{reg}$             |
| 2     | On  | $Q_b = \frac{P_{hp, evap}}{4.2 * (T_{b, out} - 6.5)}$           | $T_{b, in} = 6.5$                 |
|       | Off | (-)   | (-)                               |
| 3     | (-) | (-)   | (-)                               |
| 4     | (-) | (-)   | (-)                               |

Table 4-2 - ATES flow and temperature equations outside office hours

## **4.4 DISCUSSION**

The simulation of building loads and states is the method needed to complete the reference model. Other than the (physics based) methods in chapters 2 and 3, the loads are influenced by a complex combination of external factors and human interaction with the building. This makes accurate simulation of the buildings loads a lot more complex than plotting and fitting data of a single physical characteristic.

The data analysis methods showed a large scattering of values. If the primary goal of this method would be to do an accurate prediction of the loads for each specific hour, the used method would not be suitable. A much more extensive and detailed method is required to include effects of for instance varying occupation, solar heat load, wind speed and startup effects (during early hours). For this research however, the long-term averages should be sufficient to detect structural deviations or predict stored energy over longer periods.

As mentioned before: the building has to behave predictable before its behavior can be predicted. This is especially a requirement if data based modeling is used, because the results can only be as good as the used input data allows. A lot of effort should be put into the buildings software to justify additional research on load prediction for the case study building. Trials (non-published) to find relations between the additional input variables (sun, wind, occupancy and time of day) did not show any solid relations.

For future buildings these BMS-data based methods probably are going to be even more interesting. Higher insulation values and better heat recovery makes the building less dependent on the outdoor temperature. Buildings will be kept 24/7 at a constant temperature, making the effects of user behavior more apparent. Even for the (slightly older) case-study building, modeling would give better results if all rooms were kept at a constant temperature.

## 5. MODEL APPLICATION

---

The developed reference model is the key element in the implementation of both continuous commissioning and model predictive control practices. An analysis of the potential results of implementation of these methods is presented in this chapter.

The potential of continuous commissioning is analyzed by comparing a simulated year with a year of actual measurements. Using this method the structural deviations between simulation and measurement results can be found. The structural and significant deviations are assumed to be detectable by continuous commissioning.

The potential of model predictive control is analyzed by simulating a simple MPC strategy. By evaluating this strategy model over a 20-years period, an analysis is made to determine if MPC is capable of maintaining the ATES energy balance on long-term.

Even if the long-term simulation proves MPC can keep the ATES in thermal balance, the results are only valid if the building can be operated according to the reference model (continuous commissioning). On the other hand, implementation of continuous commissioning is no guarantee for a reliable ATES system, as long as an ATES balance is not achieved. Both methods have to be applied successfully to make the researched concept work.

### 5.1 CONTINUOUS COMMISSIONING ANALYSIS

This section compares the simulation results of the reference model with measurements logged by the building management system. The results are compared to the same dataset (2013) as used for curve fitting in the separate methods of chapters 3 and 4. For the ideal case, the simulation and the measurements match exactly. However, there are three possibilities that can cause structural deviating results:

- The reference model is not accurate enough
- The building software does not operate according to the defined states
- Physical leaks cause flows outside the defined state diagrams

The found structural deviations are assumed to be detectable by an implemented continuous commissioning method. The data is analyzed as function of the outdoor temperature and building state (during/outside office hours). The detected deviations are analyzed and the possible causes are determined. The original data of the graphs can be found in Appendix I.

#### 5.1.1 DATA ANALYSIS DURING OFFICE HOURS

The simulated data for this comparison is generated using the logged weather data of 2013 and the ATES temperature distribution on 1-1-2013 as start condition. The results are evaluated on generated heat, generated cold, stored heat and stored cold.

##### **Generated heat**

The generated heat is evaluated using the amount of district heating and the heat generated by the heat pump (Figure 5-1). The use of district heat is in line with the simulation results, except for the (small) uses above 4°C. This is probably caused by startup problems or malfunctioning of the heat pump. Although the amount is small (a few thousand kWh), this shouldn't be present.

The heat generated by the heat pump has multiple zones of interest. Below 0°C the simulation results are in line with measurements. Between 2°C and 14°C, the measurements are structurally lower than expected. This can be caused by the temperatures of the central heating curve, which are adjusted (raised) during the year. This results in more recovered heat and though less heat-

pump-generated heat. Above 20°C the heat pump is in cooling mode and measured data is again in line with the simulation.

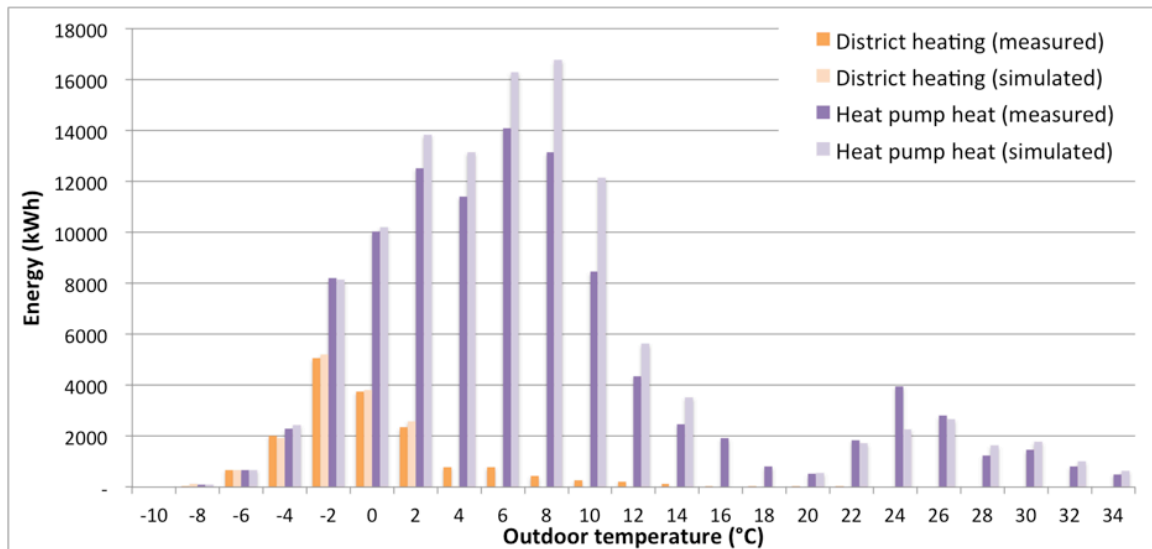


Figure 5-1 - Generated heat during office hours

### Stored cold

The generated and stored cold is evaluated in Figure 5-2. The heat pump generated cold is coupled to the heat pump generated heat, so these values have the same deviations. As showed in the simulation results, below 4 °C it is expected that the amount of cold generated at the heat pump evaporator side should be equal to the stored cold. The measurements show a structural deviation of 30%, which was also visible in the load analysis of chapter 4. Above 4°C a part of the generated cold is used for building cooling (state 2), which explains the mismatch between generated and stored.

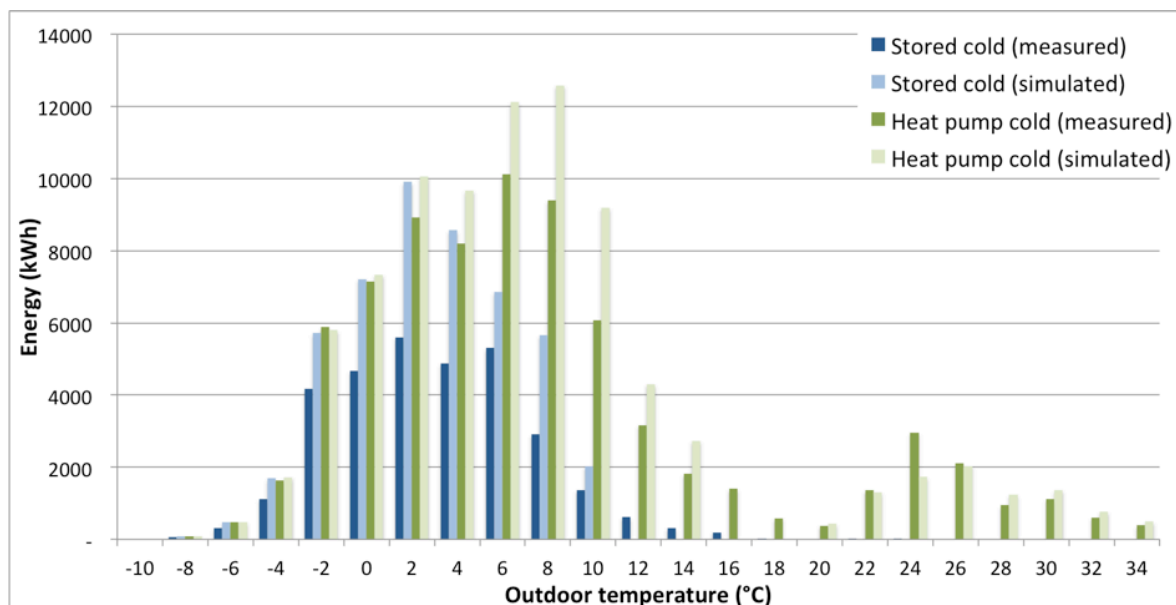


Figure 5-2 - Stored cold during office hours

### Stored heat

The stored heat is evaluated in Figure 5-3. At higher outdoor temperature (>20 °C) the data is matching. Between 15°C and 20°C there is a deviation which is hard to explain. Simulation of this 'partial load' area is always difficult, because the loads are very low and the number of hours is large. A possible explanation is that the night ventilation pre-cools the building and reduces the cooling load. Below 12 °C the measurements show there is still heat stored, but according to the

simulation model the HVAC should be operating in state 2 (free cooling via AHU). The use of ATES cooling during these temperatures is caused by missing software implementation of state 2 and manual override of settings. Around 10 MWh of heat is needlessly stored below 12°C.

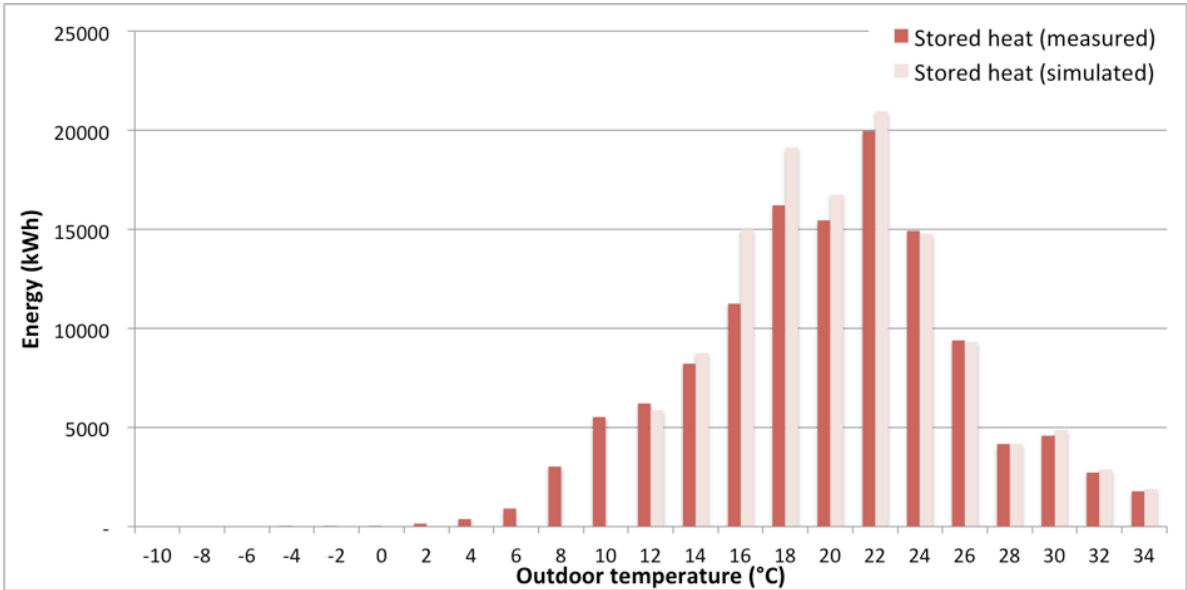


Figure 5-3 - Stored heat during office hours

### 5.1.2 DATA ANALYSIS OUTSIDE OFFICE HOURS

A similar evaluation is done for the data outside office hours (night and weekend). Because the cold can be generated by both the heat pump and regeneration state, these are analyzed separately before analyzing stored cold.

#### Generated heat

Figure 5-4 shows the use of district heating is much too high. The simulated use is zero over the entire graph, while in measurements there are two ranges of significant use. Below 4°C the use seems to be caused by the leakage between cold and warm circuit and above 10°C the use is caused by the software bug. Heat pump use is structurally too high during almost all states, which caused by heated water leaking to the cold water circuit (as already indicated in section 4.2.3 and appendix J).

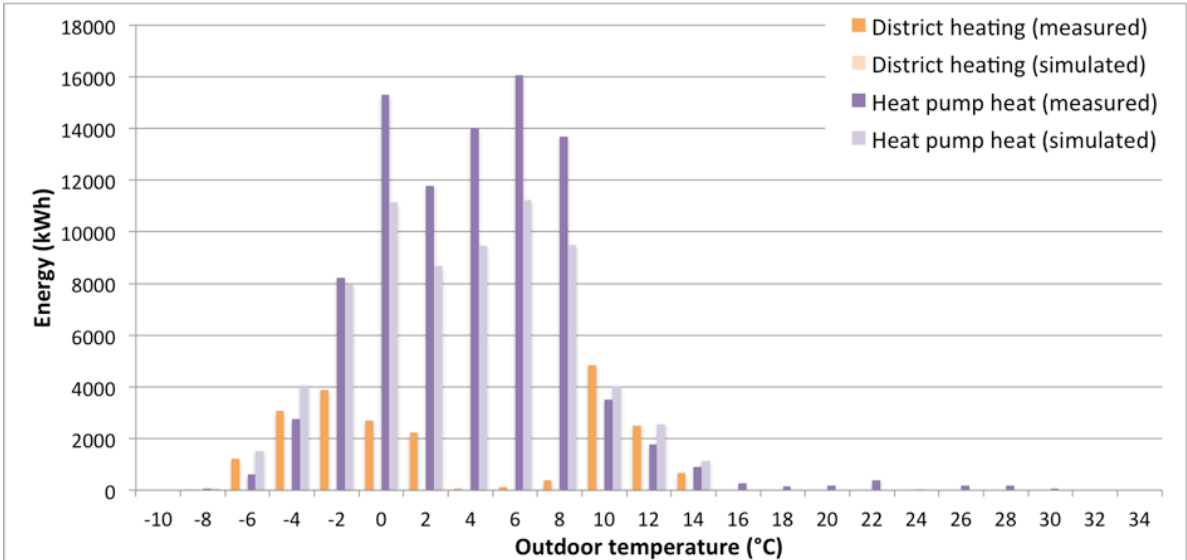


Figure 5-4 - Generated heat outside office hours

### Generated cold

Outside office hours, the generated cold (Figure 5-5) is produced by both the heat pump and regeneration. The regeneration shows a larger deviation when close to 4°C. This is probably caused by the air leaks from the exhaust air, increasing the intake air temperature. Another cause could be the mismatch between sensors of outdoor temperature and the intake air, because they are placed at different locations at the roof. The simulation model of chapter 3 is based on the intake air temperature after the HRW, which is in measurements often >1°C higher than the outdoor temperature. The deviations between the heat pump values are proportional to the deviations in the previous graph (Figure 5-4).

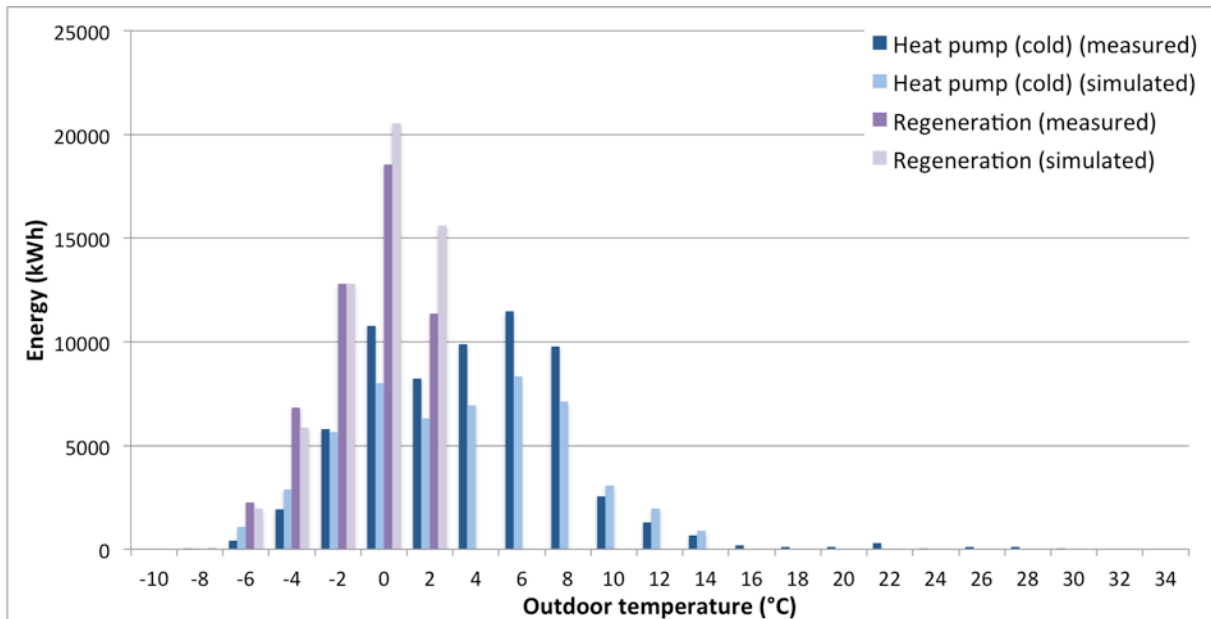


Figure 5-5 - Generated cold outside office hours

### Stored heat

The stored heat graph (Figure 5-6) is very simple. Outside office hours the only source of cooling is night ventilation, but the ATES system should be never used. The simulation shows zero heat storage, while the measurements show a total of 13 MWh of stored heat. Again, this is caused by the same software bug already mentioned in section 4.2.3 (Figure 4-4) and appendix K.

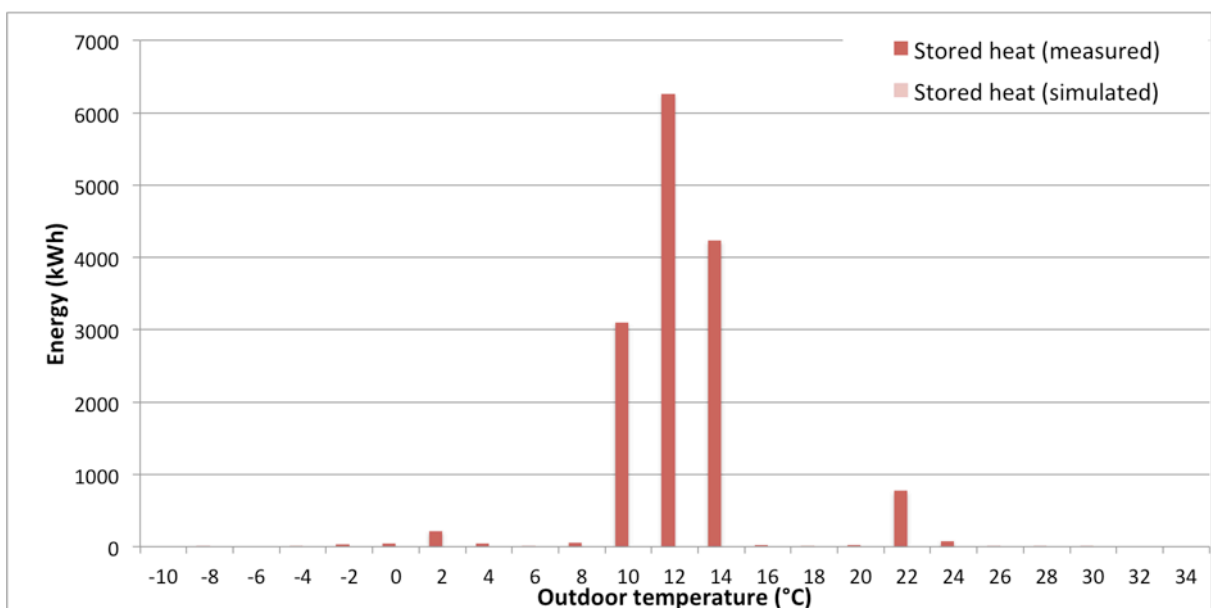


Figure 5-6 - Stored heat outside office hours



### Cold storage

The stored cold graph (Figure 5-7) shows a similar characteristic as during office hours (Figure 5-2). The amount of generated cold does not correspond with the amount of stored cold. Again, the leaking between the heating and cooling system is responsible for the deviation.

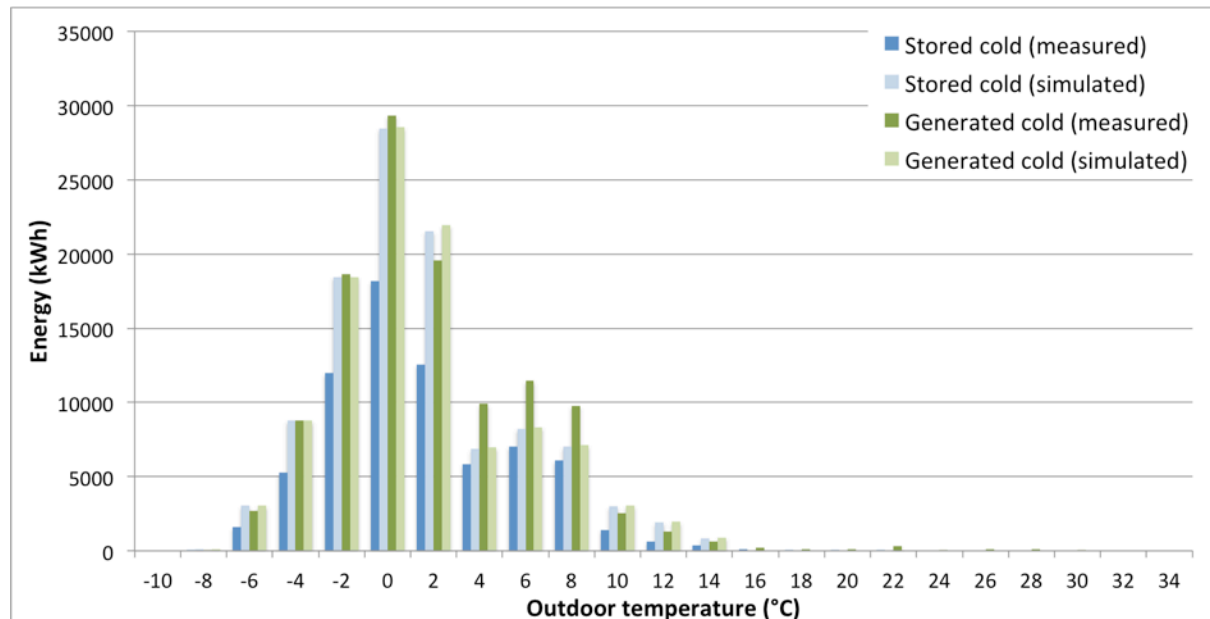


Figure 5-7 - Stored cold outside office hours

### 5.1.3 EVALUATION

The comparison of measurements and simulation revealed serious deviations in the building, causing the structural imbalance of the ATES (Table 5-1). Instead of a surplus of heat, the building should have produced a surplus of cold in 2013. This means the energy used for regeneration could have been reduced significantly. Even using this simple analysis method, a lot of problems could be narrowed to a specific cause. Measurements on leaks and analysis of the control software (Appendix J and K) showed the expected problems indeed caused the deviations.

|                  |       | Energy (MWh) |           | Deviation      |              |
|------------------|-------|--------------|-----------|----------------|--------------|
|                  |       | Measured     | Simulated | Absolute (MWh) | Relative (%) |
| Stored cold      | Day   | 31.6         | 48.2      | -16.6          | -34.5%       |
| Stored heat      |       | 125.1        | 124.4     | 0.7            | +0.5%        |
| Heat pump cold   |       | 74.8         | 85.4      | -10.6          | -12.5%       |
| Heat pump heat   |       | 103.6        | 115.2     | -11.6          | -10.1%       |
| District heating |       | 16.5         | 14.4      | 2.1            | +14.9%       |
| Stored cold      | Night | 71.1         | 108.2     | -37.1          | -34%         |
| Stored heat      |       | 14.9         | 0.0       | 14.9           | inf.         |
| Regeneration     |       | 51.8         | 56.9      | -5.0           | -9%          |
| Heat pump cold   |       | 64.0         | 52.3      | 11.7           | +22%         |
| Heat pump heat   |       | 90.1         | 71.3      | 18.8           | +26%         |
| District heating |       | 21.7         | 0.0       | 21.7           | inf.         |
| Stored cold      | Total | 102.6        | 156.4     | -53.8          | -34%         |
| Stored heat      |       | 140.0        | 124.4     | 15.6           | +13%         |
| Regeneration     |       | 51.8         | 56.9      | -5.0           | -9%          |
| Heat pump cold   |       | 138.7        | 137.7     | 1.0            | +1%          |
| Heat pump heat   |       | 193.7        | 186.5     | 7.2            | +4%          |
| District heating |       | 38.2         | 14.4      | 23.9           | +166%        |

Table 5-1 - Summed results

## 5.2 MODEL PREDICTIVE CONTROL ANALYSIS

In the previous section the goal of the analysis was to check if the expected amounts of heat and cold were actually stored in the ATES. The goal of this section is to control the amount of stored energy, to ensure that a thermal balance is maintained in the ATES system. It makes only sense to apply this method if the expected stored energy is (approximately) equal to the actual stored energy. The results of the method are only meaningful if the buildings performance and the reference model have a good match (for instance <5% overall deviation).

### 5.2.1 METHOD INTRODUCTION

Model predictive control (MPC) is a generic term for several predictive methods to control input variables of a process. The essence of MPC is to use a model of the process to predict future evolution of the system [12]. For every time interval, the input variable(s) of the model are determined to reach a *future target state* starting from the *current system state*. To analyze if MPC is suitable to maintain the ATES balance, first the storage goal (the target state) is defined and secondly the MPC method is applied.

If the amount of stored heating and cooling energy without regeneration is analyzed, it is clear that the case-study building has a structural surplus of stored heat. This makes the stored amount of heat the leading input variable for the method and the amount of (compensating) regenerated cold the variable 'to be controlled'. The amount of heat stored in the summer season must be compensated by the amount of cold in the winter season. This also means the MPC method will only be evaluated during winter season.

During the winter season there are two sources of cold: cold generated by the heat pump and by regeneration. The cold generated by the heat pump is influenced by the heating load of the building, which is coupled to the outdoor temperatures and is *uncontrollable*. The amount of regeneration is influenced by the setpoint temperature below which the regeneration is active. The higher the setpoint, higher the probability regeneration is active. This means the amount of regenerated cold is *controllable* by increasing or decreasing the chance on outdoor temperatures below the setpoint. Combined, this means the total amount of stored cold becomes controllable.

The storage goal is the required amount of stored energy at the end of the winter. There are two approaches to define the storage goal: keeping the energy balance around zero or maintaining a certain amount of stored cold water as energy buffer. Both methods reach a yearly balance, but the difference is found in the offset of this balance. Because the building relies solely on the ATES' cold-water storage for its active cooling, it makes sense to store additional cold water to improve reliability. For this simulation an energy balance of minus 100 MWh is used as target for the end of the winter. This value is arbitrary, but can be argued using the assumption of a typical cooling load (per summer) around 100 MWh. For a balance around 0 MWh, the target at the end of the winter would be -50 MWh and balance at the end of the summer +50 MWh. To account for the worst-case scenario of a very warm summer (+50% heat) and a soft winter (-50% cold), a target value of -100 MWh seems justified.

The implementation of this method has two steps. First the amount of regeneration, needed to reach minus 100 MWh at the end of the winter (using a reference winter dataset), is calculated. The curve of the stored amount of energy (using the result of this calculation) is stored as 'goal curve'. Using the 'actual weather dataset', the building is simulated and the progress of the storage is compared to the (reference) storage curve. Every first day of the week, the reference weather dataset is used to calculate the needed setpoint to get back on the goal curve.

### 5.2.2 METHOD APPLICATION

This section gives an example of application of the method for three years. First the goal curve is defined and next the MPC implementation is showed. As reference winter dataset the winter of 2008-2009 is used, as this winter is the most recent 'reference climate year' [49]. By simulating the energy stored during the winter as function of the regeneration setpoint, the graph of Figure 5-8 is plotted.

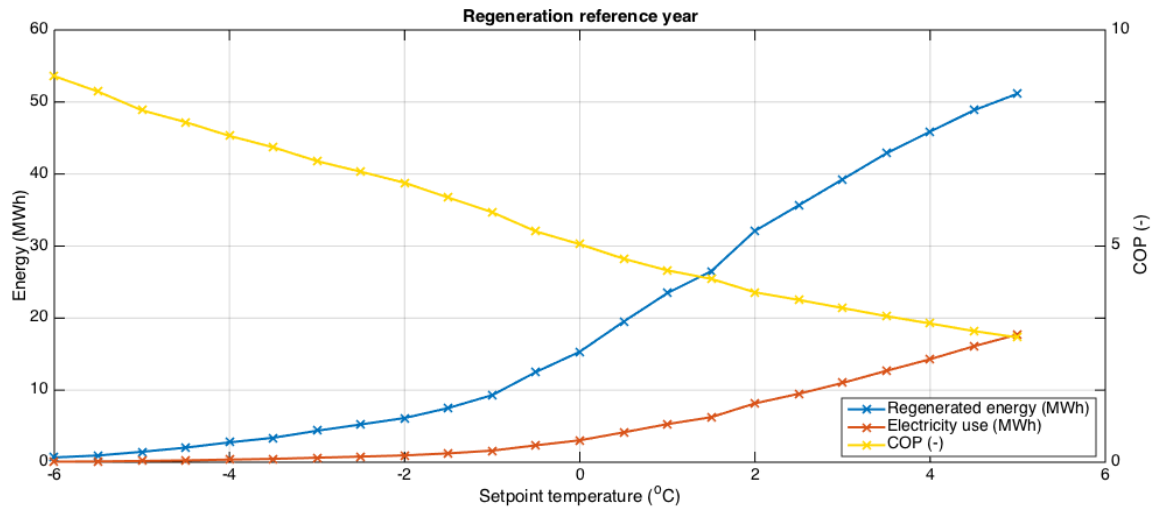


Figure 5-8 - Regeneration curves after reference winter

The amount of cold stored by the heat pump during the reference winter is 88.1 MWh. If for instance the energy balance is +21 MWh at the start of the winter, 121 MWh of cold must be stored to reach the goal of -100 MWh. If the amount of cold stored by the heat pump is distracted,  $121 - 88 = 33$  MWh is left which must be generated using regeneration. As visible in Figure 5-8 the setpoint temperature should be 2 °C. If the reference model is simulated using the setpoint of 2 °C and starting at 21 MWh ATES balance, the reference curve shows indeed an ATES balance of -100 MWh at the 1th of April (Figure 5-9).

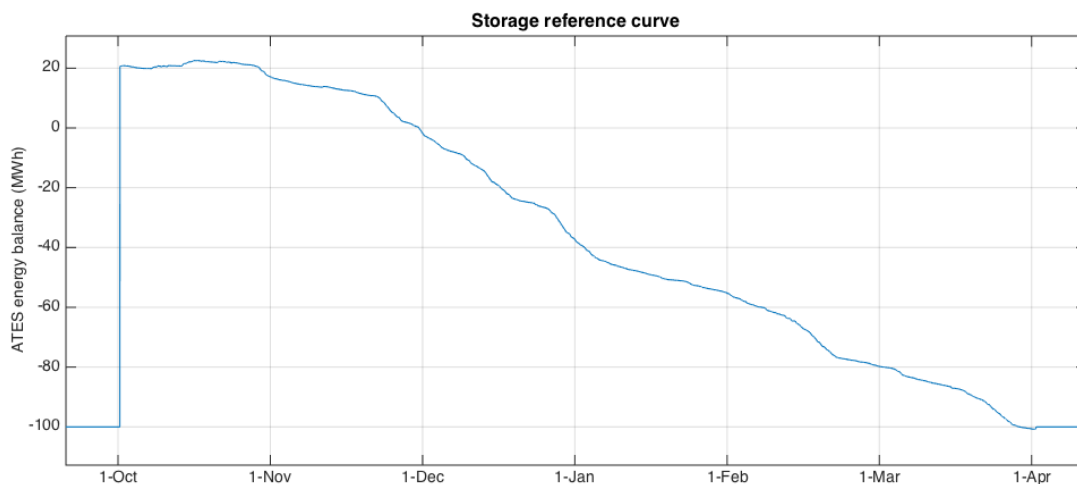


Figure 5-9 - Storage reference curve example

This curve is the target curve for the MPC model. Every first day of the week, a simulation the prediction horizon of 4 weeks is simulated (similar to Figure 5-8) to determine the setpoint at which the target curve is met after 4 weeks. If the actual winter is warmer than the reference winter, the setpoint increases to compensate for the less generated cold by the heat pump (and vice versa for a colder winter). Figure 5-10 shows the results of three years of MPC simulation. As clearly visible in the last year, the setpoint is 4°C (max. value) when the actual stored energy

is above the goal curve and  $-5^{\circ}\text{C}$  (min. value) if too much cold is stored. If the curves match, the setpoint is in between these values.

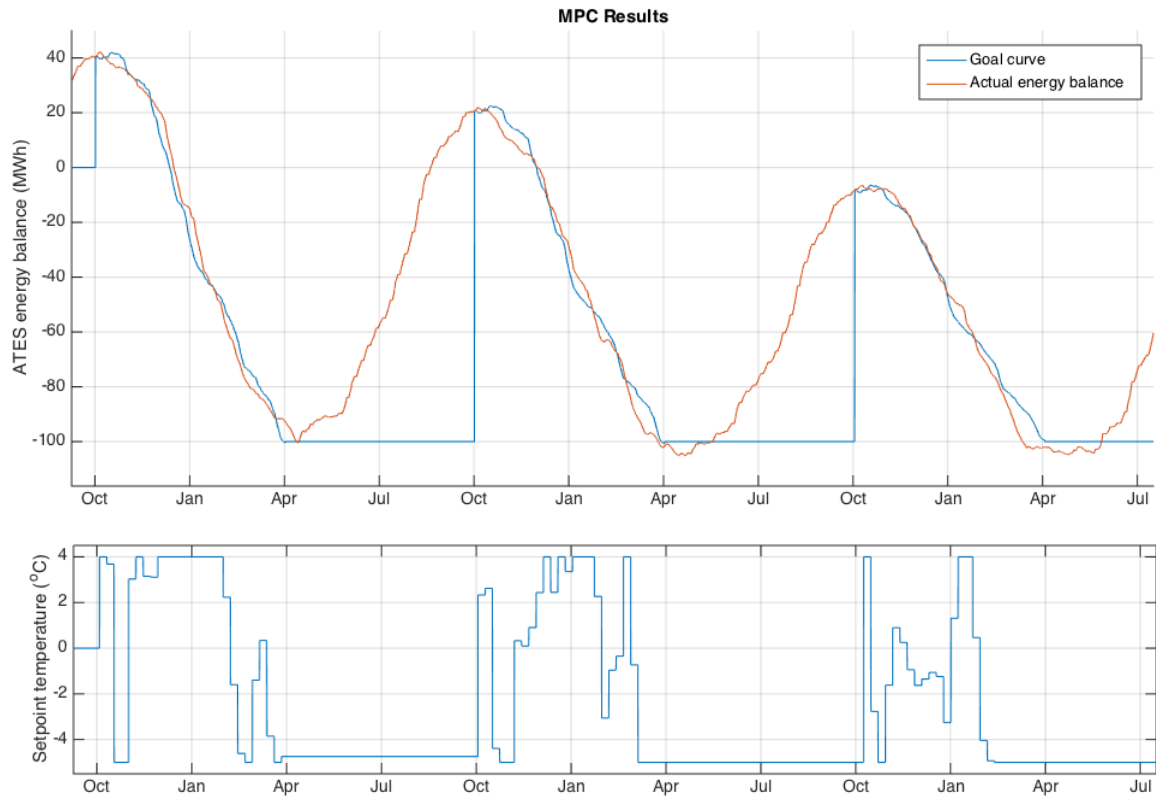


Figure 5-10 - MPC energy storage simulation and setpoint temperatures

### 5.2.3 LONG-TERM RESULTS

To test if the method is capable of maintaining the ATES balance over a longer period, a dataset of 25 years is used. The dataset is collected from a nearby weather station ('De Bilt') [50] and data from 1990 until 2014 is used. The result is shown in Figure 5-11.

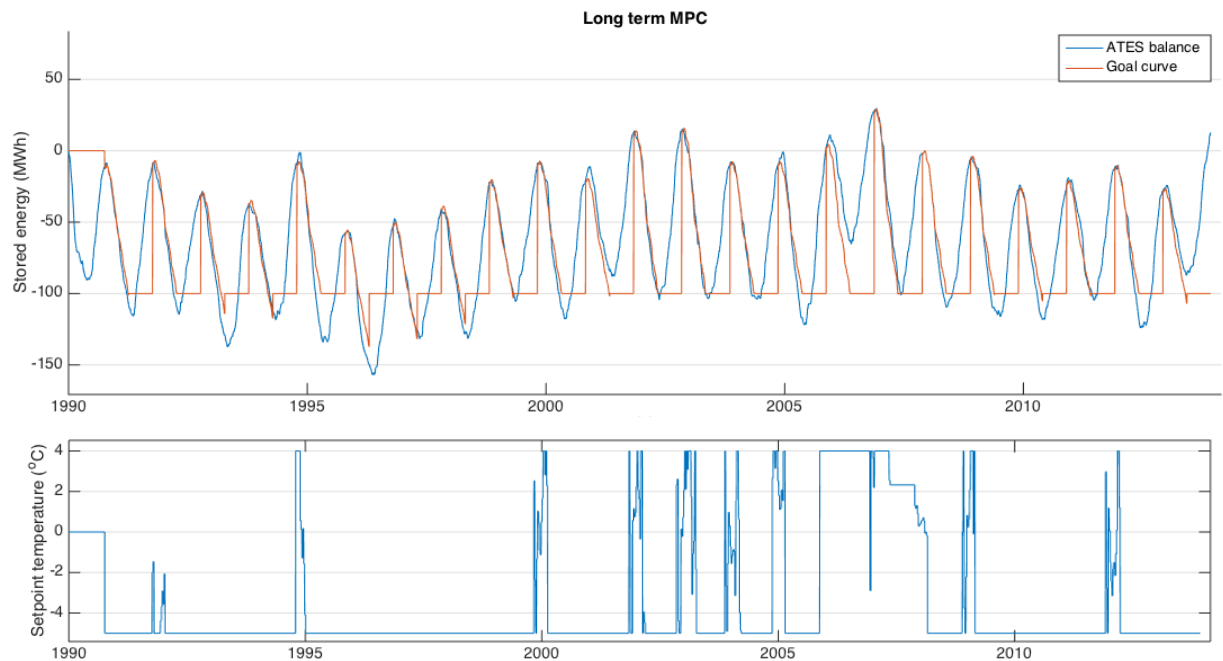


Figure 5-11 - Long term MPC simulation

The graph shows that in the first half of the simulation hardly any regeneration is needed. The stored amount of cold is often even larger than the storage goal, even without regeneration. If this is a structural problem, a regeneration method to store additional heat should be developed. After 2005 an example is visible of the opposite problem. Two warm summers combined with a soft winter that cannot supply enough cold to reach the storage goal. On average however, the MPC method proved to be capable of maintaining the ATES balance over a longer period.

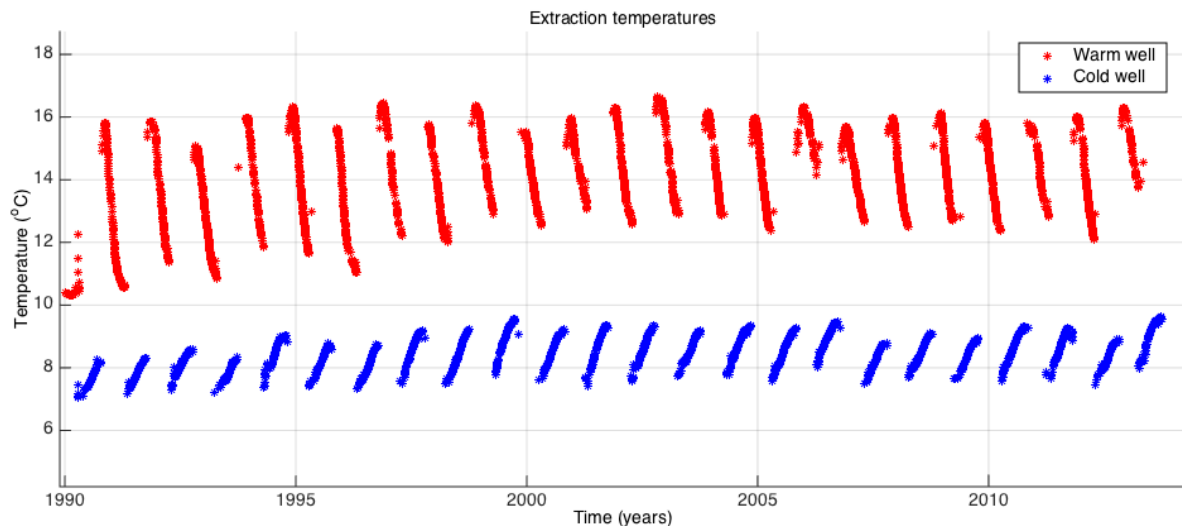


Figure 5-12 - Extraction temperatures

Figure 5-12 shows the extraction temperatures during the simulation. The creation of a 'cold buffer' by using a lower target than strictly needed, showed that a combination of a warm winter and between hot summers does not have a significant influence on the extraction temperatures. The extracted cooling water is always below 10°C, which is enough to supply the designed cooling capacity to the building.

### 5.3 DISCUSSION

The main goal of this chapter is to show the importance of a good reference model in gaining control over an ATES system. Once the model is complete, the troubleshooting of the building problems and testing a MPC method was relatively easy.

The comparison between the measurements and the reference model indicates which problems could be found using continuous commissioning. Reducing the deviations (between measurements and simulation model) by rewriting the HVAC control software and fixing the leaking components will solve the majority of the imbalance problems. The analysis explicitly did not include a method to implement the continuous commissioning, only an analysis which deviations are likely to be detectable using the reference model.

The used method for MPC is relatively simple and has room for improvement. The main goal was to show that even using something unpredictable as the weather as input, it is still possible to control the amount of stored energy in the ATES (within a certain range). The applied method tried to reach a certain fixed goal, but the necessity of a fixed goal is debatable. A predefined (or dynamic) upper and lower limit to the storage levels could also be enough to provide long term balance. However, the presented results are intended as a 'prove of concept' and do not pretend to be the best possible method.

## 6. CONCLUSIONS AND RECOMMENDATIONS

---

This chapter evaluates the results of this research, based on the main research questions of the first chapter. In the second section recommendations for further research are given, based on the results of this project. This chapter mainly contains the scientific research related results. The more practical results and recommendations are given in appendices J to L.

### 6.1 CONCLUSIONS

The first (and mayor) part of the research is focused on the development of an ATES and building reference model. A main requirement was to develop a model that is mainly based on learning the building behavior from building data and requires minimal human interaction. The more these methods can be automated, the more likely it is they can be implemented successfully.

The development of the ATES model was quite challenging because the lack of measurement data and the absence of suitable ATES simulation models. Conclusions that can be drawn from the ATES modeling method are:

- The use of an axisymmetric grid and the streamline method proved to be an effective method to quickly simulate this (low- $\Delta T$ ) ATES system. Caution should be taken in applying this method to other ATES systems, because it is not thoroughly validated and cannot cope with high natural groundwater flows, inhomogeneous ground structures and non-axisymmetric interferences.
- The developed data reconstruction method did produce a usable dataset, but is too labor intensive to be actually implemented. ATES systems should always measure the groundwater temperatures and flows if a system like developed in this research is planned to implement.
- The used data logging method, based on measurements extracted from different systems at different moments in time is only useful for steady states. It is almost impossible to simulate the unsteady start-stop behavior.

The developed HVAC model is partly based on the actual (measured) performance of components and partly on the designed (combined) behavior of the system. The developed methods proved that simulation on component level using the building data is possible and results are accurate. Conclusions for the separate components:

- The AHU main component is the central coil. Behavior can be accurately simulated using the heat transfer function and the dehumidification curve. These are also the main physical phenomena that should be monitored to notice performance degradation.
- The combined analysis of all local cooling components showed quite uniform behavior as function of the indoor temperature and cooling load. This is specific behavior for the case study building. Buildings with varying occupation or larger solar influence are probably less easy to predict using this method.
- The heat pump behavior *as individual component* accurately to analyzed and simulated, but the prediction of the condenser temperature showed to be very complex. It is debatable if the model should be capable of simulating this behavior more accurately or the actual installation should behave more predictable.
- A general remark based on the experience with data analysis is the importance of calibrated temperature sensors and the presence of flow sensors. The accuracy of the simulation depends heavily on the accuracy of the input data.

The prediction of loads proved to be difficult because the available load data is very scattered, caused by often changing room temperature setpoints and heating curves. By summing all loads it was possible to reconstruct the behavior of the building as function of the central heating curve.

- The load on the local cooling is highly dependent on the central heating curve. Especially during 'partial-load' season (10-20°C) the method is not very accurate. Because the loads are relative low during this temperature range, the influence on the ATES is minimal. To accurately measure the load curves, an optimal heating curve should be chosen and locked in the software system. Also variations in room temperature setpoints should be minimized.
- Because the heat pump is a simple on/off design, the minutes of activity are the main result of the heating load simulation. The generated curves are average values over a year. The use of these averages makes the results only valid over a longer term (multiple months), but not on hour-to-hour basis.

For the whole model the general conclusion can be given that it produces accurate simulation results for the **actual** behavior of the building. It is explicitly not intended as tool to show how the building **theoretically** should perform, but only to detect deviations from historical performance.

The second part of the research questions is about analyzing if continuous commissioning and model predictive control are suitable methods to maintain the ATES balance. The combination of both should ensure that the stored amount of energy is according to the model (on short-term) and the total amounts of stored heat and cold maintain storage balance (the long-term cumulative effect).

The continuous commissioning analysis showed several structural problems in the building. Because the models of the separate components are accurate, the problems are caused by the distribution network, in hardware (valves) and software (building states).

- The problems of the hardware, the leaking valves, are mainly detected by analyzing the conservation of energy. The amount of energy extracted at one side of the system should be supplied at the other side. Temporary imbalances can be caused by the thermal mass of pipes and vessels, but on the long term these should level out. The cold storage deviations of more than 30% were clearly detectable and showed to be caused by leaks (appendix J).
- The problems of the software are detected by analyzing if the supplied or extracted energy of each component corresponds with the expected building state. The significant deviations in the analysis are indeed caused by software bugs and missing implementation of states (appendix K).
- The main conclusion of the analysis is that a significant part of the heat surplus is unnecessary and can be avoided. These deviations would be detected if continuous commissioning (using the developed reference model) was implemented.

Using the model predictive control method it was proven that it is possible to keep the ATES in balance without human interaction, but using an autonomously operating software system. Implementation of the developed method could significantly improve reliability and eliminate the need for human interventions in the storage strategy, which significantly reduces costs. The used method is a proof-of-concept and does not pretend to be the optimal solution.

The research proved that developing a reference model based on partly designed (the states) and partly historical performance (the data fits) of the building is a very useful tool. Using this reference model both structural deviations can be detected and ATES balance can be maintained.

## 6.2 RECOMMENDATIONS

The methods and results presented in this research can be a starting point for further research. This section gives selection of possibly interesting topics.

### ***Further validation of the ATES model***

The developed model showed to be very effective (especially on simulation speed), but validation of the method proved to be difficult due to missing aquifer side data. Further development and validation of the method can provide a very useful tool for MATLAB and Simulink simulations. Validation could be done by comparison to validated software results and by analyzing measurements of multiple case study ATES systems throughout the Netherlands.

### ***Automatic calibration of temperature and moisture sensors***

The methods used in this research are quite sensitive for sensor accuracy. Especially with modern high temperature cooling / low temperature heating distribution, a  $\Delta T$  of  $< 2K$  is quite common. Uncalibrated sensor measurements with deviations of  $> 0.5K$  are unapplicable for simulation and monitoring of these systems, because they cause measurement errors of over 25%. Development of automated sensor calibration methods should be very useful. Next to technical solutions this could also be done using software logic. For instance by comparing temperatures of two sensors placed in the same duct or pipe or comparing moisture sensors to measurements of a nearby (calibrated) weather station.

### ***Insights in the need of a thermal balance in the ATES***

The goal of this research was set on maintaining a yearly thermal balance. However, it is never proved that this is the best solution for the system. It could be possible that it is better to store much smaller or larger amounts of cold water. It could also be a possibility that minimizing regeneration, unto the limits of the legally permitted imbalance, significantly reduces energy use without causing noticable performance issues.

### ***Implementation of smart grid energy prices in the regeneration strategy***

Regeneration is a typical process suitable to adapt to low energy prices. There is no high priority to regenerate on an exact moment in time, as long as the goal is reached at the end of the winter. Optimal use of variable electricity prices (caused by day/night tariffs, a surplus of electricity production by PV panels or smart-grid based price variations) can minimize the costs of regeneration.

### ***Application and further development of methods for other buildings***

All used methods are specifically designed for the Kropman Utrecht office. Development and validation of more 'BMS data based'-methods is needed if these monitoring methods are going to be implemented in all kinds of HVAC systems. For the ideal case, a toolkit of modeling methods can be developed, minimizing the effort to implement the methods in a large number of buildings.

### ***BMS data correlation analysis***

A lot of leakage effects could be detected by discovering two sensors followed the same temperature variation pattern. For instance, the correlation between cooling and heating return water temperatures indicated a leakage between both. By applying a correlation or spectral analysis over all logged data, links between values could be detected. These can be valid, for instance between a room temperature setpoint and the measured room temperature. They can also be invalid, when for instance water temperatures are correlated between two unrelated parts of the system. The other way around, broken components can be detected if two values have no correlation at all, while they should.



## REFERENCES

---

- [1] "IF Technology." [Online]. Available: [www.iftechnology.nl](http://www.iftechnology.nl). [Accessed: 21-Aug-2014].
- [2] NEN, "NEN 7120 - (Energieprestatie van gebouwen - Bepalingsmethode)," 2012.
- [3] R. Segers, "Rendementen en CO<sub>2</sub> -emissie van elektriciteitsproductie in Nederland , update 2012," 2014.
- [4] Unica Ecopower, "White paper - Behaalt uw WKO het maximale rendement ?," 2012.
- [5] Unica Ecopower, "Komt een WKO bij de dokter," 2013.
- [6] H. T. W. Bouwmeester, "Wko 3x beter," 2013.
- [7] A. van Wijck, "Bronproblemen," *De Ingenieur*, pp. 15–27, Nov-2012.
- [8] K. J. van der Maas, "Rendementsverbetering van een warmte- koude opwek en opslag systeem," 2013.
- [9] R. N. H. Claessen, "Improving the accuracy of ATES system design predictions," 2013.
- [10] C. Hoogervorst, "De energieneutrale wijk in nederland," 2009.
- [11] J. C. Visier and M. Jandon, "Commissioning tools for improved energy performance," 2004.
- [12] Y. Ma, F. Borrelli, B. Hancey, A. Packard, and S. Bortoff, "Model Predictive Control of thermal energy storage in building cooling systems," *Proceedings of the 48th IEEE Conference on Decision and Control (CDC) held jointly with 2009 28th Chinese Control Conference*, pp. 392–397, Dec. 2009.
- [13] H. Robert, R. Bars, and U. Schmitz, *Predictive Control in Process Engineering*, no. D. Wiley, 2011.
- [14] M. Behrendt, "MPC scheme basic," 2009. [Online]. Available: [http://upload.wikimedia.org/wikipedia/commons/thumb/1/11/MPC\\_scheme\\_basic.svg/2000px-MPC\\_scheme\\_basic.svg.png](http://upload.wikimedia.org/wikipedia/commons/thumb/1/11/MPC_scheme_basic.svg/2000px-MPC_scheme_basic.svg.png). [Accessed: 15-Dec-2014].
- [15] R. L. Bak, "Kantoren in cijfers 2012," 2012.
- [16] S. v.d. Burgt, "Boorprofiel Kropman Utrecht - GT15." p. 4, 2003.
- [17] Dutch Government, "Data en Informatie van de Nederlandse Ondergrond." [Online]. Available: <http://www.dinoloket.nl>. [Accessed: 19-Aug-2014].
- [18] USGS, "MODFLOW 2005." [Online]. Available: <http://water.usgs.gov/ogw/modflow/>. [Accessed: 28-Aug-2014].
- [19] T. Olsthoorn, "MFLab - Environment for MODFLOW suite groundwater modeling." [Online]. Available: <https://code.google.com/p/mflab/>. [Accessed: 28-Aug-2014].
- [20] A. Louwyck, "MaxSym - A MATLAB tool for the simulation of two-dimensional, axi-symmetric groundwater flow." .

- [21] W. Barash and M. Dougherty, "Modeling Axially Symmetric and Nonsymmetric Flow to a Well with MODFLOW, and Application of Goddard2 Well Test, Boise, Idaho," *Ground Water*, vol. 35, no. 4, pp. 602–606, 1997.
- [22] A. Louwyck, A. Vandenbohede, M. Bakker, and L. Lebbe, "Simulation of axi-symmetric flow towards wells: A finite-difference approach," *Computers & Geosciences*, vol. 44, pp. 136–145, Jul. 2012.
- [23] C. Zheng and P. P. Wang, "MT3DMS: A Modular Three-Dimensional Multispecies Transport Model for Simulation of Advection, Dispersion, and Chemical Reactions of Contaminants in Groundwater Systems; Documentation and User's Guide," Tuscaloosa, 1999.
- [24] B. M. S. Giambastiani, M. Antonellini, G. H. P. Oude Essink, and R. J. Stuurman, "Saltwater intrusion in the unconfined coastal aquifer of Ravenna (Italy): A numerical model," *Journal of Hydrology*, vol. 340, no. 1–2, pp. 91–104, Jun. 2007.
- [25] M. T. Kangas and P. D. Lund, "Modeling and Simulation of Aquifer Storage Energy Systems," *Solar Energy*, vol. 53, no. 3, pp. 237–247, 1994.
- [26] Stadswerken - Stedelijk Beheer, "Grondwatercontourkaart Gemeente Utrecht." 2013.
- [27] R. Caljé, "Future use of Aquifer Thermal Energy Storage below the historic centre of Amsterdam," no. January, 2011.
- [28] Geocomfort BV., "Technische documentatie GeoThermic GT15/30." 2011.
- [29] M. Peeters, "Hydrologische effectenberekening bij thermische energieopslagsystemen Kwantificeren van de fout bij verwaarlozing," *Stromingen*, vol. 9, no. 2, pp. 13–24, 2003.
- [30] IF Technology, "Thermisch opslagrendement, Deelrapport Werkpakket III," 2012.
- [31] P. K. Kundu, I. M. Cohen, and D. R. Dowling, *Fluid Mechanics*, Fifth edit. Academic Press, 2012.
- [32] J. S. Dickinson, N. Buik, M. C. Matthews, and A. Snijders, "Aquifer thermal energy storage: theoretical and operational analysis," *Geotechnique*, vol. 59, no. 3, pp. 249–260, 2009.
- [33] KNMI, "Maand- en jaarwaarden van de temperatuur, neerslag en luchtdruk." [Online]. Available: <http://www.knmi.nl/klimatologie/maandgegevens/>. [Accessed: 04-Sep-2014].
- [34] R. K. Sinnott, *Chemical Engineering Design*, Fourth Edi. 2005.
- [35] Wikipedia contributors, "Lambert-W function." [Online]. Available: [http://en.wikipedia.org/wiki/Lambert\\_W\\_function](http://en.wikipedia.org/wiki/Lambert_W_function). [Accessed: 02-Sep-2014].
- [36] F. P. Incropera & D. P. DeWitt, *Fundamentals of Heat and Mass Transfer*, 3rd editio. Wiley, 1990, pp. 658–660.
- [37] A. Hepbasli, "Low exergy (LowEx) heating and cooling systems for sustainable buildings and societies," *Renewable and Sustainable Energy Reviews*, vol. 16, no. 1, pp. 73–104, Jan. 2012.
- [38] Thermia Värme AB, "Thermia Robust Datasheet." .
- [39] H. Witteveen, "Toestandenbeschrijving Kropman Utrecht," 2003.

- [40] Y.-W. Wang, W.-J. Cai, Y.-C. Soh, S.-J. Li, L. Lu, and L. Xie, "A simplified modeling of cooling coils for control and optimization of HVAC systems," *Energy Conversion and Management*, vol. 45, no. 18–19, pp. 2915–2930, Nov. 2004.
- [41] J. Siegel, I. Walker, and M. Sherman, "Dirty air conditioners: Energy implications of coil fouling," *Lawrence Berkeley National*, no. 1986, 2002.
- [42] G.-Y. Jin, W.-J. Cai, Y.-W. Wang, and Y. Yao, "A simple dynamic model of cooling coil unit," *Energy Conversion and Management*, vol. 47, no. 15–16, pp. 2659–2672, Sep. 2006.
- [43] A. Van den Brink, "HAMLAB - Building Systems Toolbox." [Online]. Available: <http://archbps1.campus.tue.nl/bpswiki/index.php/Hamlab>. [Accessed: 23-Oct-2014].
- [44] Siemens, "Datasheet - Duct sensor QFM21...", vol. 220. pp. 1–8, 2008.
- [45] Solid Air, "Datasheet - OKNI 300 & 400." ham, pp. 37–62, 2012.
- [46] International Energy Agency, *Sourcebook - Condensation and Energy*. 1991.
- [47] D. K. E. Consultants, "Refrigerants." [Online]. Available: [http://www.industrialheatpumps.nl/en/how\\_it\\_works/refrigerants/](http://www.industrialheatpumps.nl/en/how_it_works/refrigerants/). [Accessed: 29-Dec-2014].
- [48] C. Fan, F. Xiao, and S. Wang, "Development of prediction models for next-day building energy consumption and peak power demand using data mining techniques," *Applied Energy*, vol. 127, pp. 1–10, Aug. 2014.
- [49] F. Imsirovic and R. Molenaar, "Comfort in tijden van klimaatverandering," *TVVL Magazine* 10, pp. 4–6, 2011.
- [50] KNMI, "Uurgegevens van het weer in Nederland." [Online]. Available: <http://www.knmi.nl/klimatologie/uurgegevens/selectie.cgi>. [Accessed: 09-Oct-2014].

## **APPENDICES**

---

|   |            |
|---|------------|
| <b>Appendix A - ING-House ATES simulation .....</b>                     | <b>A-1</b> |
| <b>Appendix B - Start-up behavior well pumps.....</b>                   | <b>B-1</b> |
| <b>Appendix C - Temperature distrubion ATES .....</b>                   | <b>C-1</b> |
| <b>Appendix D - Principle diagram air .....</b>                         | <b>D-1</b> |
| <b>Appendix E - Principle diagram water .....</b>                       | <b>E-1</b> |
| <b>Appendix F - Calibration measurements AHU .....</b>                  | <b>F-1</b> |
| <b>Appendix G - Calibration measurements water flows .....</b>          | <b>G-1</b> |
| <b>Appendix H - Analysis of load curves.....</b>                        | <b>H-1</b> |
| <b>Appendix I - Raw data of continuous commissioning analysis .....</b> | <b>I-1</b> |
| <b>Appendix J - Measurements on leaking valves .....</b>                | <b>J-1</b> |
| <b>Appendix K - Software problems.....</b>                              | <b>K-1</b> |
| <b>Appendix L - Recommended modifications and improvements .....</b>    | <b>L-1</b> |

## Appendix A - ING-HOUSE ATES SIMULATION

Because the injection and extraction temperatures of the case study object are not known, it is difficult to get an idea of the accuracy of the developed method. A simulation using the data of the ATES system of the ING-House in Amsterdam is performed to get an indication of accurateness.

### INTRODUCTION

The ING-house is commissioned in 2002 and has a GFA of 20.000 m<sup>2</sup>. The building is constructed using a lot of glazed facades to use as much solar heat as possible. To provide heating and cooling an ATES system is used. The system is a doublet system, using two wells of roughly 150 meters deep. The used grid structure is shown in Table A-1 (source<sup>1,2</sup>). Because the system is a doublet, the wells are simulated in separate axisymmetric grids using the same dimensions. Because two axisymmetric grids are used, no interference can be simulated.



Figure A-1 - Picture ING -House

| Variable          | Value [m] | Grid point |
|-------------------|-----------|------------|
| Gridsize          | 2.5       | -          |
| Top aquifer       | 40        | 16         |
| Top filter        | 50        | 20         |
| Bottom filter     | 120       | 48         |
| Bottom aquifer    | 150       | 60         |
| Simulation depth  | 160       | 64         |
| Simulation length | 100       | 40         |

Table A-1 - Used grid dimensions

### RESULTS

Using a dataset with injection flows and temperatures with 8-minute interval between 2008 and 2013 the simulation was performed (Figure A-2). Total simulation was executed in approx. 20 seconds per storage well.

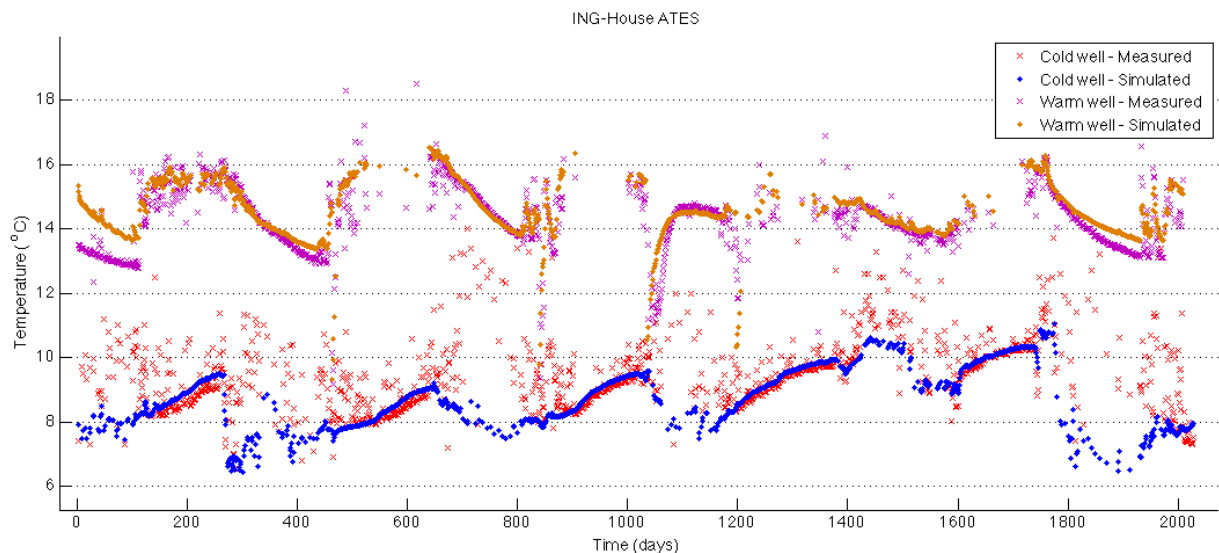


Figure A-2 - Simulation results

<sup>1</sup> <http://www.dinoloket.nl>

<sup>2</sup> R. Caljé, "Future use of Aquifer Thermal Energy Storage below the historic centre of Amsterdam", January, 2011

The average deviation between measurement and simulation is shown in Figure A-3. The deviation stays within  $\pm 0.3$  °C, except for the start-up values and the warm well values end of the simulation. The larger deviations are caused by start/stop behavior and low flows. When water flows slowly through the pipes or the pumps have been turned off for a while, the water is heated or cooled by the surrounding earth and building. The data has been filters to exclude low flows, but it is still difficult to get a smooth extraction temperature curve.

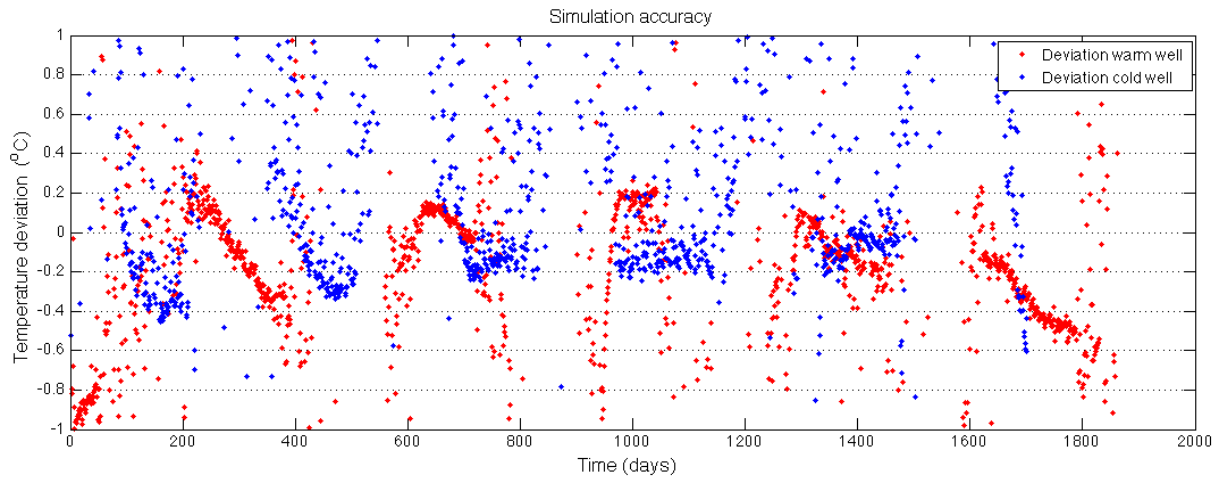


Figure A-3 - Simulation deviation

## DISCUSSION

The method to test the model using a completely different system is far from optimal, but is the best option available. Other ATES systems constructed by Kropman are mostly mono well systems or buildings of which they cannot access the ATES data.

This test was intended to get an idea of system accuracy and speed. The simulation showed that the used method is very quick compared to existing software that take hours of calculation time. The accuracy should be within 1 °C to predict the effect on the building systems. The accuracy of the simulation depends partly on the accuracy of the data. The used dataset contains a lot of start/stop and 'low flow' events, which makes it difficult to reconstruct the actual temperature of the stored water.

## Appendix B - START-UP BEHAVIOR WELL PUMPS

As already noticed in the sample dataset, the well pumps always start at full capacity (100%) and then slowly decrease to the required or minimal value (30%). Figure B-1 shows a manual measurement of this behavior.

If only the minimal capacity (30%) of the ATES is needed, the grey area is the amount of water is additional transferred between the wells. Using the pump curves derived in section 2.3.4 ( Figure B-2), the transferred water in the grey area is calculated.

The transferred amount of water is:

$$20(\text{m}^3/\text{h}) (100\%) \times 60 \text{ sec} + 13(\text{m}^3/\text{h}) (65\%) \times 260 \text{ sec} = 1.37 \text{ m}^3$$

The required amount of water (at 30%) is:

$$6(\text{m}^3/\text{h}) (30\%) \times 320 \text{ sec} = 0.53 \text{ m}^3$$

The effect of this start-up flow is particularly visible during spring and autumn. When for instance the heat pump is started two times per hour and is active for 10 minutes per cycle, roughly ( $20\text{min} \times 6 \text{ m}^3/\text{h} = 2 \text{ m}^3$ ) of chilled water ( $\sim 7^\circ\text{C}$ ) is stored and  $1.6 \text{ m}^3$  is transferred directly from the warm well ( $\sim 15^\circ\text{C}$ ) to the cold well. The averaged stored water is  $3.6 \text{ m}^3$  of  $\sim 11^\circ\text{C}$  after one hour. This indicates the effect of the start-up behavior is quite significant and does increase the temperature of the cold-water storage. To simulate the impact of this behavior, for every well pump start (after rest)  $0.8 \text{ m}^3$  is directly transferred between the wells.

It should be recommended to minimize the number of start/stop events and re-evaluate the necessity of the large start-up flow. According to GeoComfort, this is needed to be able to directly supply heating or cooling capacity. However, it is debatable if this actually needed and if the goal justifies the counter effects.

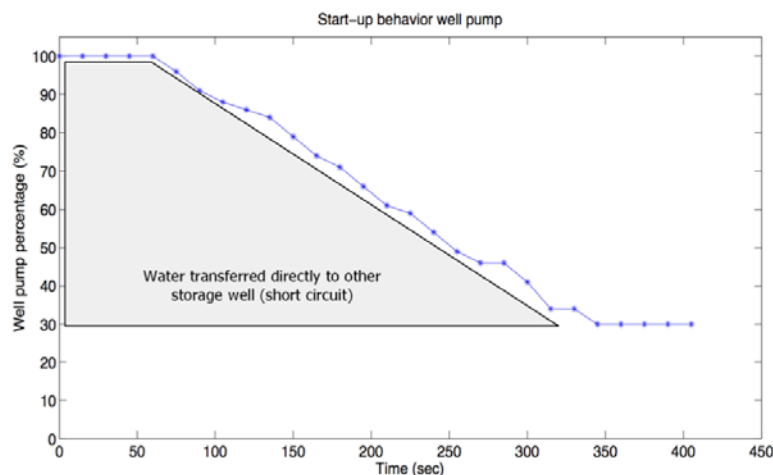


Figure B-1 - Start-up curve of well pump

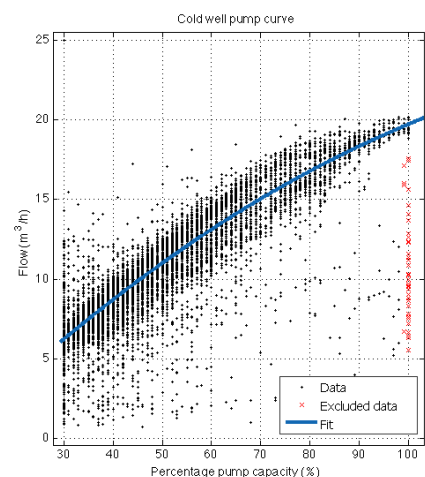
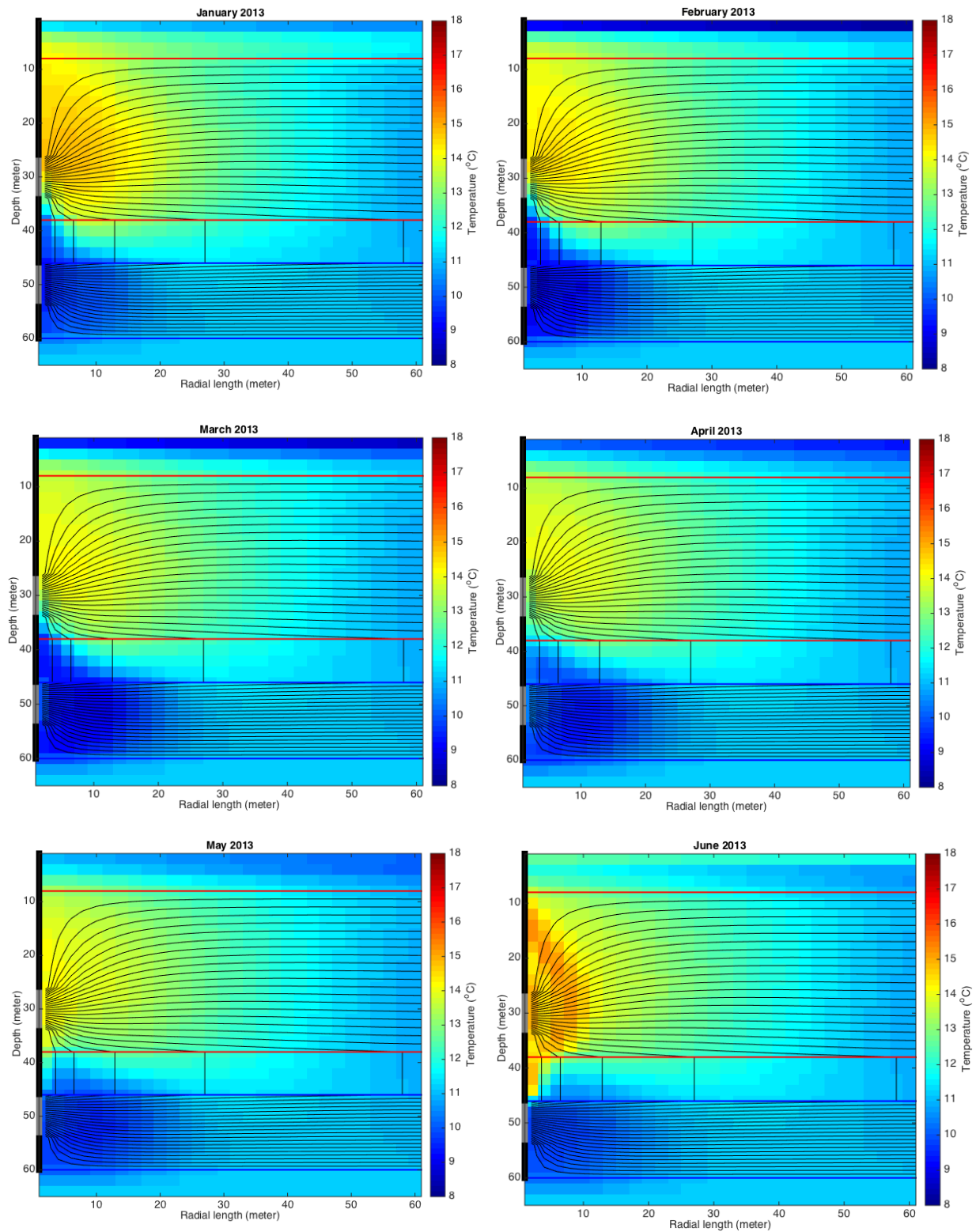


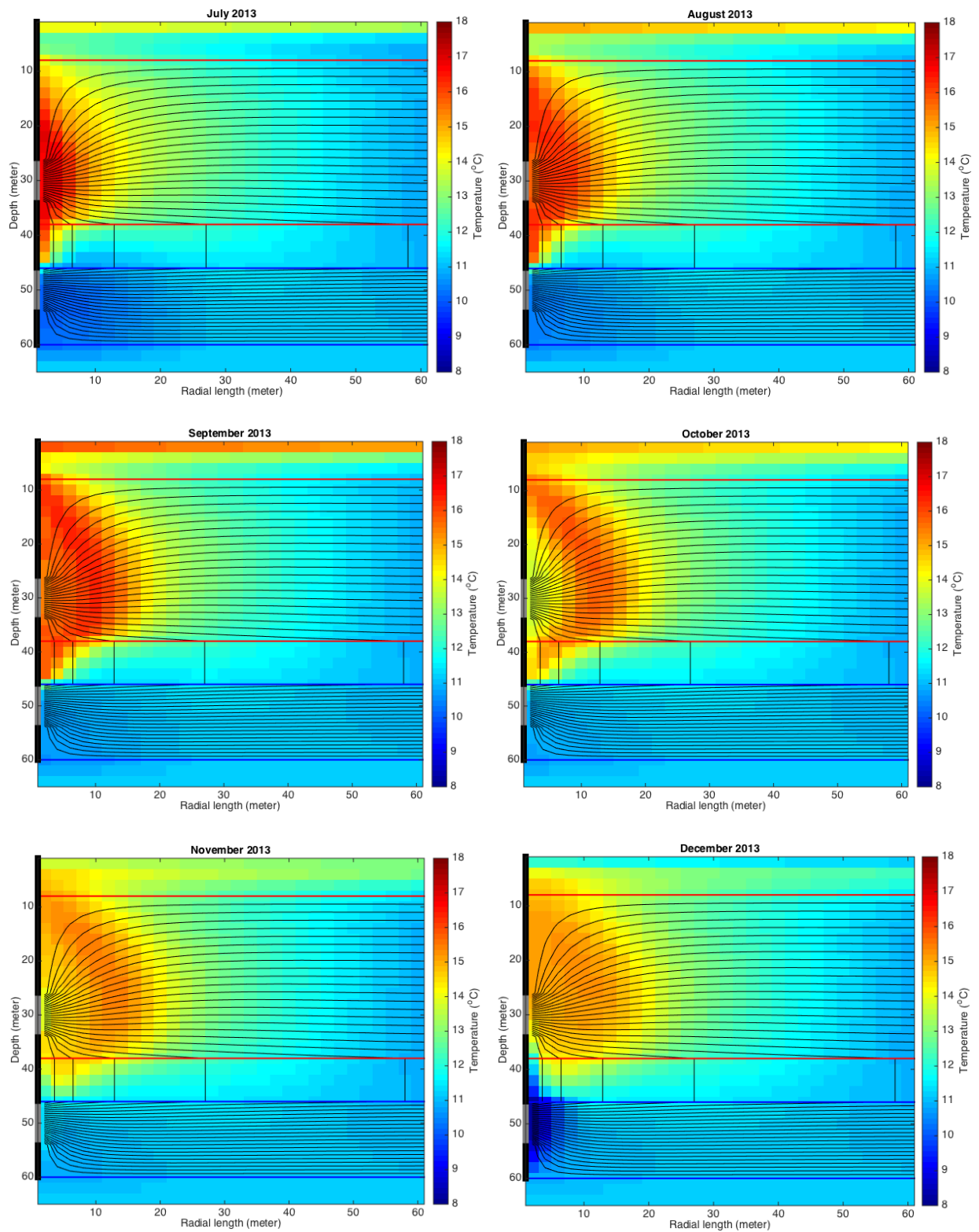
Figure B-2 – Well pump curve

## Appendix C - TEMPERATURE DISTRIBUTION ATES

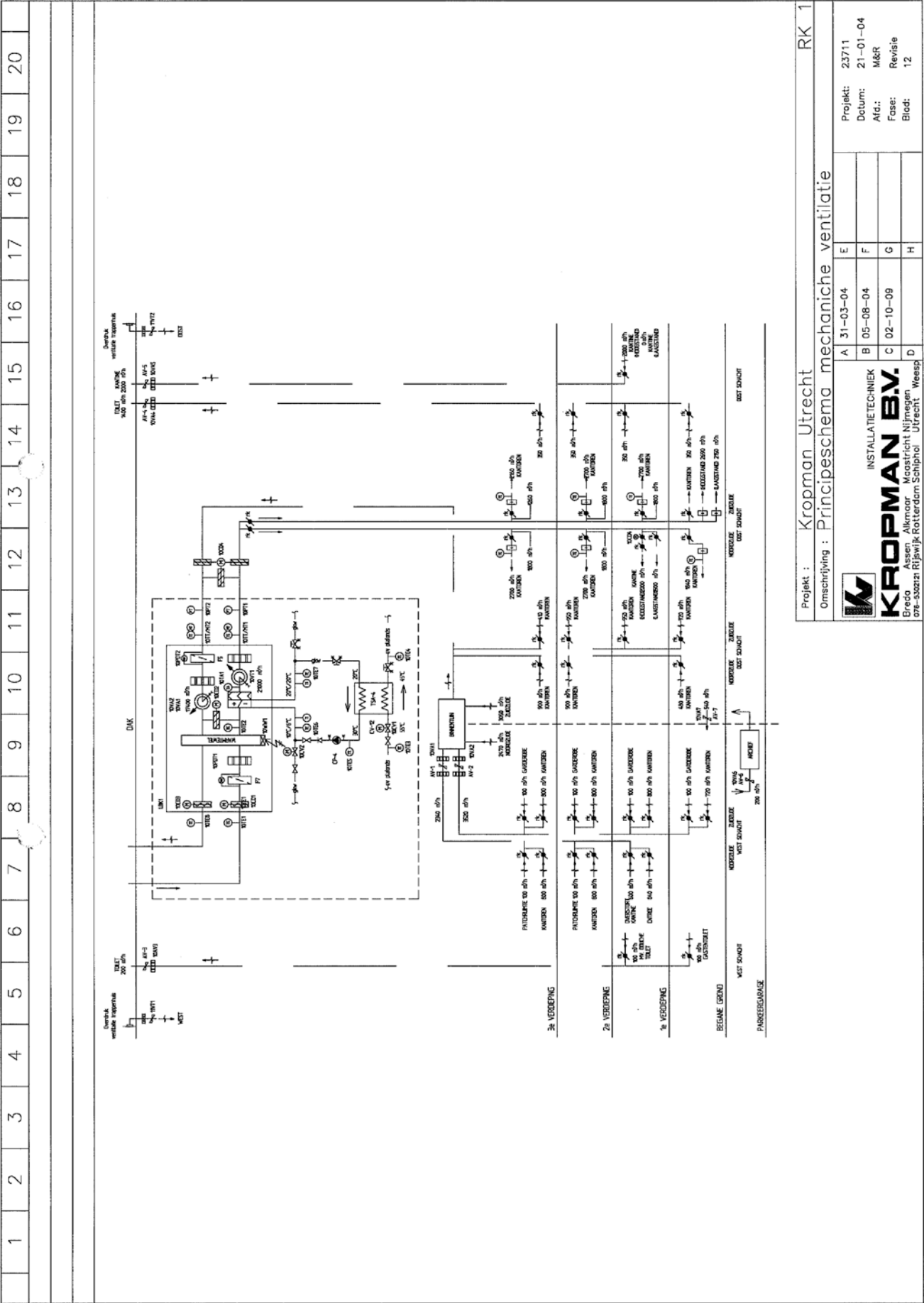
These figures show the calculated temperature distribution of the ATES system during 2013.






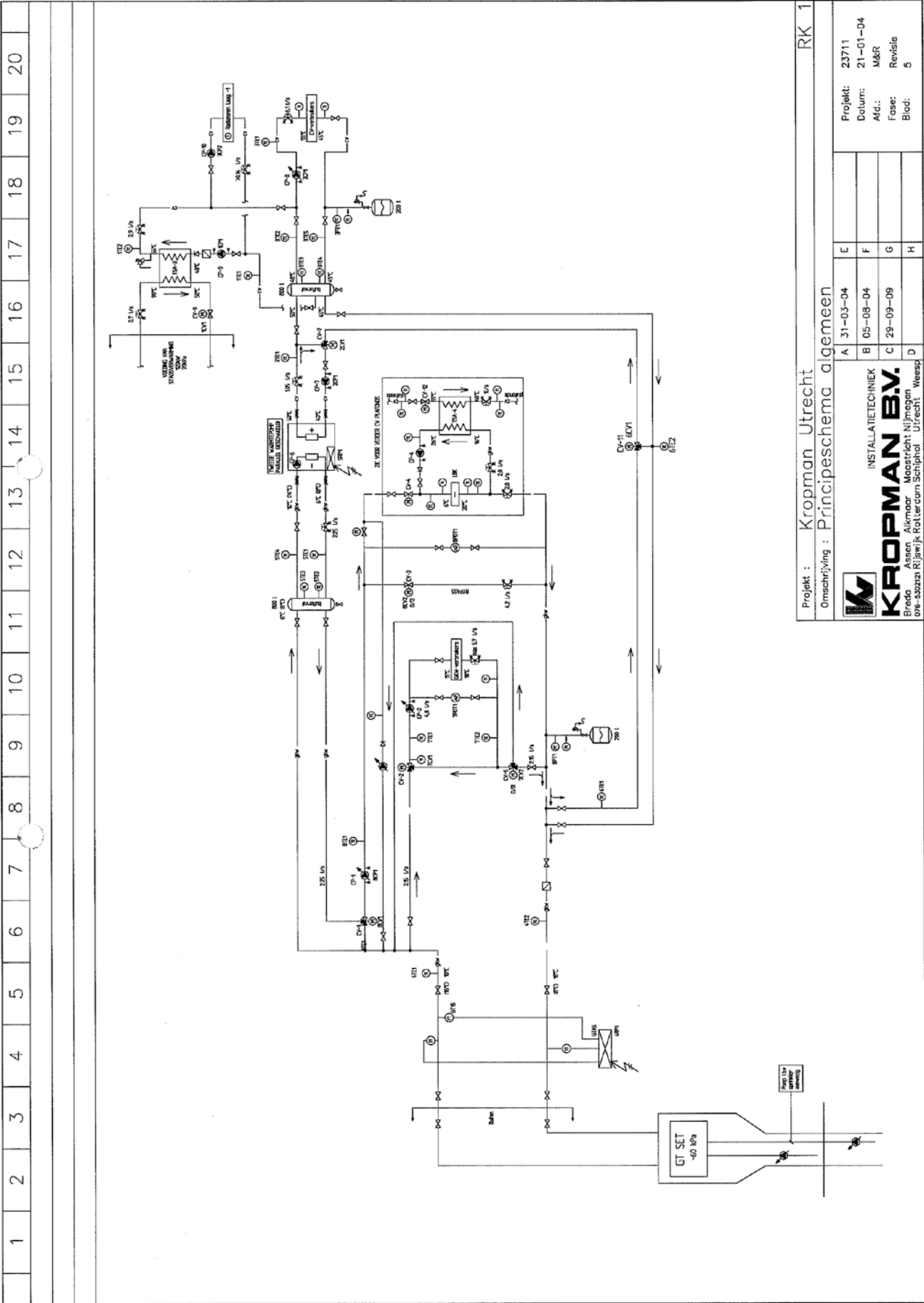


Appendix D - PRINCIPLE DIAGRAM AIR



|   |       |                 |  |
|---|-------|-----------------|--|
| RK 1  |       |                 |  |
| Project : Kropman Utrecht   |       |                 |  |
| Omschrijving : Principeschema mechanische ventilatie                                  |       |                 |  |
|  |       |                 |  |
| INSTALATIETECHNIEK  |       |                 |  |
| <b>KROPMAN B.V.</b>   |       |                 |  |
| Eredo Assen Alkmaar Moordrecht Nijmegen   |       |                 |  |
| 076-5302121 Rijswijk Rotterdam Schiphol Utrecht Weesp                                 |       |                 |  |
| Project:  | 23711 | Datum: 21-01-04 |  |
| Alc.:   | M&R   | Fase: Revisie   |  |
| Blad:   | 12    |                 |  |

Appendix E - PRINCIPLE DIAGRAM WATER



|   |          |
|---|----------|
| RK 1  |          |
| Project : Kroppman Utrecht                                  |          |
| Omschrijving : Principeschema algemeen                      |          |
| A   | 31-03-04 |
| B   | 05-08-04 |
| C   | 29-09-08 |
| D   |          |
| E   |          |
| F   |          |
| G   |          |
| H   |          |
| Project: 23711  |          |
| Datum: 21-01-04   |          |
| M&R   |          |
| Fase: Revisie   |          |
| Blad: 5   |          |
| INSTALLATIE-TECHNIEK  |          |
| <b>KROPPMAN B.V.</b>  |          |
| Breda, Assen, Alkmaar, Maastricht, Nijmegen, Utrecht, Weesp |          |
| 096-530201 Rijkswijk Rotterdam Schiphol                     |          |

## Appendix F - CALIBRATION MEASUREMENTS AHU

The AHU is the main distributor of heating and cooling loads within the installation. To accurately predict the energy demand, all temperature and moisture sensors are checked, the airflow is measured and fan heat dissipation is calculated.

### AHU SCHEMATIC INSITEVIEW OVERVIEW

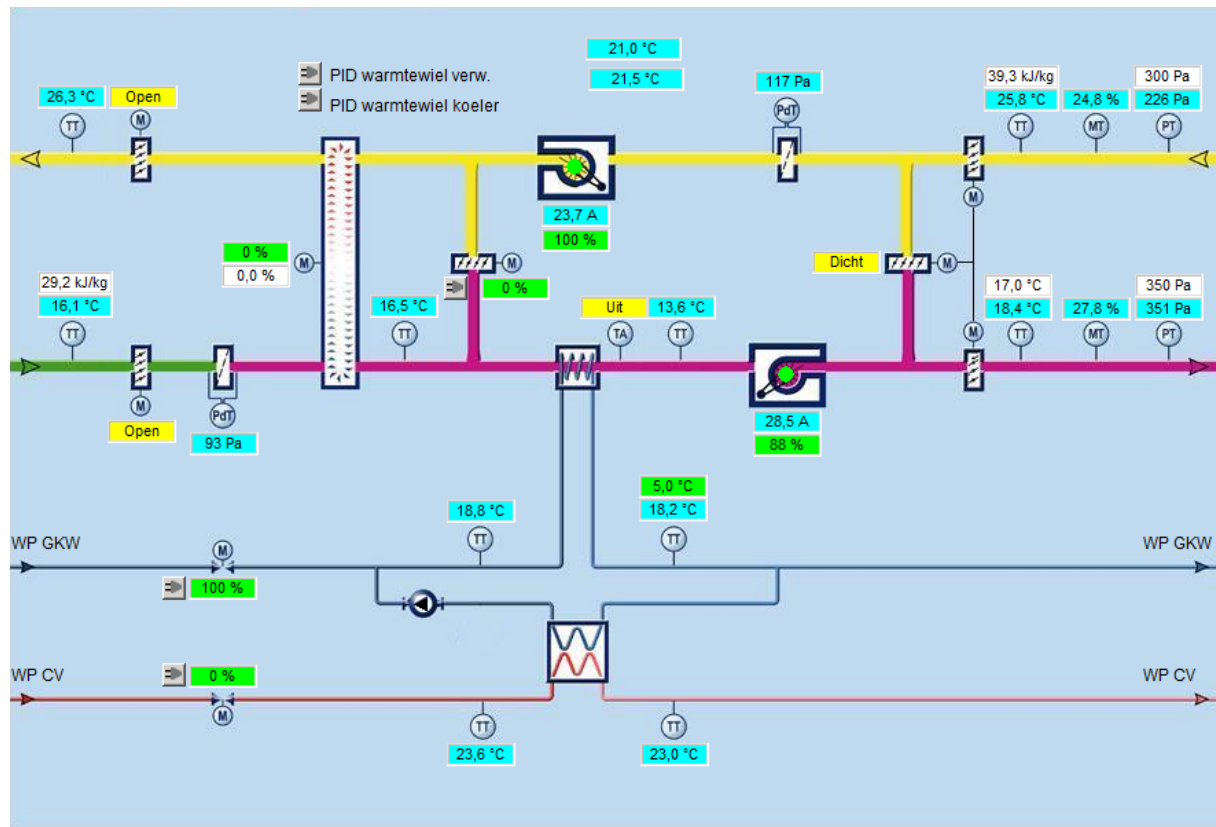


Figure F-1 - InsiteView screenshot of available air sensors

### TEMPERATURE MEASUREMENTS

The temperature (and moisture) measurements are executed with a calibrated datalogger (Testo 176H2), which records temperature and moisture values every minute for a predefined time. These measurements are compared with the InsiteView measurements to determine the offset. All calculated offsets are plotted in a histogram to determine the most frequent offset.

The accuracy of the duct sensors<sup>1</sup> coupled to InsiteView is  $\pm 0.4$  °C and the accuracy of the datalogger<sup>2</sup> is  $\pm 0.3$  °C.

<sup>1</sup> Siemens, 'Duct Temperature Sensors QAM2110' datasheet, Feb. 2008

<sup>2</sup> Testo, '176H2 - Data logger - Temperature and humidity', Mar. 2012

## 1. Intake air

Intake air temperature is measured directly in the outdoor air, exposed to the weather. Because the datalogger probe isn't waterproof, it was placed in the AHU intake duct. The large deviation between samplepoint 30 and 40 is caused because the AHU was inactive at that time (no night ventilation active). The average offset is between -0.1 and 0 degrees, so no correction is needed.

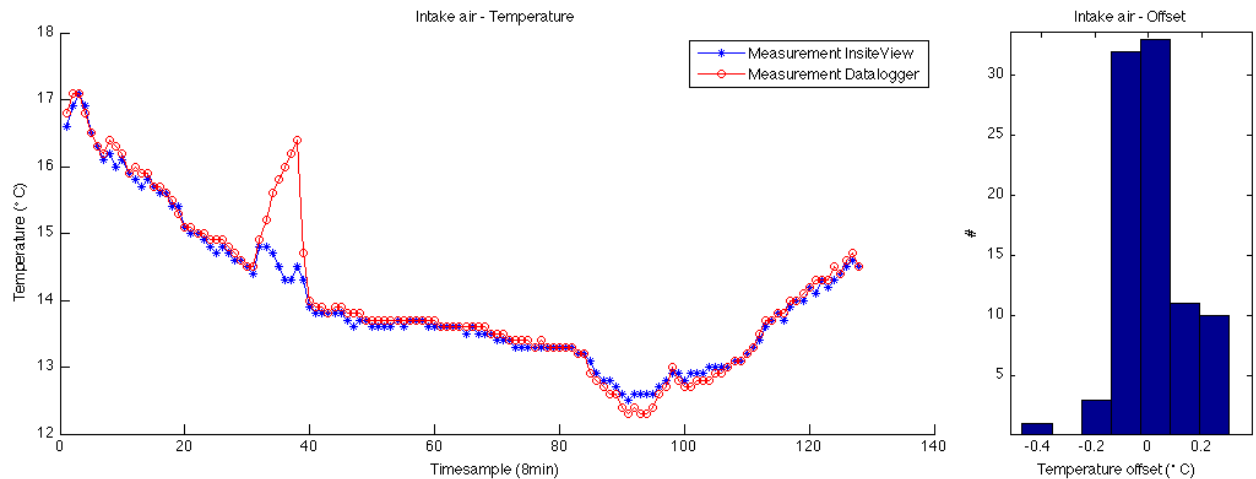


Figure F-2 - Intake air measurements

## 2. Intake air after heat recovery wheel

The air temperature after the heat recovery wheel is difficult to measure, because there is air leaking from the return channel that causes a vertical temperature gradient. This air is leaking via the seals of the heat recovery wheel and through the recirculation valve. By circulating water through the cooling coil (using earlier calibrated water temperature sensors), the average (effective) temperature of the coil can be measured. This corresponds to the average temperature of the air passing through. The average offset is +0.5 °C, which should be used to correct the historical data.

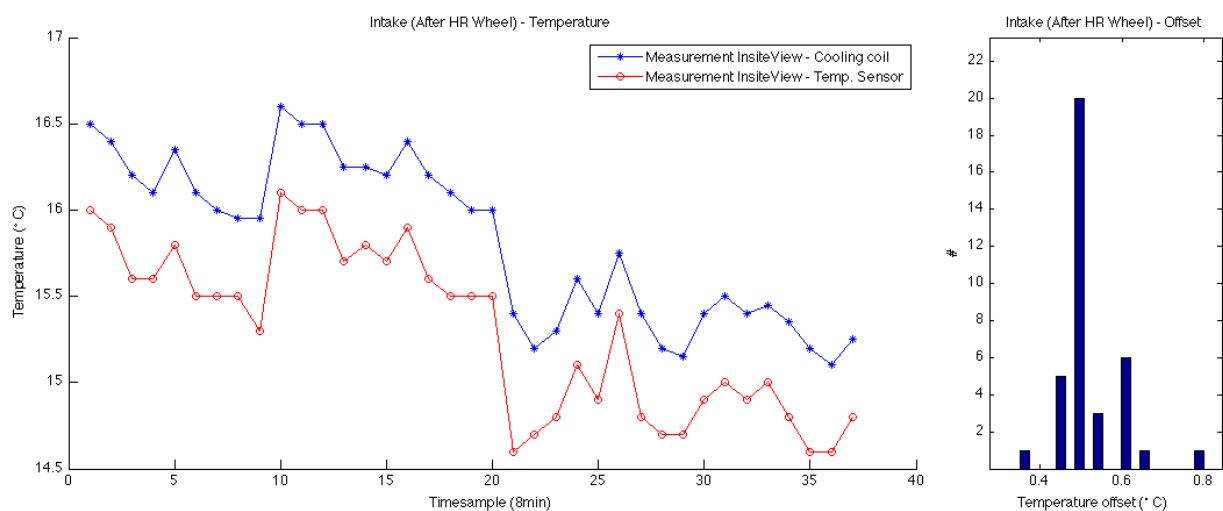


Figure F-3 - Intake air after HR wheel measurements

### 3. Supply air

The supply air temperature sensor has an offset of 0.9 °C. The historical data is corrected with this value.

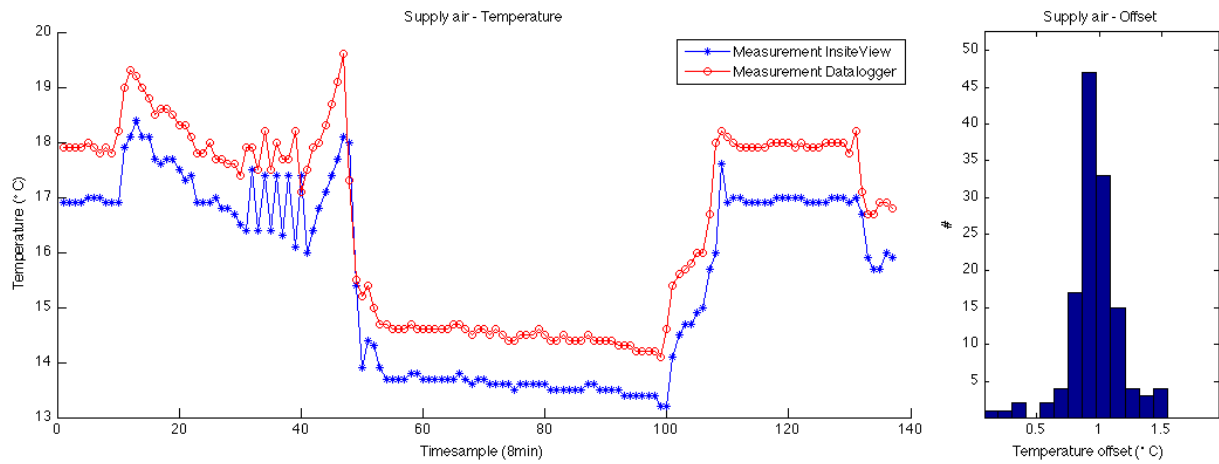


Figure F-4 - Supply air measurements

### 4. Return air

The return air has an offset of -0.4°C, which is significant enough to apply to the historical measurements. Also there seems to be bit of a proportional offset component. However, deriving this proportional relation won't be significant, because the return air is usually in the same temperature range (20-28°C).

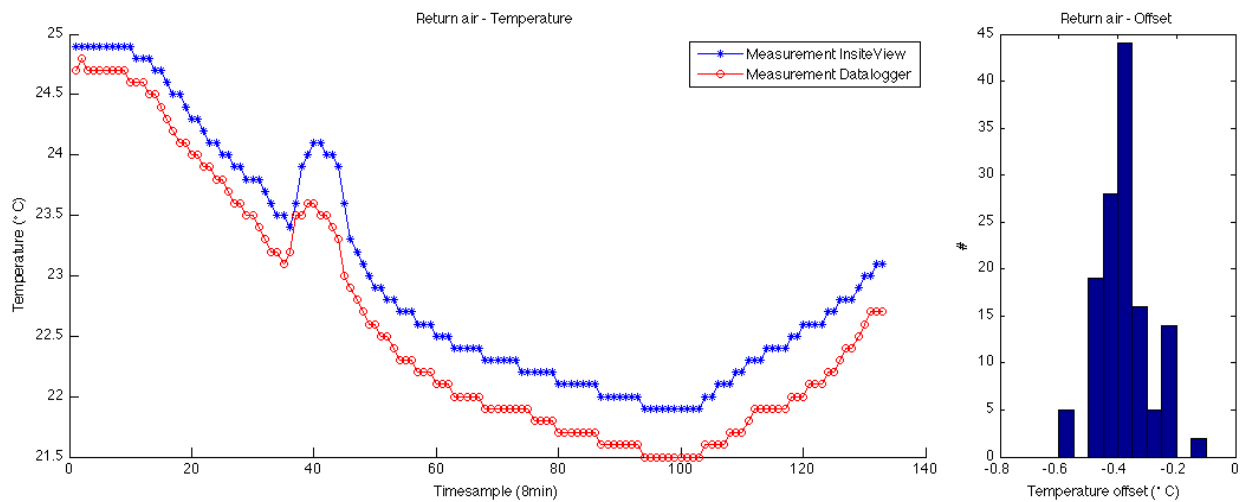


Figure F-5 - Return air measurements

## 5. Exhaust air

Similar to the return air, the exhaust air seems to have a proportional offset. It has an exact match at 25°C and roughly 0.3°C offset at 20°C. Again, this is within the accuracy of both temperature sensors, so an average offset of -0.1°C will be applied.

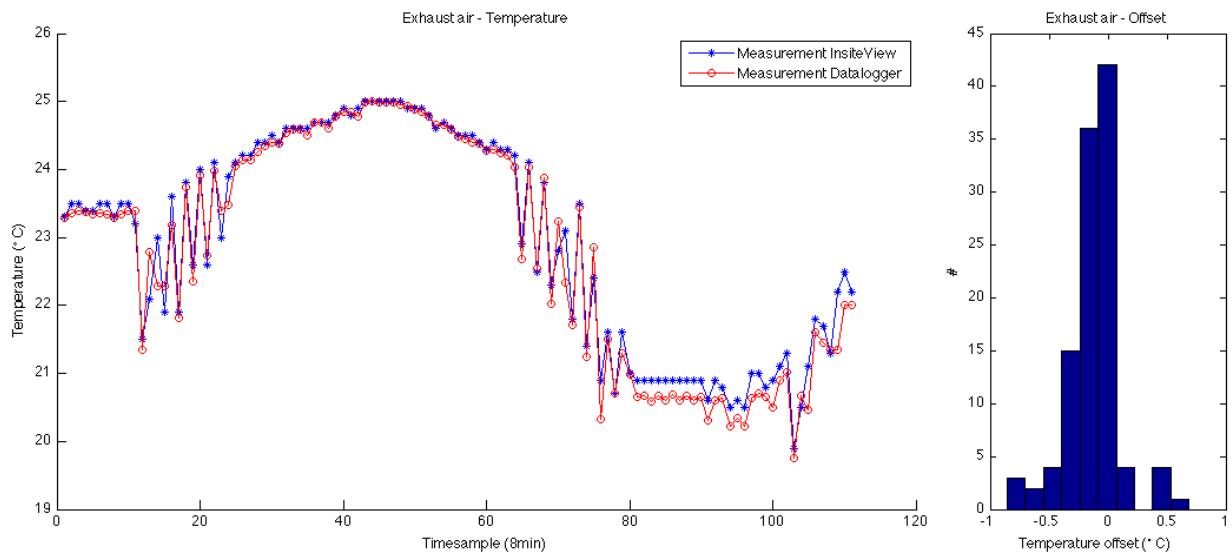


Figure F-6 - Exhaust temperature measurements

## AIR LEAKS

One of the drawback of applying a heat recovery wheel, startup valve and regeneration valve is the inevitable leaking of air between supply and return air. By measuring the caused temperature offset before and after the leaking valves, the ratios of leaking air are calculated.

### 1. Heat recovery wheel and recirculation valve

The intake air is heated by roughly 1°C when passing the (inactive) heat recovery wheel and the startup valve. To achieve this increase roughly 13% of the exhaust air must be added to the airflow. A typical leakage rate for a heat recovery wheel is 1-10%<sup>3</sup>. The remainder leaks through the recirculation valve. It's not possible to define the ratio between both leaks. The average pressure difference between both sides is ~750 Pa, so a small gap can already cause a significant leak.

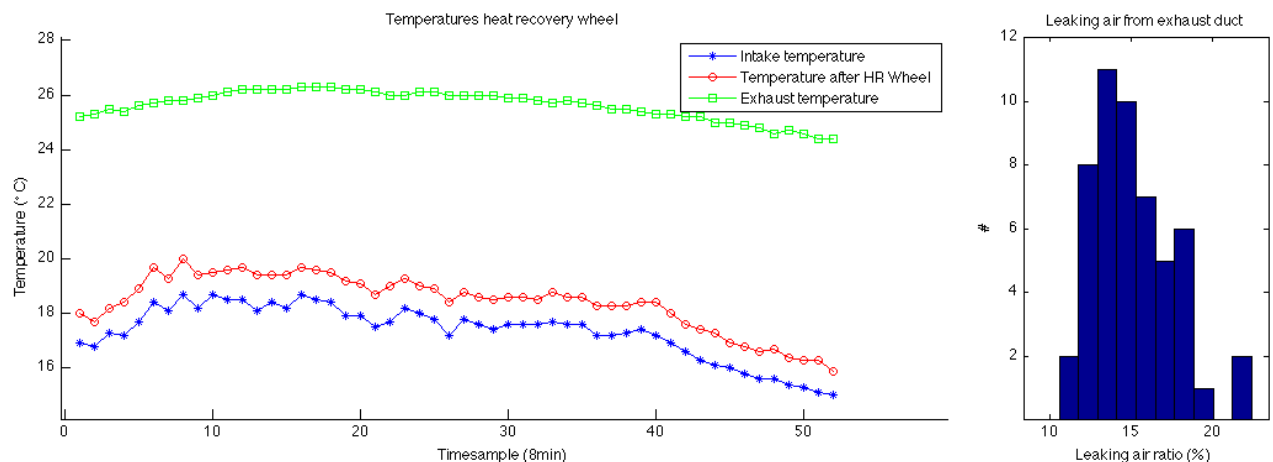


Figure F-7 - Air leak heat recovery wheel

<sup>3</sup> 'Waste heat recovery potential for HVAC systems', Sustainable Energy Authority of Ireland

## 2. Regeneration valve

The regeneration valve also leaks a significant amount of air. This causes the return air to be cooled down by the supply air. Using datalogger temperature measurements, the ratio of leaking air is determined to be  $\pm 9\%$ . The pressure drop between both supply and return air is 600 Pa.

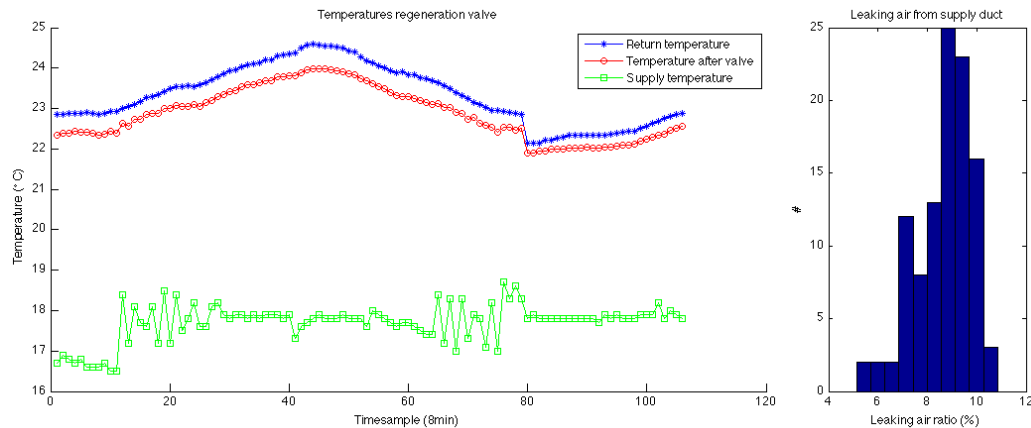


Figure F-8 - Air leak regeneration valve

## AIR FLOWS

Using an air velocity meter (TSI VELOCICALC Ventilation Meter 8385) the supply and return air duct flows are measured. Because the flow is highly turbulent (due to short and variable duct dimensions) the produced measurements are expected to have a large error (sometimes  $>25\%$  as estimated by Kropman employees). Measured values:

- Supply air:  $19.9 \cdot 10^3 \text{ (m}^3/\text{h)}$  ( $\pm 25\%$ )      Design:  $21000 \text{ (m}^3/\text{h)}$
- Return air:  $16.4 \cdot 10^3 \text{ (m}^3/\text{h)}$  ( $\pm 25\%$ )      Design:  $17400 \text{ (m}^3/\text{h)}$

These values are within range of the design values, but due to low accuracy not useable for the research.

A somewhat more reliable method is to reconstruct the airflow using the energy required to heat up the airflow. Because the water flow between the AHU heat exchanger and heating coil is constant (1.7 l/s), the temperature difference is directly related to the delivered heating power. When the heating power is divided by the temperature increase (minus fan dissipation) multiplied by the specific heat of air (1.2 kJ/K), the airflow is calculated. Figure F-9 shows the calculated airflow during the winter of 2013 is roughly  $23000 \text{ m}^3/\text{h}$ . This value is in line with the design flow of  $21000 \text{ m}^3/\text{h}$  plus  $\sim 10\%$  leaking air.

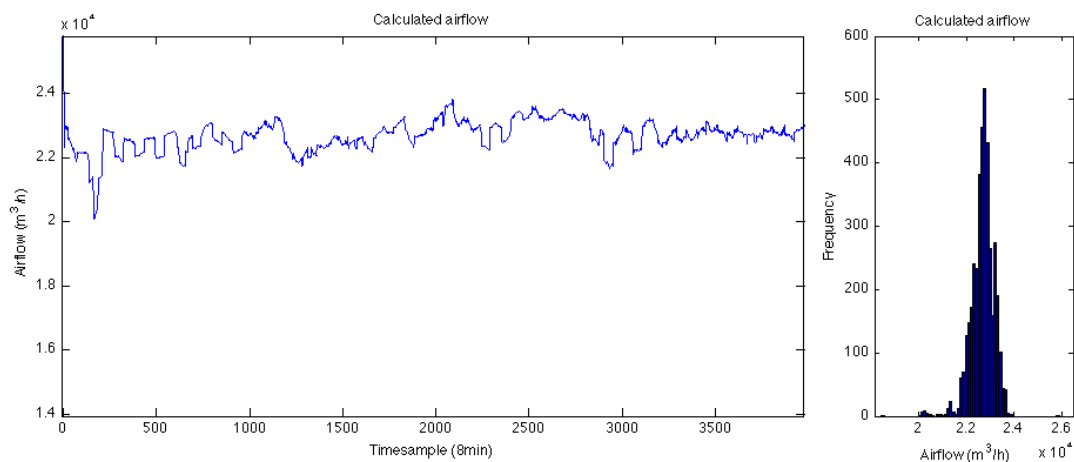


Figure F-9 - Calculated supply airflow using measured heating power



Using the same method, the airflow during regeneration mode can be determined. Because heating of air circulated through the regeneration valve is not an existing AHU state, the state must be manually created outside office hours. Because it takes a while before the whole systems has reached a steady state, only one measurement is done. When 43.8 kW of heat was added, the airflow was heated by 5.1 °C, which equals 25700 m<sup>3</sup>/h airflow.

The airflow of the exhaust air cannot be measured this way, because of the absence of a heating or cooling coil. However, a rough estimation can be done using the air filter pressure drop, which is roughly proportional<sup>4</sup> to the airflow. When the regeneration valve is closed, the pressure drop over the intake filter decreases from 102 Pa to 90 Pa. This equals a proportional airflow decrease from 25700 m<sup>3</sup>/h to 22700 m<sup>3</sup>/h, about equal to the 23000 m<sup>3</sup>/h results from the measurement above.

The pressure drop over the exhaust filter decreases from 160 Pa to 120 Pa, equal to a decrease from 25700 m<sup>3</sup>/h to 19300 m<sup>3</sup>/h. This seems a bit high, because the design flow is only 17400 m<sup>3</sup>/h. The difference is caused by the leaking air through the regeneration valve. Because this value won't be used in the model, further measurements and calculations are not necessary. Using these values as assumption, the air balance of Figure F-10 is derived.

Taking the leaking airflows in account, the measurements and calculated flows do match better. All flows in this graph are estimations based on various tricks. Turbulent airflows in an AHU are very difficult to measure and this graph should be seen as an indication.

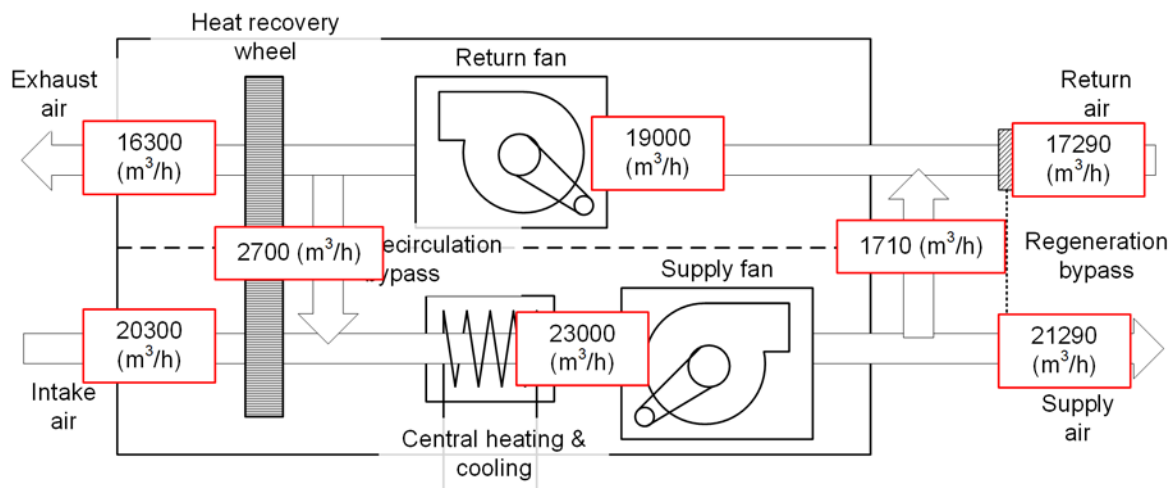


Figure F-10 - Calculated air leaks through valves and HRW

<sup>4</sup> ASHRAE Handbook – HVAC Systems and Equipment, 2008

## DISSIPATION AHU FANS

A typical AHU fan heats the air with roughly 1°C (common rule of thumb). This increase depends on the required pressure difference over the fan and the airflow. By measuring the  $\Delta T$ , the fan efficiency can be derived.

### 1) Intake fan

The histogram shows an average temperature increase of 1.3°C. Using the assumption that the airflow is 23000 (m<sup>3</sup>/h), the thermal dissipation is calculated at 9.8 kW. This is 87% of the electricity use of the fan.

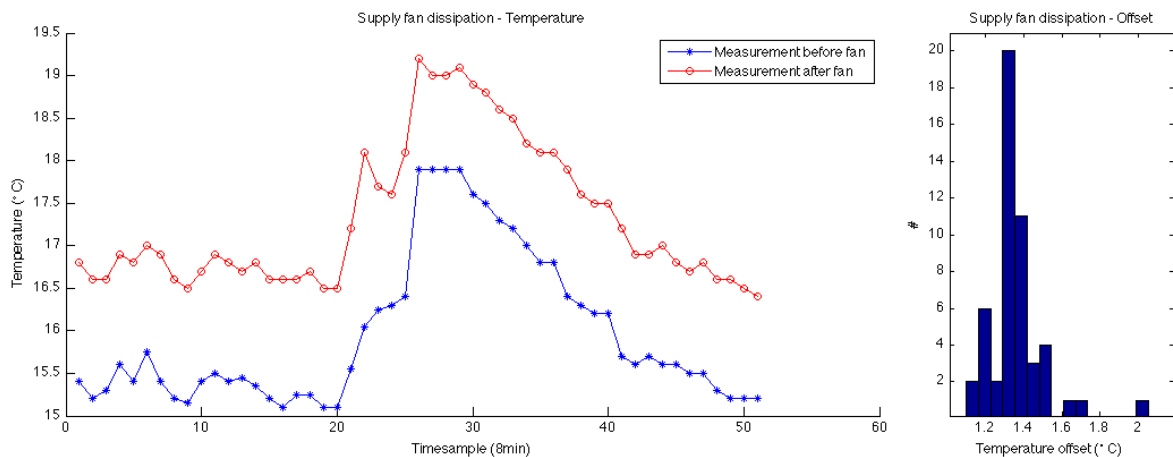


Figure F-11 - Dissipation intake fan

### 2) Exhaust fan

The exhaust measurement points 10-25 are disturbed because of heat recovery wheel activity. Between points 30-45 there is also some heat recovery wheel activity visible. Points 25-65 are used to define the temperature offset histogram, showing a 1°C offset. Assuming the exhaust airflow of 19000 (m<sup>3</sup>/h), the dissipation is calculated at 6.4 kW. This is 67% of the electricity use of the fan.

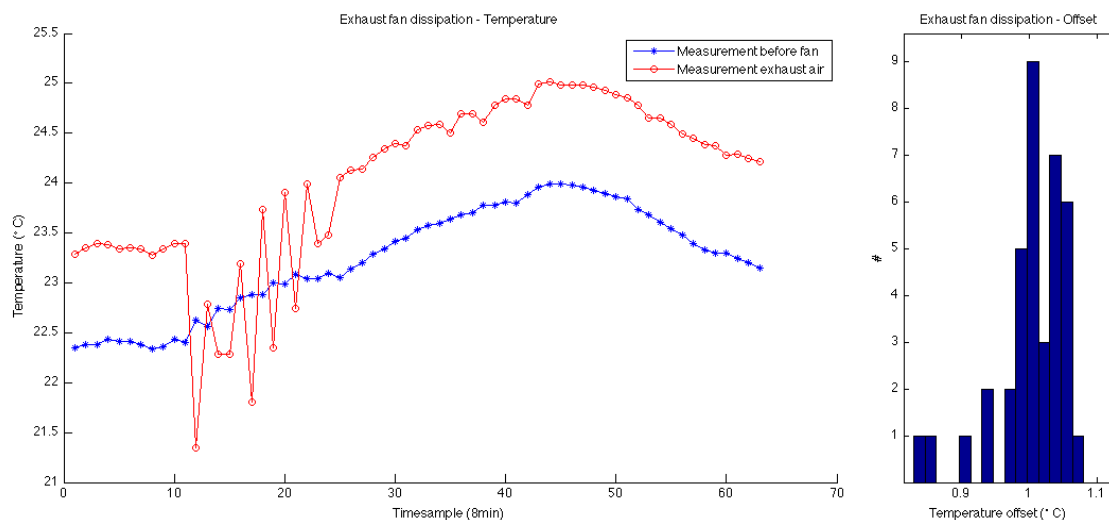


Figure F-12 - Dissipation exhaust fan

The variation in supply (87%) and exhaust (67%) fan dissipation is partly caused by the pressure difference that is generated. The supply fan generates 840 Pa pressure difference and the exhaust fan 740 Pa.

## MOISTURE SENSORS

There are three moisture sensors used in the installation, two in the buildings air ducts and one on the roof as part of the weather station. The duct sensors are capacitive relative humidity sensors, so they can be compared without correcting for the temperature sensor offset. The duct sensors have an accuracy<sup>5</sup> of 3% and the data logger probe has an accuracy<sup>6</sup> of 2%.

### 1. Supply air RH sensor

The supply air RH sensor has an offset of roughly 7%. The instabilities in the first part of the measurement are caused by instable supply air temperatures.

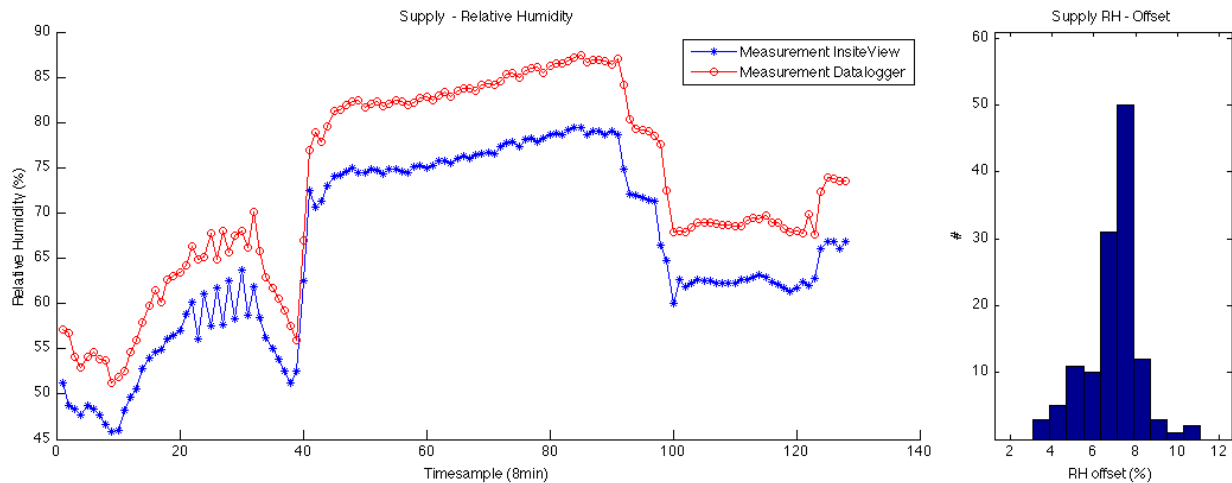


Figure F-13 - Supply air moisture sensor

### 2. Return air RH sensor

The return air RH sensor has an offset of roughly 3%. Although this is within the error margin of the duct sensor, it makes sense to apply this correction because the offset seems very constant.

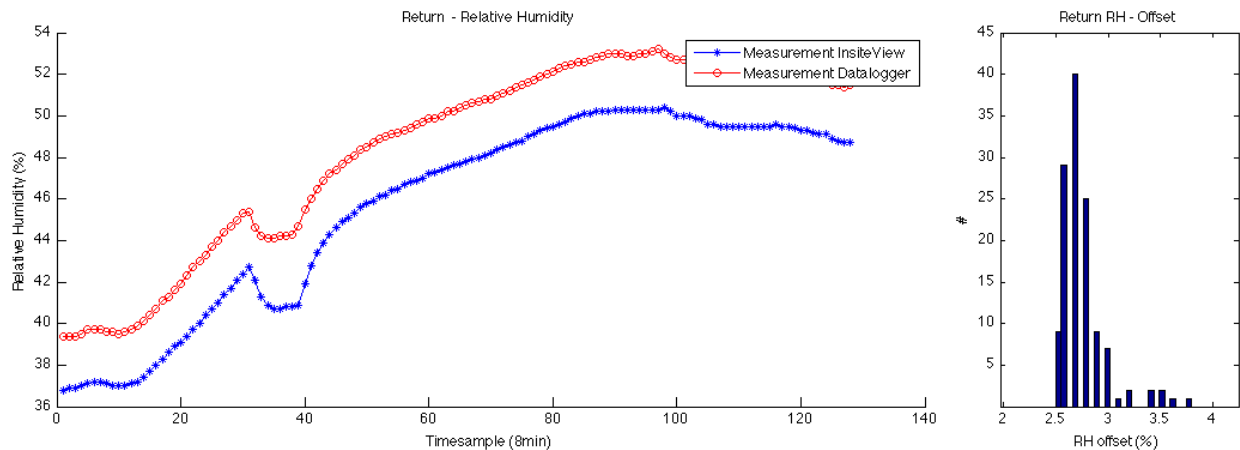


Figure F-14 - Return air moisture sensor

### 3. Weather station RH sensor

The moisture sensor of the weather station is checked by comparing the calculated absolute humidity with the absolute humidity of the supply air in the simulation method in section 2.2. This sensor proved to be accurate, because dehumidification converged to zero far above the dew-point temperature.

<sup>5</sup> Siemens, 'Duct Sensors QFM2100' datasheet, Jul. 2008

<sup>6</sup> Testo, '176H2 - Data logger - Temperature and humidity', Mar. 2012

### HEAT RECOVERY WHEEL

The heat recovery wheel (also known as rotary heat exchanger) is a large cylindrical aluminum disk, perforated with a fine mesh of channels. The wheel is mounted with the upper half in the exhaust air and the lower half in the intake air. It can rotate perpendicular to the airflows. The warm (i.e. 25 °C) exhaust air will heat up the upper half of the disc and the cold intake air (i.e. 5 °C) will cool down the lower half. When the wheel is rotated the warm half will release its heat to the intake air and vice versa. By varying the angular velocity of the wheel, the amount of transferred heat can be controlled.

The recovery efficiency is expressed using equation F-1. The equation calculates the ratio between the maximal achievable temperature increase ( $T_{\text{exhaust}} - T_{\text{intake}}$ ) and the actual achieved temperature increase ( $T_{\text{afterhr}} - T_{\text{intake}}$ ). Because the exhaust flow is lower than the intake flow, it is corrected by the flow ratio. A typical heat recovery wheel has an efficiency of roughly 80%.

$$\eta_{\text{hrw}} = \frac{T_{\text{exhaust}} - T_{\text{intake}}}{T_{\text{afterhr}} - T_{\text{intake}}} * \frac{\phi_{\text{intake}}}{\phi_{\text{exhaust}}} \quad (\text{F-1})$$

Figure F-15 shows the efficiency of the heat recovery wheel. At maximum rpm the efficiency is around 80%, which is in line with theoretical efficiency. The graph shows also there is no efficiency improvement above 40% angular velocity. At this velocity the wheel reaches a constant temperature distribution apparently. Applying a different gear ratio to the wheel would make it easier to control.

The dataset is filtered on all HRW activity between 1 and 99% during office hours and while startup valve is inactive. The line at 30% is the periodic setting to avoid jamming or clogging of the wheel. The values of 100% are left out, because this is the startup speed and results in a random collection of startup values.

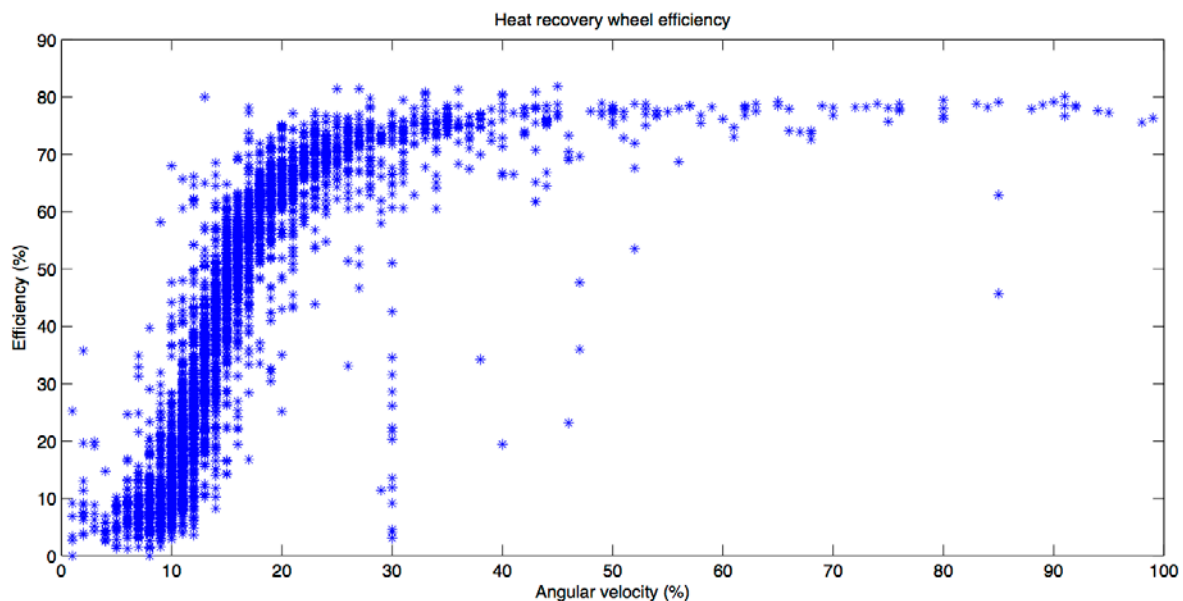


Figure F-15 - Heat recovery wheel efficiency

## Appendix G - CALIBRATION MEASUREMENTS WATER FLOWS

The majority of temperature, flow, pressure and moisture sensors used in the HVAC system is installed during commissioning in 2004 and have never been calibrated or checked since. Because the method developed in this project does heavily depend on accuracy of the historical data, a quick check of the used sensors is performed using recently calibrated measuring equipment. The main purpose of these measurements is to establish if recorded values are within usable error range. If not, the measurements are used to define the offset.

### CONSTANT WATER FLOWS

All measurements are executed with a calibrated 'TA-Hydrionics Scope', using pressure differential measurements over balancing valves. The internal software of the measuring device is used to calculate flows. Typical 'rule of thumb' error range of these measurements is 10%, depending on both balancing valve setting<sup>1</sup> and pressure measurement precision<sup>2</sup>.

#### 1. Heating circuit AHU – 10CP1 – CP-4

|                        |   |
|------------------------|---|
| Measurement conditions | - Chilled water valve closed<br>- Measurement performed at balancing valve in return pipe |
| Pump type              | UPS 40-120F   |
| Valve type             | Staf 50   |
| Design flow            | 2.0 [l/s]   |
| Measurement 2004       | 1.64 [l/s] (3.2 [kPa] – position 4.0 – Kv 33)   |
| Measurements 2014      | 1.7 (±0.2) [l/s] (3.5 [kPa] – position 4.0 – Kv 33)                                       |

#### 2. District heating – 1CP1 – CP-9

|                        |   |
|------------------------|---|
| Measurement conditions | - Measurement performed at balancing valve in return pipe<br>- District heating not active (valve closed) |
| Pump type              | UPS 40-180  |
| Valve type             | Staf 50   |
| Design flow            | 2.9 [l/s]   |
| Measurement 2004       | 2.72 [l/s] (8.8 [kPa] – position 4.0 – Kv 33)   |
| Value used in Priva    | 0.271 [l/s]   |
| Measurement 2014       | 2.8 (±0.3) [l/s] (9.9 [kPa] – position 4.0 – Kv 33)   |

#### 3. Heat pump condenser side – 2CP1 – CP-7

|                        |  |
|------------------------|--|
| Measurement conditions | - Measurement performed at balancing valve<br>- Heat pump not active<br>- Influence valve 2CV1 tested, influence not significant (<5%) |
| Pump type              | UPS 32-120F  |
| Valve type             | Stad 40  |
| Design flow            | 1.05 [l/s]   |
| Measurement 2004       | 1.131 [l/s] (4.5 [kPa] – position 4.0 – Kv 19.2)   |
| Value used in Priva    | 1.65 [l/s]   |
| Measurement 2014       | 1.8 (±0.2) [l/s] (11.0 [kPa] – position 4.0 – Kv 19.2)   |

<sup>1</sup> Tour & Andersson, 'TA Hydrionics, TA Scope – Inregelinstrument' datasheet, Oct. 2013

<sup>2</sup> Tour & Andersson, 'TA Hydrionics, STAF/STAF-SG– Inregelafsluiter' datasheet, Mar. 2013

#### 4. Heat pump evaporator side – CP-6

|                        |   |
|------------------------|---|
| Measurement conditions | - Included in heat pump<br>- Measurement performed at balancing valve<br>- Heat pump active |
| Pump type              | N/a   |
| Valve type             | Staf 50   |
| Design flow            | 2.25 [l/s]  |
| Measurement 2004       | 2.36 [l/s] (6.6 [kPa] – position 4.0 – Kv 33)   |
| Value used in Priva    | 2.0 [l/s]   |
| Measurement 2014       | 2.3 ( $\pm 0.2$ ) [l/s] (5.8 [kPa] – position 4.0 – Kv 33)                                  |

#### WATER TEMPERATURE SENSORS

Temperature measurements are also performed with the 'TA-Hydrionics Scope' using the temperature probe, measured directly in the water at circuit valves. All measurements were monitored for at least 2 minutes to ensure steady state and measurement accuracy. Only a few sensors could be measured directly. Especially the valves in the cold circuit are often blocked by fitted extension pieces. These pieces allow pressure measurements, but no temperature measurements. For this reason several measurements are performed using reconstruction via other (checked) temperature sensors. Water temperature sensors have a design accuracy<sup>3</sup> of  $\pm 0.3\text{K}$ . The TA-Scope probe has an accuracy<sup>4</sup> of  $<0.2\text{K}$ . An offset correction is only applied when the error is  $>0.1\text{K}$ .

##### 1. District heating return – 1TE2

|                      |  |
|----------------------|--|
| Measurement method   | - Direct at balancing valve            |
| ISV readout          | $35.9 \pm 0.1\text{ }^{\circ}\text{C}$ |
| TA-Scope Measurement | $36.0 \pm 0.1\text{ }^{\circ}\text{C}$ |
| Correction           | -                                      |

##### 2. District heating supply – 1TE1

|                    |  |
|--------------------|--|
| Measurement method | - Indirect via 1TE2<br>- Circulation pump (CP-9) active for 10 minutes to reach equilibrium temperature in heat exchanger<br>- District heating valve closed |
| ISV readout 1TE2   | $35.4 \pm 0.1\text{ }^{\circ}\text{C}$   |
| ISV readout 1TE1   | $35.5 \pm 0.1\text{ }^{\circ}\text{C}$   |
| Correction         | -  |

##### 3. AHU heating/cooling coil return – 10TE7

|                      |  |
|----------------------|--|
| Measurement method   | - Direct at balancing valve            |
| ISV readout          | $17.4 \pm 0.1\text{ }^{\circ}\text{C}$ |
| TA-Scope Measurement | $17.0 \pm 0.1\text{ }^{\circ}\text{C}$ |
| Correction           | - $0.4\text{ }^{\circ}\text{C}$        |

<sup>3</sup> Siemens, 'Immersion Temperature Sensors, QUA 3010' datasheet, Nov. 2006

<sup>4</sup> Tour & Andersson, 'TA Hydrionics, TA Scope – Inregelinstrument' datasheet, Oct. 2013

#### *4. AHU heating/cooling coil supply – 10TE6*

|                    |  |
|--------------------|--|
| Measurement method | - Indirect by creating constant water temperature in circuit<br>- Using 10TE7 as reference |
| ISV readout 10TE7  | 17.4 ± 0.1 °C  |
| ISV readout 10TE6  | 17.3 ± 0.1 °C  |
| Correction         | - 0.3 °C   |

#### *5. Heat pump condenser side return – 2TE1*

|                      |                             |
|----------------------|-----------------------------|
| Measurement method   | - Direct at balancing valve |
| ISV readout          | 32.9 ± 0.1 °C               |
| TA-Scope Measurement | 32.9 ± 0.1 °C               |
| Correction           | -                           |

#### *6. Heat pump condenser side supply – 2TE2*

|                    |   |
|--------------------|---|
| Measurement method | - Indirect by creating constant water temperature in circuit<br>- Using 2TE1 as reference |
| ISV readout 2TE1   | 30.1 ± 0.1 °C   |
| ISV readout 2TE2   | 30.0 ± 0.1 °C   |
| Correction         | -   |

#### *7. Local cooling group return – 7TE2*

|                      |                             |
|----------------------|-----------------------------|
| Measurement method   | - Direct at balancing valve |
| ISV readout          | 16.7 ± 0.1 °C               |
| TA-Scope Measurement | 16.6 ± 0.1 °C               |
| Correction           | -                           |

#### *8. Local cooling group supply – 7TE1*

|                    |  |
|--------------------|--|
| Measurement method | - Indirect by creating circuit shortcut (7CV1 @ 0%)<br>- Using 7TE2 as reference |
| ISV readout 7TE2   | 16.7 ± 0.1 °C  |
| ISV readout 7TE1   | 16.6 ± 0.1 °C  |
| Correction         | -  |

### 9. Multiple sensors in chilled water circuit

Because of the thick insulation layer on the chilled water circuit piping, the majority of the measurement valves are equipped with an extension part for flow measurements. These extension parts prevent direct measurement of water temperatures because they block access to the original measurement valve. The remaining temperature sensors of the chilled water circuit are checked by creating a steady state throughout the whole building circuit. These values are compared to the measured AHU coil temperature sensors.

The total water volume of the evaluated system is 1.4 m<sup>3</sup>; based on 100 meter piping ( $\pm 5$  liter /meter), 800 liter buffer vessel and 70 liter AHU coil water content. The system flow during the experiment was 7.8 (m<sup>3</sup>/h), so the entire water mass is circulated every 10 minutes. The measurement duration is 18 samples of 8 minutes (2:24 hours).

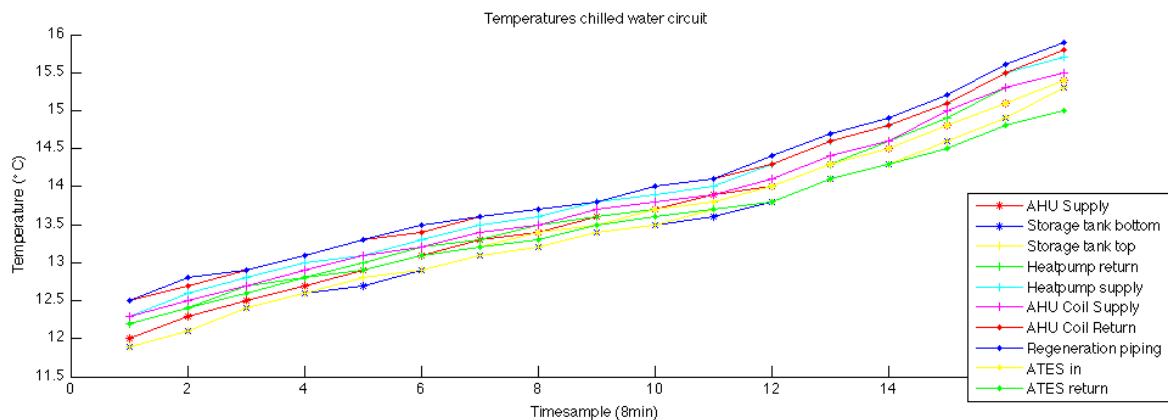


Figure G-1 - Absolute water temperatures

The absolute temperature plot shows a constantly increasing temperature on all temperature sensors, which suggests there is a heat source somewhere in the system. The average temperature increases roughly with 1 degree/hour. The added heat is partly dissipated during transport through the ATEs system. As visible in figure E-2 the offset of the ATEs return sensor temperature is constant during the first 8 measurements, but changes while the average circuit temperature increases.

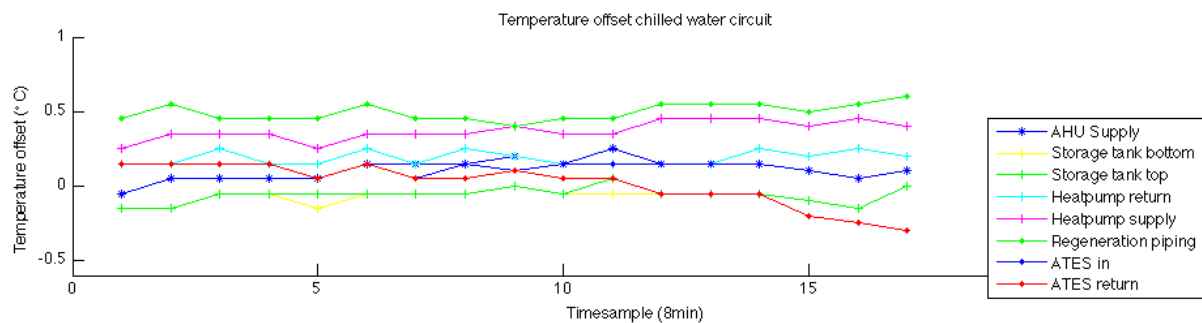


Figure G-2 - Temperature offset from AHU coil measurements



|                      |   |
|----------------------|---|
| Measurement method   | <ul style="list-style-type: none"> <li>- ATES, heat pump, AHU and local cooling are blocked</li> <li>- Water circulated at 7.8 m<sup>3</sup>/h</li> <li>- AHU sensors 10TE6 and 10TE7 used as reference</li> <li>- Measured sensors: <ul style="list-style-type: none"> <li>* 4TE2 – ATES supply flow</li> <li>* 4TE1 – ATES return flow</li> <li>* 5TE3 – Chilled water buffer top sensor</li> <li>* 5TE2 – Chilled water buffer lower sensor</li> <li>* 5TE4 – Heat pump evaporator supply flow</li> <li>* 5TE1 – Heat pump evaporator return flow</li> <li>* 8TE1 – AHU supply flow</li> <li>* 8TT2 – Regeneration bypass</li> </ul> </li> </ul> |
| Averaged offset 4TE2 | 0.1 °C  |
| Averaged offset 4TE1 | 0.1 °C  |
| Averaged offset 5TE3 | -0.1 °C   |
| Averaged offset 5TE2 | 0.0 °C  |
| Averaged offset 5TE4 | 0.4 °C  |
| Averaged offset 5TE1 | 0.2 °C  |
| Averaged offset 8TE1 | 0.1 °C  |
| Averaged offset 8TT2 | 0.5 °C  |

The used method for sensor calibration is not a very solid way, but is the only possible option. It can be concluded that there are no very large deviations, which was the main goal. Also the temperature increase (equal to 1.6 kW of constant heating) is interesting to notice. Appendix H explains two possible causes for this heat source.

## Appendix H - ANALYSIS OF LOAD CURVES

The generated scatterplots of the heating and cooling load can be used for reconstruction of the thermal building characteristics. The summed heating and cooling loads represent the total energy flow needed to keep the building at the average indoor temperature of 22.5°C. From a 'black box' perspective this equals the amount of energy entering or leaving the building via the sum of transmission, ventilation and internal heat loads.

### DURING OFFICE HOURS - DATA ANALYSIS

If the heating and cooling loads during daytime are summed, the graph of Figure H-1 can be plotted. This graph can be fitted by equation H-1.

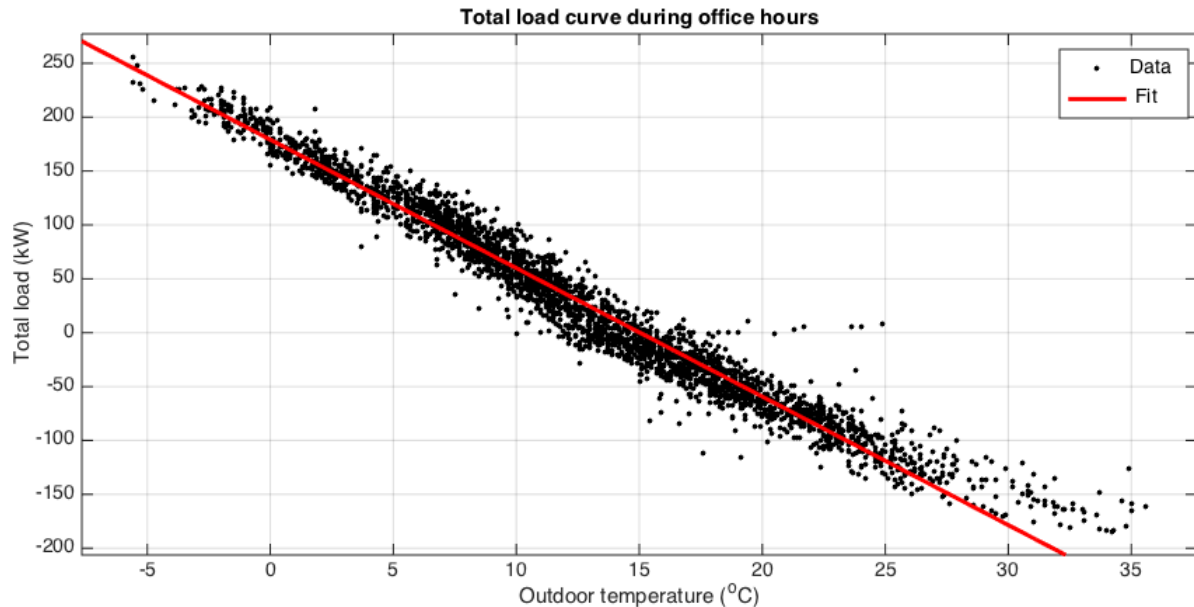


Figure H-1 - Summed load profile during office hours

$$P_{total} = 179.1 - 11.9 T_{outdoor} \quad (R^2: 0.993) \quad (H-1)$$

From this fit two building characteristics are derived:

- The internal heat load is equal to the cooling load, when the average indoor temperature equals the outdoor temperature (22.5°C) → 88.7 kW
- The transmission is the slope of the curve minus the ventilation losses (6.4 kg/s \* 1.2 kJ/kgK = 7.7 kW/K). → 4.2 kW/K

### DURING OFFICE HOURS – COMPARISON WITH THEORETICAL ANALYSIS

The analyzed values can be compared to theoretical estimations of the internal heat load and the building transmission. First the internal heat load is estimated and next the transmission value.

#### INTERNAL HEAT LOAD

For the internal heat load the solar irradiance, building use and thermal mass are evaluated.

##### Solar irradiance variation

The sunlight passing through the windows is absorbed by the interior and provides an internal heat gain. The Kropman building is equipped with automatic sun blinds that can reduce solar irradiance by 75% in two steps. Using 280 m<sup>2</sup> of windows on the south façade and a transmission of 0.6, a quick calculation is done. When the sun heats the south façade with an intensity of 600 W/m<sup>2</sup> (sunny day & sunscreens down), 300 W/m<sup>2</sup> (light clouds & sunscreens 50%) or 150 W/m<sup>2</sup>

(cloudy day & sunscreens up) the internal heat load will be in all cases increased with 25.2 kW of sunlight. For this reason no proportional relation between the solar intensity and internal heat load can be found in the data. Although the sun definitely influences the internal heat load, the average value is expected to be 25 kW with a 100% variation.

#### *Presence*

The Kropman office is has a very variable occupation. During start and end of the office hours hardly 10 people are present, while during the mid-day peak around 150 people are in the building. Assuming 100 watts of body heat and 200 watts of computer equipment, the internal heat load varies between 3 and 45 kW along with the presence of employees. The average heat load is 25 kW with a 100% variation throughout the day.

Slightly related to the presence of employees is the lighting in the building. The building has around 20 kW of lighting installed and because of the open office design there is only one light switch per wing floor. If one person is present, all the lights on the floor are turned on. The smaller offices are equipped with presence detection, and will be turned on only 50% of the time. These offices occupy 20% of the floor space, which means 10% (2kW) variation.

#### *Thermal mass*

As introduced, because of the small temperature variation the thermal mass of the building core is expected to play a minor role in the general building behavior. However on short-term and local scale, the thermal mass of the building interior is expected to assist in leveling out the variance in internal heat load. For instance, when 10 people enter a meeting room it will take a while for the space to heat up. This heat is stored in the interior and released after these people leave. Based on a rough guess, a variation reduction of 50% is assumed.

#### *Total internal heat load*

Table H-1 shows the summed and expected internal heat load and its variation. The AHU supply fan is included in this calculation; due to the heating of supply air it becomes an internal heat load. The total value of 78 kW is roughly comparable to the measured 88 kW.

| Component               | Average value (kW) | Variation      |
|-------------------------|--------------------|----------------|
| Solar irradiance        | 25 kW              | ±25 kW         |
| Body heat               | 8 kW               | ±8 kW          |
| Equipment               | 17 kW              | ±17 kW         |
| Lighting                | 20 kW              | ±2 kW          |
| AHU supply fan          | 8 kW               | 0 kW           |
| Thermal mass (interior) | 0 kW               | - 50%          |
| <b>Total</b>            | <b>78 kW</b>       | <b>± 26 kW</b> |

Table H-1 - Expectation of internal heat load during office hours

#### *THERMAL CONDUCTIVITY VALUE*

The total conductivity value of the building can be calculated by summing the separate constructive parts of the building shell, based on quick assumptions used in the design. Table H-2 shows the calculation for this case. The calculation also includes infiltration through the buildings façade. The analyzed value of 4.2 kW/K is in accordance with the calculated 3.8 kW/K.

| Component    | Specific value                          | Area                | Conductivity |
|--------------|---|---------------------|--------------|
| Walls        | 2.5 [m <sup>2</sup> K/ W]               | 720 m <sup>2</sup>  | 288 [W/K]    |
| Windows      | 2.2 [W/m <sup>2</sup> K]                | 1080 m <sup>2</sup> | 2376 [W/K]   |
| Roof         | 2.5 [m <sup>2</sup> K/ W]               | 1120 m <sup>2</sup> | 448 [W/K]    |
| Floor        | 2.5 [m <sup>2</sup> K/ W]               | 1120 m <sup>2</sup> | 448 [W/K]    |
| Infiltration | 0.15 [m <sup>3</sup> /sm <sup>2</sup> ] | 1800 m <sup>2</sup> | 324 [W/K]    |
| Total        | -                                       | -                   | 3.8 [kW/K]   |

Table H-2 - Estimation of the total conductivity value

### OUTSIDE OFFICE HOURS – DATA ANALYSIS

Outside office hour the same plot can be made. Because of the software bug mentioned in the report and appendix K, all values above 10°C are excluded from the fit.

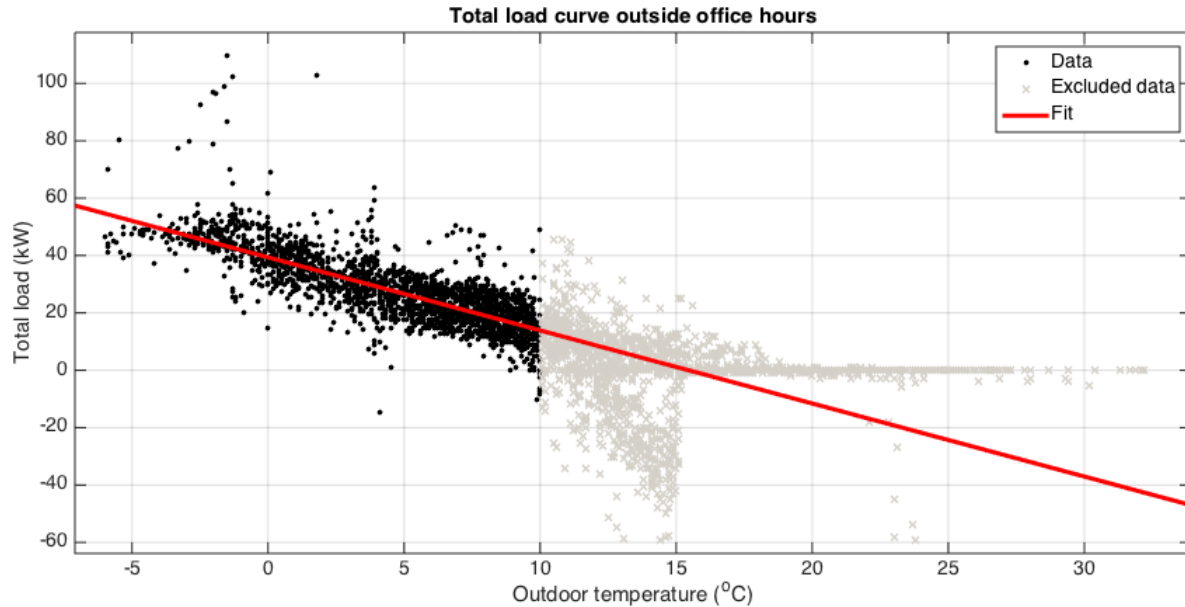


Figure H-2 - Summed load profile outside office hours

$$P_{total} = 39.3 - 2.5 T_{outdoor} \quad (R^2: 0.927) \quad (H-2)$$

Using the same method as during office hours, the following characteristics can be derived:

- Internal heat load: 17.0 (kW)
- Transmission: 2.5 (kW/K)

### OUTSIDE OFFICE HOURS – THEORETICAL ANALYSIS

The theoretical analysis is somewhat more difficult, because the building is not used. The internal heat load is created by a bit of standby electricity (measured around 10 kW) use of equipment and some small solar gains. This is in accordance to the measured 17 kW.

Because only half the building is heated during nighttime (both sides of the first floors and the restaurant at the second floor), the transmission should also be roughly half the transmission during daytime. The other floors do have a small amount of heating, because the warm water is still circulated through all chilled beam units. The transmission of 2.5 kW/K is roughly half the transmission during office hours and seems reasonable.

# Appendix I - RAW DATA OF CONTINUOUS COMMISSIONING ANALYSIS

| Temp  |      | Hours |      | Outside office hours |       |                   |      |                     |      |                       |       |                      |       |                   |       |       |       |     |       |
|-------|------|-------|------|----------------------|-------|-------------------|------|---------------------|------|-----------------------|-------|----------------------|-------|-------------------|-------|-------|-------|-----|-------|
|       |      |       |      | ATES                 |       |                   |      | District heating    |      |                       |       | Heat pump            |       |                   |       | AHU   |       |     |       |
|       |      |       |      | Cold stored (kWh)    |       | Heat stored (kWh) |      | Supplied heat (kWh) |      | Evaporator side (kWh) |       | Condenser side (kWh) |       | Regenerated (kWh) |       |       |       |     |       |
| Meas. | Sim. | Meas. | Sim. | Meas.                | Sim.  | Meas.             | Sim. | Meas.               | Sim. | Meas.                 | Sim.  | Meas.                | Sim.  |                   |       |       |       |     |       |
| -10   | -    | -     | -    | -                    | -     | -                 | -    | -                   | -    | -                     | -     | -                    | -     | -                 | -     | -     |       |     |       |
| -9    | -    | -     | -    | -                    | -     | -                 | -    | -                   | -    | -                     | -     | -                    | -     | -                 | -     | -     |       |     |       |
| -8    | -    | -     | -    | -                    | -     | -                 | -    | -                   | -    | -                     | -     | -                    | -     | -                 | -     | -     |       |     |       |
| -7    | 1    | 41    | -62% | 107                  | 1     | inf.              | 32   | inf.                | 0    | 40                    | 0%    | 40                   | 57    | 0%                | 57    | inf.  | 67    |     |       |
| -6    | 14   | 801   | -46% | 1480                 | -     | 511               | inf. | 296                 | -45% | 536                   | 419   | -44%                 | 755   | 1141              | 21%   | 944   |       |     |       |
| -5    | 15   | 784   | -50% | 1559                 | -     | 711               | inf. | 125                 | -77% | 545                   | 188   | -75%                 | 768   | 1124              | 11%   | 1013  |       |     |       |
| -4    | 24   | 1348  | -45% | 2446                 | 2     | inf.              | 995  | inf.                | 393  | -52%                  | 827   | 563                  | -52%  | 1164              | 1843  | 14%   | 1619  |     |       |
| -3    | 63   | 3902  | -38% | 6315                 | 11    | inf.              | 2073 | inf.                | 1544 | -25%                  | 2052  | 2183                 | -24%  | 2890              | 4994  | 17%   | 4265  |     |       |
| -2    | 102  | 6024  | -40% | 10033                | 16    | inf.              | 2990 | inf.                | 2606 | -17%                  | 3129  | 3698                 | -16%  | 4407              | 7011  | 7%    | 6902  |     |       |
| -1    | 87   | 5956  | -29% | 8408                 | 13    | inf.              | 884  | inf.                | 3204 | 27%                   | 2526  | 4527                 | 28%   | 3547              | 5801  | 2%    | 5897  |     |       |
| 0     | 157  | 9843  | -34% | 14890                | 15    | inf.              | 1438 | inf.                | 5702 | 32%                   | 4321  | 8062                 | 34%   | 6033              | 10276 | -3%   | 10627 |     |       |
| 1     | 148  | 8324  | -39% | 13562                | 30    | inf.              | 1256 | inf.                | 5079 | 38%                   | 3673  | 7247                 | 42%   | 5099              | 8279  | 16%   | 9915  |     |       |
| 2     | 104  | 5108  | -40% | 8525                 | 37    | inf.              | 852  | inf.                | 3118 | 33%                   | 2342  | 4454                 | 38%   | 3231              | 4981  | 20%   | 6191  |     |       |
| 3     | 189  | 7432  | -43% | 13015                | 178   | inf.              | 1377 | inf.                | 5121 | 29%                   | 3968  | 7317                 | 34%   | 5441              | 6363  | 32%   | 9416  |     |       |
| 4     | 150  | 2477  | -11% | 2780                 | 35    | inf.              | 49   | inf.                | 4102 | 45%                   | 2821  | 5827                 | 51%   | 3847              | -     | -     | -     |     |       |
| 5     | 232  | 3367  | -17% | 4078                 | 6     | inf.              | 11   | inf.                | 5791 | 40%                   | 4132  | 8168                 | 46%   | 5602              | -     | -     | -     |     |       |
| 6     | 251  | 3518  | -17% | 4230                 | -     | -                 | 61   | inf.                | 5756 | 34%                   | 4285  | 8075                 | 40%   | 5781              | -     | -     | -     |     |       |
| 7     | 265  | 3521  | -12% | 3992                 | 2     | inf.              | 62   | inf.                | 5700 | 41%                   | 4050  | 7985                 | 47%   | 5433              | -     | -     | -     |     |       |
| 8     | 330  | 3612  | -15% | 4246                 | 8     | inf.              | 114  | inf.                | 5917 | 37%                   | 4308  | 8282                 | 44%   | 5751              | -     | -     | -     |     |       |
| 9     | 263  | 2465  | -11% | 2765                 | 45    | inf.              | 268  | inf.                | 3872 | 37%                   | 2816  | 5398                 | 44%   | 3742              | -     | -     | -     |     |       |
| 10    | 222  | 830   | -49% | 1632                 | 1089  | inf.              | 2452 | inf.                | 1428 | -14%                  | 1663  | 1967                 | -11%  | 2199              | -     | -     | -     |     |       |
| 11    | 230  | 564   | -59% | 1373                 | 2012  | inf.              | 2397 | inf.                | 1120 | -20%                  | 1398  | 1544                 | -16%  | 1841              | -     | -     | -     |     |       |
| 12    | 228  | 366   | -66% | 1063                 | 3175  | inf.              | 1830 | inf.                | 817  | -25%                  | 1085  | 1111                 | -22%  | 1421              | -     | -     | -     |     |       |
| 13    | 195  | 244   | -71% | 856                  | 3091  | inf.              | 674  | inf.                | 487  | -44%                  | 869   | 649                  | -43%  | 1134              | -     | -     | -     |     |       |
| 14    | 196  | 236   | -72% | 836                  | 3739  | inf.              | 635  | inf.                | 358  | -59%                  | 880   | 494                  | -56%  | 1136              | -     | -     | -     |     |       |
| 15    | 217  | 148   | inf. | -                    | 495   | inf.              | 49   | inf.                | 295  | inf.                  | -     | 406                  | inf.  | -                 | -     | -     | -     |     |       |
| 16    | 235  | 83    | inf. | -                    | 6     | inf.              | -    | inf.                | 124  | inf.                  | -     | 160                  | inf.  | -                 | -     | -     | -     |     |       |
| 17    | 188  | 45    | inf. | -                    | 11    | inf.              | -    | inf.                | 84   | inf.                  | -     | 116                  | inf.  | -                 | -     | -     | -     |     |       |
| 18    | 216  | 24    | inf. | -                    | 7     | inf.              | -    | inf.                | 72   | inf.                  | -     | 96                   | inf.  | -                 | -     | -     | -     |     |       |
| 19    | 131  | 4     | inf. | -                    | 9     | inf.              | -    | -                   | 35   | inf.                  | -     | 49                   | inf.  | -                 | -     | -     | -     |     |       |
| 20    | 96   | 3     | inf. | -                    | 15    | inf.              | -    | -                   | 79   | inf.                  | -     | 111                  | inf.  | -                 | -     | -     | -     |     |       |
| 21    | 79   | 3     | inf. | -                    | 9     | inf.              | -    | -                   | 54   | inf.                  | -     | 74                   | inf.  | -                 | -     | -     | -     |     |       |
| 22    | 76   | 1     | inf. | -                    | 58    | inf.              | -    | -                   | 116  | inf.                  | -     | 157                  | inf.  | -                 | -     | -     | -     |     |       |
| 23    | 50   | -     | -    | -                    | 718   | inf.              | -    | -                   | 177  | inf.                  | -     | 236                  | inf.  | -                 | -     | -     | -     |     |       |
| 24    | 27   | -     | -    | -                    | 76    | inf.              | -    | -                   | 35   | inf.                  | -     | 46                   | inf.  | -                 | -     | -     | -     |     |       |
| 25    | 22   | -     | -    | -                    | -     | -                 | -    | -                   | -    | -                     | -     | -                    | -     | -                 | -     | -     | -     |     |       |
| 26    | 20   | -     | -    | -                    | 8     | inf.              | -    | -                   | 85   | inf.                  | -     | 113                  | inf.  | -                 | -     | -     | -     |     |       |
| 27    | 6    | -     | -    | -                    | 4     | inf.              | -    | -                   | 46   | inf.                  | -     | 61                   | inf.  | -                 | -     | -     | -     |     |       |
| 28    | 4    | -     | -    | -                    | 4     | inf.              | -    | -                   | 50   | inf.                  | -     | 62                   | inf.  | -                 | -     | -     | -     |     |       |
| 29    | 3    | -     | -    | -                    | 7     | inf.              | -    | -                   | 84   | inf.                  | -     | 112                  | inf.  | -                 | -     | -     | -     |     |       |
| 30    | 2    | -     | -    | -                    | 4     | inf.              | -    | -                   | 43   | inf.                  | -     | 58                   | inf.  | -                 | -     | -     | -     |     |       |
| 31    | 4    | -     | -    | -                    | -     | -                 | -    | -                   | -    | -                     | -     | -                    | -     | -                 | -     | -     | -     |     |       |
| 32    | 2    | -     | -    | -                    | -     | -                 | -    | -                   | -    | -                     | -     | -                    | -     | -                 | -     | -     | -     |     |       |
| 33    | -    | -     | -    | -                    | -     | -                 | -    | -                   | -    | -                     | -     | -                    | -     | -                 | -     | -     | -     |     |       |
| 34    | -    | -     | -    | -                    | -     | -                 | -    | -                   | -    | -                     | -     | -                    | -     | -                 | -     | -     | -     |     |       |
| 35    | -    | -     | -    | -                    | -     | -                 | -    | -                   | -    | -                     | -     | -                    | -     | -                 | -     | -     | -     |     |       |
| Sum   | 4844 | 71074 | 34%  | 108191               | 14936 | 100%              | 0    | 21721               | 100% | 0                     | 63951 | 22%                  | 52266 | 90072             | 26%   | 71279 | 51813 | -9% | 56858 |

| Temp | Hours | Meas. | Sim. | Meas. | Sim. | Meas. | Sim. | Meas. | Sim. | Meas. | Sim. | Meas. | Sim. | Meas. | Sim. |
|------|-------|-------|------|-------|------|-------|------|-------|------|-------|------|-------|------|-------|------|
| -10  | -     | -     | -    | -     | -    | -     | -    | -     | -    | -     | -    | -     | -    | -     | -    |
| -9   | -     | -     | -    | -     | -    | -     | -    | -     | -    | -     | -    | -     | -    | -     | -    |
| -8   | -     | -     | -    | -     | -    | -     | -    | -     | -    | -     | -    | -     | -    | -     | -    |
| -7   | 1     | 41.0  | -62% | 107.1 | 1.0  | inf.  | 32.0 | inf.  | 0.2  | 40.3  | 0%   | 40.2  | 56.7 | 0%    | 56.6 |
| -6   | 14    | 57.2  | -46% | 105.7 | -    | 36.5  | inf. | 21.1  | -45% | 38.3  | 29.9 | -44%  | 53.9 | 81.5  | 21%  |
| -5   | 15    | 52.3  | -50% | 103.9 | -    | 47.4  | inf. | 8.3   | -77% | 36.4  | 12.5 | -75%  | 51.2 | 74.9  | 11%  |
| -4   | 24    | 56.2  | -45% | 101.9 | 0.1  | inf.  | 41.4 | inf.  | 16.4 | -52%  | 34.4 | 23.4  | -52% | 48.5  | 76.8 |
| -3   | 63    | 61.9  | -38% | 100.2 | 0.2  | inf.  | 32.9 | inf.  | 24.5 | -25%  | 32.6 | 34.6  | -24% | 45.9  | 79.3 |
| -2   | 102   | 59.1  | -40% | 98.4  | 0.2  | inf.  | 29.3 | inf.  | 25.5 | -17%  | 30.7 | 36.3  | -16% | 43.2  | 68.7 |
| -1   | 87    | 68.5  | -29% | 96.6  | 0.1  | inf.  | 10.2 | inf.  | 36.8 | 27%   | 29.0 | 52.0  | 28%  | 40.8  | 66.7 |
| 0    | 157   | 62.7  | -34% | 94.8  | 0.1  | inf.  | 9.2  | inf.  | 36.3 | 32%   | 27.5 | 51.4  | 34%  | 38.4  | 65.5 |
| 1    | 148   | 56.2  | -39% | 91.6  | 0.2  | inf.  | 8.5  | inf.  | 34.3 | 38%   | 24.8 | 49.0  | 42%  | 34.4  | 55.9 |
| 2    | 104   | 49.1  | -40% | 82.0  | 0.4  | inf.  | 8.2  | inf.  | 30.0 | 33%   | 22.5 | 42.8  | 38%  | 31.1  | 47.9 |
| 3    | 189   | 39.3  | -43% | 68.9  | 0.9  | inf.  | 7.3  | inf.  | 27.1 | 29%   | 21.0 | 38.7  | 34%  | 28.8  | 33.7 |
| 4    | 150   | 16.5  | -11% | 18.5  | 0.2  | inf.  | 0.3  | inf.  | 27.3 | 45%   | 18.8 | 38.8  | 51%  | 25.6  | -    |
| 5    | 232   | 14.5  | -17% | 17.6  | 0.0  | inf.  | 0.0  | inf.  | 25.0 | 40%   | 17.8 | 35.2  | 46%  | 24.1  | -    |
| 6    | 251   | 14.0  | -17% | 16.9  | -    | -     | 0.2  | inf.  | 22.9 | 34%   | 17.1 | 32.2  | 40%  | 23.0  | -    |
| 7    | 265   | 13.3  | -12% | 15.1  | 0.0  | inf.  | 0.2  | inf.  | 21.5 | 41%   | 15.3 | 30.1  | 47%  | 20.5  | -    |
| 8    | 330   | 10.9  | -15% | 12.9  | 0.0  | inf.  | 0.3  | inf.  | 17.9 | 37%   | 13.1 | 25.1  | 44%  | 17.4  | -    |
| 9    | 263   | 9.4   | -11% | 10.5  | 0.2  | inf.  | 1.0  | inf.  | 14.7 | 37%   | 10.7 | 20.5  | 44%  | 14.2  | -    |
| 10   | 222   | 3.7   | -49% | 7.4   | 4.9  | inf.  | 11.0 | inf.  | 6.4  | -14%  | 7.5  | 8.9   | -11% | 9.9   | -    |
| 11   | 230   | 2.5   | -59% | 6.0   | 8.7  | inf.  | 10.4 | inf.  | 4.9  | -20%  | 6.1  | 6.7   | -16% | 8.0   | -    |
| 12   | 228   | 1.6   | -66% | 4.7   | 13.9 | inf.  | 8.0  | inf.  | 3.6  | -25%  | 4.8  | 4.9   | -22% | 6.2   | -    |
| 13   | 195   | 1.3   | -71% | 4.4   | 15.9 | inf.  | 3.5  | inf.  | 2.5  | -44%  | 4.5  | 3.3   | -43% | 5.8   | -    |
| 14   | 196   | 1.2   | -72% | 4.3   | 19.1 | inf.  | 3.2  | inf.  | 1.8  | -59%  | 4.5  | 2.5   | -56% | 5.8   | -    |
| 15   | 217   | 0.7   | inf. | -     | 2.3  | inf.  | 0.2  | inf.  | 1.4  | inf.  | -    | 1.9   | inf. | -     | -    |
| 16   | 235   | 0.4   | inf. | -     | 0.0  | inf.  | -    | inf.  | 0.5  | inf.  | -    | 0.7   | inf. | -     | -    |
| 17   | 188   | 0.2   | inf. | -     | 0.1  | inf.  | -    | inf.  | 0.4  | inf.  | -    | 0.6   | inf. | -     | -    |
| 18   | 216   | 0.1   | inf. | -     | 0.0  | inf.  | -    | inf.  | 0.3  | inf.  | -    | 0.4   | inf. | -     | -    |
| 19   | 131   | 0.0   | inf. | -     | 0.1  | inf.  | -    | inf.  | 0.3  | inf.  | -    | 0.4   | inf. | -     | -    |
| 20   | 96    | 0.0   | inf. | -     | 0.2  | inf.  | -    | inf.  | 0.8  | inf.  | -    | 1.2   | inf. | -     | -    |
| 21   | 79    | 0.0   | inf. | -     | 0.1  | inf.  | -    | inf.  | 0.7  | inf.  | -    | 0.9   | inf. | -     | -    |
| 22   | 76    | 0.0   | inf. | -     | 0.8  | inf.  | -    | inf.  | 1.5  | inf.  | -    | 2.1   | inf. | -     | -    |
| 23   | 50    | -     | -    | -     | 14.4 | inf.  | -    | inf.  | 3.5  | inf.  | -    | 4.7   | inf. | -     | -    |
| 24   | 27    | -     | -    | -     | 2.8  | inf.  | -    | inf.  | 1.3  | inf.  | -    | 1.7   | inf. | -     | -    |
| 25   | 22    | -     | -    | -     | -    | -     | -    | -     | -    | -     | -    | -     | -    | -     | -    |
| 26   | 20    | -     | -    | -     | 0.4  | inf.  | -    | inf.  | 4.3  | inf.  | -    | 5.7   | inf. | -     | -    |
| 27   | 6     | -     | -    | -     | 0.7  | inf.  | -    | inf.  | 7.7  | inf.  | -    | 10.2  | inf. | -     | -    |
| 28   | 4     | -     | -    | -     | 1.0  | inf.  | -    | inf.  | 12.4 | inf.  | -    | 15.6  | inf. | -     | -    |
| 29   | 3     | -     | -    | -     | 2.3  | inf.  | -    | inf.  | 28.0 | inf.  | -    | 37.4  | inf. | -     | -    |
| 30   | 2     | -     | -    | -     | 2.0  | inf.  | -    | inf.  | 21.3 | inf.  | -    | 28.9  | inf. | -     | -    |
| 31   | 4     | -     | -    | -     | -    | -     | -    | -     | -    | -     | -    | -     | -    | -     | -    |
| 32   | 2     | -     | -    | -     | -    | -     | -    | -     | -    | -     | -    | -     | -    | -     | -    |
| 33   | -     | -     | -    | -     | -    | -     | -    | -     | -    | -     | -    | -     | -    | -     | -    |
| 34   | -     | -     | -    | -     | -    | -     | -    | -     | -    | -     | -    | -     | -    | -     | -    |
| 35   | -     | -     | -    | -     | -    | -     | -    | -     | -    | -     | -    | -     | -    | -     | -    |
| Sum  | 4844  | -     | -    | -     | -    | -     | -    | -     | -    | -     | -    | -     | -    | -     | -    |

Summed

Averaged per hour

|      |       | During office hours |           |                   |           |                     |           |                       |           |                      |           |
|------|-------|---------------------|-----------|-------------------|-----------|---------------------|-----------|-----------------------|-----------|----------------------|-----------|
|      |       | ATES                |           | District heating  |           | Heat pump           |           |                       |           |                      |           |
|      |       | Cold stored (kWh)   |           | Heat stored (kWh) |           | Supplied heat (kWh) |           | Evaporator side (kWh) |           | Condenser side (kWh) |           |
| Temp | Hours | Measured            | Simulated | Measured          | Simulated | Measured            | Simulated | Measured              | Simulated | Measured             | Simulated |
| -10  | 0     | -                   | -         | -                 | -         | -                   | -         | -                     | -         | -                    | -         |
| -9   | 0     | -                   | -         | -                 | -         | -                   | -         | -                     | -         | -                    | -         |
| -8   | 2     | 55                  | -31%      | 79                | -         | 41                  | -71%      | 81                    | 0%        | 113                  | 0%        |
| -7   | 0     | -                   | -         | -                 | -         | -                   | -         | -                     | -         | -                    | -         |
| -6   | 8     | 202                 | -36%      | 316               | -         | 527                 | 16%       | 313                   | -3%       | 437                  | -3%       |
| -5   | 4     | 118                 | -25%      | 158               | -         | 140                 | -32%      | 166                   | 3%        | 229                  | 1%        |
| -4   | 12    | 313                 | -34%      | 473               | 5         | 591                 | 7%        | 443                   | -8%       | 618                  | -9%       |
| -3   | 31    | 813                 | -34%      | 1224              | 17        | 1436                | 4%        | 1193                  | -4%       | 1666                 | -5%       |
| -2   | 76    | 2206                | -27%      | 3016              | 8         | 2963                | -2%       | 3090                  | 1%        | 4289                 | 0%        |
| -1   | 68    | 1966                | -27%      | 2702              | 5         | 2094                | -4%       | 2794                  | 2%        | 3915                 | 2%        |
| 0    | 81    | 2125                | -34%      | 3242              | 23        | 1920                | -3%       | 3269                  | -1%       | 4587                 | 0%        |
| 1    | 98    | 2545                | -36%      | 3977              | 9         | 1824                | 1%        | 3874                  | -4%       | 5443                 | -3%       |
| 2    | 139   | 3401                | -40%      | 5709              | 34        | 1342                | -28%      | 5160                  | -11%      | 7261                 | -9%       |
| 3    | 101   | 2204                | -47%      | 4194              | 123       | 1001                | 35%       | 3766                  | -12%      | 5257                 | -10%      |
| 4    | 109   | 2180                | -51%      | 4489              | 167       | 537                 | inf.      | 3786                  | -17%      | 5254                 | -15%      |
| 5    | 140   | 2704                | -34%      | 4074              | 211       | 249                 | inf.      | 4417                  | -14%      | 5114                 | -11%      |
| 6    | 172   | 3032                | -18%      | 3707              | 348       | 431                 | inf.      | 5136                  | -14%      | 5979                 | -12%      |
| 7    | 182   | 2269                | -28%      | 3160              | 554       | 357                 | inf.      | 4991                  | -19%      | 6133                 | -15%      |
| 8    | 225   | 1738                | -46%      | 3246              | 1438      | 310                 | inf.      | 5469                  | -24%      | 7198                 | -21%      |
| 9    | 186   | 1176                | -51%      | 2419              | 1603      | 133                 | inf.      | 3936                  | -27%      | 5386                 | -23%      |
| 10   | 202   | 781                 | -61%      | 2024              | 2524      | 89                  | inf.      | 3203                  | -35%      | 4965                 | -32%      |
| 11   | 201   | 582                 | inf.      | -                 | 3016      | 186                 | inf.      | 2860                  | -32%      | 4234                 | -29%      |
| 12   | 175   | 387                 | inf.      | -                 | 3032      | 156                 | inf.      | 1874                  | -27%      | 2564                 | -24%      |
| 13   | 151   | 226                 | inf.      | -                 | 3189      | 54                  | inf.      | 1298                  | -25%      | 1739                 | -21%      |
| 14   | 144   | 176                 | inf.      | -                 | 3529      | 48                  | inf.      | 916                   | -42%      | 1575                 | -39%      |
| 15   | 159   | 141                 | inf.      | -                 | 4710      | 69                  | inf.      | 908                   | -22%      | 1163                 | -17%      |
| 16   | 164   | 132                 | inf.      | -                 | 5280      | 24                  | inf.      | 790                   | inf.      | 1083                 | inf.      |
| 17   | 152   | 65                  | inf.      | -                 | 5984      | 5                   | inf.      | 611                   | inf.      | 835                  | inf.      |
| 18   | 169   | 14                  | inf.      | -                 | 8333      | 1                   | inf.      | 331                   | inf.      | 440                  | inf.      |
| 19   | 131   | 8                   | inf.      | -                 | 7902      | -                   | -         | 260                   | inf.      | 362                  | inf.      |
| 20   | 79    | -                   | -         | -                 | 5809      | 0                   | inf.      | 66                    | 52%       | 43                   | 53%       |
| 21   | 116   | -                   | -         | -                 | 9642      | 0                   | inf.      | 313                   | -19%      | 388                  | -16%      |
| 22   | 111   | -                   | -         | -                 | 10604     | 0                   | inf.      | 392                   | -26%      | 529                  | -24%      |
| 23   | 85    | 1                   | inf.      | -                 | 9367      | -                   | -         | 968                   | 24%       | 780                  | 27%       |
| 24   | 61    | -                   | -         | -                 | 7628      | -                   | -         | 1500                  | 123%      | 672                  | 127%      |
| 25   | 51    | 1                   | inf.      | -                 | 7301      | -                   | -         | 1462                  | 38%       | 1057                 | 40%       |
| 26   | 34    | -                   | -         | -                 | 5262      | -                   | -         | 1146                  | 17%       | 979                  | 15%       |
| 27   | 26    | -                   | -         | -                 | 4156      | -                   | -         | 959                   | -8%       | 1048                 | -7%       |
| 28   | 10    | -                   | -         | -                 | 1797      | -                   | -         | 403                   | -26%      | 546                  | -26%      |
| 29   | 13    | -                   | -         | -                 | 2365      | -                   | -         | 542                   | -22%      | 695                  | -21%      |
| 30   | 11    | -                   | -         | -                 | 1998      | -                   | -         | 482                   | -19%      | 599                  | -19%      |
| 31   | 14    | -                   | -         | -                 | 2590      | -                   | -         | 635                   | -17%      | 767                  | -17%      |
| 32   | 7     | -                   | -         | -                 | 1364      | -                   | -         | 312                   | -18%      | 382                  | -18%      |
| 33   | 7     | -                   | -         | -                 | 1376      | -                   | -         | 296                   | -23%      | 383                  | -22%      |
| 34   | 6     | -                   | -         | -                 | 1191      | -                   | -         | 253                   | -22%      | 327                  | -22%      |
| 35   | 3     | -                   | -         | -                 | 582       | -                   | -         | 133                   | -19%      | 165                  | -18%      |
| Sum  | 3916  | 31561               | -35%      | 48210             | 125076    | 16524               | 14387     | 74794                 | -12%      | 85442                | -10%      |
| Temp | Hours | Measured            | Simulated | Measured          | Simulated | Measured            | Simulated | Measured              | Simulated | Measured             | Simulated |
| -10  | 0     | -                   | -         | -                 | -         | -                   | -         | -                     | -         | -                    | -         |
| -9   | 0     | -                   | -         | -                 | -         | -                   | -         | -                     | -         | -                    | -         |
| -8   | 2     | 28                  | -31%      | 40                | -         | 20                  | -71%      | 40                    | 0%        | 57                   | 0%        |
| -7   | 0     | -                   | -         | -                 | -         | -                   | -         | -                     | -         | -                    | -         |
| -6   | 8     | 25                  | -36%      | 39                | -         | 66                  | 16%       | 39                    | -3%       | 40                   | -3%       |
| -5   | 4     | 30                  | -25%      | 40                | -         | 35                  | -32%      | 41                    | 3%        | 40                   | 1%        |
| -4   | 12    | 26                  | -34%      | 39                | 0         | 49                  | 7%        | 37                    | -8%       | 40                   | -9%       |
| -3   | 31    | 26                  | -34%      | 39                | 1         | 46                  | 4%        | 38                    | -4%       | 40                   | -5%       |
| -2   | 76    | 29                  | -27%      | 40                | 0         | 39                  | -2%       | 41                    | 1%        | 40                   | 0%        |
| -1   | 68    | 29                  | -27%      | 40                | 0         | 31                  | -4%       | 41                    | 2%        | 40                   | 2%        |
| 0    | 81    | 26                  | -34%      | 40                | 0         | 24                  | -3%       | 40                    | -1%       | 41                   | 0%        |
| 1    | 98    | 26                  | -36%      | 41                | 0         | 19                  | 1%        | 40                    | -4%       | 41                   | -3%       |
| 2    | 139   | 24                  | -40%      | 41                | 0         | 10                  | -28%      | 37                    | -11%      | 42                   | -9%       |
| 3    | 101   | 22                  | -47%      | 42                | 1         | 10                  | 35%       | 37                    | -12%      | 42                   | -10%      |
| 4    | 109   | 20                  | -51%      | 41                | 2         | 5                   | inf.      | 35                    | -17%      | 42                   | -15%      |
| 5    | 140   | 19                  | -34%      | 29                | 2         | 2                   | inf.      | 32                    | -14%      | 37                   | -11%      |
| 6    | 172   | 18                  | -18%      | 22                | 2         | 3                   | inf.      | 30                    | -14%      | 35                   | -12%      |
| 7    | 182   | 12                  | -28%      | 17                | 3         | 2                   | inf.      | 27                    | -19%      | 34                   | -15%      |
| 8    | 225   | 8                   | -46%      | 14                | 6         | 1                   | inf.      | 24                    | -24%      | 32                   | -21%      |
| 9    | 186   | 6                   | -51%      | 13                | 9         | 1                   | inf.      | 21                    | -27%      | 29                   | -23%      |
| 10   | 202   | 4                   | -61%      | 10                | 12        | 0                   | inf.      | 16                    | -35%      | 25                   | -32%      |
| 11   | 201   | 3                   | inf.      | -                 | 15        | 1                   | inf.      | 14                    | -32%      | 21                   | -29%      |
| 12   | 175   | 2                   | inf.      | -                 | 17        | 1                   | inf.      | 11                    | -27%      | 15                   | -24%      |
| 13   | 151   | 1                   | inf.      | -                 | 21        | 0                   | inf.      | 9                     | -25%      | 12                   | -21%      |
| 14   | 144   | 1                   | inf.      | -                 | 25        | 0                   | inf.      | 6                     | -42%      | 11                   | -39%      |
| 15   | 159   | 1                   | inf.      | -                 | 30        | 0                   | inf.      | 6                     | -22%      | 7                    | -17%      |
| 16   | 164   | 1                   | inf.      | -                 | 32        | 0                   | inf.      | 5                     | inf.      | 7                    | inf.      |
| 17   | 152   | 0                   | inf.      | -                 | 39        | 0                   | inf.      | 4                     | inf.      | 5                    | inf.      |
| 18   | 169   | 0                   | inf.      | -                 | 49        | 0                   | inf.      | 2                     | inf.      | 3                    | inf.      |
| 19   | 131   | 0                   | inf.      | -                 | 60        | -                   | -         | 2                     | inf.      | 3                    | inf.      |
| 20   | 79    | -                   | -         | -                 | 74        | 0                   | inf.      | 1                     | 52%       | 1                    | 53%       |
| 21   | 116   | -                   | -         | -                 | 83        | 0                   | inf.      | 3                     | -19%      | 3                    | -16%      |
| 22   | 111   | -                   | -         | -                 | 96        | 0                   | inf.      | 4                     | -26%      | 5                    | -24%      |
| 23   | 85    | 0                   | inf.      | -                 | 110       | -                   | -         | 11                    | 24%       | 9                    | 27%       |
| 24   | 61    | -                   | -         | -                 | 125       | -                   | -         | 25                    | 123%      | 11                   | 127%      |
| 25   | 51    | 0                   | inf.      | -                 | 143       | -                   | -         | 29                    | 38%       | 21                   | 40%       |
| 26   | 34    | -                   | -         | -                 | 155       | -                   | -         | 34                    | 17%       | 29                   | 18%       |
| 27   | 26    | -                   | -         | -                 | 160       | -                   | -         | 37                    | -8%       | 40                   | -7%       |
| 28   | 10    | -                   | -         | -                 | 180       | -                   | -         | 40                    | -26%      | 55                   | -26%      |
| 29   | 13    | -                   | -         | -                 | 182       | -                   | -         | 42                    | -22%      | 53                   | -21%      |
| 30   | 11    | -                   | -         | -                 | 182       | -                   | -         | 44                    | -19%      | 54                   | -19%      |
| 31   | 14    | -                   | -         | -                 | 185       | -                   | -         | 45                    | -17%      | 55                   | -17%      |
| 32   | 7     | -                   | -         | -                 | 195       | -                   | -         | 45                    | -18%      | 55                   | -18%      |
| 33   | 7     | -                   | -         | -                 | 197       | -                   | -         | 42                    | -23%      | 55                   | -22%      |
| 34   | 6     | -                   | -         | -                 | 199       | -                   | -         | 42                    | -22%      | 54                   | -22%      |
| 35   | 3     | -                   | -         | -                 | 194       | -                   | -         | 44                    | -19%      | 55                   | -18%      |

Summed

Averaged per hour

## Appendix J - MEASUREMENTS ON LEAKING VALVES

The results of the continuous commissioning analysis (but also the load curves in an earlier stage) suggest that there are some leaks or other problems in the system. Not all generated cold is stored in the ATES system. This appendix shows how causes could be detected using data analysis, the measurements on the leakage and an explanation for the leakage.

### DATA ANALYSIS

By analyzing plots of the measured data, already a lot the leaking could have been detected.

#### LEAKING 3-WAY VALVE LOCAL COOLING SUPPLY (7CV1)

This valve is placed as mixing valve to achieve the required supply temperature to the local cooling group (to avoid condensation). By mixing some return water to the supply water the temperature is increased. When fully opened the local cooling supply water should have the same temperature as the water supplied by the ATES system. Figure J-1 shows the valve cannot reach the setpoint temperature after time sample 90, although valve setting is 100% open.

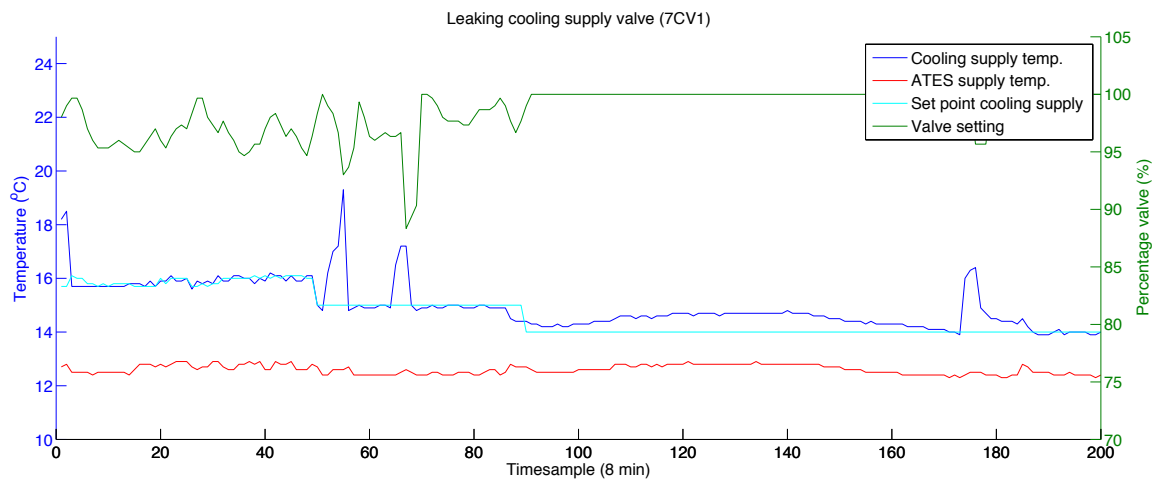


Figure J-1 - Supply valve (7CV1)

#### LEAKING 3-WAY VALVE LOCAL COOLING RETURN (7CV2)

This valve is placed as distribution valve to direct water flow towards series configuration with the heat pump or parallel on the ATES system. Figure J-2 shows a significant deviation between the water temperature leaving the heat pump and the temperature flowing to the ATES when the local cooling pump is started. The water flow is continuously around 3 m<sup>3</sup>/h.

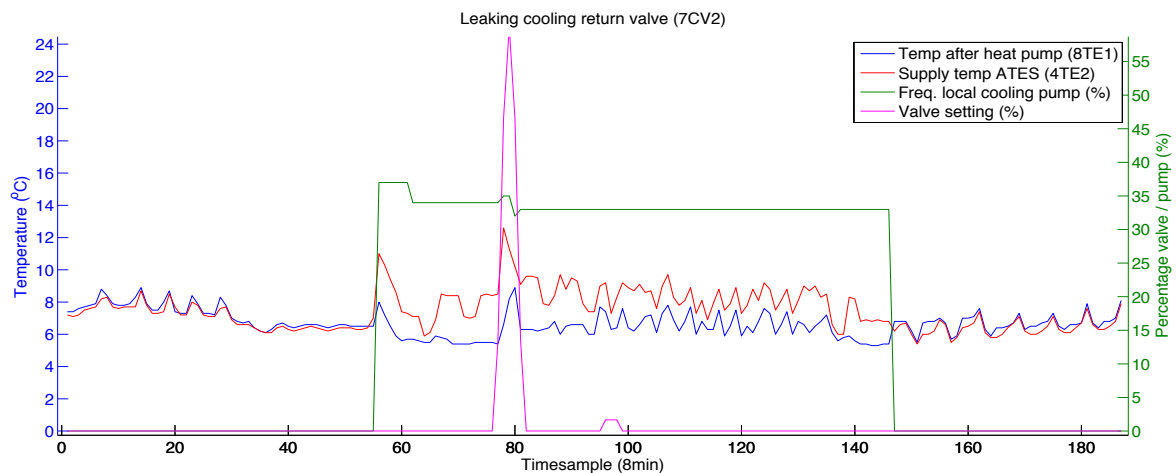


Figure J-2 - Return valve (7CV2)

### LEAKING 3-WAY VALVE BETWEEN HEATING AND COOLING SYSTEM (6CV1)

Figure J-3 shows the return temperature of the combined cooling systems (local + AHU) and the supply temperature to the heat pump condenser. Because valve is 100% opened and the circulation pump is continuously running (not logged, but linked to the valve), these temperatures should be exactly the same. The supply temperature to the heat pump is significantly higher, which suggests there is heated water leaking to the supply flow via 6CV1 and/or 2CV2. This leak causes a lower COP of the heat pump in cooling mode, resulting in less cooling power.

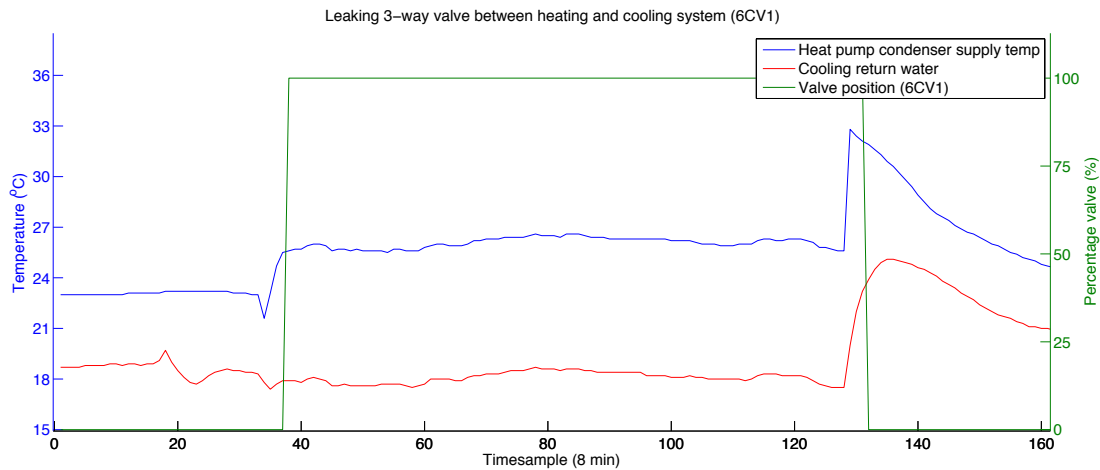


Figure J-3 - Valve between heating and cooling circuit (6CV1)

### LEAKS BETWEEN HEATING AND COOLING CIRCUIT

There is continuously water leaking between the heating and cooling system. This can be noticed when only one of the two systems is active (Figure J-4). During summer (the upper graph) the heating return water temperature is often equal to the cooling return water temperature. During winter (the lower graph) the return temperature of the cooling circuit is gets a lot higher than 20°C and the temperature pattern follows the heating return temperature variations.

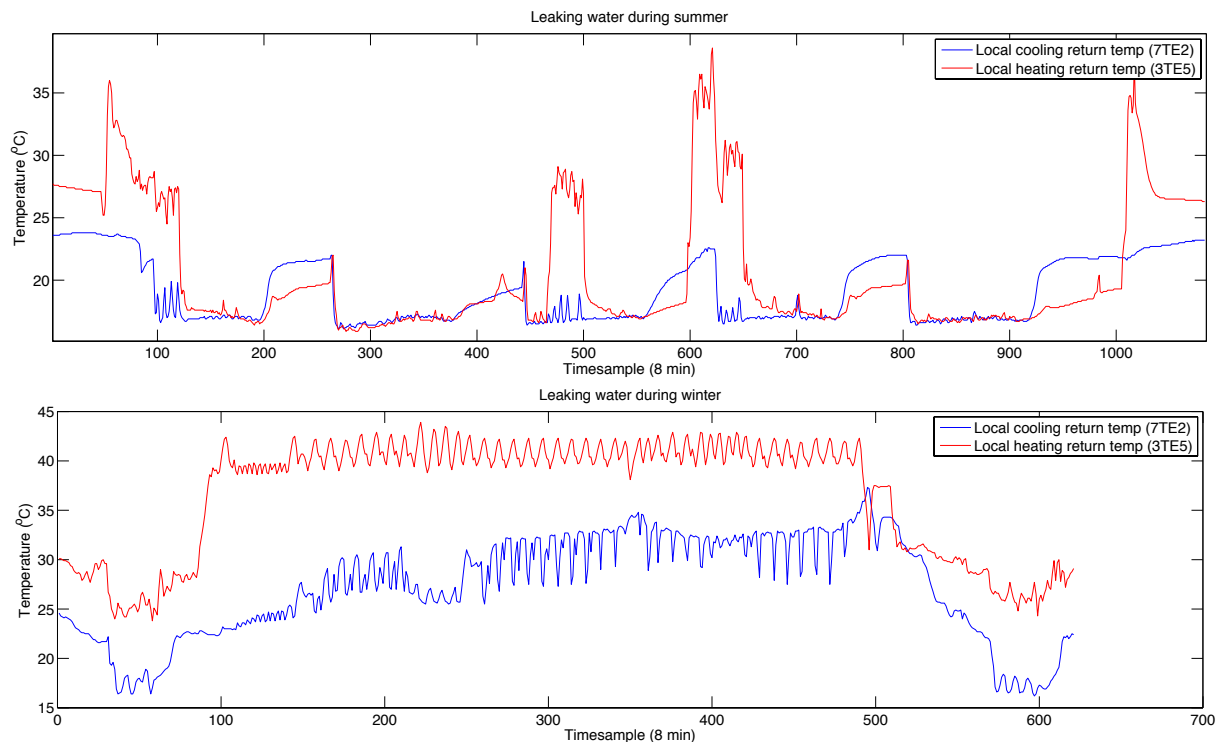


Figure J-4 - Water leaks between heating and cooling circuits



The fact that the temperature profiles follow each other quite accurately indicates already that there is a significant flow. The cold water leaking through the heating systems does not have a large influence, because the heating system is not active during the summer days. The heat leaking through the cooling system does significantly lower the cold storage effectiveness and the heat pump efficiency.

#### HEATING OF THE CHILLED WATER BUFFER

When the cooled water system isn't used for a longer period, the cooled water buffer vessel slowly heats up. During long weekends of inactivity, the temperature can reach up to 40°C. Measurements showed the circulation pump at the evaporator side in continuously running, even when the heat pump is not used. When analyzing historical data (Figure J-5) the effect can be clearly seen. The heat source could be the heat created by the circulation pump or active carter heating of the heat pump. The effect on the yearly performance of the overall system won't be very large, but it still is a waste of electricity and creates an error in the heat pump monitoring system. Also, supplying 40°C water to the heat pump evaporator cannot be very healthy.

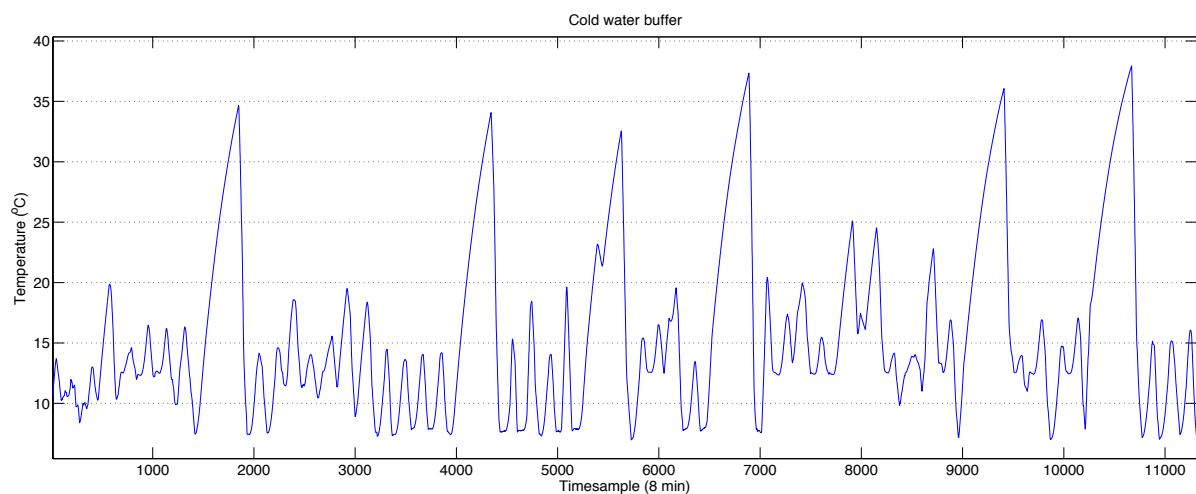


Figure J-5 - Cold water buffer vessel temperatures

#### MEASUREMENTS

An attempt was done to measure the actual leakage through the system. Because there are no balancing valves in the routes of possible leakage, an actual flow measurement is not possible. Also the amount of leakage is variable and depends on the setting of all valves throughout the building (the internal heating or cooling load). These measurements shouldn't be seen as absolute values, but as indication.

#### Measurement states

- A. Regeneration circuit pump 50% - Heat pump off
- B. Regeneration circuit pump 80% - Heat pump off
- C. Regeneration circuit pump 50% - Heat pump on
- D. Regeneration circuit pump 80% - Heat pump on
- E. Regeneration circuit off – Heat pump on

|                        | State A | State B | State C | State D | State E |
|------------------------|---------|---------|---------|---------|---------|
| Flow sensor ATEs       | 6.1     | 8.6     | 10.8    | 13.5    | 5.4     |
| Flow over AHU valve    | 8.0     | 11.2    | 7.5     | 10.0    | -       |
| Flow over bypass valve | -       | -       | 6.4     | 6.4     | 6.5     |
| Sum                    | -       | -       | 13.9    | 16.4    | -       |
| Leak                   | 1.9     | 2.6     | 3.1     | 2.9     | 1.1     |

Table J-1 - Measurements of leaking flows in (m<sup>3</sup>/h)

The values in Table J-1 are worst-case values, during very cold periods (as regeneration is active). During higher outdoor temperatures, the local heating supply water valves are closed and leaks are significantly less. There is not a method to calibrate the ATES flow sensor, because there are no balancing valves in series with the sensor without possible leaking routes in between. During minimal flow ( $<4 \text{ m}^3/\text{h}$ ) and manually closed valves between heating/cooling systems, the sensor readouts match the balancing valve readouts within  $0.2 \text{ m}^3/\text{h}$ .

The amount of energy transferred is hard to estimate, because this largely depends on the temperature of the leaked water. The load curves in chapter 4 provide a good indication on how significant the leaks are.

## LEAKAGE CAUSES

The leakage between the heating and cooling system is caused by a design fault. The open connection between the return water of the cooling system and the supply water for the heating system creates a pressure offset (Figure J-6) between the heating and the cooling system. This offset is equal to the pressure drop over the ATES system. The leakage is proportional to the flow over the ATES system and changes in the ATES flow are visible in the system pressure of the heating system.

The distribution system of the building is constructed using  $\pm 100$  change-over systems for local climate control. Each change-over system uses four valves to ensure the heating and cooling circuits are separated. If one of these valves is not working / closing properly, water flows directly from the highest pressure to the lowest pressure. In this case it implies water flowing from the heating circuit to the cooling circuit.

Another possible weak point is the mixing valve (7CV2) in the return flow of the local cooling. This causes cold water to the ATES supply. Because the water stays in the cold-water circuit, this causes no inefficiencies. The only negative effect is more water has to be circulated by the pump, causing a bit more energy use.

The pressure distribution diagram in Figure J-6 is the situation during office hours and in state 2. If the local cooling pump is not active (state 1), the pressure difference over the supply side of the change-over systems becomes even larger. In state 3 the local cooling group is in parallel configuration to the ATES, equalizing the pressure difference between both return circuits and minimizing leakage. In state 4 the heat pump is not active, so leakage has no negative effect.

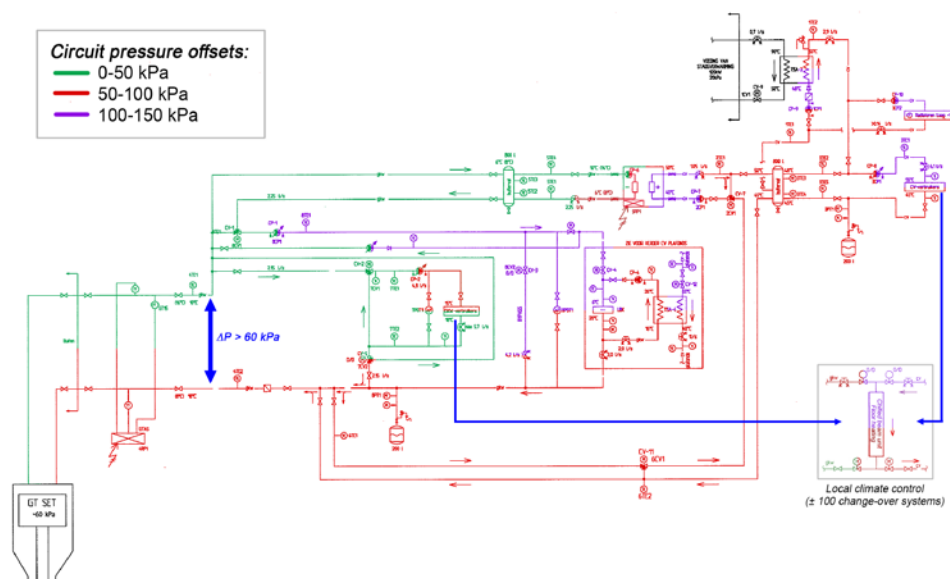
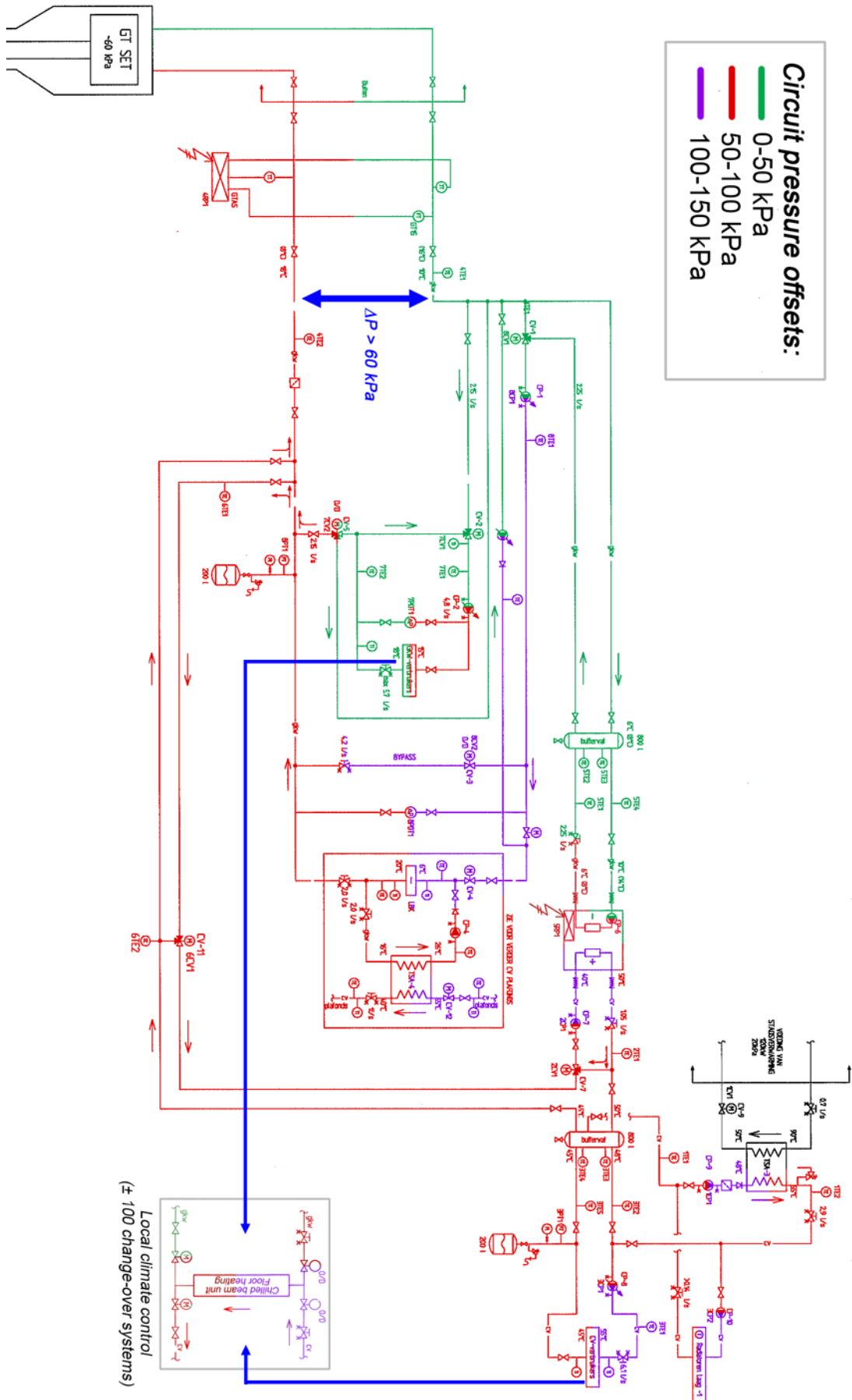


Figure J-6 - Pressure offsets in hydronic circuit (larger version next page)



## CONCLUSION

In short the following problems are found in the HVAC hardware:

- All used 3-way valves are leaking (far more than the design value)
- The open connection between the heating and cooling system is a design fault
- A unknown number of change-over systems is leaking
- The heat pump keeps heating the cold water buffer

None of these problems is very exotic, but all together they cause significant cold storage problems. Most remarkable is that all problems are visible in the historical data since the commissioning in 2004. This means the system has never operated correctly. For a specialized company, it could be expected that someone noticed these problems over the 10-year period of use. On the other hand, the fact that nobody noticed something underpins the need for systems like CC. Using the CC result a good indication was given where to look and what the impact of problems is.

Using this analysis three-design practices can be derived:

- 1) If 3-way valves are needed, decide if mixing or switching is required and choose the appropriate valve (ball or mixing valve).
- 2) Always expect a percentage (~5-10%) of the change-over valves to leak or otherwise not function correctly. This automatically means that during system design, a pressure difference between both sides of the change-over system must be avoided at all times.
- 3) Drawing a quick estimation of the pressure distribution in the principle diagram is a good habit. It quickly points out the critical valves and potential leakage points. The number of these points should be minimized and if they are unavoidable, good quality valves must be applied.

## Appendix K - SOFTWARE PROBLEMS

The main (Priva based) building software was designed in 2004 and was changed several times by several employees and using several software versions over the last 10 years. In the meantime, a fast amount of setpoint changes was done by people changing settings without a specific knowledge about the total building software. As a result, no one fully understands the behavior of the building software anymore and the frequently changing of setpoints only makes the performance worse. To give an impression of the problems, this appendix will give a small introduction categorized per state.

### STATES DURING OFFICE HOURS

#### State 1 (only heating)

- The transport of chilled water from the heat pump to the ATES is controlled by three PID's and three temperature sensors. This complex solution often results in no water transport at all, causing the heat pump to switch in protection mode and district heating is used.
- The floor heating systems (1<sup>st</sup> floor and restaurant) are using a heating curve based on the outdoor temperature with no feedback loop the room temperature. The used setpoint for the restaurant for instance does not make any sense without feedback loop.
- The additional radiator circulation pump is started if the restaurant temperature is below the setpoint value (which has no relation to the actual temperature).
- The district heating is using a lower heating curve temperature (42°C) than the heat pump (50°C), while the heat pump has the most profit of a low heating curve. This should be the other way around.

#### State 2 (free cooling + heating)

The official software description suggests the following method to apply free cooling:

##### *Vrije koeling*

*De gkw verbruikers worden in serie geschakeld aan de LBK. Het circuit van de gkw verbruikers (cp-2) injecteerd drukloos op het circuit van cp-1 (circuit gkw LBK). Buitenlucht wordt voorverwarmd met de koeler van de LBK en de gkw verbruikers koelen lokaal na in het gebouw.*

Translated:

##### *Free cooling*

*The local cooling users are coupled in series with the AHU. The circuit of the local cooling (CP-2) injects (without pressure difference) on the circuit of CP-1 (chilled AHU circuit). Outside air is preheated using the cooling coil of the AHU and the local cooling users supply cooling in the building.*

This method is needed because otherwise the ATES must be used to deliver this cooling capacity. Because the ATES uses a temperature difference of roughly 7°C (15 – 8) and the minimum ground water flow is around 1.5 l/s, the minimum cooling capacity is ± 40 kW. On lower demands the system will pump cold water into the warm storage. This function is completely missing in the software.

#### State 3 (active cooling + heating)

- Both systems are continuously switching between parallel and series configuration (which takes 5 minutes), causing a malfunctioning local cooling system (far to high supply temperatures) and very chaotic start/stop behavior of the ATES system.
- A setpoint is used to block the heat recovery above 16°C to supply additional heating load for the heat pump (and so more cold storage). However, the heat pump is usually blocked above 15°C. This is a typical example of complications caused by adjusted setpoints without understanding the complete system.

#### *State 4 (only cooling)*

- If the heat pump is not disabled while supplying central cooling, the chilled water is supplied to the AHU coil. If the central cooling load is for example <5 kW and the heat pump produces >40 kW the heat pump goes into protection mode to prevent freezing
- As long if the heat pump is active but in protection mode, the ATES cooling mode is also blocked and as result the whole cooling system is not working.
- Because of the low heating curve temperature (<30°C), there is hardly any heat stored in the buffer vessel. The heat pump is started and stopped very often, making the problem even worse.
- If water precooling is active, the heat pump stops working if the AHU supply valve gets below 50%. However, if this valve is below 70% the by-pass valve (8CV2) is opened. As result: If the heat pump is started, it never stops again until the system is shut down.

### **STATES OUTSIDE OFFICE HOURS**

#### *State 1 (regeneration)*

- The flow over the AHU is controlled using a 'percentage setting' of the circulation pump (50-80%). The actual flow depends on the behavior of other flows in the system and the pressure drop over the total system. A good habit is to use pressure-controlled systems.
- The heat pump circuit is partly controlled by the return temperature of the regeneration circuit, creating unpredictable behavior.

#### *State 2 (heating)*

- Between 10-15°C the night ventilation is started, the heat pump is blocked, district heating is operational and ATES cooling is used, creating a huge waste of energy.
- If (due to high temperatures during office hours) the heat pump was blocked, the buffer vessel is obviously not on the right temperature. If the night heating is started, district heat is used for reheating because the system 'thinks' the heat pump does not have enough capacity for reheating the buffer (while it was blocked).

#### *State 3 (night ventilation)*

- Night ventilation is stopped if the indoor temperature is 1°C below the outdoor temperature, which is impossible with a fan dissipation of 1.3 °C.
- Night ventilation is stopped if the average temperature of the building is below 20°C, while all setpoints during summer are around 23-24°C.

#### *State 4 (rest)*

- It occurs that after a warm summer weekend and warm night (mainly >23 °C), the average temperature in the building gets above 27°C. A kind of active (ATES) cooling mode for these cases would be useful.

### **SUMMARY**

This appendix shows the issues in the software of the general HVAC system. In all local (office level) climate control settings there are again a lot of inconsistencies, but these are not that much of concern for the general building model. The problems are described as discovered in the used software in 2013. In the meanwhile (using some workarounds) a number of these problems is fixed or is less critical. To fix all these problems the best solution is probably to start again from scratch. Methods as described in this research are only useful if the buildings software is also bug-free and behaves predictable.

## Appendix L - RECOMMENDED MODIFICATIONS AND IMPROVEMENTS

Using the methods described in this research, it is possible to transform the Kropman Utrecht building into the world's first building with a fully implemented combination of Continuous Commissioning and Model Predictive Control. This requires a considerable amount of new software development to automate data processing, implement continuous commissioning and determine the control strategy. However, before these methods are applicable a number of modifications and improvements on the buildings HVAC system are needed. The recommended modifications are grouped three priority classes:

- A. High priority: should definitely be done, regardless future plans
- B. Medium priority: should be done to improve monitoring possibilities, implement CC and MPC or perform more research on the building
- C. Low priority: should be seen as additions that can be considered for further optimization

The recommendations are grouped in hardware and software related modifications and improvements.

### HARDWARE

The recommendations for the hardware part are given using the main principle diagram, with the specific components colored red.

#### AIR HANDLING UNIT

The following recommendations are given for the AHU configuration:

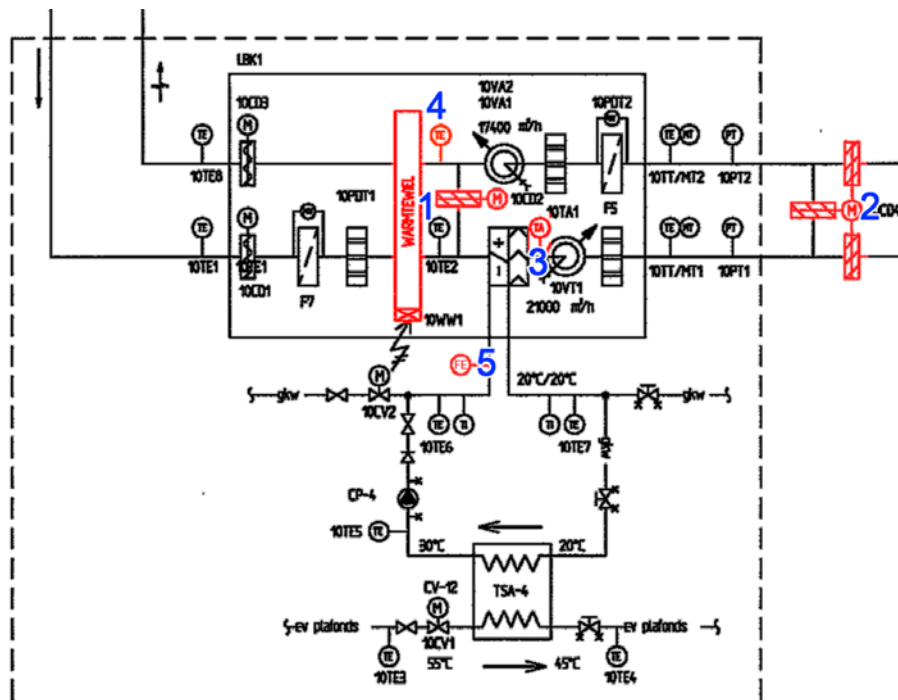


Figure L-1 - Principle diagram AHU with additions

#### 1. (High) Minimize air leaks recirculation valve and HRW

As shown in appendix F (Figure F-10) the air leak between intake and exhaust is estimated over 2500 (m<sup>3</sup>/h), which is far more than the combined typical air leak of a HRW and a valve. HRW air seals should be checked or improved and the valve should be replaced for airtight versions.

## 2. (High) Minimize air leaks regeneration valves

As shown in appendix F (Figure F-10) the air leak through regeneration valve is 1700 (m<sup>3</sup>/h) between supply and return air. This is direct annihilation of cooling or heating energy. During regeneration it is also visible that the supply and return duct valves are not airtight. These valve settings must be recalibrated or the valves must be replaced by airtight versions.

## 3. (Medium) Recalibration or replacement of sensor

The sensor between the coil and fan is ignored during this research, because it produces strongly deviating and inconsistent values. This sensor should be recalibrated or replaced.

## 4. (Medium) Placement of additional temperature sensor

It is a good practice to place a temperature sensor after every component that influences the air temperature. Using this additional temperature sensor the  $\Delta T$  of the exhaust fan and the efficiency of the HRW can be directly monitored.

## 5. (Medium) Placement of additional flow sensor

Placement of an additional flow sensor makes the used methods a lot easier to implement. It eliminates the need for flow assumptions based on manual measurements. Using this flow sensors it is also possible to do real-time AHU load monitoring.

## 6. (Low) Optimize fan configuration during regeneration

In the current configuration both supply and return fans are active during regeneration. A significant energy saving could be achieved if only one fan needs to be active. A higher airflow could be achieved if the pressure drop (over the HRW (twice) and the two filters) was reduced by installing bypasses.

## 7. (Low) Consider application of a dry cooler

A dry cooler for regeneration (instead of the AHU) can significantly reduce energy costs and increase regeneration capacity. A payback time calculation can reveal if this is a smart choice on long-term.

### LOCAL COOLING GROUP

The following recommendations are given for local cooling group:

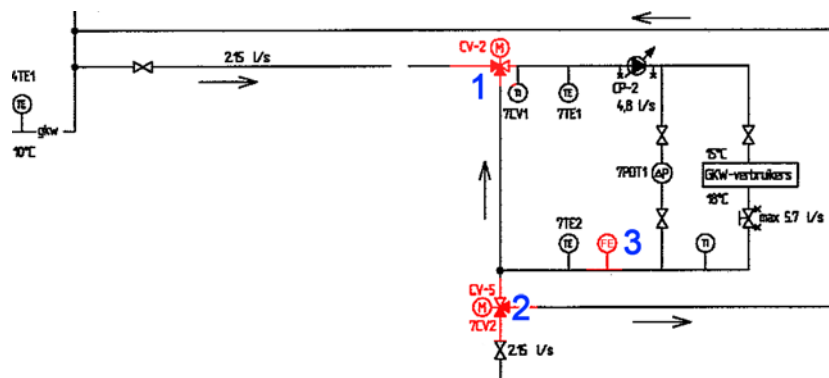


Figure L-2 - Principle diagram local cooling group with additions

## 1. (High) Minimize mixing valve leakage

As visible in Figure J-1 the valve is barely capable of reaching the needed supply water temperature due to leakage. The valve should be replaced or readjusted.

## 2. (High) Replace mixing valve for switching type

The goal of this valve is switching between to return water pipes. The (leaking) mixing valve must be removed and a switching type (ball valve) should be installed. As shown in the pressure distribution diagram, this is a critical spot in the system so the valve has to be 100% watertight.



### 3. (Medium) Placement of flow sensor

Placement of a flow sensor allows to directly measure the supplied local cooling load, using the flow and the two temperature sensors.

## HEAT PUMP AND HEATING SYSTEM

The following recommendations are given for the heating system:

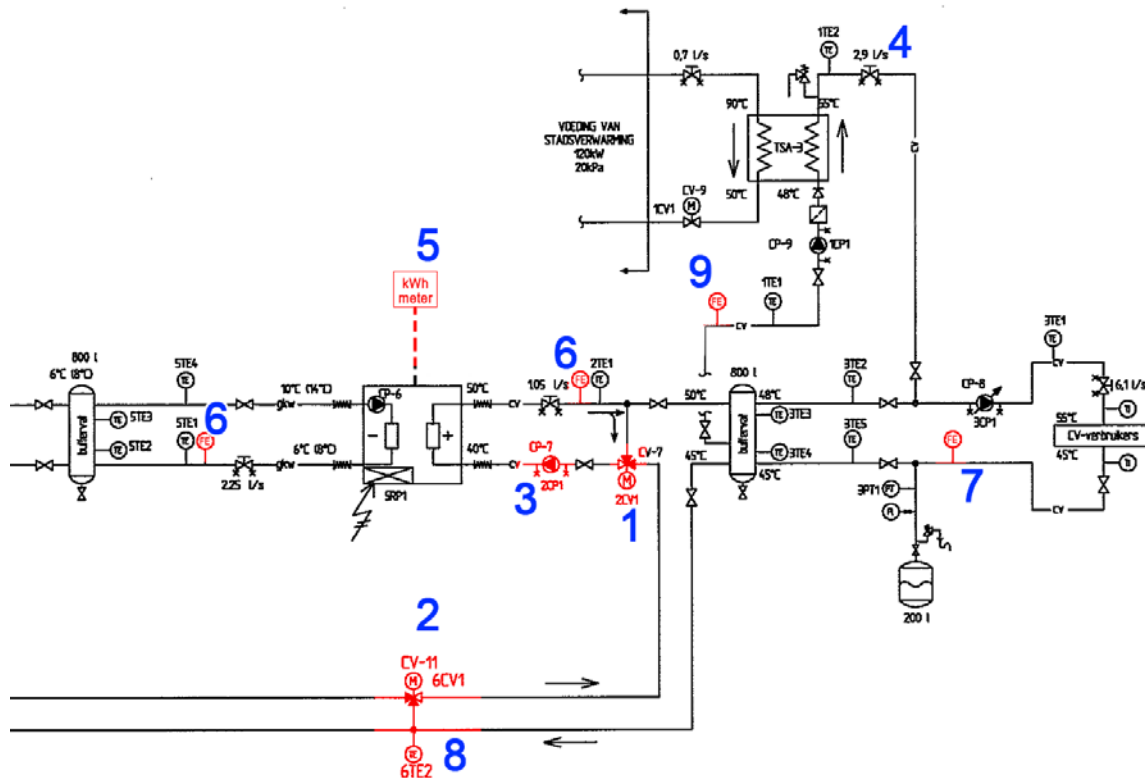


Figure L-3 - Principle diagram heat pump and heating system with additions

### 1. (High) Minimize mixing valve leakage

This 3-way mixing valve is continuously mixing the supply and return water, causing a higher supply water temperature to the heat pump. This increases condenser temperature and lowers the COP and heating capacity.

### 2. (High) Redesign valve setup

This construction is intended to separate the heating and cooling circuit during normal operation and transport the heat to the ATEs if heat pump is used for pre-cooling of the AHU water. This single (3-way) mixing valve must be replaced two 3-way ball valves or three 2-way valves to ensure water can never flow freely between both circuits.

### 3. (High) Increase condenser flow

The pump should be replaced by a larger type, to reduce  $\Delta T$  over the condenser. A smaller  $\Delta T$  ( $< 5K$ ) makes it easier to follow the heating curve and reduces condenser temperature.

### 4. (High) Fix BMS used energy calculation

In the BMS the use of district heat is logged, only a flow of 0.3l/s is used for heat load calculations. This should be adjusted to 2.9 to log the actual (tenfold) district heat use.

### 5. (Medium) Add electricity meter to heat pump

By logging the used electricity of the heat pump, the monitoring method for the heat pump gets more robust. Also heating of the cold-water buffer (Figure J-5) was detected earlier.

#### 6. (Medium) Add flow meters to heat pump circuits

By placing flow meters in both circuits of the heat pump the delivered heating and cooling capacity can be monitored more accurately. Using the combination of pump and balancing valve it is assumed that a constant flow is maintained, but an additional sensor is more accurate.

#### 7. (Medium) Add flow meters to heat distribution circuit

By measuring the flow through the heating circuit the actual heating load can be measured more accurately. In the original principle diagram a separate circuit for a radiators group is visible. This should be included in the main heating circuit.

#### 8. (Medium) Relocate temperature sensors

This temperature sensor is placed on a junction of three pipes. Measuring a temperature on a junction makes no sense, because it is never clear which temperature is measured. The sensor should be relocated to the right.

#### 9. (Medium) Add flow meters to the district heating circuit

This temperature sensor is placed on a junction of three pipes. Measuring a temperature on a junction makes no sense, because it is never clear which temperature is measured. The sensor should be relocated to the right.

#### 10. (Low) Reconsider implementation of heating curve

In the current configuration the heating curve is used to control the supplied water temperature and the maximum temperature of the buffer. The higher temperature during winter causes lower heat pump efficiency and though a lower heating capacity. Especially when district heating is active it makes sense to operate the condenser at the lowest temperature trajectory possible (25/35) and use the district heating for reaching the heating curve temperature (35/45).

### ATES SYSTEM

The following recommendations are given for the ATES system:

#### 1. (Medium) Place temperature and flow sensors

As discussed in chapter 2, the monitoring of the ATES system becomes significant easier if both temperatures and flows of the groundwater are measured.

#### 2. (Medium) Improve logging accuracy

As shown in section 2.3.1 the logging of the ATES system is not consistent. Improvement of the data acquisition method and logging the warm and cold well pumps behavior separately is recommended.

#### 3. (Medium) Discuss well pump software with GeoComfort

First, as explained in appendix B, the well pumps always start at 100% capacity causing a direct short cut between warm and cold wells. Secondly, the minimum capacity of 30% is too high for the used heat pump. For a  $\Delta T$  of 8K between the wells at 6 m<sup>3</sup>/h, at least 56 kW of heat load is needed. The heat pump delivers around 40 kW, requiring a minimal flow of 4 m<sup>3</sup>/h or lower. Both issues should be discussed with a GeoComfort software engineer.

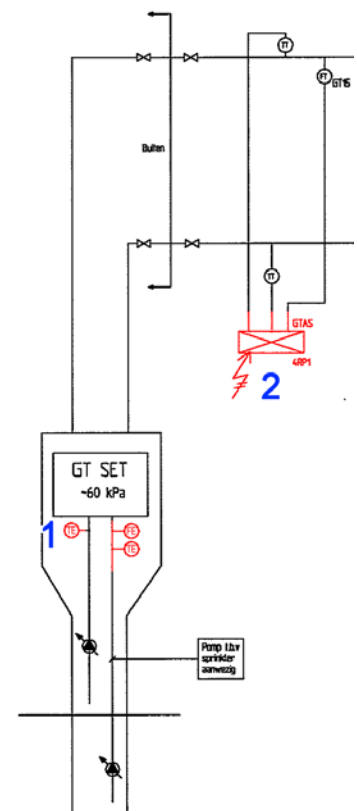


Figure L-4 – Principle diagram ATES system with additions

## SOFTWARE RELATED RECOMMENDATIONS

The following recommendations are given for all software-related parts:

### **1. (High) Rewrite the main control software**

As already introduced in appendix K, there are a lot of issues with the main (Priva-based) control software. A new rewritten version of the control software should implement all states as separate software components. The 'top-level' of the software should only decide in which state the HVAC-system operates and when to switch between states. The separate state components only contain software for the needed system parts during that state, making programming, debugging and optimizing a lot easier. Changes in the software during winter cannot influence the behavior during summer, because this are separate software parts.

### **2. (Medium) Simplify local climate control**

It proved to be hardly possible to find accurate relations for the load simulation of the building. This was mainly caused by the structure of room temperature setpoints. In several offices the setpoint is at 10 °C (full cooling) during absence and at 23 °C (full reheating) during presence. Because office doors are usually left open and occupancy changes often, this makes no sense. One central setpoint for the whole floor (with the possibility to define an offset per office), controlled by a heating curve (22°C during winter, 24°C during summer for instance), significantly reduces the heating and cooling loads. The use of presence sensors per room is useless.

### **3. (Medium) Implement a fixed AHU heating curve**

During the analyzed year (2013) the heating curve for ventilation air (AHU) is changed at least 10 times. Several employees have access to the BMS and change the heating curve setpoints (for the total building) if the temperature in a specific room is too high or low. An optimized heating curve should be developed and locked (as fixed values) in the control software.

### **4. (Medium) Night ventilation optimization**

Because night ventilation does not directly influence the ATES system, no attention is paid to this state. However, for building comfort it is an important feature. In the current configuration the operation mainly depends on the outdoor temperature. Using the data of indoor temperatures, the need for night ventilation can be defined. For instance, if more than 25% of the rooms are warmer than the setpoint temperature, night ventilation is started. Night ventilation can also be coupled to the weather forecast. Above 23°C night ventilation is not active. This causes the building (and thermal mass) temperature to rise up to 30°C for rare cases (weekends with tropical temperatures). The system has not enough cooling capacity to extract this heat, causing comfort issues for days. If for instance 50% of the rooms gets above 25 °C and outdoor temperatures are not suitable for night ventilation, cooling using the ATES system should be used.

### **5. (Low) Increase data logging speed**

In the current system, the logging of all sensors takes around 5 minutes. This is too slow for data analysis, because the behavior can change significantly in the meantime. Using modern computer hardware it should not be a problem to log all data within 1 second, to create an accurate snapshot of the buildings systems.